The University of Sheffield

Department of Biomedical Science
Sheffield
United Kingdom
European Union

Analysis of 4E-BP effectors with cellular protective potential *in vitro* and *in vivo* by quantitative mass spectrometry

---

Thesis submitted in fulfilment of the degree of Doctor of Philosophy

by

Simon Christoph Sattler

Supervisors
Dr. Alexander J. Whitworth
Prof. Carl G. W. Smythe

Advisors
Prof. Carl G. W. Smythe
Prof. Mikko Juusola

September 2016

Abstract

Translation initiation factor 4E binding proteins (4E-BP) are crucial for
stress resistance and the survival of cells upon encountering different stres-
sors. In particular, they are cell protective and able to rescue the Parkinson's
disease phenotype of patient cells and in *Drosophila* models. 4E-BPs are in-
hibitors of cap-dependent translation, the predominant form of translation in
eukaryotes. However, an estimated 10 - 15 % of mRNAs can initiate transla-
tion cap-independently via internal ribosome entry sequences (IRES), which
become predominant when 4E-BPs block cap-dependent translation. Al-
though a lot is already known about the upstream regulation of 4E-BP activ-
ity, much less is known about its downstream effectors, and the mechanism
by which they are responsible for the protective effect. Here, I developed two
inducible stable cell lines overexpressing wildtype 4E-BP1 (4E-BP1[WT]),
the most abundant isoform in humans or a constitutively active form carry-
ing two point mutations (4E-BP1[TA]). Likewise, two *Drosophila* lines were
generated overexpressing the wildtype orthologue of 4E-BP1 (d4E-BP[WT])
or its constitutively active form (d4E-BP[TA]). Stable isotope labelling of
these cells and flies allowed the quantification of individual protein abun-
dances after 4E-BP overexpression and the identification of upregulated pro-
teins by mass spectrometry. Bioinformatic analyses of the mass spectrome-
try data revealed that many antioxidant, mitochondrial and lipid metabolic
proteins were enriched among the proteins upregulated upon 4E-BP overex-
pression. Cell viability assays confirmed that 4E-BP1 overexpression rescues
cells from the toxic effects of the mitochondrial complex I inhibitor rotenone.
The effect was reduced after knockdown of different 4E-BP1 effectors iden-
tified by prior quantitative proteomics.

Wir stehen selbst enttäuscht
und sehn betroffen,
den Vorhang zu
und alle Fragen offen.

BERTOLT BRECHT: DER GUTE MENSCH
VON SEZUAN. 1943

So ends the play,
the curtain closed
and all questions open.

BERTOLT BRECHT: THE GOOD PERSON
OF SZECHWAN. 1943

Acknowledgements

Contents

Chapter 1

Introduction

1.1 Mechanisms of protein translation

The regulation of protein synthesis has been in the focus of interest for decades. Since the DNA structure and their principal transcription mechanism has been revealed, many researchers investigated the regulation of protein production on the level of mRNA transcription, the first step of protein biosynthesis. The mRNA becomes synthesised during the complex process of transcription in which many different proteins with varied functions are involved. It became clear that transcription is indeed a strongly regulated process, but it revealed that the following mRNA translation is not only a subsequent non-controlled automatism, but is itself a strongly regulated process. Translation describes the process of protein synthesis out of single amino acids on the ribosomes, based on the mRNA template, and is the second major step of protein synthesis. Regulation of protein synthesis by modifying translation allows cells to respond quicker to extra- and intracellular changes without time and energy consuming synthesis of new transcripts. Many studies have shown that the ability of cells to regulate translation is crucial, e.g. to resist different cellular stressors as reviewed by Holcik and Sonenberg (2005).

The process of translational regulation and the proteins involved are diverse, but can be differentiated into global and mRNA-specific regulation. On the one hand, global regulation enhances or decreases the amount of all synthesised proteins, while on the other hand mRNA-specific regulation modifies the translation of defined mRNA subtypes with characteris-

tic sequences or secondary structures in the 5' and/or 3' untranslated region. Local translation of distinct mRNAs in polarised cells is a special case of mRNA-specific translational regulation. This mechanism is required to translate specific mRNAs e.g. at the synapses of neuronal cells or during embryonic development. For this purpose, mRNAs can be actively transported to distinct cell compartments. For example, at the synapses it is crucial to translate proteins quickly from pre-existing mRNAs in respond to pre- or postsynaptic stimuli e.g. to strengthen the synaptic connection for learning processes (Kandel, 2001; Steward, 1997). However, the focus in this study laid on global translation regulation.

The process of translation in eukaryotes takes place in the cytoplasm and is divided into three major steps: initiation, elongation and termination (Fig. 1.1). The initiation is critical, because it marks the last highly controlled step of protein biosynthesis. When the translation passed through the initiation step, the whole protein will be translated. mRNA translation is the most energy consuming process in cells (Buttgereit and Brand, 1995), which is why it is crucial for cellular survival to regulate the process tightly, in particular under stress when resources are limited. Basically, two different variants of global translation initiation were described so far: cap-dependent and cap-independent translation. Their initiation principles differ and are described separately below.
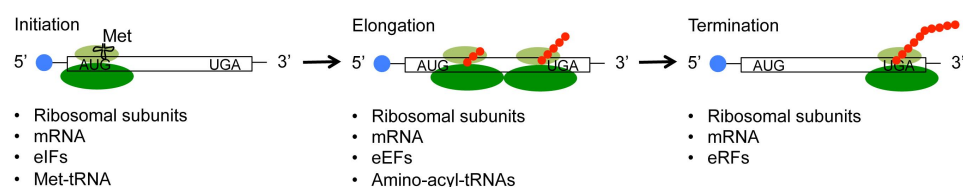
Figure 1.1: Process of mRNA translation. Initiation factors (eIFs) catalyse the association of ribosomal subunits with the mRNA followed by a screen of the mRNA for the start codon AUG. During elongation, tRNAs carry amino acids to the ribosomes and bind sequence specifically to the mRNA. Amino acids become connected by elongation factors (eEFs) and ribosomes in order to synthesise a peptide chain. The synthesis takes place in 3' direction. When the ribosomes reach a stop codon on the mRNA, release factors (eRFs) terminate translation and release the different compounds.

After initiation, the mRNA is translated into a protein chain at the ribosomes with the support of different elongation factors (eEFs) beginning at the 5' end and translating in the 3' direction. tRNA delivers single amino acids, which bind sequence specifically to the mRNA and are connected to the nascent polypeptide under energy consumption by ribosomes. As soon

as the ribosome reaches a stop codon on the mRNA, release factors (eRFs) bind, release the newly synthesised protein chain from the ribosomes and terminate the translation process.

1.1.1 Cap-dependent translation initiation

The predominant form of translation initiation under normal conditions in eukaryotes was described after many studies by Merrick (1992). At its beginning, initiator factor 3 (eIF-3), eIF-1, eIF-1A and eIF-5 bind the small ribosomal subunit (40S) to form the 43S pre-imitation complex and prime ribosomes for loading tRNA and mRNA. tRNA binding the first amino acid methionine is delivered by eIF-2 to the pre-initiating complex (Fig. 1.2B).

In the meantime, the mRNA binds eIF-4F, a complex consisting of three subunits: eIF-4E, which binds the 5' cap structure of mRNAs, eIF-4A, a RNA helicase, which removes mRNA secondary structures, and eIF-4G, a scaffold protein. The cap structure is characterised by a methylated and poly-phosphorylated guanine (Fig. 1.2A). Binding of mRNA by eIF-4F primes mRNA for translation and is a tightly regulated and rate-limiting step during translation. The mRNA-eIF-4F complex is loaded onto the pre-initiating complex. During this process, eIF-4G binds the poly(A)-binding protein (PABP) at the 3' end to stabilise the protein-mRNA complex (Wells et al., 1998). This brings the 5' and 3' ends close together during initiation of translation and may explain why many regulatory elements for translation are located at the 3' end of mRNAs although the elongation starts from the 5' end.

Subsequently, the mRNA is scanned by the pre-initiating complex for the start codon AUG. After identifying it, the large ribosomal subunit (60S) is recruited by eIF-5B to complete the initiation complex. eIF-2 is removed from the complex before translation begins. New contributing and regulating factors are discovered constantly and amend our understanding of translation initiation.

1.1.2 Cap-independent translation initiation

Alternatively to cap-dependent translation, approximately 10 - 15 % of all mRNAs (Komar et al., 2012) were estimated to be able to initiate translation cap-independently via internal ribosome entry sequences (IRES), which

are up to 200 nucleotides long secondary mRNA structures that recruit ribo-
somal complexes (Fig. 1.2A) (Holcik and Sonenberg, 2005; Johannes et al.,
1999; Pestova et al., 2001). This cap-independent translation bypasses the
recruitment of initiation factors like eIF-4E, which require binding the 5' cap
structure to initiate translation. Originally, viral mRNAs were identified to
allow cap-independent translation via IRES and it was quite surprising when
these structures were also identified in mammalian cells. However, IRES ele-
ments from viral and cellular origins may differ as several labs reported that
cellular IRES translation initiation was much less effective than initiation by
viral IRES (Gilbert, 2010; Kozak, 2005; Merrick, 2004; Shatsky et al., 2010).
This means that cap-dependent translation is by far the predominant form
of translation in cells, if it is not suppressed by certain regulators.

Viral mRNA typically do not require cap-dependent translation, which
is why it was hypothesised that cap-independent translation is evolution-
ary older and later superseded by cap-dependent translation. For this rea-
son, our knowledge about the mechanism of cap-independent translation
is mostly based on viral IRES, which makes it difficult to draw inference
about the mechanism of cellular IRES regulation in eukaryotes. In particu-
lar, several structural differences between viral and cellular IRES have been
described. Cellular IRES are shorter (Komar and Hatzoglou, 2005, 2011),
but more diverse in their secondary structure and less stable than viral IRES
(Komar and Hatzoglou, 2011; Xia and Holcik, 2009) and share no common
motif (Baird et al., 2007). However, when one considers the available infor-
mation about viral IRES, different pathways of IRES-initiated translation
can be proposed (Fig. 1.2B). For instance, polio virus mRNA IRES seems
to mimic the cap-structure to recruit eIFs, which means that in this case
cap-independent translation may proceed similar to cap-dependent trans-
lation (Marcotrigiano et al., 2001). Given that cellular mRNAs all have
cap-structures, it is quite hard to believe that this pathway would be of
any benefit in cells. On the other hand, the hepatitis C virus mRNA IRES
have been described to initiate translation independently of the eIF-4F com-
plex (Pestova et al., 1998). Furthermore, cricket paralysis virus mRNA
IRES were found to recruit ribosomes via elongation factors instead of ini-
tiation factors (eEF-1A) (Wilson et al., 2000). Several studies have also
described that some viruses do not need eIF-2 to initiate translation, but
utilise eIF-2A, eIF-2D, eIF-5B or other factors to transport tRNA bound

amino acids to the ribosomes (Dmitriev et al., 2010; Kim et al., 2011; Pestova et al., 2008; Robert et al., 2006; Thakor and Holcik, 2012; Ventoso et al., 2006). The exact mechanism may be dependent on the IRES structure of individual mRNAs. To make things even more complicated, alternative initiation factors have also been identified, so called IRES trans-acting factors (ITAFs). It has been proposed that they stabilise IRES structures or serve as additional mediators between ribosomes and mRNAs (Komar and Hatzoglou, 2011; Lewis and Holcik, 2008). The identification of other key players and contributors to the IRES-initiated translation may increase the number translation pathways further.
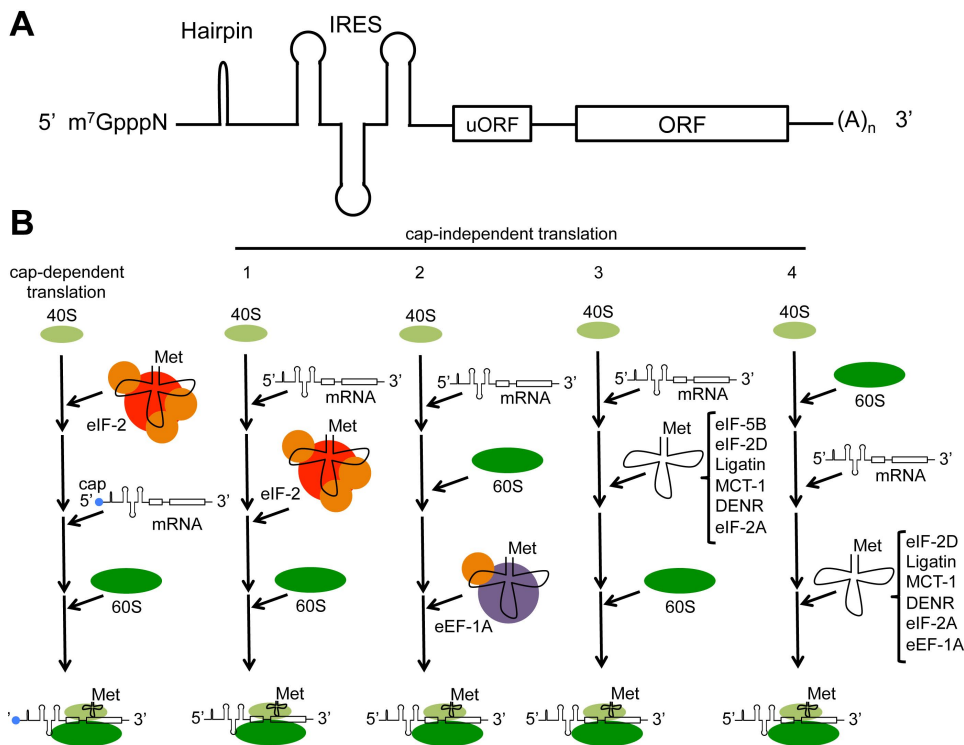
Figure 1.2: Different models of mRNA translation initiation. (A) Composition of a mRNA with translation initiating 5' cap structure m^7GpppN and IRES structure. 5' hairpins can interfere with translation initiation as well as upstream open reading frames (uORF), which can reduce translation of the coding open reading frame (ORF). The poly(A) tail $(A)_n$ is also crucial to stabilise the initiating complex. Source: Gebauer and Hentze (2004) (B) Cap-dependent translation begins with the recruitment of the tRNA-bound first amino acid methionine to the primed 40S ribosomal subunit by eIF2. The cap structure of the mRNA is bound by the eIF-4F complex and shuttled to the ribosomes. The standard model of cap-independent translation understands that the IRES structure acts similar as the cap-structure to bind initiation factors, but do not require the cap-binding eIF-4F complex (1), while in other cases it was described that IRES can recruit eEFs to initiate translation (2). Further studies propose thateIF-2 is replaced by eIF-2A and other factors to recruit tRNA bound methionine to the mRNA (3), which could even involve eEFs (4).

Interestingly, many mRNAs containing IRES seem to be important for cell growth, differentiation and regulation of apoptosis and may be crucial for regulation of cell survival and death (Holcik et al., 2000a; Holcik and Sonenberg, 2005). Indeed, IRES-mediated translation was found upregulated under conditions of cell stress, when cap-dependent translation is inhibited. Still, cells require specific mRNAs to be translated even when general translation is switched off to survive critical conditions. IRES-dependent translation bridges this gap, which is why it becomes the upregulated upon different stressors.

1.2 Molecular regulation and impact of 4E-BP

Diverse pathways and proteins can interfere with the initiation of cap-dependent translation and block the protein translation either in global or mRNA-specific way. The ability of cells to change the spectrum of synthesised proteins is crucial e.g. to respond appropriately to intra- or extracellular stressors like hypoxia, nutrient deprivation, heat shock or endoplasmic reticulum stress by misfolded proteins. To save energy, global protein expression is usually reduced in response to stressors, while synthesis of stress-response proteins, like chaperones, increases (Harding et al., 2000; Holcik et al., 2000b). A common mechanism to modulate translation is to inhibit the binding of the translation initiation factor eIF-4E to the 5' cap structure by blocking the eIF-4E binding site of eIF-4G. Binding proteins (4E-BPs) occupy the binding site of eIF-4E and stop the completion of translation initiation. Several proteins with this capacity are involved in embryonic development like Maskin, which is crucial for the regulation of maternal mRNA translation (Stebbins-Boaz et al., 1999) or Cup, which enables the establishment of the anteroposterior axis formation in *Drosophila melanogaster* (Nakamura et al., 2004; Nelson et al., 2004; Wilhelm et al., 2003). Interestingly, it has been reported for Cup that the repressed mRNA is associated with polysomes anyway (Clark et al., 2000). It is not clear yet whether this is a common result for many eIF-4E binding proteins, but it indicates that inhibition of translation initiation may not necessarily be achieved by blocking of ribosomal assembly.

Aside from embryogenesis, cap-dependent translation is also blocked in response to cellular stress. IRES elements containing mRNA translation be-

comes predominant and ensures cellular survival by translation of e.g. the anti-apoptotic X-chromosome linked inhibitor of apoptosis (XIAP) (Holcik et al., 1999). However, the XIAP antagonist pro-apoptotic protease-activating factor 1 (APAF1) is also regulated by IRES-dependent translation (Coldwell et al., 2000). The ratio of both proteins is crucial for the fate of the cell under stress. Another example for the cellular protective effect of IRES-dependent translated proteins is HIAP2, which belongs to the IAP family as well as XIAP. This protein is up-regulated in a response to intracellular stress induced by misfolded proteins and delays stress-induced apoptosis (Warnakulasuriyarachchi et al., 2004).

1.2.1 Structure and Function

4E-BP is a protein with three known human isoforms 4E-BP1-3 (Pause et al., 1994; Sonenberg and Dever, 2003). The binding partner eIF-4E exhibits a two- to threefold larger binding preference for 4E-BP2 compared to 4E-BP1/3 under physiological conditions, despite many structural similarities between the different isoforms (Fukuyo et al., 2011; Tomoo et al., 2005). 4E-BPs interact with eIF-4E through the binding motif YXXXXLΦ (where X stands for any amino acid and Φ for a hydrophobic residue) (Altmann et al., 1997; Fukuyo et al., 2011). They mimic the eIF-4E binding site of eIF-4G, compete with it and prevent the formation of the cap-binding eIF-4F complex (Fig. 1.3A and B).

4E-BP's functions are regulated by different kinases via a complex mechanism of phosphorylation. A stepwise phosphorylation blocks the access of the 4E-BP binding site to eIF-4E and ends the inhibition of cap-dependent translation. Nine 4E-BP1 phosphorylation sites have been described so far: Thr37, Thr41, Thr46, Thr50, Ser65, Thr70, Ser83, Ser101 and Ser112 (Fadden et al., 1997; Heesom et al., 1998; Shin et al., 2014b; Wang et al., 2003). The functional differences between different human 4E-BP variants are not very well elucidated yet. 4E-BP1 is by far the best studied isoform, which is why the focus of this study laid on this paralogue. All 4E-BP isoforms are ubiquitously expressed, but with varying amounts in different organs. 4E-BP1 is enriched in adipose tissue, skeletal muscle and the pancreas, while 4E-BP2 is strongly expressed in the brain and seems to be important for memory formation and synaptic plasticity. 4E-BP3 expression seems to be increased in cells of the immune system, but available data for this isoform

A

B

C

	regulatory motif	eIF4E-binding site	TOS motif	
	RAIP	**YxxxxLΦ**	**FEMDI**	Identity to 4E-BP1
4E-BP1				
4E-BP2				60%
4E-BP3				57%

D

```
MSGGSSCSQTPSRAIPA-TRRVVLGDGVQLPPGDYSTTPGGTLFSTTPGGTRIIYDRKFLME human 4E-BP1
MSAGSSCSQTPSRAIP—-TRRVALGDGVQLPPGDYSTTPGGTLFSTTPGGTRIIYDRKFLME mouse 4E-BP1
MSASPTARQAITQALPMITRKVVISDPIQMP-EVYSSTPGGTLYSTTPGGTKLIYERAFMKN Drosophila Thor
                                 37        46
```

```
CRNSPVTKTPPRDLPTIPGVTSPSSDEPPMEASQSHLRNSPEDKRAGGEESQFEMDI human 4E-BP1
CRNSPVAKTPPKDLPAIPGVTSPTSDEPPMQASQSQLPSSPEDKRAGGEESQFEMDI mouse 4E-BP1
LRGSPLSQTPPSNVPSCLLRGTPRTPFRKCVPVPTELIKQTKSLKIEDQEQFQLDL  Drosophila Thor
   65   70
```

Figure 1.3: Structure of 4E-BP and its binding behaviour in different species. (A) Ribbon diagrams demonstrate the binding of eIF-4G, human 4E-BP1 and *Drosophila* homologue Thor to eIF-4E, which is shown in a schematic representation below (B). Source: Peter et al. (2015) (C) shows the primary structure of human 4E-BP1-3 with threonine (T) and serine (S) phosphorylation sites and conserved motifs. TOS is required for the interaction with mTORC1. The primary sequences of 4E-BP1 in human, mouse and of *Drosophila* Thor show that in particularfour highlighted phosphorylation sites required for eIF-4E release are very well conserved in different species (D).

is thin. Although the sequence identity of 4E-BP1 and 4E-BP2 is only 60 % and 57 % between 4E-BP1 and 4E-BP3 (Martineau et al., 2013), the eIF-4E binding motif and the phosphorylation sites, which regulate the activity of the protein seem very well conserved, not only in humans but also across other species including mouse and *Drosophila* (Fig. 1.3C and D). In fact, in *Drosophila*, only one 4E-BP ortholog exists, called Thor. The phosphorylation sites Thr37, Thr41, Thr46, Thr50, Ser65 and Thr70 are conserved in Thor, but Ser83 is replaced by Thr while Ser101 and Ser112 are replaced by Gln.

1.2.2 4E-BP regulation by TOR

In vitro studies have revealed that 4E-BP's activity is controlled by phosphorylation through the target of rapamycin (TOR) kinase. In mammalian systems, TOR is abbreviated as mTOR. The 4E-BP1 phosphorylation sites Thr37, Thr46, Ser65 and Thr70 were characterised to be particularly important for the regulation by mTOR. At first, Thr37 and Thr46 become phosphorylated by mTOR, which is the priming event of a hierarchical phosphorylation cascade and seems to be relatively independent of external stimuli (Gingras et al., 1999). Subsequently, Thr70 becomes phosphorylated before Ser65 (Fig. 1.4). These steps are sensitive to external stimuli and crucial to release 4E-BP1 from the binding to eIF-4E. Interestingly, the inhibition of mTOR by rapamycin leads to a dephosphorylation of Thr70 and Ser65, but only barely affects Thr37 and Thr46 phosphorylation in HEK293 cells (Gingras et al., 2001). A possible conclusion may be that the phosphorylation of Thr70 and Ser65 is the rate-limiting step, while Thr37/Thr46 are constitutively phosphorylated. Furthermore, there is some evidence that Thr70 and Thr65 are not directly phosphorylated by mTOR, in contrast to Thr37/46, but regulated by an mTOR-dependent kinase or phosphatase, which may explain the different sensitivities of these sites for rapamycin (Burnett et al., 1998; Heesom and Denton, 1999; Peterson et al., 1999; Schalm et al., 2003). Studies in mouse embryonic fibroblasts revealed a much stronger inhibitory effect on mTOR by competitive inhibitors like Torin1, which binds to the mTOR ATP-binding site (Thoreen et al., 2009) and results in a phosphorylation decrease of 4E-BP1 residues Thr37/46 and Ser65. However, for 4E-BP1 to be released from eIF-4E all four phosphorylation sites are essential. Phosphorylation of Thr70 and Ser65 only is insufficient for release (Gingras et al., 2001).

TOR itself is a key regulator of protein synthesis in response to extracellular and intracellular signals. It is a target of many different pathways and regulates proteins which affect cap-dependent and cap-independent translation. The name target of rapamycin was chosen after studies in yeasts revealed that TOR was inhibited by rapamycin (Helliwell et al., 1994; Kunz et al., 1993). The allosteric inhibition is facilitated by the peptidyl-prolyl cis-trans isomerase FKBP12 after binding to rapamycin (Brown et al., 1994; Chiu et al., 1994; Sabatini et al., 1994). The allosteric binding domain in the C terminus, the FKBP12-rapamycin binding site (FRB), lies right next
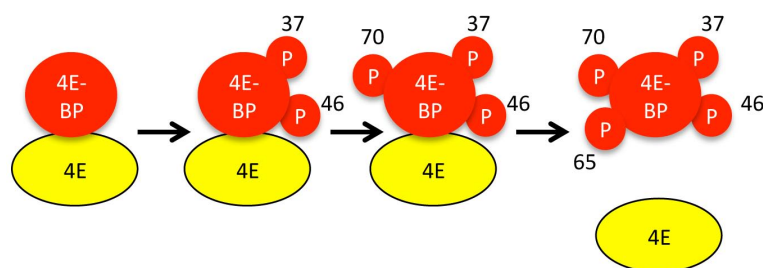
Figure 1.4: Process of 4E-BP1 phosphorylation. To inactivate it, 4E-BP1 is phosphorylated in a cascade beginning with Thr37 and Thr46, followed by Thr70 and Ser65. All four sites have to be phosphorylated in order to release eIF-4E.

to the functional kinase domain (Fig. 1.5A). However, mTOR cannot phosphorylate its substrates autonomously but has to recruit helper proteins. Two protein complexes were described to form around mTOR: mTORC1 and mTORC2 (Fig. 1.5B). In addition to mTOR, mTORC1 consists of raptor, which is crucial for phosphorylation of substrates (Beugnet et al., 2003; Choi et al., 2003; Nojima et al., 2003; Schalm et al., 2003), mLST8, which stabilises the mTOR-Raptor complex in response to nutrient supply (Kim et al., 2003) and some other proteins with partly not completely clarified functions. mTORC1 activates on the one hand the ribosomal S6 kinases (S6K1/2), which enhances cap-dependent translation initiation and translation elongation, while on the other hand it inactivates 4E-BPs, the promoter of cap-independent translation. The other mTOR complex, mTORC2, also recruits mLST8, but rictor and SIN1 instead of raptor. mTORC2 seems incapable to phosphorylate S6K or 4E-BP, but phosphorylates other targets like Akt, a kinase which activates mTORC1 for its part. Hence, the substrate specificity of mTOR is clearly determined by the associated factors. The upstream regulation of both mTOR complexes differ. One example is their different response to rapamycin. While mTORC1 can be inhibited effectively depending on the cell context, mTORC2's activity is only blocked after a very long treatment (Sarbassov et al., 2006). In contrast to human 4E-BP1/2, 4E-BP3, which is not very well studied, does not seem to be controlled by mTORC1 (Tsukumo et al., 2016). Instead, the protein is transcribed during prolonged mTORC1 inhibition and may play a different physiological role compared to the other two isoforms. Here, I focus on the regulation of mTORC1 as mTORC2 is not directly responsible for the activity of 4E-BP1/2.

mTORC1 is regulated by many different pathways. Its activity is reduced upon nutrition deprivation, which means that 4E-BP1 becomes active under these conditions. This is facilitated by a defined stabilisation of the raptor-mTOR association, which hinders mTOR binding its substrates effectively (Kim et al., 2002).
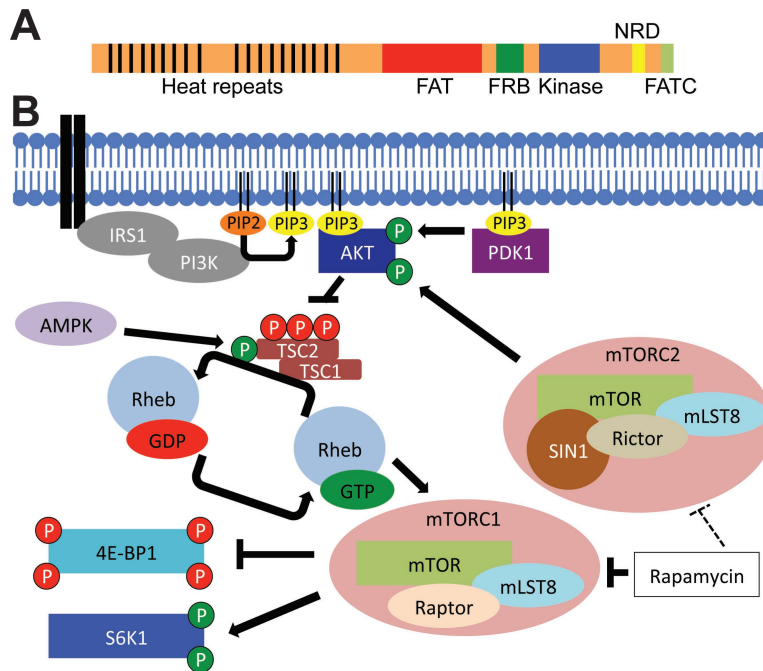
Figure 1.5: Structure and regulation of mTOR. (A) mTOR is composed of 20 tandem HEAT repeats (Huntignton, EF3, A subunit of PP2A, TOR1) for protein-protein interactions and two FAT domains (FRAP, ATM, TRAP) of which is one located at the C-terminus (FATC). They may be necessary for the functionality of the catalytic domain. mTOR also contains a putative negative regulatory domain (NRD). However, most importantly for its function are the kinase domain and the FRB site (FKB12–rapamycin binding), which is crucial for the inhibitory effect of rapamycin. (B) mTOR forms two distinct complexes with other proteins: mTORC1 and mTORC2. Both have different up- and downstream targets, but interfere with each other. The mTOR inhibitor rapamycin mostly affects mTORC1 and hardly mTORC2. Red P-sites indicate phosphorylations, which lead to an inactivation of the protein, while green P-sites indicate protein activation by phosphorylation. See text for further details.

Growth factors like insulin or IGF alter mTORC1 activity as well. One mechanism of mTORC1 activation by growth factors is via the phosphoinositide-3-OH kinase (PI3K) pathway (Brunn et al., 1996; Cheatham et al., 1994; Chung et al., 1994; Gingras et al., 1998; Mèndez et al., 1996; Sharma et al., 1998; Ueki et al., 2000; von Manteuffel et al., 1996). Akt kinase, one of the downstream effectors of PI3K, is the mediating kinase, which activates mTORC1 (Gingras et al., 1998) by inhibiting tuber-

ous sclerosis complex 2 (TSC2), a negative regulator of mTORC1 (Inoki et al., 2002; Jaeschke et al., 2002; Gao et al., 2002; Manning et al., 2002; Tee et al., 2002). TSC2 acts as a heterodimer with TSC1 and inactivates the mTOR promoter Ras homologue enriched in brain (Rheb) (Castro et al., 2003; Garami et al., 2003; Tee et al., 2003). Alternatively, growth factors can also activate mTOR via phospholipase D (PLD), which hydrolyses phospholipids and generates phosphatidic acids. These degradation products were also found to activate mTOR (Fang et al., 2001, 2003).

As mTOR is a major control node to regulate energy intensive processes like translation, mTOR is also regulated by the cellular energy level. The 5'-AMP-activated protein kinase (AMPK) is an intracellular sensor for the AMP/ATP ratio and was identified to inhibit mTOR activity when it is activated by a sinking energy level (Kimura et al., 2003). AMPK acts by phosphorylating and activates TSC2 (Inoki et al., 2003) or hinders the raptor-mTOR interaction (Gwinn et al., 2008).

1.2.3 Non-TOR regulation of 4E-BP

For a long time, it was generally believed that mTORC1 is the only kinase controlling 4E-BP1's activity. The phosphorylation states of mTORC1 substrates 4E-BP1 and S6K1 are commonly utilised to evaluate the activity of mTORC1. More recently, evidence has emerged that other kinases, along with phosphatases, modulate the activity of 4E-BP and interfere with the canonical mTOR pathway by manipulating its downstream targets.

Ataxia telangiectasia mutated (ATM), a serine/threonine protein kinase which acts as a stress sensor upon double strand breaks, apoptosis and genotoxic stress was identified to phosphorylate 4E-BP1 at Ser112 *in vitro* and *in vivo* (Yang and Kastan, 2000). Like mTOR, ATM's activity is promoted by insulin. Although Ser112 was not reported so be crucial for eIF-4E binding, it highlights the physiological potential of other 4E-BP1 phosphorylation sites, which have not been elucidated yet. It was also reported that 4E-BP1 phosphorylation is controlled in a cell cycle dependent manner, suppressing its activity by phosphorylating Thr70 through cyclin-dependent kinase 1 (CDK1) (Greenberg and Zimmer, 2005; Heesom et al., 2001). During mitosis, 4E-BP1 remains phosphorylated to promote cap-dependent translation. Aside from stress response, this emphasises another potential function of 4E-BP1 to regulate the kind of protein translation depending on the cell

cycle. The mitogen-activated protein kinase p38 was also described to phosphorylate 4E-BP1 in murine and human cells at all four sites in response to UVB radiation (Liu et al., 2002) or TNF-α-induced apoptosis (Janzen et al., 2011), which promotes apoptosis. Furthermore, there is evidence that serine/threonine-protein kinase pim-2 is able to phosphorylate 4E-BP1 directly at position Ser65 in human cell lines (Fox et al., 2003). Another identified non-TOR kinase targeting 4E-BP1 in HEK293T cells and the *Drosophila* ortholog Thor was the leucine-rich repeat serine/threonine-protein kinase 2 (LRRK2/dLRRK) (Imai et al., 2008). It phosphorylates 4E-BP1 at the positions Thr37/46 and initiates the phosphorylation cascade thereby, although another study in mice was unable to confirm this interaction (Trancikova et al., 2012).

Some of the pathways, which regulate 4E-BP1 aside from mTORC1 are very cell/tissue specific or dependent on the metabolic context. For instance, Cheng et al. (2011) have reported that in *Drosophila* neuronal progenitor cells (neuroblasts), Thor is not phosphorylated by TOR under dietary restriction, but by the anaplastic lymphoma kinase tyrosine kinase receptor (Alk). Alk is localised to the cell membrane and activates the PI3K cascade, but whether the phosphorylation of 4E-BP is directly facilitated by Alk itself or by a kinase cascade initiated by Alk is still not clear. In different cancer cell lines, glycogen synthase kinase-3β (GSK-3β) was identified to phosphorylate and inactivate 4E-BP1 at Thr37/46 and potentially also Ser70 and Ser65 (Shin et al., 2014a).

Casein kinase 1$_\epsilon$ was recently found phosphorylating 4E-BP1 on two new sites, Thr41 and Thr50 (Shin et al., 2014b). The knowledge about these sites is still limited, but first investigations suggest that phosphorylation on these sites can reduce the activity of 4E-BP1 and its binding to eIF-4E.

Although the mechanism of 4E-BP1 phosphorylation by mTOR is understood very well, much less is known about the process of dephosphorylation. However, two studies in intestinal epithelial cells and cardiac myocytes paid attention to this reversal mechanism and have shown that oxidative stress promotes dephosphorylation by protein phosphatase 1 and 2A (PP1/PP2A) (Guan et al., 2007; Pham et al., 2000). Interestingly, another study in HEK293 and HCT116 cells by Liu et al. (2013) has elucidated that protein phosphatase 1G (PPM1G) is responsible for the basal dephosphorylation of 4E-BP1. These findings suggest that dephosphorylation of 4E-BP1 may be

controlled by proteins of two different phosphatase families, phosphoprotein phosphatases (PPP) and metal-dependent protein phosphatases (PPM), in a cell context or situation-dependent manner.

Very recently, a study on rat chondrocytes revealed that 4E-BP1's phosphorylation state can even contradict mTOR's activity. These cells were reported to respond with inhibition to fibroblasts growth factor (FGF), while most other cells proliferate. Ruoff et al. (2016) showed that FGF stimulates mTOR activity, but also dephosphorylates 4E-BP1, which is crucial for the behaviour of the cells and overrides the mTOR signal. Although the mechanism is not entirely clear yet, the findings indicate an involvement of PP2A in the regulation of 4E-BP1 under these conditions.

1.3   Role of 4E-BP in cancer

mTOR and 4E-BP1 have been studied intensively for their role in the development of cancer. The reason for this is that the mTOR inhibitor rapamycin was identified as a potent anti-cancer drug (Law, 2005). The rapamycin analogues everolimus and temsirolimus were successfully approved for anti-cancer treatment by the FDA (Battelli and Cho, 2011). The ability of the mTOR pathway to regulate growth and proliferation depending on extra- and intracellular growth signals makes it a very attractive key target for cancer treatment. Furthermore, many mTOR pathway proteins showed proto-oncogenic potential including mTOR itself. Over the years many examples and details about the role of 4E-BP1 and its regulating mTOR pathway in cancer have been elucidated.

It is already known that the PI3K/Akt pathway, which activates mTOR and inhibits 4E-BP1, is up-regulated in many different subtypes of cancer (Vivanco and Sawyers, 2002). For instance, the GTPase Ras, which binds and activates PI3K, is activated in approximately 30 % of all epithelial tumours (Downward, 2003). Furthermore, TSC1/2 loss of function mutations led to hamartomas development (Jones et al., 1999) and the mTOR activator Rheb was reported to be overactive in cancer cell lines (Im et al., 2002). Interestingly, S6K1 seems to be negligible for the oncogenic potential of the mTOR pathway (Hsieh et al., 2010; She et al., 2010). More important is the other downstream effector 4E-BP1, which acts as a tumour suppressor through the ability to stop the cell cycle in G1 phase and to block cell trans-

formation (Lynch et al., 2004). While 4E-BP1 controls cell proliferation, it was reported that it has no effect on cell growth (Dowling et al., 2010). The cell cycle progression block of 4E-BP1 is repealed when mTOR becomes active, which hyperphosphorylates 4E-BP1, increases the concentration of free eIF-4E and supports tumour progression (Avdulov et al., 2004; Qu et al., 2016). Recent findings revealed that mTOR downstream proteins with enhanced translation rate in prostate cancer are responsible for cell proliferation, metastasis and invasion. Experiments in mice showed a significant therapeutic benefit of the new mTOR ATP site inhibitor INK128 for prostate cancer metastasis, for which there is presently no cure (Hsieh et al., 2012). eIF-4E itself is also known for a while as a protein with proto-oncogenic potential as a protein, which is rate-limiting in cap-dependent translation (De Benedetti and Rhoads, 1990; Graff et al., 1995; Lazaris-Karatzas et al., 1990). The loss of cellular tumour antigen p53, a pro-apoptotic protein in cancer also promotes mTORC1 activity (Feng et al., 2005).

Surprisingly, over the recent years several studies described a non-canonical function of 4E-BP1 as a tumour promoting protein (reviewed by Musa et al. 2016; Qin et al. 2016; Wang et al. 2016a). This seems to be counterintuitive considering the function and regulation of 4E-BP1 as suppressor of cap-dependent translation. Nonetheless, several studies revealed 4E-BP1 overexpression in different cancers associated with poorer prognosis for patients (Chao et al., 2015; Karlsson et al., 2011, 2013; Ray et al., 2004), while degradation of 4E-BP1 had anti-cancer effects (Lai et al., 2013). It was suggested that certain subtypes of tumours may capture 4E-BP1 to benefit from its ability to resist stress. Invasive growing cancers are often cut off from nutrition and oxygen. Thus, 4E-BP1 and its upregulated cap-independent translated genes may promote survival under these conditions. It may be even possible that in the very same tumour subsets of cells down-regulate 4E-BP1 to grow exponentially, while other cells induce 4E-BP1 overexpression to survive an unfavourable environment (Braunstein et al., 2007). Several genes with important roles in tumourigenesis have been identified to be translated cap-independently (Walters and Thompson, 2016). These include the pro-apoptotic genes *APAF-1* (Coldwell et al., 2000) and *P53* (Hertz et al., 2013; Ray et al., 2006), but also the proto-oncogenes *XIAP* (Holcik et al., 1999; Saffran and Smiley, 2009) and *MYC* (Nanbru et al., 1997; Stoneley et al., 1998). The implications of 4E-BP1's multifunc-

tionality for future cancer treatment are currently under investigation.

1.4 Role of 4E-BP in neurodegenerative diseases

Aside from its importance for cell proliferation and protein synthesis, the TOR pathway is also crucial for the plasticity of the central nervous system (CNS). To establish long term memory it is necessary to create new synaptic connections, which requires specific protein synthesis (Kandel, 2001). However, inactivation of TOR and subsequent activation of 4E-BP blocks the essential protein synthesis and inhibits the formation of long term memories, as it was described for the sea slug *Aplysia californica* (Casadio et al., 1999). A further study showed that mTOR and 4E-BP1 are not only localised in the cell body, but also in dendrites to control neuronal plasticity (Tang et al., 2002). Translational inhibition impairs synaptic plasticity by inhibiting axonal pathfinding, which is crucial for the formation of new synapses as a study in *Xenopus* retinal cells showed (Campbell and Holt, 2001). All these data demonstrate how important the balance of 4E-BP1 and mTOR is for the correct function of the CNS and how easy a disorder may affect it. For this reason, it is no surprise that 4E-BP plays also a crucial role in neurologic diseases like Alzheimer's (AD) and Parkinson's disease (PD).

AD is a neurodegenerative disorder with associated dementia and other neuropsychological symptoms. Characteristic plaques of misfolded Amyloid β (Aβ) peptides accumulate in the brain tissue of patients as well as neurofibrillary tangles of hyperphosphorylated tau, a microtubules associated protein. Besides tau, hyperphosphorylated mTOR was also found in AD (Griffin et al., 2005). The subsequent inactivation of 4E-BP1 and activation of the positive mTOR effector S6K1 was associated with tau formation in these patients (An et al., 2003). Furthermore, the inhibition of mTOR reduces the Aβ level and improves dementia symptoms in mice (Spilman et al., 2010). It was suggested that the inhibition of mTOR leads to amelioration of AD phenotypes in mice by promoting overexpression of chaperones via 4E-BP1 activation (Pierce et al., 2013). On the other hand, it was speculated that the amyloid precursor protein (APP), which accumulates in Aβ sheets during AD is synthesised via cap-independent translation and thus promotion of cap-independent translation via 4E-BP1 activation may be counterproductive for AD (Beaudoin et al., 2008; Liu, 2015). Further data

emphasised the contradictory characteristics of the mTOR pathway in an AD background. Activation of mTOR and subsequent inhibition of 4E-BP1 can rescue cells exposed to Aβ (Shang et al., 2012), while blockage of mTOR may lead to neuronal atrophy in AD models (Chano et al., 2007). Contradictory effects of mTOR inhibition in neurodegenerative diseases can also be due to overlapping effects. As a key regulator of many cellular pathways, mTOR has also an effect on autophagy via inhibition of Ulk1 and Atg13, which initiate autophagy (Yang and Klionsky, 2010). Thus, mTOR inhibition causes upregulation of autophagy as well, a self-consuming mechanism involved in cell survival, preservation of cellular nutrient level under stress, intracellular organelle homeostasis and removal of toxic and aggregated proteins. Hence, it is important to notice that overlapping effects of 4E-BP/S6K and autophagy cannot be completely excluded in mTOR inhibition studies, which may explain different conclusions depending on the concrete experimental set-up.

PD is another neurodegenerative disease with characteristic motoric disorders like rigor and tremor. The primary neurons affected are dopaminergic neurons of substantia nigra, a brain region which is crucial for initiation and execution of voluntary movements. Patients show typical accumulations of α-synuclein in so called intracellular Lewy bodies. Although one study found some evidence that blocking the mTOR pathway leads to neuronal death and mTOR restoring may rescue them (Malagelada et al., 2006), a broad range of studies support the neuroprotective effect of active 4E-BP1 by mTOR inhibition. For instance, in transgenic mice it was shown that mTOR inhibition led to decreased α-synuclein accumulation and neuroprotection (Crews et al., 2010). Furthermore, the treatment with rapamycin and subsequent activation of the *Drosophila* 4E-BP, Thor, prevents loss of dopaminergic neurons in *Drosophila* PD models and ameliorates the mitochondrial defects in human cells of PD patients (Tain et al., 2009). Also, it has been elucidated that loss of the mitochondrial serine/threonine-protein kinase PINK1, which is linked to autosomal recessive PD, impairs dephosphorylation of 4E-BP1 and cap-independent protein translation after hypoxia and prevents upregulation of HIF-1α, a transcription factor which promotes cell viability upon hypoxia (Lin et al., 2014a). These data suggests that PINK1 is responsible for stress induced initiation of cap-independent translation and links it to 4E-BP1 directly for the first time. Even though PD is mostly sporadic, several genes

have been associated with the development of familial PD. Among them are the above mentioned kinase PINK1 and the E3 ubiquitin-protein ligase parkin, which act together in mitochondrial autophagy, α-synuclein and LRRK2 (Moore et al., 2005). Ottone et al. (2011) showed that eIF-4E and parkin interact and that diminution of eIF-4E suppresses many parkin mutant phenotypes. LRRK2 has been proposed to be an inactivator of 4E-BP1 and studies in *Drosophila* revealed that gain of function mutations with associated chronic phosphorylation of Thor destroyed dopaminergic neurons and reduced stress resistance in *Drosophila* (Imai et al., 2008). Altogether, protein translation in PD has received little attention, but its importance for the development of PD is increasing. Recently, Taymans et al. (2015) discussed the potential of protein translation deregulation as a game changer for PD pathogenesis and demanded more unbiased screening experiments to identify proteins with cellular protective potential in PD.

A common feature of neurodegenerative diseases is the intra- and extracellular aggregation of misfolded protein, e.g. α-synuclein in PD or tau in AD. Allard et al. (2013) found that inhibition of mTOR or eIF-4E is able to reduce the amount of accumulated prion proteins *in vitro*, which causes e.g. Creutzfeldt-Jakob Disease. These results indicate that 4E-BP1 is able to reverse the accumulation of proteins, which is a very prominent characteristic of neurodegenerative diseases and may have a positive impact on disease progression. However, it is important to keep in mind that several studies concluded the opposite effect of 4E-BP1 on neurodegeneration. As discussed above, Beaudoin et al. (2008) and Liu (2015) suggested that APP translation in AD may be promoted by 4E-BP1 activation, while Malagelada et al. (2006) found that mTOR inhibition deteriorated the phenotype of PD models. Thus, the underlying mechanisms of 4E-BP1's protective potential may be more complex than expected previously. This could point to a yet unknown effect of mTOR/4E-BP1 or emphasise that the rescuing potential of 4E-BP1 may be dosage dependent.

1.5 Role of 4E-BP in ageing

Ageing is a major contributor for the development of different diseases by the accumulation of inherited and acquired risk factors. In multicellular organisms, it includes distinct pathogenic events like higher mortality, loss of organ

function and higher susceptibility for neurodegenerative diseases. Previously harmless DNA mutations may lead to a pathological phenotype when other risk factors were acquired over time. Thus, a constant by-product of ageing is cellular stress and the ability to cope with it may determine how long and how healthy an organism can live. For this reason, the mTOR/4E-BP1 pathway was studied for a long time for its ability to protect cells from age related stressors.

A common way to extend lifespan in different species is dietary restriction, which must not be mistaken for malnutrition. TOR is an important regulator of cell response towards nutritions and its inhibition was consistently reported to be associated with life span extension in different species including *Drosophila* flies (Bjedov et al., 2010; Kapahi et al., 2004) and mice (Harrison et al., 2009; Miller et al., 2011). Furthermore, a study in yeast confirmed that dietary restriction could not prolong life span when *TOR* was knocked out (Kaeberlein et al., 2005). Both major TOR effectors S6K and 4E-BP were described to contribute to the life extending properties of TOR inhibition. In *Drosophila*, Thor loss reduced the life span extension by dietary restriction, while a constitutively active Thor was able to prolong life span even under rich nutrient conditions (Zid et al., 2009). The study by Zid et al. revealed also the upregulation of mitochondrial proteins involved in ATP generation by Thor upon dietary restriction. These data emphasise the involvement of the translational switch from cap-dependent to cap-independent translation as a crucial step to cope with age dependent cellular stress. Furthermore, Demontis and Perrimon (2010) found that constitutively active Thor preserved *Drosophila* muscle cells from accumulating aggregates of misfolded proteins during ageing and maintaining proteostasis. Additionally, the overexpression of Thor in muscle cells had also a systemic effect by decreasing the energetic demand of muscles, it changes the feeding behaviour and establishes a fasting-like nutrient intake, which slows the ageing of other organs, too. This study emphasises again the tissue specific effects of 4E-BP. The study was confirmed by Kapahi et al. (2004), who showed that dominant-negative forms of TOR or S6K in fat or muscle tissue are sufficient to trigger life span extension.

1.6   Quantitative proteomic studies *in vitro* and *in vivo*

Proteomic studies describe the investigation of all proteins in a cell, a cell compartment or an organism. The genome of an organism defines its basic proteome, but also short and long term environmental changes affect the proteomic composition and relative proportions of proteins. Proteomic studies also take posttranscriptional and posttranslational regulations into account as well as the protein turnover rate. It measures the end of the gene expression cascade, which is more closely related to the biological function than the transcriptome level. The challenges to characterise a proteome already begin with its definition. After the human genome was completely sequenced for the first time, we learned by subsequent studies that it consists of approximately 20,000 coding genes (Clamp et al., 2007). If one follows the traditional theory that one gene encodes for one protein, the human proteome would consist of 20,000 proteins. However, protein biosynthesis is regulated on many different levels, which complicates the estimation. Gene transcription depends very much on the cell type and environmental situation, which means that not all genes are transcribed in all cells at the same time. Splicing and post-translational modifications enhance complexity even further. For this study, the protein definition of the UniProt database was applied: One gene transcribes for one protein and alternative splice variants were only considered as a different protein, if there is a clear difference in sequence or function. Using this definition, approximately 10,000 proteins could be identified in a human cell line theoretically. This value represents a guidance value for a completely characterised proteome (Cox and Mann, 2011).

The breakthrough for proteomic investigations was the constant improvement of mass spectrometers. A mass spectrometer characterises charged ions of peptides or proteins by their mass to charge ratio (m/z). Current devices can measure mixes of several ten thousand ions in a single run with a precision <1 Da. Coupled with an *in silico* reference database, peptides and proteins can be identified with high accuracy. Typically, proteins of cells or organisms will be digested by an enzyme prior to mass spectrometry analyses, basically because of two reasons: the mass spectrometer are more sensitive for low molecular weight molecules and the digestion pro-

duces several peptides per protein. As only one or two peptides are sufficient to identify a protein, digestion increases the chance to identify a certain protein in a complex protein mix. This strategy of identifying proteins by their peptides is also known as "bottom-up" proteomic.

To quantify proteins, two basic strategies are currently possible in proteomic research: labelled or label-free quantification, in which the labelled option is clearly more sensitive. Among different label strategies, the stable isotope labelling (SILAC) is the most widely spread method, which was developed in 1999 by three different laboratories (Gygi et al., 1999; Oda et al., 1999; Pasa-Tolic et al., 1999). It requires the incorporation of amino acids with light (^{12}C, ^{14}N) or heavy isotopes (^{13}C, ^{15}N). When the samples are combined and analysed, peptides appear as pairs with a defined mass difference and their relative abundance difference can be determined. Samples for label-free quantification do not get combined prior to mass spectrometric analysis, but are analysed separately. Quantification is executed by the signal intensity of the same peptides in sample and control. This approach is robust enough for large ratio changes. In 2008, the first report of whole proteome quantification in yeast using SILAC was published (de Godoy et al., 2008). Since then, the technology was adapted and successfully applied in *Drosophila* (Sury et al., 2010), mice (Krüger et al., 2008) and further organisms (Fredens et al., 2011; Larance et al., 2011), which demonstrates that the technology is developed enough to perform high-throughput proteomics in complex *in vivo* models.

1.7 Aim of this thesis

During the last years, many different studies have revealed the impact of 4E-BP1 for cellular survival, life span enhancement and a broad range of disorders and diseases like cancer or neurologic disorders like AD or PD. Although the mechanism of 4E-BP1 activation by use of mTOR inhibitor rapamycin is already applied in practical treatment of patients to avoid organ rejection after transplantation, no 4E-BP1 manipulating drug with the potential to cure one of these neurologic disorders has been released yet. This makes it crucial to get a better idea of the 4E-BP1 pathway, in particular to understand how 4E-BP1/Thor is able to rescue the PD symptoms in cellular and *Drosophila* models (Tain et al., 2009). PD is an

upcoming challenge for an ageing society like in all countries of the Western world. Approximately 1 % of the elderly population is affected by this neurodegenerative disease, but no disease-modifying treatment is available yet.

One major reason for the insufficient understanding of the mTOR pathway is that the downstream effectors of 4E-BP1 and their impact for the effect of 4E-BP1 still remain unclear. During this study, I aimed to investigate the downstream mechanism of 4E-BP1 and assess the impact of its downstream effectors for cellular survival. The initial aim was to establish an inducible cell line of non-cancer origin expressing wildtype or constitutively active human 4E-BP1. Here, constitutively active 4E-BP1 carried two point mutations, which caused a replacement of threonine by alanine in positions 37 and 46 in order to stop the phosphorylation cascade at its beginning. Such a cell line had the potential to allow an observation of changes in the proteome upon 4E-BP1 overexpression and activation. It makes it possible to control 4E-BP1 expression precisely without affecting the upstream regulating mTOR kinase directly. This cellular model would be used for quantitative proteomic mass spectrometry analyses. With the described approach I aimed to reveal translationally upregulated proteins in response to 4E-BP1. Highly upregulated proteins should be selected subsequently and investigated as to whether these 4E-BP1 effectors are able to protect cells from stress.

To complement the *in vitro* analysis, I also aimed to study the downstream effectors of 4E-BP *in vivo*. The purpose was to find differences and similarities between up- and downregulated proteins upon 4E-BP overexpression in order to investigate the conservation of certain effectors with cellular protective potential. *Drosophila melanogaster* was chosen as the *in vivo* model in this study, because of the finding that overexpression of d4E-BP rescues the PD phenotype in fly models of this disease. As with the *in vitro* model, two transgenic *Drosophila* lines would be generated overexpressing wildtype or constitutively active d4E-BP, carrying the same Thr37/46 to alanine mutations as their *in vitro* counterparts. Both transgenic lines should be utilised for quantitative proteomic mass spectrometry experiments as an *in vivo* comparison to the *in vitro* results.

The investigation of the cellular protective mechanism of the protein 4E-BP1 may open a new door to a better understanding of a broad range

of diseases. Indeed, 4E-BP1 could be a general key target for outbreak and progress, but also treatment of different challenging diseases of our time. For example, many different studies have already revealed the importance of 4E-BP1 for initiation or prevention of cancer respectively. However, the mechanism behind it is still unknown and prevents physicians, researchers and pharmaceutical companies from finding new ways to treat patients. Knowledge about the key target is the first step for the development of powerful therapies.

Although rapamycin is already known for a long time, it cannot be used as a general medication to activate 4E-BP1, because of its immunosuppressive effect. The identification of a more specific downstream target of 4E-BP1 could help to find new drugs to activate these effectors. This study can contribute to reveal these effectors and to assess their importance for the protective effect of 4E-BP1 in living organisms.

Especially for patients of PD is it important to find new approaches to treat this disease. Despite long years of research, neither the mechanism of PD is completely understood nor a powerful cure developed. This study could reveal how 4E-BP1 contributes neuronal rescue from degeneration. The findings may contribute to extend our picture of PD, how it works and how it could be treated.

Chapter 2

Material and Methods

2.1 Cell culture techniques

2.1.1 Reagents and media

All media, reagents and mixes utilised in cell culturing are listed here. Reagents and chemicals were bought from Sigma-Aldrich, unless indicated otherwise. All media were sterile filtered using Stericup filters (#SCGPU05RE, Millipore) and stored at 4 °C.

1x PBS, pH 7.4
> 150 mM NaCl (#BP-358212, Fisher Scientific)
> 2.7 mM KCl (#P9541)
> 10 mM Na_2HPO_4 (#444425M, VWR)
> 1.8 mM KH_2PO_4 (#P0662)

Normal culture medium for HeLa cells
> 89 % MEM with HEPES and GlutaMAX (#42360-032, Gibco)
> 10 % FBS (#F4135)
> 1 % Penicillin-Streptomycin (#P0906)

Normal culture medium for HEK293, RPE1, HTC116 and MCF7 cells
> 89 % DMEM with nutrient mixture F-12 Ham (#8062)
> 10 % FBS (#F4135)
> 1 % Penicillin-Streptomycin (#P0906)

Normal culture medium for SH-SY5Y cells and fibroblasts
> 88 % DMEM with nutrient mixture F-12 Ham (#8062)
> 10 % FBS (#F4135)
> 1 % non-essential amino acids (#M7145)
> 1 % Penicillin-Streptomycin (#P0906)

Cell freezing media
 50 % FBS (#F4135)
 40 % Normal culture medium (see above)
 10 % DMSO (#276855)

Flp-In T-REx host cell medium
 90 % DMEM with nutrient mixture F-12 Ham (#8062)
 10 % FBS (#F4135)
 100 µg/ml Zeocin (#R250-01, Gibco)
 15 µg/ml Blasticidin (#BP2647-50, Fisher Scientific)

Flp-In T-REx expression cell medium
 90 % DMEM with nutrient mixture F-12 Ham (#8062)
 10 % tetracycline free FBS (#631106, Clontech)
 150 µg/ml Hygromycin B (#10687-010, Life technologies)
 15 µg/ml Blasticidin (#BP2647-50, Fisher Scientific)

Cell viability assay medium
 90 % DMEM/F12 medium, no phenol red (#21041, Gibco)
 10 % tetracycline free FBS (#631106, Clontech)

Normal culture medium for *Drosophila* S2R+ cells
 89 % Schneider's *Drosophila* medium with L-Glutamine (#21720-024, Gibco)
 10 % FBS (#F4135)
 1 % Penicillin-Streptomycin (#P0906)

2.1.2 Human cell lines

In order to overexpress 4E-BP1 and to investigate its behaviour, different human cell lines were screened: HeLa cells, derived from cervical cancer tissue, HCT116 cells, derived from colon cancer tissue and kindly gifted by Dr. Emma Bruce-Jones (RNAi facility, University of Sheffield), SH-SY5Y cells, derived from bone marrow tissue of a neuroblastoma patient, primary fibroblasts, RPE1 cells, derived from retinal pigmented epithelium and HEK293 cells, derived from human embryonic kidneys and kindly gifted by Prof. Elizabeth Smythe (University of Sheffield). MCF7 cells, which were used to assess downstream effects of 4E-BP1, derived from breast cancer tissue and were a kind gift from Dr. Irene Cantón (Centre for Stem Cell Biology, University of Sheffield).

2.1.2.1 Cell culture handling

All human cell lines were permanently maintained in an incubator at 37 °C with 95 % O_2 and 5 % CO_2 atmosphere. Cells were grown in T25 (#136196, Thermo Scientific) or T75 flasks (#658170, Greiner Bio One) and passaged in a 1:10 or 1:5 ratio all 3 - 5 days after they reached full confluence. Before passaging, cell media were pre-warmed to 37 °C to prevent temperature shock. Initially, existing media were aspirated and cells were washed with 1x PBS to remove serum traces. To detach cells from flask surface, 2.5 % trypsin (#15090-046, Gibco) diluted in 1x PBS was added till the bottom of the flask was fully covered and cells were returned to the incubator for 3 - 10 min. Subsequently, 10 ml (T75 flask) or 5 ml (T25 flask) media were added to stop trypsin and cells were resuspended by manually pipetting before passaging.

2.1.2.2 Plasmid transfection

Cells were seeded into 12 well plates (#150628, Thermo Scientific) and grown to full confluency for transfection. Plasmids were delivered to all human cells, but T-REx HEK293 cells, by Effectene transfection reagent (#301425, Qiagen) according to manufacturer's instructions. Cells were transfected with 600 ng pCMV vector DNA, carrying the gene of interest. The DNA was incubated at room temperature in 100 µl EC buffer together with 3.2 µl Enhancer for 5 min, which condenses DNA. Subsequently, 2.5 µl Effectene was added to the mix and incubated for further 8 min. The transfection mix was added to the cell media directly. Cells were used for experiments 48 h after transfection.

2.1.2.3 Generating Flp-In T-REx HEK293 Expression cell lines

The Flp-In T-REx system has been developed by Life Technologies and allows the generation of stable cell lines, in which overexpression of the gene of interest can be induced by adding tetracycline to the cell media. Flp-In T-REx HEK293 host cells were kindly gifted by Christopher Webster and Dr. Adrian Higginbottom (SITraN, University of Sheffield). These host cells carried a Flp Recombination Target (FRT) site, linked to a zeocin resistance gene, and a tetracycline repressor gene, linked to a blasticidin resistance gene, stably integrated into their genome (Fig. 2.1). Host cells

were maintained by blasticidin and zeocin in Flp-In T-REx host cell medium.
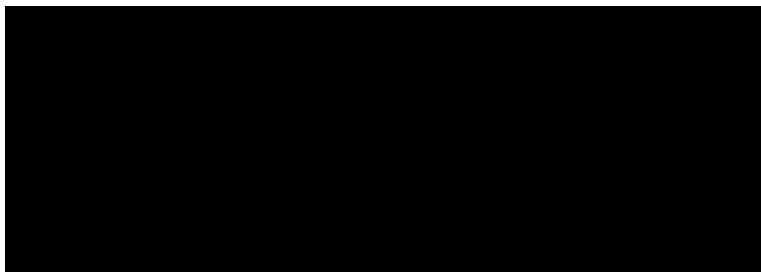
Figure 2.1: Structure of FRT and TetR gene in Flp-In T-REx host cells. The cells have a FRT site and a tetracycline repressor gene stably integrated into their genome, linked to zeocin and blasticidin resistance genes. Both genes are controlled by constitutively active promoters. Fig. from Flp-In T-REx Core Kit Manual, Life Technologies (2000).

To integrate *4E-BP1* stably in the cell genome at the FRT site, *4E-BP1* was cloned into pcDNA5/FRT/TO expression vectors (#K6500-01, Life Technologies) (see section 2.2 for details) and co-transfected with pOG44 vectors, encoding for Flp recombinase (Fig. 2.2).
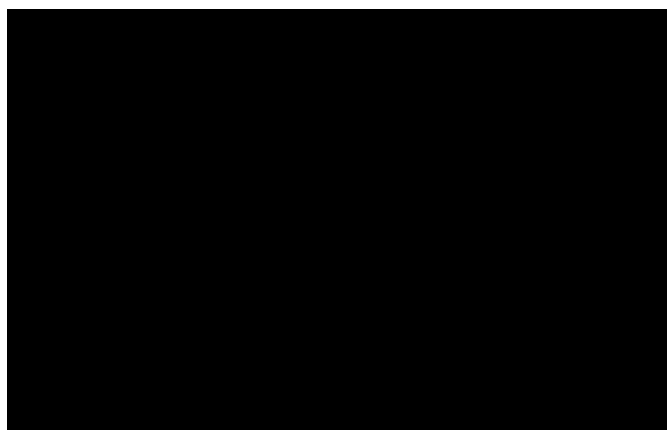
Figure 2.2: Transfection vectors to generate Flp-In T-REx expression cells. pcDNA5/FRT/TO vector carried the gene of interest flanked by its promoter P_{CMV}, the activity of which is dependent on the occupation of the following tetracycline binding site (2x $TetO_2$). The FRT site allowed homologous recombination with the corresponding site in T-REx HEK293 cells, mediated by Flipase (FLP) encoded on the pOG44 vector. Recombination success was monitored by acquired hygromycin resistance of cells. Fig. from Flp-In T-REx Core Kit Manual, Life Technologies (2000).

For transfection of T-REx HEK293 host cells, cells were grown in Petri dishes of 10 cm diameter (#430591, Corning). Just before transfection, cells were washed with 1x PBS and the medium replaced by 10 ml serum reduced medium Opti-MEM (#11058-021, Life technologies). 2.4 µg pcDNA/FRT/TO and 21.6 µg pOG44 vector DNA were incubated in 1.5 ml

Opti-MEM for 5 min as well as 60 µl Lipofectamine 2000 transfection reagent (#11668019, Life technologies) in a separate aliquot of equal Opti-MEM volume. Both aliquots were united and incubated for 20 min before transferring them to the cells. The pOG44 vector carried a gene encoding for the Flp recombinase, Flipase. It catalysed a site-specific homologous recombination between the FRT site in the cellular genome and the pcDNA/FRT/TO vector and integrates the *4E-BP1* transgene along with the tetracycline dependent promoter and a hygromycin B resistance gene, while this integration event destroys the zeocin resistance gene (Fig. 2.3). Transfected cells were maintained in the incubator for 4 h before replacing the media by antibiotic-free normal HEK293 cell media. 48 h later, cells were split in a ratio of 1:10 and passaged into ten new Petri dishes with Flp-In T-REx expression cell medium containing hygromycin B as a negative selector. All untransfected cells died due to hygromycin B within the following days, while positively transfected cells survived and formed colonies. The expression cell medium was replaced every other day. After 10 d, positive cell colonies were clearly definable. Twelve colonies per *4E-BP1* construct were isolated and detached from the Petri dish by local application of trypsin and transferred to a 24 well plate (#CLS3527, Sigma-Aldrich) for amplification. During the next passage, each colony was transferred into 4 wells on a 12 well plate. In three of these wells, cells were maintained in T-REx host cell medium for 10 d to check them on their zeocin sensitivity. When the recombination has taken place at the correct position on the FRT site, cells exhibited zeocin sensitivity, but hygromycin B resistance. Only when zeocin sensitivity was confirmed in all three replicates of one clone, this clone was amplified from the fourth well and maintained for further experiments. To induce overexpression of 4E-BP1 in T-REx HEK293 cell clones, cells were treated with 1 µg/ml tetracycline (#58346, Calbiochem) from 30 min to 48 h (Fig. 2.3).
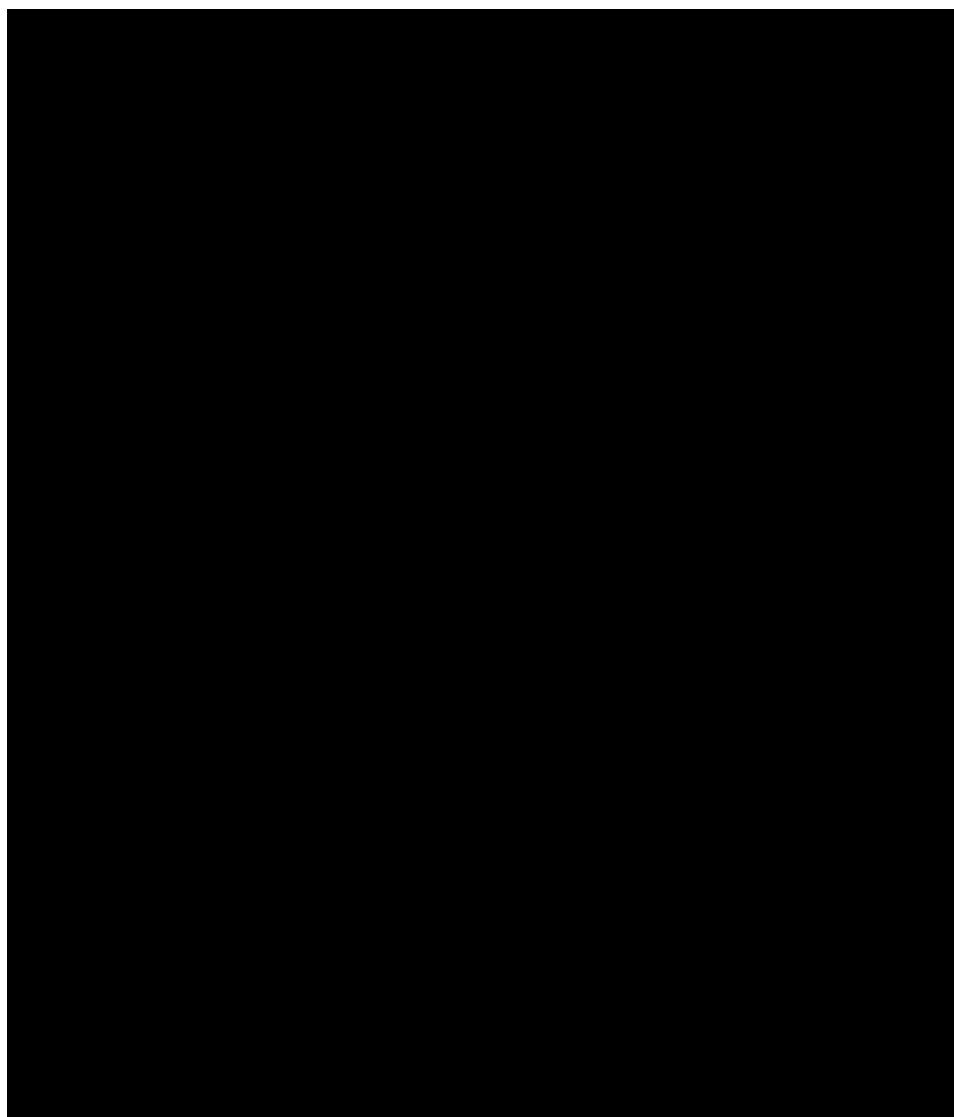
Figure 2.3: Process of GOI integration into the Flp-In T-REx host cell genome and transgene induction. The Flipase, encoded on the pOG44 vector, catalysed homologous recombination between the FRT sites in the genome and on the pcDNA5/FRT/TO vector and integrated the *4E-BP1* transgenes (GOI) along with the hygromycin B resistance gene into the genomic DNA, while it destroyed the zeocin resistance gene at the same time. The addition of tetracycline to the cell media induced transcription of the *4E-BP1* constructs. Fig. from Flp-In T-REx Core Kit Manual, Life Technologies (2000).

2.1.3 Cell viability assay

To assess the viability of T-REx HEK293 cell clones, two different assays were performed. One way to assess cell viability was to measure the total cellular ATP amount by utilising the CellTiter-Glo Luminescent Cell Via-

bility Assay by Promega (#G7571) according to manufacturer instructions. The assay determined the number of viable cells in culture based on quantity of ATP present. ATP, the molecular unit of intracellular energy transfer, is a nucleoside with three high-energy phosphate bonds, which are comparatively unstable. For this reason, cells have to recycle it permanently, which makes it one of the early indicators of apoptosis and necrosis. In the assay, ATP catalysed the oxygenation of luciferin to oxyluciferin upon light emission. This luminescence signal was detected.

Another way was the utilisation of Sigma-Aldrich's Cell Counting Kit - 8 (#96992) according to manufacturer instructions. It is a colorimetric assay for assessing cell metabolic activity. The detection reagent was reduced in the presence of cellular dehydrogenases to a water soluble formazan dye. The absorbance of the dye was detected at 460 nm.

20,000 cells per well were plated on 96 well plates with transparent bottom (#6005225, PerkinElmer), suspended in 80 µl cell viability assay medium. If viability assay was performed after RNA knockdown (see section 2.2.11) in a 384 well plates format (#6007460, PerkinElmer), 7000 cells were plated per well. 24 h later, cells were treated with 1 µg/ml tetracycline to induce 4E-BP1 overexpression or 1 µl medium as negative control. To stress cells, they were treated with different concentrations of paraquat (#36541, Sigma-Aldrich), rotenone (#R8875, Sigma-Aldrich), sodium azide (#S2002, Sigma-Aldrich) or mito-paraquat (generated by Thomas Bright, Murphy laboratory, MBU Cambridge) after further 24 h. Cell viability was assessed 24 - 96 h after toxification. Luminescence or absorbance was measured in the Varioskan Flash Multimode Reader (Thermo Scientific).

2.1.4   Cell culture of *Drosophila* cell lines and plasmid transfection

In order to investigate the functionality of plasmids, which were generated with the purpose of integration in *Drosophila* genome and overexpression of proteins *in vivo*, *Drosophila* S2R+ cells were grown and transfected. Cells were stored in an incubator at 25 °C and standard atmosphere. T75 and T25 flasks were used to amplify cells. All 3 - 4 days, S2R+ cell were passaged at a ratio of 1:10 or 1:5. For this purpose, cell media were replaced before cells were removed from the flask surface by cell scrapers (#541070, Starlab) and resuspended by manual pipetting before being passaged.

To transfect *Drosophila* S2R+ cells, they were seeded into 12 well plates and Effectene transfection reagent was used to deliver plasmids (see 2.1.2.2 for details). 300 ng DNA of the *FLAG-d4E-BP* transgenes in a pUAST.attB vector were combined with an equal amount of pCASPER-Actin-PolyA vector DNA in 75 µl EC buffer and along with 2.4 µl Enhancer per well. pCASPER-Actin-PolyA encodes for the GAL4 protein using the actin promoter. GAL4 binds the UAS enhancer on the pUAST.attB vector to induce transcription and overexpression of *FLAG-d4E-BP* constructs. After 5 min incubation, 6 µl Effectene was added and the whole mix incubated for 8 min before adding it to the cell media. Cells were harvested for analysis by immunoblotting three days after transfection.

2.1.5   Freezing cell cultures for long-term storage

To freeze human cell lines, cells were amplified in T75 flasks and detached from the flask surface by trypsin as described in section 2.1.2.1. After resuspending cells in 10 ml medium, they were transferred into 15 ml tubes (#352097, Corning) and centrifuged at 1,000 rpm for 5 min. The supernatant was aspirated and the cell pellets resuspended in 1 ml cell freezing medium. Subsequently, cultures were transferred into cryovials (#5000-0012, Nalgene) and placed at -80 °C for 24 h, while swimming in 2-propanol (#278475, Sigma-Aldrich), before being permanently stored in liquid nitrogen tanks. 2-propanol assured a slow and gentle freezing process, which reduced cell death by membrane rupture.

2.2   Molecular Biology

2.2.1   Reagents and media

All reagents and mixes utilised for molecular biology in this study are listed here. Reagents and chemicals were bought from Sigma-Aldrich, unless indicated otherwise.

1x TBE buffer, pH 8.3
  89 mM Tris base (#103156X, VWR)
  89 mM Boric Acid (#B7901)
  3 mM EDTA (#E6758)

6x DNA loading buffer
  30 % Glycerol (#G7757)

0.25 % Bromphenol Blue (#B0126)

Cloning and Sequencing PCR mix (per reaction)

10 µl Phusion HF buffer (#B0518S, NEB)

1 µl 10 µM dNTP mix (#N0447, NEB)

2 µl 10 µM forward Primer

2 µl 10 µM reverse Primer

5 µl DNA template

1 µl Phusion HF DNA polymerase (#M0530, NEB)

29 µl ddH$_2$O

Genotyping PCR mix (per reaction)

2 µl NH$_4$ reaction buffer (#BIO-21040, Bioline)

0.8 µl 50 mM MgCl$_2$ (#BIO-21040, Bioline)

1 µl 10 µM forward Primer

1 µl 10 µM reverse Primer

2 µl DNA template

0.2 µl BIOTAQ DNA polymerase (#BIO-21040, Bioline)

0.6 µl 10 µM dNTP mix (#N0447, NEB)

0.6 µl DMSO (#276855)

11.8 µl ddH$_2$O

Digestion mix (per reaction)

40 µl PCR product or 5 µg plasmid DNA

2 µl FastDigest Endonuclease 1

2 µl FastDigest Endonuclease 2

5 µl 10x FastDigest buffer

1 µl ddH$_2$O

Ligation mix (per 10 µl reaction)

75 ng PCR product

25 ng Plasmid

1 µl 10x reaction buffer (#M0202, NEB)

1 µl T4 DNA ligase (#M0202, NEB)

DNA extraction buffer

100 mM Tris-HCl, pH 9 (#T5941)

100 mM EDTA (#E6758)

1 % SDS (#862010)

100 µg/ml Ribonuclease A (#R4875)

2.2.2 Primers

All primers used for PCR or qRT-PCR in this project were bought from Sigma-Aldrich and are listed below. Primers for qRT-PCR were designed

with ProbeFinder (v. 2.49, Roche) and were always intron spanning to avoid biasing effects with genomic DNA.

Name	Orientation	Length	Tm in °C	Sequence (5'-3')	Application
h4E-BP1	forward	33	68	GCGCAAGCTTGGGATGTCCGGGGGCAGCAGCTG	PCR
h4E-BP1	reverse	33	68	GCGCCTCGAGCCCCCTAGGGCGAAGGTGGCTTT	PCR
CMV	forward	21	52	CGCAAATGGGCGGTAGGCGTG	PCR
BGH	reverse	18	52	TAGAAGGCACAGTCGAGG	PCR
FLAG-d4E-BP	forward	55	58	GCGCGAATTCATGGATTACAAGGATGACGATGACAAGACCATGTCCGCTTCACCC	PCR
Kozak-FLAG-d4E-BP	forward	33	65	GCGCGAATTCCAAAATGGATTACAAGGATGACG	PCR
-2nd start-codon-d4E-BP	forward	55	58	GCGCGAATTCATGGATTACAAGGATGACGATGACAAGACCTCCGCTTCACCCACC	PCR
pAT322	reverse	23	58	AAATCTCTGTAGGTAGTTTGTCC	PCR
pKS69	reverse	26	58	GCGCTCTAGACTACAGATCCAGTTGG	PCR
pUAST	forward	22	65	GCAACTACTGAAATCTGCCAAG	PCR
pUAST	reverse	22	65	CACACCACAGAAGTAAGGTTCC	PCR
ext-Thor	forward	20	63	GCGAGAAGAGAGCGAGAGAG	PCR
ext-Thor	reverse	20	63	GACCACAAGGGATCGGTCTA	PCR
int-Thor	forward	20	63	AAGTTCCTTCCGGAAAGTGG	PCR
int-Thor	reverse	20	63	GTGCTCGGGATTATCTTCCA	PCR
q-d4E-BP	forward	18	60	CCAGATGCCCGAGGTGTA	qRT-PCR
q-d4E-BP	reverse	21	60	AGCCCGCTCGTAGATAAGTTT	qRT-PCR
18S	forward	27	60	TCTAGCAATATGAGATTGAGCAATAAG	qRT-PCR
18S	reverse	27	60	AATACACGTTGATACTTTCATTGTAGC	qRT-PCR
ATPV0A2	forward	21	60	TCCCAGCCAGTAAAACAAGTG	qRT-PCR
ATPV0A2	reverse	20	60	GTGACAACCAGCAGCACTCT	qRT-PCR
CYR61	forward	18	60	AGTGCCGCCTTGTGAAAG	qRT-PCR
CYR61	reverse	20	60	TGGTCTTGCTGCATTTCTTG	qRT-PCR

Name	Orien-tation	Length	Tm in °C	Sequence (5'-3')	Appli-cation
DHCR24	forward	19	60	CTACTACCACCGCCACACG	qRT-PCR
DHCR24	reverse	20	60	GTTGTTGCCAAAGGGGATAA	qRT-PCR
FHL2	forward	18	60	AGGAGAGGGGAGCAGAGC	qRT-PCR
FHL2	reverse	20	60	GCCAAAGAGAGATTCGTTGC	qRT-PCR
FTL	forward	18	60	GCTGAACCAGGCCCTTTT	qRT-PCR
FTL	reverse	21	60	TCCAGGAAGTCACAGAGATGG	qRT-PCR
GSTM3	forward	20	60	CCAATGGCTGGATGTGAAAT	qRT-PCR
GSTM3	reverse	19	60	TCCAGGAGGTAGGGCAGAT	qRT-PCR
HADHB	forward	20	60	ACACTGTCACCATGGCTTGT	qRT-PCR
HADHB	reverse	19	60	CTGGCCAGAAGCAATCAAG	qRT-PCR
HMOX1	forward	21	60	CAGTCAGGCAGAGGGTGATAG	qRT-PCR
HMOX1	reverse	20	60	AGCTCCTGCAACTCCTCAAA	qRT-PCR
HSPA13	forward	20	60	GGCAAGATTTTTACCGCAGA	qRT-PCR
HSPA13	reverse	23	60	CAGAAAACTCAACCATTCCATTT	qRT-PCR
MYOM1	forward	22	60	TTCCCAGGATTCAGAAGCTATT	qRT-PCR
MYOM1	reverse	18	60	CAGTGCGGGACACACATC	qRT-PCR
PC1	forward	23	60	GCACTACTTCATCGAGGTCAACT	qRT-PCR
PC1	reverse	19	60	CGTGGATCTGAGCATGGAC	qRT-PCR
PPT1	forward	20	60	GCAGCAAGGCTACAATGCTA	qRT-PCR
PPT1	reverse	19	60	AGGGCATCTCTGAGCCACT	qRT-PCR
SERPINB6	forward	25	60	GAAAGTCTTGTGATTTCCTCTCAT	qRT-PCR
SERPINB6	reverse	20	60	CTACGGCGCTGATAAAGTCA	qRT-PCR
TIA1	forward	18	60	AGGGAGCTGGACCTGGAG	qRT-PCR
TIA1	reverse	21	60	TCTGGAAAGGTTACCGACGTA	qRT-PCR
TOMM40L	forward	20	60	CGAGCTAAGGCTGTCTTCCA	qRT-PCR
TOMM40L	reverse	20	60	CGATACTCGCCATCAAACTG	qRT-PCR
GAPDH	forward	20	60	TCGCTCTCTGCTCCTCCTGTTC	qRT-PCR
GAPDH	reverse	20	60	CGACCAAATCCGTTGACTCCGACC	qRT-PCR

2.2.3 siRNAs utilised

All siRNAs utilised in this project are listed below and were purchased from the RNAi facility, University of Sheffield. Non-targeting control siRNAs 1, 2 and 3 were ordered from Dharmacon (#D-001810-01-20, #D-001810-02-20, #D-001810-03-20).

siRNA target mRNA	siRNA sequences (5'-3')
ATP6V0A2	GUAGAGAAAUGGCGUGUGA
	GAACAAAUUCUACGUUGGU
	GAACCGGAGUGGCUACACA
	GAAUGACAGCGUCGUUAGA
CYR61	GGGCAGACCCUGUGAAUAU
	GGCCAGAAAUGUAUUGUUC
	GGUCAAAGUUACCGGGCAG
	GCAGCAAGACCAAGAAAUC
DHCR24	CAACACAUCUGCACUGCUU
	GAAAUGAGGCAGAGCUCUA
	GGAGUACAUUCCCUUGAGA
	CAUCAUCCCUGCCAAGAAG
FHL2	GAAACUCACUGGUGGACAA
	GAACGGCAGUGGCAUAACG
	GCAGUGCGUUCAGUGCAAA
	GCGAUGACUUUGCCUACUG
FTL	GCGAGUAUCUCUUCGAAAG
	UCAAGAAGCCAGCUGAAGA
	GGGCGAGUAUCUCUUCGAA
	AGACUCACUUCCUAGAUGA
GSTM3	GGGAAAUUCUCAUGGUUUG
	UUACAGCUCUGACCACGAA
	CAACAUGUGUGGUGAGACU
	CAACAAGCCUGUAUGCUGA
HADHB	GAGCAGCGCUUACGGGUUU
	GCAGGGCCAUGCUAUGAUA
	CAACAUAUGCUACUCCAAA
	GGAUUGACCAUGAAUGAUA
HMOX1	GGCAGAGGGUGAUAGAAGA
	ACACUCAGCUUUCUGGUGG
	AGAGAAUGCUGAGUUCAUG
	GAGGAGAUUGAGCGCAACA
HSPA13	GGUAAUAAAUGAACCCACA
	UAUGUUGGCUCUCGACUAU
	GCAUAAGCUGCAUACGUAA
	AGUGAUUGGUAUUGAUCUU
MYOM1	GAAACAAGGUCCUCACUUU
	GAUAUCACCUGUCUUGAAA
	GGACUCCGGUCACUGGUUA
	CCAAAGAGCUGGUCGGGUA
PC	GAAAGCAGAUGAAGCCUAU
	GAGCUGAUGUGGUGGAUGU

siRNA target mRNA	siRNA sequences (5'-3')
	GGAUAAUGCUUCCGCCUUC
	UCUCUGAGCGAGCGGACUU
PPT1	GGAGACAACUAACUAAAGU
	GAAGUAGCACCCAAAUUAA
	GAGAUCAACCCACAUUAGA
	AGAAAAUGUAGGCGCGAAA
SERPINB6	CAGCAAGACCAACGGGAUU
	AGAAAGAACUCACUUACGA
	GGGUAAAGACAACUCGAAG
	UCAUCAUGCUUCCGGACGA
TIA1	GACGGAAGAUAAUGGGUAA
	GAACAACUAAUGCGUCAGA
	GUACAUAUGAGUCAAAUAC
	UAUGAUAAAUCCCGUGCAA
TOMM40L	GACACAACAUUCUCCUUUG
	GAGGCUUGGUGGAUAGUAA
	GGAGAUGACUACACAGCCA
	CCAGGUGGCGCACACUAUA

2.2.4   Plasmids utilised

All plasmids utilised in this project are listed below.

Transgene	Vector	Species	Source
4E-BP1[WT]	pCMV6-XL5	Human	Elena Ziviani
4E-BP1[TA]	pCMV6-XL5	Human	Elena Ziviani
FLP	pOG44	Human	Invitrogen (#V6005-20)
d4E-BP[WT]	pAT322	*Drosophila*	Aurelio Teleman, DKFZ Heidelberg, Germany
d4E-BP[TA]	pAT324	*Drosophila*	Aurelio Teleman, DKFZ Heidelberg, Germany
Actin-GAL4	pCASPER-Actin-PolyA	*Drosophila*	David Strutt, University of Sheffield

2.2.5   Polymerase chain reaction (PCR)

PCR was performed to either amplify plasmid DNA sequences for cloning into new vectors, DNA sequencing or to genotype transformed *E. coli* bacteria. The PCR program for the Eppendorf Mastercycler Personal is described below. The annealing temperature (Tm) is dependent on the used primer pair (see section 2.2.2) and the extension time varied depending on the length of the PCR product. For cloning and sequencing PCR reactions, a Phusion HF DNA polymerase with a proofreading function was used to

avoid point mutations, while genotyping PCR reactions required a simple BIOTAQ polymerase without proofreading function (see section 2.2.1 for details).

After the PCR run, the PCR products were loaded on 1 % agarose gels, composed of either UltraPure Agarose (#16500, Life technologies) for cloning and sequencing PCRs or standard agarose (#BIO-41025, Bioline) for genotyping PCRs with 0.5 µg/ml ethidium bromide (#E8751, Sigma-Aldrich) and dissolved in 1x TBE buffer. The gel floated in 1x TBE buffer within the gel tray. Gels ran at 120 V for 30 min to separate PCR products of different sizes. The PCR products were analysed under UV light. As a size reference, 5 µl HyperLadder 1 kb (#BIO-33053, Bioline) were loaded on the gel and ran along with the PCR products.

Step	Name	Temperature in °C	Time in s
1	Initialisation	98	300
2	Denaturation	98	10
3	Annealing	Different	30
4	Extension	72	15 - 60
5	Repeat steps 2 - 4 (30x)		
6	Final extension	72	300
7	End	4	∞

2.2.6 Gel purification and vector integration of PCR products

After cloning and sequencing PCRs, products were cut out of agarose gels and purified using the QIAquick Gel Extraction Kit (#28706, Qiagen) according to manufacturer instructions to clean up specific PCR products of a distinct size. For sequencing, purified PCR products were sent to the Core Genomic Facility at the Medical School of the University of Sheffield.

To integrate PCR products into a new vector after clean-up, the products and the convenient vector were digested with the same two sequence specific endonucleases to produce specific sticky ends, which were used to ligate the product into the vector in the correct orientation. To achieve this, vector and PCR products have to be designed to contain the appropriate endonuclease recognition sequences. Digestion was performed at 37 °C for 15 min with the digestion mix listed in section 2.2.1. The used endonucleases *Eco*RI (#FD0274), *Hind*III (#FD0504), *Xho*I (#FD0694) or *Xba*I (#FD0684) were all purchased from Thermo Scientific. Subsequently, the digestion products were cleaned up again, either by gel purification as de-

scribed above if waste DNA exceeded 100bp or by filter purification. In the latter case, equipment from the above mentioned gel extraction kit was used. Digestion product were diluted by 250 µl PB buffer and loaded in a filter tube, which was centrifuged for 30 s at 13,000 rpm and the flow through discarded. Filters were washed with 750 µl PE buffer before the clean digestion product was eluted with 30 µl ddH$_2$O. To complete integration, the digested PCR products were ligated into the vector with the ligation mix (see section 2.2.1) at 16 °C for 24 h.

2.2.7 Transformation

Plasmids were amplified in high efficient 10-β competent *E. coli* bacteria (#C3019H, NEB) for later applications. To transform bacteria with plasmids, 50 µl *E. coli* were defrosted on ice for 10 min and the whole ligation mix (see section 2.2.1) was added to the bacteria after integration and maintained on ice for 30 min. Bacteria were heat shocked at 42 °C for 30 s to increase incorporation of plasmids and incubated on ice for further 5 min. Subsequently, bacteria were suspended in 950 µl SOC medium (#S1797, Sigma-Aldrich) and placed at 37 °C for 1 h while shaking at 300 rpm, before 100 µl of the transformation mix was spread on a 2 % LB agar plate (#A1296, Sigma-Aldrich) containing 100 µg/ml ampicillin (#A0166, Sigma-Aldrich) to select positively transformed bacteria. The bacteria were grown at 37 °C for 16 h and single colonies were isolated subsequently.

2.2.8 Plasmid preparation

Following plasmid transformation of *E. coli* bacteria, ten single colonies were picked with pipette tips, transferred to a master LB agar plate and subsequent tip stirring in 13.8 µl ddH$_2$O, which was used to confirm successful integration by PCR (see section 2.2.5). One positively transformed colony was picked from the master agar plate and amplified in the appropriate volume of 2 % LB Broth medium (Sigma-Aldrich) at 37 °C. Plasmids from *E.coli* grown in small volumes till 5 ml were isolated using the QIAprep Spin Miniprep Kit (#27106, Qiagen), while larger volumes till 100 ml required the HiSpeed Plasmid Midi Kit (#12643, Qiagen). Manufacturer's instructions were followed in both cases. Plasmid concentrations were measured with the NanoDrop spectrophotometer 1000 (Thermo Scientific).

2.2.9 Quantitative real-time PCR (qRT-PCR)

The RNeasy Mini Kit (#74106, Qiagen) was used, according to manufacturer instructions, to extract mRNA from 3 - 5 pooled individual *Drosophila* flies per genotype or cells grown to full confluence on 24 well plates.

To quantify the relative amount of specific mRNAs, qRT-PCR was performed. In preparation, 1 µg total RNA per sample were transcribed into cDNA using the ProtoScript First Strand cDNA Synthesis Kit (#E6300, NEB) with random primer mix according to manufacturer's instructions.

For quantification, the signal intensity of mRNAs in qRT-PCR were normalised against a reference gene. In this study *Drosophila* 18S rRNA, part of the ribosomes, or human *Glyceraldehyde 3-phosphate dehydrogenase (GAPDH)* were used as references. qRT-PCR was performed on Green/White Hard-Shell 96-well PCR plates (#HSP9645, Bio Rad) with a reaction volume of 10 µl per well. The reaction mix consisted of 1 µl cDNA, 5 µl iQ Sybr Green Supermix (#1708880, Bio Rad), 0.6 µl 5 µM forward and reverse primers (see section 2.2.2) and 2.8 µl ultra pure water (#W3500, Sigma-Aldrich). Plates were sealed with Microseal B seals (#MSB1001, Bio Rad), centrifuged briefly and loaded into the CFX 96 Touch Real-Time PCR Detection System (Bio Rad). All samples were assayed in triplicates and the average value was taken for subsequent analyses.

During the qRT-PCR run, Sybr Green dye binds cDNA and the resulting fluorescent complex emits green light ($\lambda_{\mathrm{max}} = 520$ nm) after excitation with blue light ($\lambda_{\mathrm{max}} = 497$ nm). The emitted light increases proportional to cDNA, while it undergoes multiplication. When all dye is bound to cDNA, the fluorescence reaches a threshold level. Comparing the number of PCR cycles, described as threshold cycle C_{T}, which are necessary to reach this threshold level allows the calculation of relative expression ratios between samples.

The qRT-PCR program used to measure C_{T} values of multiple samples is listed below. The melt curve measurements at the end of the qRT-PCR cycle were necessary to gain information on the specificity of amplification. Only one peak should have been detectable, otherwise this may indicate non-specific primer binding, primer dimers formation or contaminations with other DNAs or mRNAs.

Step	Name	Temperature in °C	Time in s	
1	Initialisation	95	180	
2	Denaturation	95	30	
3	Annealing	60	30	
4	Extension	72	30	Real time measurement
5	Repeat steps 2 - 4 (40x)			
6		95	30	
7	Melt curve analysis	60	30	
8		55	10	Melt curve measurement
9	Increase step 8 by 1°C until 95°C is reached			

The described method of Livak and Schmittgen (2001) was used to calculate the relative fold change of expression between different samples. The average threshold cycle value of the gene of interest ($C_{T(GOI)}$) was normalised to the average threshold cycle value of the reference genes 18S or *GAPDH* ($C_{T(Ref)}$) and the resulting ΔC_T was calculated:

$$\Delta C_T = C_{T(GOI)} - C_{T(Ref)}$$

Once the samples were normalised to their reference genes, the experimental samples (e.g. d4E-BP overexpressing *Drosophila*) must be normalised to a control sample (e.g. wildtype *Drosophila*). The resulting $\Delta\Delta C_T$ was calculated:

$$\Delta\Delta C_T = C_{T(Experimental\ sample)} - \Delta C_{T(Control\ sample)}$$

Finally, to produce a normalised expression ratio between experimental and control samples, $2^{-\Delta\Delta CT}$ is calculated for each value. Here, the control sample is equal to 1, with experimental samples representing relative expression levels.

To evaluate the efficiency of qRT-PCR primers, cDNA dilution series were produced and the C_T values measured with constant primer concentrations. The data points were fitted to decadic logarithmic curve and the primer efficiency (E) calculated based on the slope of the curve (S):

$$E = (10^{\frac{-1}{S}} - 1) \times\ 100$$

2.2.10 Extraction of DNA from *Drosophila* for PCR

To extract DNA from *Drosophila*, 2 - 10 individual flies of the same genotype were pooled together and homogenised in 100 µl DNA extraction buffer (see

2.2.1) and incubated for 30 min at 70 °C to degrade RNA. The degradation was stopped by adding 22.4 µl 5 M potassium acetate (#P171-500, Fisher Scientific) and incubating the samples on ice for further 30 min. Subsequently, the samples were centrifuged at 14,000 rpm for 15 min to remove tissue debris and the supernatant was transferred to a new tube, mixed with phenol-chloroform (#17908, Fisher Scientific) in a ratio of 1:1 (v/v) and centrifuged again for 10 min. The aqueous phase was collected, mixed with chloroform 1:1 and centrifuged again. After this step, the aqueous phase was mixed with 2-propanol (#A416-4, Fisher Scientific) in a ratio of 1:0.5 and centrifuged for 10 min to precipitate DNA. The supernatant was discarded and the pellet washed with 150 µl 70 % ethanol (#BP28184, Fisher Scientific). The pellet was dried on air and resuspended in 10 µl ddH$_2$O.

2.2.11 RNA knockdown

In order to knockdown RNAs of specific genes, cells were transfected with small interfering RNAs (siRNA). siRNA are synthetic double-stranded RNAs, which act like artificial micro RNAs (miRNAs). They bind complementary mRNAs and prevent their translation. When siRNAs enter the cell, they bind to the protein complex Dicer, which cuts siRNAs into smaller parts. One strand of the fragmented siRNA is taken up by the RNA-induced Silencing Complex (RISC). The siRNA sequences guide RISC to specific mRNA targets, which leads to their degradation and to gene silencing.

5 µl 150 nM siRNA (see 2.2.3) were incubated with 5 µl transfection reagent 1.2 % Dharmafect 1 (#T-2001-01, GE Healthcare Dharmacon) in phenol red free DMEM/F12 medium (#21041, Gibco) on 384 well plates (#6007460, PerkinElmer) for 30 min at room temperature. Dharmafect formed vesicle complexes with siRNAs to deliver them to the cells. After incubation, 7000 cells per well were plated in 35 µl Cell viability assay medium as described in 2.1.3. Cells were incubated with siRNA complexes for further 30 min at room temperature, before they were moved to 37 °C incubators.

If cells were transfected with green fluorescent oligonucleotides siGLO (#D-001630-01, GE Healthcare Dharmacon) to assess the siRNA transfection protocol, cells were fixed 48 h after transfection with 50 µl 4 % PFA (#P6148, Sigma-Aldrich) in 1x PBS per well for 15 min. The PFA solution

contained also 2 µg/ml Hoechst 33342 dye (#4082S, Cell Signaling) to stain cell nuclei. Fixed cells were washed three times with 1x PBS before analysed in an ImageXpress Micro system (Molecular Devices).

2.3 Immunoblot

2.3.1 Reagents and media

All media, reagents and mixes utilised in this study are listed here. Reagents and chemicals were bought from Sigma-Aldrich, unless indicated otherwise. RIPA buffer was sterile filtered using Stericup filters (#SCGPU05RE, Millipore) and stored at 4 °C.

RIPA buffer (sterile filtered)
    50 mM Tris-HCl pH 7.5 (#T5941)
    150 mM NaCl (#BP-358212, Fisher Scientific)

Cell Lysis buffer
    88.4 % RIPA buffer
    1 % Triton X-100 (#T9284)
    10 % Glycerol (#G7757)
    2 mM EGTA (#E8145)
    1 mM MgCl$_2$ (#M8266)
    50 µM MG-132 (#M8699)
    1x cOmpmplete Mini, protease inhibitor tablet (#11836170001, Roche)
    10 mM N-Ethylmaleimide (#E3876)

Fly Lysis buffer
    20 mM HEPES pH 7.6
    350 mM NaCl
    20 % Glycerol (#G7757)
    1 % NP-40 (#ab142227, Abcam)
    0.5 mM EDTA (#E6758)
    0.1 mM EGTA (#E8145)
    1 mM MgCl$_2$ (#M8266)
    1x cOmpmplete Mini, protease inhibitor tablet (#11836170001, Roche)
    1x PhosSTOP, phosphatase inhibitor tablet (#04906845001, Roche)

4x SDS Sample buffer
    240 mM Tris-HCl pH 6.8 (#T5941)
    8 % SDS (#862010)
    40 % Glycerol (#G7757)
    1 % β-Mercaptoethanol (#M6250)
    0.008 % Bromphenol Blue (#B0126)

2.3.2 Antibodies

All antibodies used in this study were diluted in 1x PBST with 5 % milk powder.

Antibody type	Name	Source	Product code	Dilution	Host animal
Primary	Actin	Millipore	MAB1501	1:10,000	Mouse
Primary	4E-BP1	Cell Signaling	9452	1:1,000	Rabbit
Primary	Phospho-4E-BP1 (Thr37/46)	Cell Signaling	9459	1:1,000	Rabbit
Primary	Non-phospho-4E-BP1 (Thr46) (87D12)	Cell Signaling	4923	1:1,000	Rabbit
Primary	TFAM	Cell Signaling	7495	1:1,000	Rabbit
Primary	HSP90	Enzo Life Sciences	ADI-SPA-846	1:1,000	Rabbit
Primary	DYKDDDDK-Tag (FLAG)	Cell Signaling	2368	1:1,000	Rabbit
Secondary	HRP-conjugate Anti-Mouse	Abcam	ab6789	1:5,000	Goat
Secondary	HRP-conjugate Anti-Rabbit	Molecular Probes	G21234	1:5,000	Goat

2.3.3 Cell lysis

Cells were seeded into 12 well microtiter plates (#CLS3513, Corning) and lysed after grown to full confluence. In preparation of cell lysis, the media was replaced by 100 µl Cell Lysis buffer (see section 2.3.1). Cells were dislodged from the surface by a pipette tip and repeated pipetting. The harvested cells were transferred to microcentrifuge tubes and put on ice instantly. To store lysates, they were frozen down at -20 °C.

2.3.4 Fly lysis

Four to ten individual flies of the same genotype were anaesthetised with CO_2 and transferred to 1.5 ml microcentrifuge tubes filled with 150 µl Fly Lysis buffer. Flies were squished by mechanical force till all flies were visibly disrupted and put on ice immediately. Tubes were centrifuged at 4000 rpm for 7 min to remove tissue debris and supernatants were transferred to fresh tubes. To store lysates, they were frozen down at -20 °C.

2.3.5   Protein quantification

To quantify proteins of lysed cells or flies, Bradford assays were performed. In preparation, Bradford reagent (#B6916, Sigma-Aldrich) was diluted with ddH$_2$O at a 1:1 ratio. 1 µl of the lysate was added to 1 ml of diluted Bradford reagent and incubated at room temperature for 30 min. To measure the samples, they were transferred into cuvettes (#67.742, Sarstedt) and analysed in a BioPhotometer (Eppendorf) at 595 nm.

2.3.6   SDS-PAGE and membrane transfer

To prepare the cell and fly lysates for gel electrophoresis, 50 µg samples with 1x SDS Sample Buffer (see section 2.3.1) were boiled at 95 °C for 5 min to remove secondary, tertiary and quaternary protein structures. Subsequently, samples were centrifuged briefly before loaded onto polyacrylamide gels.

Polyacrylamide gels were hand-cast to the appropriate concentration using a Bio Rad Mini-PROTEAN Tetra Handcast System (#1658006FC) to manufacturer instructions. Gels were mounted in electrophoresis chambers, which were filled with 1x Tris/Glycine/SDS running buffer (#1610772EDU, Bio Rad). Additional to the samples, 5 µl of Precision Plus Protein Standard All Blue (#1610373, Bio Rad) was loaded onto a separate lane to analyse the molecular weights of proteins. Gels run at 150 V through the stacking gel, which was increased to 180 V while running the protein mix through the resolving gel.

In order to immobilise proteins, they were transferred onto PVDF membranes (#1620177, Bio Rad). For this purpose, gels were removed from electrophoresis chambers and transferred to a transfer cassette bathed in 1x Tris/Glycine transfer buffer (#1610771EDU, Bio Rad) containing 20 % or 40 % methanol (#10499560, Fisher Scientific) when transferring fly proteins. Inside the cassette, a PVDF membrane was placed on top of the gel. The membrane was activated before by short incubation in pure methanol. On top and bottom of membrane and gel, both were cased by two layers of chromatography paper (#WHA3001672, Whatman) on each side, followed by outer fibre pads. This pack made sure that the gel was maintained in a close and permanent contact to the membrane for an efficient transfer. The transfer cassette was placed in the transfer chamber together with an ice block. The chamber was filled with transfer buffer completely. The transfer

was conducted at 200 V for 60 min for proteins smaller than 50 kDa or at 300 V for 90 min for heavier proteins.

After completion of protein transfer, membranes were bathed in 1x PBST (1x PBS (see section 2.1.1) with 0.2 % Tween 20 (#BP337, Fisher Scientific)) with 5 % milk powder (Premier Foods) for 1 h at room temperature to saturate unspecific protein bindings. Before usage, milk was centrifuged at 4000 rpm for 20 min to remove undissolved powder conglomerates. Subsequently, membranes were incubated with primary antibodies from 1 h to overnight at room temperature or at 5 °C. For this process, membranes were either sealed in plastic bags or put in 50 ml falcon tubes. Membranes were rocked the whole time to guarantee an even antibody distribution. If different primary antibodies were applied to the membranes, they were cut after protein transfer and treated with different antibodies separately. Subsequently, membranes were washed with 1x PBST while shaking vigorously for 3x 10 min. The secondary HRP-conjugated antibodies were applied to membranes for 45 min while rocking them at room temperature. Following further 3x 10 min washing steps, membranes were exposed using either Enhanced Chemiluminescence Western Blotting Detection Reagent or Enhanced Chemiluminescence Prime Western Blotting Detection Reagent (#RPN2106 and #RPN2232, Amersham). Here, membranes were incubated between 1 and 3 min before exposure to light-sensitive photographic films (#28906835, Amersham) for 1 s to 1 h depending on the signal intensity. Chemiluminescence is initiated when the HRP enzyme oxidises the chemiluminescent substrate luminol with hydrogen peroxide, which causes light emission. As HRP is the limiting factor in this experimental set-up, light emission is proportional to the enzyme present, which gives information about the amount of detected protein. An automatic film developer was used to develop exposed films.

2.3.7 Data analyses

Developed films were scanned using the CanoScan Toolbox X (Canon). Scanned lanes were straightened using the 'Straighten' tool of ImageJ (v1.46r, Rasband, National Institute of Health, USA). Quantification of immunoblots was also performed with ImageJ using the histogram analyses of brightness of individual bands. Brightness and contrast was adjusted using Adobe Photoshop CS5.

2.4 *Drosophila* genetics

2.4.1 *Drosophila* husbandry

Drosophila flies were raised and maintained in plastic tubes containing corn-meal agar media and baker's yeast. Flies were kept at 18 °C for storage. All fly stocks consisted of three copies, which were transferred into fresh tubes every one to two weeks.

To select flies for experiments or crossings, they were anaesthetised by CO_2. Generally, crosses consisted of 4 - 8 females and 2 - 5 males. Crosses were performed at 25 °C, which reduced *Drosophila's* generation time to approximately 10 days. Parental flies were flipped into fresh vials every three days to increase longevity and egg-laying potential.

2.4.2 *Drosophila* lines

Below are the fly stocks listed which were used to create the Drosophila genotypes utilised in this study.

Stock name	Genotype	Source
w[1118]	w[1118] isogenic 2,3	Bloomington
Thor[2]	y w; Thor[2] II	Bernal et al. (2004)
Thor[GS]	y w; P{GSV2}GS51290/SM1	KYOTO stock center
park[25]	w; park[25]/TM6B-GFP	Greene et al. (2003)
Pink1B9	w; Pink1[B9]/FM7-GFP	J Chung
FLAG-d4E-BP[WT]	M{3xP3-RFP.attP'}ZH-51C (with M{vas-int.Dm}ZH-2A)/CyO	this study
FLAG-d4E-BP[TA]	M{3xP3-RFP.attP'}ZH-51C (with M{vas-int.Dm}ZH-2A)/CyO	this study
FLAG-d4E-BP[WT]	y w; P{UAS-FLAG-4E-BP[WT]}attP1/CyO	this study
FLAG-d4E-BP[TA]	y w; P{UAS-FLAG-4E-BP[TA]}attP1/CyO	this study
d4E-BP[WT]	w; P{UAS-4E-BP[WT]/CyO	Miron et al. (2001)
da-GAL4	w; P{da-GAL4}	Bloomington
elav-GAL4	w; P{elav-GAL4}	Bloomington
Dmef-GAL4	w; P{Dmef-GAL4}	Bloomington
24B-GAL4	w; P{24B-GAL4}	Bloomington
hh-GAL4	w; P{hh-GAL4}P{UAS-RFP}/ TM6B	David Strutt

2.5 *Drosophila* behavioural assays

2.5.1 Climbing assay

Adult *Drosophila* flies were sorted according to their genotype and maintained in groups of up to 25 flies in fresh tubes at 25 °C overnight. The next day, these tubes were transferred to the experimental room, which was adjusted to a temperature of 23 °C. The flies were incubated for an hour for acclimatisation before they were transferred into experimental climbing tubes without food and incubated for another hour. Subsequently, one tube per experiment was inserted in position one of the climbing apparatus. The apparatus consists of six upper and six lower tubes, at which the upper tubes are affixed to a slide. During the experiment, the flies had 10 s time to climb from a lower tube to an upper tube, followed by a transfer of flies, which reached the upper tube, to the next tube. This process was repeated five times per experiment. Finally, flies in each tube were counted and scored from 0 to 5. A climbing index was calculated by dividing the accumulated scored fly values by the total number of flies.

2.5.2 Viability assay

To assess whether overexpression of FLAG-d4E-BP can rescue the reduced viability of *park* and *Thor* double knockout flies, parental flies were crossed at 25 °C and eclosing offspring were counted. The relative ratio of flies with expected genotype was calculated and normalised to positive control. Furthermore, the average eclosion time was calculated as a further indicator for developmental dysfunctions.

2.5.3 Ageing and toxicity assay

Flies were raised under standard conditions at 25 °C in order to investigate the life span of *Thor* knockout flies. Every day the number of dead flies were counted and the remaining flies transferred into new tubes after approximately three days. The median survival was used as an indicator to compare the lifespan of different *Drosophila* genotypes.

To evaluate how different genotypes of flies can resist stress, adult male flies of equal genotypes were transferred into empty plastic tubes without food in groups of 18 to 25. The flies were starved for approximately four

hours at 25 °C before filter paper soaked with 200 µl 5 mM paraquat in
5 % sucrose (#S7903, Sigma-Aldrich) solution was placed into the tubes.
The solution was replaced every day, while tubes with filter papers were
replaced every third day. The number of dead flies was recorded every day
to distinguish the median survival under stress.

2.6   Immunofluorescence of *Drosophila* larvae wing discs

All media, reagents and mixes utilised for immunofluorescence are listed
here. Reagents and chemicals were bought from Sigma-Aldrich, unless indi-
cated otherwise.

PBST
    99.9 % PBS (see section 2.1.1)
    0.1 % Triton X-100 (#T9284)

Mowiol mounting medium
    3.3 mM Mowiol 4-88 (#81381)
    51.5 % 200 mM Tris-HCl pH 8.5 (#T5941)
    20.4 % Glycerol (#G7757)
    2.5 % DABCO (#290734)
    25.6 % ddH$_2$O

2.6.1   Larvae dissection and antibody labelling

Third instar larvae were picked after they crawled up the tube walls to pu-
pate. For dissection, they were transferred into a watch glass filled with 1x
PBS. With two sharp forceps, the larvae were pulled apart at the posterior
end. The carcass was cleaned of floating fat and connective tissue and turned
inside out to expose the wing discs, which were still attached. The carcass
was fixed with 4 % PFA (#P6148, Sigma-Aldrich) in 1x PBS for 25 min.,
washed three times 5 min. each with 0.1 % Triton X-100 in PBS (here-
inafter called PBST) and blocked unspecific binding by 1 % BSA (#A2058,
Sigma-Aldrich) in PBST for 1 h. Subsequently, wing discs were stained with
anti-FLAG antibody (1:50 in blocking solution, see section 2.3.2) at 5 °C
overnight. After 24 h, antibodies were removed and the wing discs washed
three times 10 min each with PBST before labelling with secondary anti-
bodies (anti-rabbit Alexa Fluor 488, Molecular Probes, #A-11008, 1:400)

for 2 h. After three further washing cycles, the wing discs were removed from the carcass and mounted on slides with Mowiol mounting medium, covered with glass slips and sealed with nail polish.

2.6.2 Fluorescence microscopy

For this study, the Olympus FV1000 Fluoview confocal system (Olympus corporation) with a 40x objective was used to visualise the fluorophore labelled wing discs. Two laser lines, 488 nm and 534 nm, were utilised to excite Alexa Fluor 488 and RFP respectively. All images were recorded sequentially.

2.7 Quantitative mass spectrometry

2.7.1 Reagents and media

All media, reagents and mixes utilised in this study are listed here. Reagents and chemicals were bought from Sigma-Aldrich, unless indicated otherwise. All media were sterile filtered using Stericup filters (#SCGPU05RE, Millipore) and stored at 4 °C.

MS Lysis buffer
> 96 % RIPA buffer (see 2.3.1)
> 4 % SDS (#862010)

Light SILAC medium
> 90 % Control DMEM-F12 medium R0K0 (#LM038, Dundee Cell Products)
> 10 % SILAC dialysed FBS (MWCO 10,000 Da, #DS1002, Dundee Cell Products)
> 150 µg/ml Hygromycin B (#10687-010, Life technologies)
> 15 µg/ml Blasticidin (#BP2647-50, Fisher Scientific)

Heavy SILAC medium
> 90 % Labelled DMEM-F12 medium R10K8 (#LM040, Dundee Cell Products)
> 10 % SILAC dialysed FBS (MWCO 10,000 Da, #DS1002, Dundee Cell Products)
> 150 µg/ml Hygromycin B (#10687-010, Life technologies)
> 15 µg/ml Blasticidin (#BP2647-50, Fisher Scientific)

Cell MS Solution 1
> 60 % ddH$_2$O
> 40 % Acetonitrile (#271004)
> 200 mM Ammonium Bicarbonate (#09830)

Cell MS Solution 2

    50 % ddH$_2$O

    50 % Acetonitrile (#271004)

    50 mM Ammonium Bicarbonate (#09830)

Cell MS Solution 3

    91 % ddH$_2$O

    9 % Acetonitrile (#271004)

    40 mM Ammonium Bicarbonate (#09830)

Cell MS Solution 4

    45 % ddH$_2$O

    50 % Acetonitrile (#271004)

    5 % Formic Acid (#F0507)

MS Reduction buffer

    100 % ddH$_2$O

    50 mM Ammonium Bicarbonate (#09830)

    10 mM DTT (#D0632)

MS Alkylation buffer

    100 % ddH$_2$O

    50 mM Ammonium Bicarbonate (#09830)

    55 mM Iodoacetamide (IAM, #I1149)

Urea Lysis buffer

    100 mM Tris-HCl pH 8 (#T5941)

    8 M Urea (#U5378)

    10 mM TCEP (#646547)

4x Fly MS Sample buffer

    200 mM Tris-HCl pH 8 (#T5941)

    40 % Glycerol (#G7757)

    4 % SDS (#862010)

    4 mM EDTA (#E6758)

    20 mM TCEP (#646547)

    0.01 % Bromophenol Blue (#B0126)

Fly Coomassie Staining Solution

    50 % Methanol (#10499560, Fisher Scientific)

    10 % Acetic acid (#320099)

    0.1 % Coomassie Brilliant Blue R-250 (#20278, Thermo Scientific)

Fly Coomassie De-Staining Solution

    40 % Methanol (#10499560, Fisher Scientific)

10 % Acetic acid (#320099)

Fly MS Solution 1
    50 % ddH$_2$O
    50 % Acetonitrile (#271004)
    20 mM Tris-HCl pH 8 (#T5941)

Fly MS Solution 2
    20 mM Tris-HCl pH 8 (#T5941)
    5 mM CaCl$_2$ (#449709)
    12.5 ng/µl protease

Fly MS Solution 3
    36 % ddH$_2$O
    60 % Acetonitrile (#271004)
    4 % Formic acid (#F0507)

2.7.2   Stable isotope labelling by amino acids in cell culture (SILAC)

SILAC is a simple and very precise approach to label proteins of cells. This label allows quantification of relative quantitative changes in mass spectrometry. Here, previously generated T-REx HEK293 cell clones were labelled. These cells were grown in heavy medium, containing arginine and lysine with ^{13}C and ^{15}N isotopes (see section 2.7.1). These labelled amino acids have the same chemical properties as their light counterparts, because they differ only in mass due to higher numbers of neutrons in the atomic nuclei of carbon and nitrogen. Control cells were grown in light medium, containing arginine and lysine with ^{12}C and ^{14}N isotopes. Before the cells were used for quantitative mass spectrometry experiments, they were cultured in these media for twelve cell doubling cycles minimum to assure that all proteins were completely labelled. The subtle difference in mass of the same proteins in differently labelled cells allows relative quantification of proteins by mass spectrometry.

2.7.3   Stable isotope labelling of *Drosophila*

Flies of the parental generation were mated on sugar-yeast-agar (SYA) food with or Lys(0) or Lys(6) labelled yeast. Yeast is the only amino acid source

in the food, which ensures that the F1 generation will incorporate Lys(0) or Lys(6) into their proteome during their development to adult flies.

To prepare 100 ml SYA food, 70 ml ddH$_2$O were heated to boiling point in a microwave. 1.5 g agar (#A1296, Sigma-Aldrich) was added and boiled several times till it was completely dissolved. Subsequently, 5 g D-(+)-glucose (#G8270, Sigma-Aldrich) and 10 g Lys(0) or Lys(6) labelled *Saccharomyces cerevisiae* (#234004300 or #234924330, Silantes) were added and everything stirred until food was homogeneous. Extra 17 ml ddH$_2$O were added and food was placed in a 60 °C water bath to cool down before 3 ml 15 % nipagin solution (#H5501, Sigma-Aldrich) were added as an anti-fungal agent. The food was toped up with ddH$_2$O to 100 ml, was filled in fly breeding bottles, was sealed and stored overnight at 4 °C. Fresh food was utilised on the next day to mate flies.

Three days after mating, parental flies were removed from SYA food for optimal development of offspring. Mating and development of F1 generation flies took place at 25 °C.

To separate fly heads from their bodies, flies raised on SYA food were transferred to 15 ml tube and shock frozen on dry ice. Flies were vortexed five times at maximum speed to decapitate flies by centrifugal forces. The frozen carcasses were passaged through a fine sieve, which retained the bodies, but let the heads pass. About 50 heads were squished in MS Lysis buffer (see section 2.7.1) by mechanical force till all heads were visibly disrupted. The disrupted heads were boiled for 5 min at 95 °C before they underwent three freezing-thawing cycles in liquid nitrogen and in a 37 °C water bath. DNA was sheered by passing lysates 15 times through a 25G Gauge needle. Tissue debris were spun down by centrifugation with 14,000 rpm for 10 min at 10 °C. Supernatants were transferred to fresh Protein LoBind tubes. Protein yield was quantified in a BCA assay.

2.7.4   Protein and peptide preparation

2.7.4.1   In-gel T-REx HEK293 cell protein fractionation, digestion and peptide extraction

Cells were grown to full confluence in T75 flasks prior harvesting and lysing. For initial experiments, Cell Lysis Buffer with detergents Triton X-100 and glycerol was utilised (see section 2.3.1). Later, cells were harvested with MS

Lysis buffer containing SDS as single detergent (see section 2.7.1). Cells were scraped from the flasks with 1 ml lysis buffer per flask after washing with 1x PBS three times and lysates were transferred to Protein LoBind tubes (#022431081, Eppendorf). In case cells were lysed with Cell Lysis buffer, lysates were utilised for fractionation straight away, but if cells were lysed in MS Lysis buffer, lysates were boiled for 10 min at 95 °C followed by three freezing-thawing cycles in liquid nitrogen and a 37 °C water bath prior fractionation. Furthermore, lysates were passaged 15 times throw a 25 G Gauge needle (#305122, BD) to shear DNA. Lysates of both lysis buffers were centrifuged subsequently at 14,000 rpm for 10 min at 10 °C. Supernatants were transferred to fresh tubes and utilised for fractionation.

Protein yield of lysates were quantified by Bradford assay as described in section 2.3.5, in case that Cell Lysis buffer was utilised, or by BCA assay kit (#23235, Thermo Fisher Scientific) according to manufacturer's instructions, if MS Lysis buffer was utilised. The reason was that SDS is incompatible with Bradford.

For quantitative mass spectrometry, equal protein amounts of cell lysates from cells grown in light or heavy SILAC media were combined with 1x SDS Sample buffer (see section 2.3.1), boiled for 5 min at 95 °C and loaded on 4 - 20 % Tris-Glycine SDS precast gels (#EC6028BOX, Invitrogen) along with 5 µl of Precision Plus Protein Standard All Blue. Gels were mounted in electrophoresis chambers, which were filled with 1x Tris/Glycine/SDS running buffer. Proteins were separated with 150 V for 15 min, before voltage was increased by 30 V till the end of the run.

After proteins were separated on the gel, gels were stained with Instant-Blue (#ISB1LUK, Expedeon) overnight at 4 °C. On the next day, gels were rinsed several times with ddH$_2$O, before the lanes were cut out from the gels and fractionated in 9 to 21 equal sized pieces under a laminar flow hood. These pieces were cut into 1 mm^3 cubes and were transferred into individual Protein LoBind tubes. The gel pieces were covered with 200 µl MS Solution 1 (see section 2.7.1) and were incubated in a 37 °C water bath for 30 min. Supernatants were discarded subsequently and this step repeated two to three times till gel pieces were completely destained. Proteins in destained gel pieces were reduced by DTT in 200 µl MS Reduction Buffer per piece. Gel pieces incubated in this buffer for 1 h at 56 °C in a heating block. After the supernatant was discarded, proteins were alkylated by

IAM in 200 µl MS Alkylation buffer per gel piece. Incubation took place at room temperature for 30 min in the dark. Subsequently, all gel pieces were washed twice with 200 µl 50 mM ammonium bicarbonate per piece for 15 min, before they were washed once with 200 µl MS Solution 2 per piece for 15 min at 37 °C. The gel pieces were dried down in a vacuum concentrator for 30 min till they lost all liquidity. The dried gel pieces were treated with 20 µl 0.02 µg/µl Trypsin Gold solution (#V5280, Promega). After 5 min of incubation, trypsin was diluted with 50 µl MS Solution 3 and incubated with the gel pieces at 37 °C for 16 h. After protein digestion, the supernatants were transferred to fresh Protein LoBind tubes and peptides were extracted from gel pieces in several steps. Initially, 20 µl acetonitrile were added to the gel pieces and incubated for 15 min at 37 °C. Subsequently, 50 µl 5 % formic acid were added to the gel pieces and incubated for further 15 min at 37 °C before the supernatants were transferred to the supernatant tube from trypsin digestion. Peptide extraction with acetonitrile and formic acid was repeated once again, before 50 µl MS Solution 4 was added to the gel pieces and incubated at 37 °C for 30 min. The supernatants were combined with previous supernatants and the gel pieces discarded. Extracted peptides were dried down in a vacuum concentrator at 40 °C and 0 bar till all fluid was evaporated.

2.7.4.2 In-gel *Drosophila* protein fractionation, digestion and peptide extraction

Prior to fractionation, proteins were reduced and alkylated in solution. Samples were mixed with Fly MS Sample buffer to dilute to 1x final buffer concentration. The buffer contained TCEP as reducing agent. Samples incubated at 37 °C for 30 min. After samples were cooled down to room temperature, a final concentration of 15 mM IAM was added to alkylate samples. Incubation took place for 30 min in the dark. Excess IAM was quenched by 25 mM DTT, which was added before samples were loaded on a 4 - 20 % Tris-Glycine SDS precast gel (#EC6028BOX, Invitrogen) along with 5 µl of Precision Plus Protein Standard All Blue. Gels were mounted in electrophoresis chambers, which were filled with 1x Tris/Glycine/SDS running buffer. Proteins were separated with 150 V for 15 min, before voltage was increased by 30 V till proteins were maximally separated.

After run, gels were briefly rinsed with ddH$_2$O and stained with

Coomassie solution for 20 min, followed by several de-staining steps in Coomassie de-staining solution until characteristic proteins bands became visible. Lanes were cut in equal sized pieces. Every piece was cut in 1 mm^3 cubes before transferred into 1.5 ml Eppendorf tubes, which have been rinsed with 50 % methanol before to remove dust and plasticizers.

Chopped gel pieces were washed with 500 µl ddH$_2$O per tube for 1 h, before they were washed twice with the same volume of 20 mM Tris-HCl (pH 8) for another hour. The washing solutions were discarded and replaced by 500 µl Fly MS Solution 1 and incubated for 30 min. For easier access of the protease to the proteins, gel pieces were dehydrated by incubation with 100 µl acetonitrile per piece for 10 min. Acetonitrile was discarded and the gel pieces were dried down completely in a vacuum concentrator at 40 °C and 0 bar. 25 µl Fly MS Solution 2 was added to the dried gel pieces to initiate protein digestion. Lys-C (#V1071, Promega) was the utilised protease - an endoproteinase, which cuts specifically at the carboxyl side of lysine residues. After rehydration, 30 µl Fly MS Solution 2 was added without protease and gel pieces incubated at 37 °C for 16 h. Subsequently, supernatants were transferred to fresh tubes before gel pieces were incubated twice with 40 µl Fly MS Solution 3 for 1 h to extract peptides. Supernatants of these two extraction steps were combined with those from digestion. Extracted peptides were dried down in a vacuum concentrator at 40 °C and 0 bar till all fluid was evaporated.

2.7.5 RP-HPLC and mass spectrometry measurements

Peptides were resuspended in 36 µl 0.5 % formic acid per fraction by 5 min sonication in a water bath at 22 °C. 20 µl of resuspended samples from T-REx HEK293 cells were analysed by nanoLC-MS/MS on a LTQ Orbitrap Elite (Thermo Fisher) hybrid mass spectrometer equipped with a nanospray source, coupled with an Ultimate RSLCnano LC System (Dionex). The system was controlled by Xcalibur 2.1 (Thermo Fisher) and DCMSLink 2.08 (Dionex). Peptides were desalted on-line using a micro-Precolumn cartridge (C18 Pepmap 100, LC Packings) and then separated using a 120 min reverse-phase gradient (4 - 32 % acetonitrile/0.1 % formic acid) on an EASY-Spray column, 50 cm x 50 µm ID, PepMap C18, 2 µm particles, 10 nm pore size (Thermo Scientific). The LTQ-Orbitrap Elite was operated with a cycle of one MS (in the Orbitrap) acquired at a resolution of 60,000 at m/z 400, with

the top 20 most abundant multiply-charged (2+ and higher) ions in a given chromatographic window subjected to MS/MS fragmentation in the linear ion trap. A Fourier transform mass spectrometry (FTMS) target value of 10^6 accumulated ions and an ion trap MSn target value of 10^4 accumulated ions was used and with the lock mass (445.120025) enabled. Maximum FTMS scan accumulation time of 500 ms and maximum ion trap MSn scan accumulation time of 100 ms were used. Dynamic exclusion was enabled with a repeat duration of 45 s with an exclusion list of 500 and exclusion duration of 30 s.

20 µl of resuspended samples from *Drosophila* were injected, using a Easy-nLC 1000 (ThermoFisher Scientific), onto a nanoscale reverse-phase column (50 µm inner diameter, 150 mm length, ThermoFisher Scientific) and separated by a reverse-phase gradient of increasing acetonitrile from 2 - 40.4 %, in 0.1 % formic acid, over 84 min at 300 nl/min. The mass spectrometer Orbitrap Q-exactive mass spectrometer (ThermoFisher Scientific) operated in a data-dependent MS/MS mode which alternate between a full scan mass spectrum with mass scan range 400 - 1600 Da, and MS/MS of the top 10 highest abundant ions selected from the full scan.

2.7.6 Data analysis

Mass spectrometry raw data was analysed and matched to proteomics databases by MaxQuant 1.5.0.12 (Max Planck Institute of Biochemistry, Martinsried, Germany). The raw data was matched to the in-silico trypsin digested UniProt database of human or Lys-C digested UniProt databse of fruit fly proteins (http://www.uniprot.org). At least one unique peptide pair was necessary to quantify a protein. The maximum of missed cleavage sites were two, the MS mass tolerance was 7 ppm and the MS/MS mass tolerance was 0.5 Da. Acetyl (Protein N-term) and Oxidation (M) were set as variable modifications and carbamidomethyl (C) as a fixed modification. A protein FDR of 0.01 and a peptide FDR of 0.01 were used for identification level cut offs.

The mass spectrometry data were analysed using PANTHER (http://pantherdb.org, Version 10), STRING (http://string-db.org, Version 10) and DAVID databases (https://david.ncifcrf.gov, Version 6.7). In PANTHER, genes were annotated and the functional classification displayed in pie charts and the matched proteins of every annotation group downloaded

and organised in an Microsoft Excel file.

For STRING analysis, the standard settings were kept. This means that the evidence of protein interactions were displayed for known, predicted and other interactions. Known interactions were either extracted from a curated database or experimentally determined. Predicted interactions were extrapolated by gene neighborhood, gene fusions or gene co-occurrence, "other" interactions were determined by textmining, co-expression or protein homology. The minimum required interaction score was kept at a medium confidence level of 0.4.

The DAVID functional annotation tool analysed the proteins and displayed them in a functional annotation chart. The DAVID system adapted the Fisher Exact test to determine gene enrichment of distinct annotation terms. The minimum count threshold was two proteins per annotation term. The significance level was expressed by the EASE score, a modified p-value. EASE is calculated more conservatively than the standard p-value, which is why the standard significance threshold of EASE is ≤ 0.1, but was set back to ≤ 0.05 here.

Chapter 3

Development of a human cellular model overexpressing 4E-BP1 for quantitative proteomic investigations

3.1 Hypothesis and aims

The initial aim of this study was to develop a cellular model to investigate the effects of 4E-BP1 overexpression on the proteome by quantitative mass spectrometry. The mTOR pathway and 4E-BP1 itself have been in focus of many different studies for many years, but it is only four years ago since high-throughput data has been published about the downstream effects of 4E-BP1. Although these data revealed many unknown details about how the mTOR pathway regulates translation, they do not allow a deep insight into the physiological effects of 4E-BP1 in protein synthesis. The information we have so far were either gained from cancer cell lines (Huo et al., 2012; Hsieh et al., 2012) or even non-human cell lines (Thoreen et al., 2012). Furthermore, all these studies have been performed using mTOR inhibitors, partly combined with 4E-BP1 knockout cell lines. As illustrated before, mTOR is a central kinase in a complex regulated pathway with several downstream targets, which complicates investigations on the effect of one specific downstream target, 4E-BP1. Even differences between several mTOR inhibitors on downstream effects were reported by Huo et al. (2012).

An important criteria for a suitable cell model was physiological resemblance of mTOR pathway functionality in order to prevent unpredictable effects on potential 4E-BP1 downstream targets. However, the expression of 4E-BP1 differs massively among different cell lines as shown by the Human Protein Atlas Project (http://www.proteinatlas.org, Uhlen et al. (2010)). This project quantified a huge number of different proteins in different cell lines or tissues based on antibody staining. Most interestingly, 4E-BP1 was often diminished in cell lines of cancer origin, e.g. MCF7 (Metastatic breast adenocarcinoma cell line), U-138 MG (Gliobastoma cell line), HMC1 (Mast cell leukaemia cell line), HDLM-2 (Hodgkin lymphoma cell line) and HeLa (Cervical epithelial adenocarcinoma cell line). This is not surprising at all considering the fact that 4E-BP1 is negatively regulated by the mTOR pathway. Many factors in the mTOR pathway have proto-oncogenic potential, because it mediates cell growth and cell proliferation (Dowling et al., 2010; Wullschleger et al., 2006). An important difference between cancer and immortal cell lines is the lacking contact inhibition in cancer cells. Contact inhibition is mediated by the mTOR pathway through 4E-BP1 (Azar et al., 2010), which highlights that the mTOR pathway is often dysregulated in cancer cells to allow unlimited amplification.

Not only the amount of 4E-BP1 varies between different cell lines, but also its regulation of phosphorylation and dephosphorylation. Choo et al. (2008) have reported that the effect of the allosteric mTORC1 inhibitor rapamycin on 4E-BP1 phosphorylation is cell type dependent. While rapamycin caused permanent dephosphorylation of 4E-BP1 in MCF7, PC3 and U2OS cell lines, it could be rephosphorylated in HEK293 and HeLa cells rapidly. Potentially, HEK293 and HeLa cells bear rapamycin resistant mTORC1 functions, which are lost in other cell lines. However, catalytic site ATP-competitive mTOR inhibitors dephosphorylate 4E-BP1 regardless of the cell context (Feldman et al., 2009; Liu et al., 2010; Thoreen et al., 2009). All these findings excluded commonly utilised cancer cell lines for this project, because of their changed 4E-BP1 expression level and regulation.

Additionally, it was demanded that the model overexpresses wildtype 4E-BP1[WT] or constitutively active 4E-BP1[TA]. In *in vivo* models, overexpression of wildtype 4E-BP was already sufficient to produce significant behavioral changes (Tain et al., 2009), but using a less physiological, but more active version of the wildtype protein may provide a better insight

into 4E-BP1 downstream effectors. The duration of 4E-BP1 overexpression must be controllable. Other important criteria on the cell model were the ability for easy transfection to overexpress 4E-BP1 and the origin as a human cell line. Neuronal origin of the cell line would have been an advantage, because it would increase the impact of findings in terms of applying them to PD.

3.2 Cell line selection

3.2.1 Validating the 4E-BP1 constructs in different cell lines

In a first step, it was necessary to test the functionality of *4E-BP1* constructs utilised for this study. Previously made *4E-BP1[WT]* and *4E-BP1[TA]* constructs were transfected into HeLa. This cell line is very easy to cultivate and to transfect. After transfection, the cells were treated with mTOR inhibitor rapamycin for 24 h prior to lysis and immunoblotting. The blot shows transfection success for both constructs when comparing to untransfected negative controls (Fig. 3.1). The overexpression of 4E-BP1[WT] appears to be more effective, because it results in a stronger band, but this may be deceptive. 4E-BP1[WT] occurs in different phosphorylation states with subtly different sizes. Hence, 4E-BP1[WT] spreads wider on membranes than 4E-BP1[TA], which is completely unphosphorylated. Nevertheless, at least partly 4E-BP1[WT] is more overexpressed than 4E-BP1[TA], because also nonphospho-4E-BP1 antibodies reveal stronger bands for it. Furthermore, the data clearly reveals that 4E-BP1[TA] is unphosphorylated, because the signal of total or nonphospho-specific 4E-BP1 antibodies is increased compared to controls, but not with phospho-4E-BP1-specific antibodies. This is in contrast to 4E-BP1[WT], in which case signals are raised with all three antibodies. However, there is no robust effect on phosphorylation detectable after rapamycin treatment, neither with 4E-BP1[WT] nor with 4E-BP1[TA]. This finding is consistent with previously published data, which shows that the effect of rapamycin is quickly abrogated in HeLa cells (Choo et al., 2008).

In a further step, it was investigated whether 4E-BP1[WT] can also be expressed in other human cell lines, which could be potential candidates for a cellular model. Here, RPE1, HEK293 and SH-SY5Y cells were tested. Retinal Pigmented Epithelial cells (RPE1) are immortal and non-cancer human cells derived from neuronal origin with a diploid genome of 46 chromosomes.
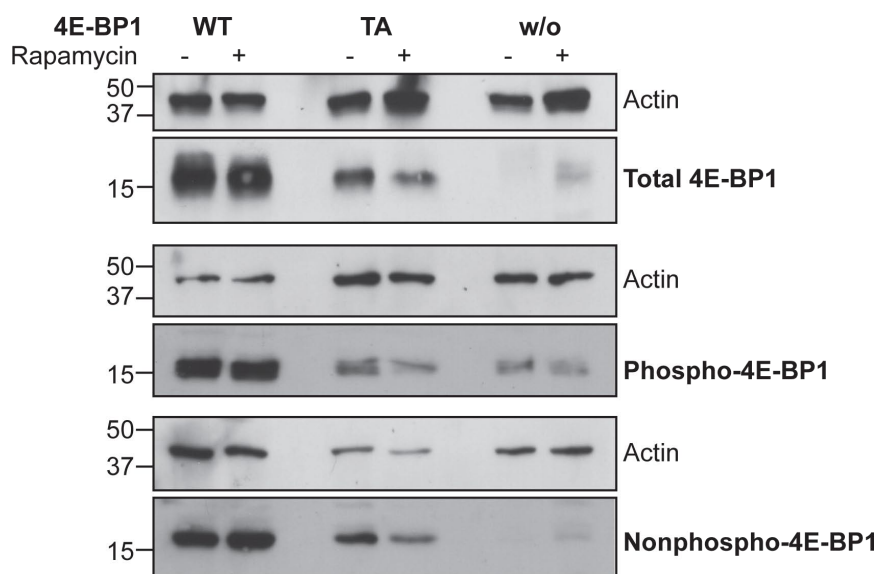
Figure 3.1: 4E-BP1 overexpression in HeLa cells. HeLa cells were transiently transfected with equal amounts of 4E-BP1[WT], 4E-BP1[TA] or no construct (w/o). After two days they were treated with 100 nM rapamycin for 24 h while the control received no treatment. 4E-BP1 state was analysed by immunoblotting with total 4E-BP1, phospho-4E-BP1 or nonphospho-4E-BP1 antibodies. The blots derived from three separate SDS-PAGES of the same biological replicate (n = 1). Actin served as loading control. The molecular weight is indicated on the left hand side in kDa.

Human Embryonic Kidney cells (HEK293) are immortal, non-cancer cells, which are very commonly used and have the advantage that a lot of reference data is already available and that results can be easily applied in many laboratories. However, compared to RPE1 cells HEK293 cells have several genetic abnormalities. They are described as hypotriploid, referring to a genotype that carries partly, but not entirely, more than two copies of every chromosome. The origin of HEK293 cells was not investigated for a long time, which is surprising given how commonly this model has been used in life science. Now, two studies give evidence that HEK293 cells have many neuronal properties and may have derived from embryonic adrenal precursor cells (Lin et al., 2014b; Shaw et al., 2002).

SH-SY5Y cells are derived from neuroblastoma cells. As a cancer cell line, it was not a preferred model, but still of interest due to its neuronal origin and its common usage to study neuronal functions *in vitro*. Also it was informative to see whether differences are detectable compared to non-cancer cell lines. The karyotype of SH-SY5Y cells consists of 47 chromosomes with trisomy 1q.
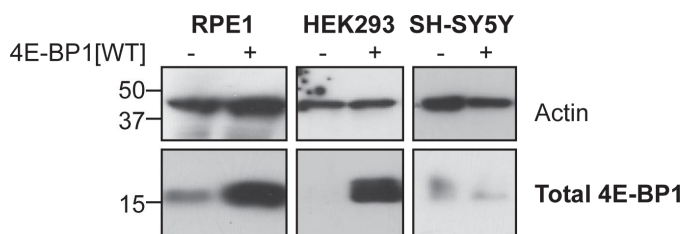
Figure 3.2: 4E-BP1[WT] over-expression in RPE1, HEK293 and SH-SY5Y cells. Cells were transiently transfected with equal amounts of 4E-BP1[WT]. After two days they were lysed and analysed by immunoblotting with total 4E-BP1 antibodies (n = 1). Actin served as loading control. The molecular weight is indicated on the left hand side in kDa.

As immunoblotting revealed, 4E-BP1[WT] was clearly overexpressed in RPE1 and HEK293 cells (Fig. 3.2). However, there has been a difference in transfection efficiency between these two cell lines. The difference between endogenous 4E-BP1 and overexpressed 4E-BP1[WT] was much larger in HEK293 than in RPE1 cells given that endogenous 4E-BP1 level in both cell lines are comparable. This topic is discussed in the following section and illustrated in figure 3.5.

Remarkably, 4E-BP1[WT] was not efficiently overexpressed in SH-SY5Y cells. Even after a long film exposure, it was only possible two detect very weak bands in control and transfected samples. This may be due to two reasons: either transfection or overexpression of 4E-BP1[WT] was unsuccessful, which is unlikely given the common use of these cells as overexpression models in research laboratories, or 4E-BP1[WT] was actively removed. The latter is conceivable given that 4E-BP1 is often downregulated in cancer cells (see section 3.1). Whatever caused the problems of 4E-BP1[WT] overexpression, SH-SY5Y cells were excluded as a potential model on the basis of these data. After confirming that 4E-BP1 constructs expressed appropriately in some human cell lines, it was important to investigate how 4E-BP1[WT] behaves in candidate cell lines in terms of its phosphorylation state. First, RPE1 cells were transfected with 4E-BP1[WT]. After two days, cells were treated with rapamycin or second generation mTOR inhibitors, Torin1 and AZD8055, for 30 min, 2 h or 6 h. Immunoblotting confirmed that 4E-BP1[WT] was overexpressed in RPE1 cells, but that rapamycin had no effect on its phosphorylation state as show in HeLa cells before (Fig. 3.3). In contrast, more potent mTOR inhibitors Torin1 and AZD8055 had a clear effect on 4E-BP1[WT] phosphorylation state. After 30 min treatment the

intensity of protein bands of the phospho-4E-BP1 antibody began to decline and were massively reduced after 2 h. Also, the appearance of the total 4E-BP1 bands changed and appeared narrower, sharper and less spread out after treatment, which is due to abolition of phosphorylated protein variants, which migrate slower on these gels. The nonphospho-4E-BP1 antibody showed no further increase of unphosphorylated protein after 30 min of second generation mTOR inhibitor treatment. Nonetheless, these results revealed that the phosphorylation state of 4E-BP1[WT] can be modified by mTOR inhibitors in RPE1 cells in a time dependent way, which supports that overexpressed 4E-BP1[WT] is also influenced by endogenous mTOR mechanisms.
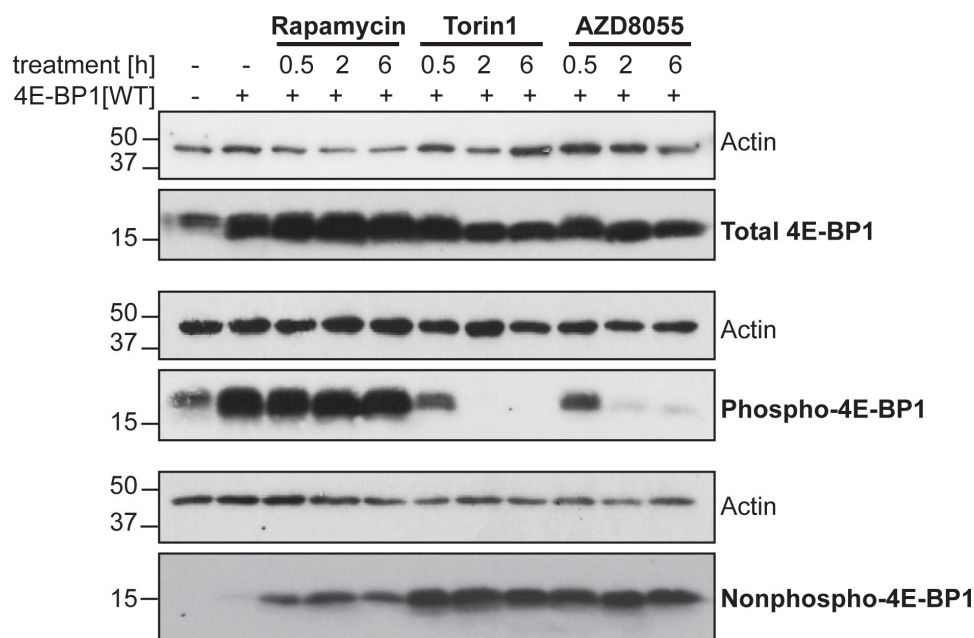
Figure 3.3: 4E-BP1[WT] phosphorylation in RPE1 cells. RPE1 cells were transiently transfected with equal amounts of 4E-BP1[WT]. After two days they were treated with 100 nM rapamycin, 250 nM Torin1 or 100 nM AZD8055 for 30 min, 2 h or 6 h. 4E-BP1 state was analysed by immunoblotting with total 4E-BP1, phospho-4E-BP1 or nonphospho-4E-BP1 antibodies. The blots derived from three separate SDS-PAGES of the same biological replicate (n = 1). Actin served as loading control. The molecular weight is indicated on the left hand side in kDa.

HEK293 cells were transiently transfected to investigate the behaviour of overexpressed 4E-BP1[WT] in these cells and the mTOR inhibitor treatment was repeated as described for RPE1 cells above. The immunoblot showed that 4E-BP1[WT] was overexpressed in HEK293 cells and that it was dephosphorylated by Torin1 and AZD8055 in a time dependent way, while

rapamycin treatment did not cause a robust change of the phosphorylation state (Fig. 3.4).

These results revealed that the 4E-BP1 constructs worked as expected and that they could be transfected successfully into different human cell lines. RPE1 and HEK293 illustrated comparable results in terms of manipulation of 4E-BP1[WT] phosphorylation state. It highlights that the important multi-protein regulator of 4E-BP1, mTORC1, acted normally. According to these results, RPE1 and HEK293 were two equal candidates for a cellular model.
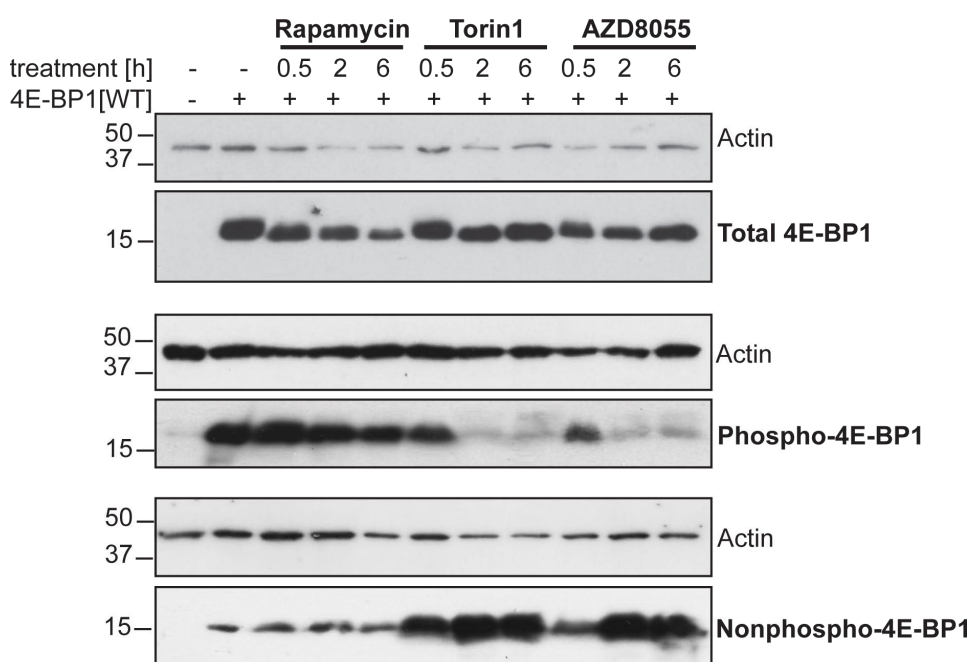
Figure 3.4: 4E-BP1[WT] phosphorylation in HEK293 cells. HEK293 cells were transiently transfected with equal amounts of 4E-BP1[WT]. After two days they were treated with 100 nM rapamycin, 250 nM Torin1 or 100 nM AZD8055 for 30 min, 2 h or 6 h. 4E-BP1 state was analysed by immunoblotting with total 4E-BP1, phospho-4E-BP1 or nonphospho-4E-BP1 antibodies. The blots derived from three separate SDS-PAGES of the same biological replicate (n = 1). Actin served as loading control. The molecular weight is indicated on the left hand side in kDa.

3.2.2 Investigating endogenous 4E-BP1 in different cell lines

After investigating the behaviour of overexpressed 4E-BP1 in different cell lines, it was important to learn more about their endogenous 4E-BP1. Endogenous 4E-BP may interfere with the effect of overexpressed 4E-BP1, so it was important to know the relative level of endogenous 4E-BP among

Figure 3.5: Endogenous 4E-BP1 in HEK293, RPE1 and SH-SY5Y cells. Two days after seeding the cells, they were treated with 250 nM Torin1 or 100 nM AZD8055 for 2 h. 4E-BP1 state was analysed by immunoblotting with total 4E-BP1, phospho-4E-BP1 or nonphospho-4E-BP1 antibodies. The blots derived from three separate SDS-PAGES of the same biological replicate (n = 1). Actin served as loading control. The molecular weight is indicated on the left hand side in kDa.
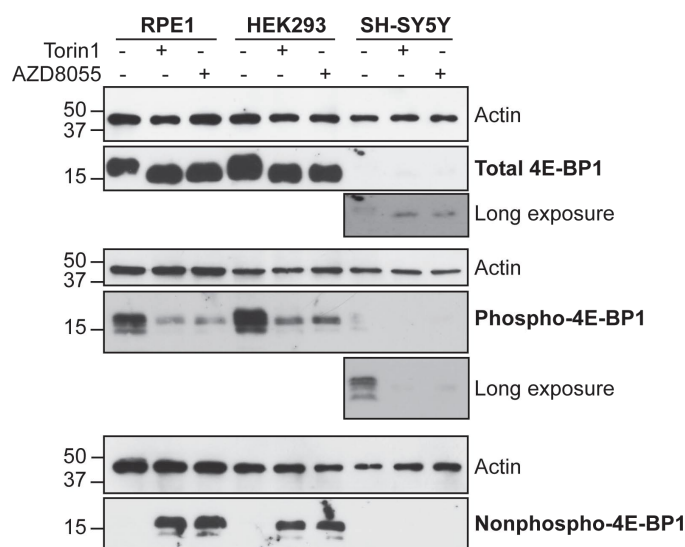
different potential candidate cell lines and to study its behaviour.

In order to do this, RPE1 and HEK293 cells, the most promising candidates form the previous experiment, were treated with mTOR inhibitors Torin1 and AZD8055 for 2 h and their lysates were immunoblotted along with SH-SY5Y cells (Fig. 3.5). These results revealed that RPE1 and HEK293 cells expressed approximately equal amounts of endogenous 4E-BP1, which was equally dephosphorylated by mTOR inhibitors. In contrast, SH-SY5Y cells had a much reduced level of endogenous 4E-BP1. Only after long film exposure weak bands became visible with total 4E-BP1 and phospho-4E-BP1 antibodies, but not with nonphospho-4E-BP1 antibodies. After mTOR inhibitor treatment, endogenous 4E-BP1 of SH-SY5Y cells seemed to be dephosphorylated as well, which indicates an active mTOR pathway regulation. These results were slightly unexpected as data published by the Human Protein Atlas Project have revealed reduced 4E-BP1 amount in several cancer cell lines, but not in SH-SY5Y cells (http://www.proteinatlas.org/ENSG00000187840-EIF4EBP1/cell/CAB005032, Fagerberg et al. (2011)). Nevertheless, it is obvious that this cancer cell line showed clear and consistent differences to the other two non-cancer cell lines regarding endogenous 4E-BP1 levels with all three antibodies used.

3.3   Generation of T-REx HEK293 4E-BP1 cells

The previous experiments have revealed that RPE1 and HEK293 cells had qualities as a 4E-BP1 overexpressing model with subtle advantages or disadvantages. However, a major advantage of HEK293 cells is that they are available as Flp-In T-REx cells, a system developed to generate inducible stable cell lines with a defined genomic integration site. It allows the generation of HEK293 cells in which the overexpression of 4E-BP1 can be induced in a time controlled way. This is a very elegant model system and a decisive factor to favour HEK293 cells.

3.3.1   Flp-In T-REx system
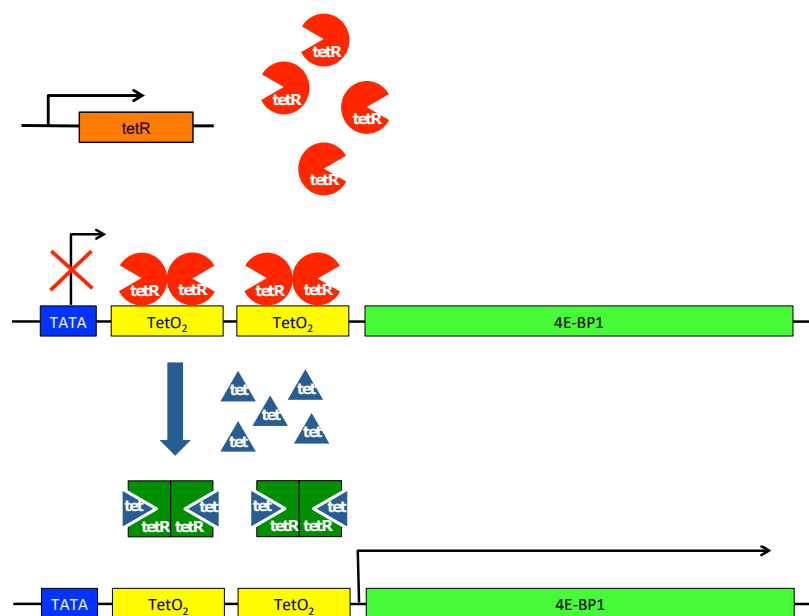
Figure 3.6: Principal of the Flp-In T-REx system. The constitutively active tetracycline repressor gene (tetR) expresses tetR, which binds to the promoter region of the stably integrated gene of interest 4E-BP1. This binding prevents 4E-BP1 from being transcribed. After adding tetracycline to the cell media, tetR is removed from 4E-BP1 promoter and the gene is transcribed.

The Flp-In T-REx system consists of two basic elements: a tetracycline repressor gene (tetR) expressed from a constitutively active promoter and the gene of interest (GOI), the promoter of which contains a tetR binding region (Fig. 3.6). The GOI is stably integrated site specifically into the genome via homologous recombination catalysed by Flp recombinase. When

tetracycline is absent in the cell media, tetR binds to the promoter region of GOI and prevents its transcription. After tetracycline is added to the media, it binds tetR, changes its structural conformation and causes its detachment from the promoter. This results in expression of the GOI.

3.3.2 Evaluation of T-REx HEK293 cells regarding their level of endogenous 4E-BP1

Before generating T-REx HEK293 cells overexpressing 4E-BP1, T-REx HEK293 and normal HEK293 cells were tested on their capability to expressed similar amounts of endogenous 4E-BP1. This was important to make sure that information about 4E-BP1 in HEK293 cells, described above, can be applied to T-REx HEK293 cells. HEK293 and T-REx HEK293 cells were treated with 1 µg/ml tetracycline for 24 h to investigate whether the activation drug itself may have an effect on endogenous 4E-BP1. The cells were lysed and the protein extract used for immunoblotting (Fig. 3.7). The total, phospho- and nonphospho-4E-BP1 immunoblots confirmed that HEK293 and T-REx HEK293 cells had the same amount of endogenous 4E-BP1 and consistent phosphorylation states. Only nonphospho-4E-BP1 showed a subtle difference between both cell types, but not massive. It should not interfere with subsequent experiments. Tetracycline treatment had no effect on the amount or phosphorylation state of 4E-BP1 in both cell types.
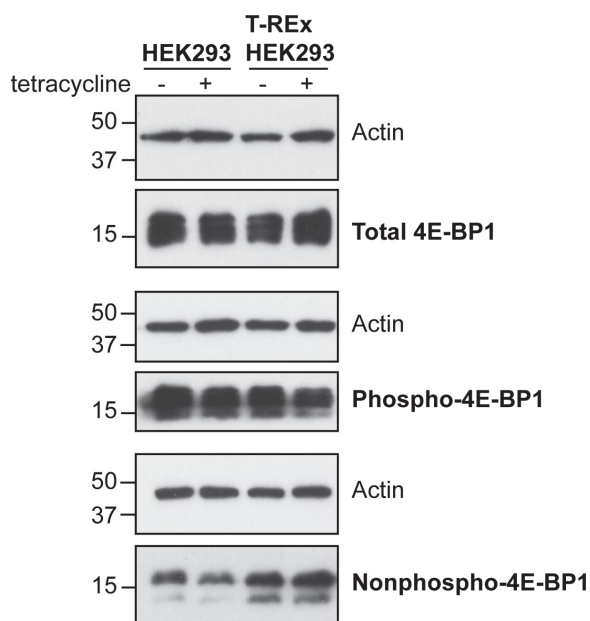
Figure 3.7: **Endogenous 4E-BP1 in HEK293 and T-REx HEK293 cells.** The cells were treated with 1 µg/ml tetracycline for 24 h. 4E-BP1 state was analysed by immunoblotting with total 4E-BP1, phospho-4E-BP1 or nonphospho-4E-BP1 antibodies. The blots derived from three separate SDS-PAGES of the same biological replicate (n = 1). Actin served as loading control. The molecular weight is indicated on the left hand side in kDa.

3.3.3 Cell transfection and clone selection

Before the Flp-In T-REx HEK293 cells overexpressing 4E-BP1 could be made, *4E-BP1* had to be cloned from the original pCMV6-XL5 vector into the pcDNA5/FRT/TO transfection vector (Fig. 3.8A). *4E-BP1[WT/TA]* were amplified from the original vector by PCR using the designed h4E-BP1 primer pair (Fig. 3.8B). The PCR products were ligated into the vector and bacteria were transformed with them. Five colonies were isolated, amplified and PCR was applied to confirm integration success with CMV and BGH primers, flanking the multiple cloning site of the vector (Fig. 3.8C). Colony 1 of *4E-BP1[WT]* transgene and colony 3 of *4E-BP1[TA]* were verified by sequencing and taken forward for use.

The generated constructs were co-transfected with the pOG44 vector, carrying the *Flp* gene, which encodes for Flipase, the recombinase catalysing the homologous recombination of the *4E-BP1* constructs and the FRT landing site. T-REx cells without integrated *4E-BP1* exhibit Zeocin resistance. The gene is responsible for maintaining the FRT landing site and is located downstream of it. Zeocin is a broadband antibiotic causing cell death by DNA double strand brakes. This resistance is destroyed by site specific *4E-BP1* integration due to separation from its start codon. The positively transfected Flp-In T-REx HEK293 cells were selected by resistance to Hygromycin B, an antibiotic inhibitor of protein biosynthesis in pro- and eukaryotes. The Hygromycin B resistance gene was co-integrated with *4E-BP1* as it was located on the same pCDNA5/FRT/TO vector. Hygromycin B acquired functionality by adapting the start codon of Zeocin after integration. After 10 days, 12 colonies were isolated and amplified separately. These colonies were triple tested on their Zeocin sensitivity. Cells which have integrated *4E-BP1* into their genome at the FRT site had lost this resistance. Only colonies with 100 % cell death in all three tests after 10 days of Zeocin treatment had integrated *4E-BP1* site-specifically and where maintained. Hygrmycin and Zeocin double resistant clones had integrated *4E-BP1* randomly into their genome and were discarded. From originally twelve clones per genotype, four T-REx *4E-BP1[WT]* clones and seven T-REx *4E-BP1[TA]* clones passed the double antibiotics selection criteria and were amplified (see section 2.1.2.3 for more details). As a third antibiotic, Blasticidin was always present in the T-REx HEK293 cell media. Blasticidin inhibits the termination step of mRNA translation and was
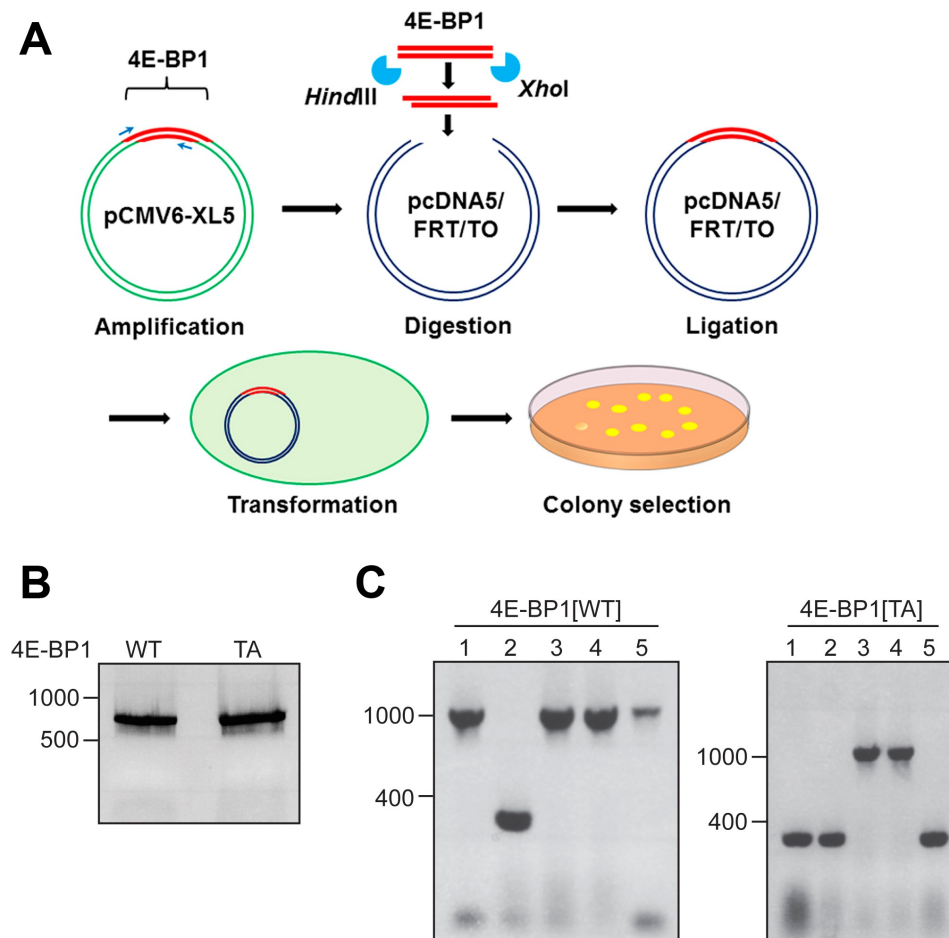
Figure 3.8: Cloning of *4E-BP1[WT]* and *4E-BP1[TA]* into pcDNA5/FRT/TO transfection vector. (A) *4E-BP1* constructs were amplified from pCMV6-XL5 vector by PCR and loaded on a 1% agarose gel (B). The calculated size was 806 bp. The PCR products were digested with *Hind*III and *Xho*I endonucleases and ligated in the new pcDNA5/FRT/TO vector. After transformation of *E. coli* bacteria with the new plasmids, single colonies were checked on their transformation success by PCR amplification of integrated 4E-BP1 genes (C). The calculated size for a successful integration was 1056 bp, while it was 270 bp without integration. The DNA size is indicated on the left hand side in bp.

linked to the tetracycline repressor gene. Thus, Blasticidin in cell media ensured the maintenance of the tetracycline repressor gene and constant production of tetracycline repressor proteins, which block the transcription of *4E-BP1* when tetracycline is absent in the media.

The amplified clones were checked for their tetracycline dependent inducibility of 4E-BP1 overexpression. For this purpose, T-REx clones were treated with 1 µg/ml tetracycline for 24 h to induce transgene expression. Tetracycline bound to the tetracycline repressor, which blocked the tran-

T-REx HEK293 4E-BP1[WT]
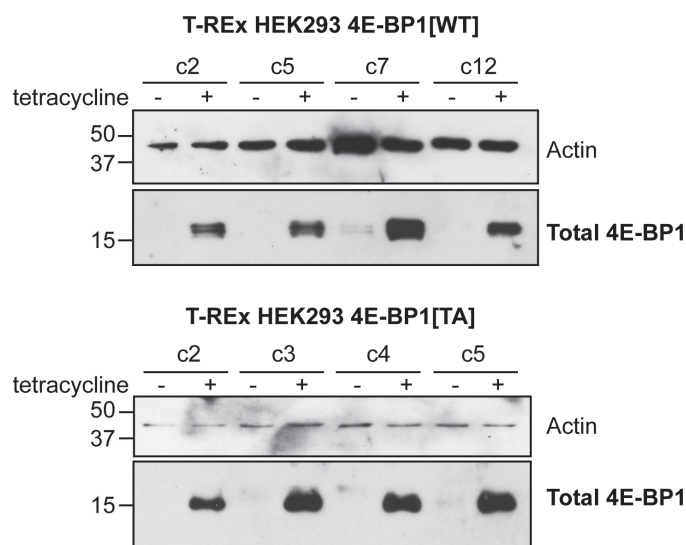
Figure 3.9: Different clones overexpressing 4E-BP1[WT] and 4E-BP1[TA] in T-REx HEK293 cells. The cells were treated with 1 µg/ml tetracycline for 24 h. 4E-BP1 was analysed by immunoblotting with total 4E-BP1 antibodies (n = 1). Actin served as loading control. The molecular weight is indicated on the left hand side in kDa.

scription of *4E-BP1* at its promoter and removed it from their. 4E-BP1 expression was analysed by immunoblotting. Four clones per genotype are displayed here (Fig. 3.9). In all cases, T-REx clones overexpressed 4E-BP1. Furthermore, the relative level of 4E-BP1 overexpression was comparable between different clones. No clone expressed very much more or less 4E-BP1 than the others, which means that all clones are equally good for subsequent experiments. However, before a certain clone could be selected for further studies, it was important to evaluate them more in detail and to learn more about how overepressed 4E-BP1 behaves in T-REx HEK293 cells.

3.3.4 Evaluation of T-REx HEK293 cell clones and selection for subsequent quantitative mass spectrometry experiments

In the next step, the level of leak 4E-BP1 expression was investigated. For this purpose, two clones of 4E-BP1[WT] T-REx HEK293 cells and two of 4E-BP1[TA] were checked on their total 4E-BP1 level by immunoblotting after grown in tetracycline free cell medium. HEK293 and T-REx HEK293 host cells were used as comparisons. The results clearly revealed that endogenous 4E-BP1 level in T-REx clones was not elevated over baseline level of HEK293 and T-REx HEK293 cells (Fig. 3.10). Thus, leaky expression was below detection level of immunoblotting and guarantees that leaky expressed 4E-BP1 will not bias later studies with these clones. The integrity of both

77

Figure 3.10: Leak expression of 4E-BP1 in different T-REx HEK293 cell clones. The cells were grown in tetracycline free media. HEK293 and T-REx HEK293 host cells indicate endogenous 4E-BP1 baseline level. 4E-BP1 was analysed by immunoblotting with total 4E-BP1 antibodies (n = 1). Actin served as loading control. The molecular weight is indicated on the left hand side in kDa.
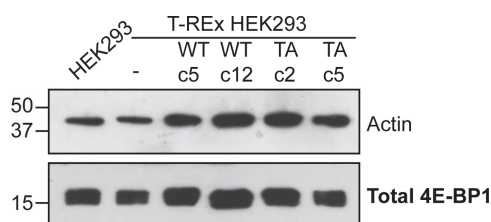
transgenes in these clones was confirmed by DNA sequencing. *4E-BP1[TA]* had two point mutations in codon 37 and 46 where adenine was replaced by guanine in both ACC/GCC codons. If not indicated otherwise, clone 5 of 4E-BP1[WT] and clone 2 of 4E-BP1[TA] were utilised for all following investigations on human cellular 4E-BP1.

Another aspect to investigate was the activity of 4E-BP1[TA]. The 4E-BP1 mutant carries the two point mutation T37A and T46A, which should activate it permanently without the option of inactivation. It is known for a long time that 4E-BP1 is inactivated by a phosphorylation cascade, beginning at the positions T37 and T46, and that blocking the cascade initiation is sufficient to inhibit phosphorylation and inactivation of 4E-BP1 (Gingras et al., 1999, 2001). Specific T37/T46 phospho- or nonphospho-4E-BP1 antibodies were used in the previous experiments to confirm that the mutations were present and working. To support that 4E-BP1[TA] in T-REx HEK293 cells was analogous to active 4E-BP1, T-REx HEK293 4E-BP1[WT/TA] were treated with mTOR inhibitor Torin1 for 2 h. Immunoblots were probed with total 4E-BP1 antibodies instead of phosphorylation site specific antibodies. Dephosphorylation of 4E-BP1 should cause a very subtle band shift due to slightly faster migration of un-phosphorylated 4E-BP1 in the gel. Thus, this band shift can be utilised as an indicator of 4E-BP1 activation. The immunoblot revealed that Torin1 treatment caused a 4E-BP1 band shift downwards in cells overexpressing 4E-BP1[WT] after Torin1 treatment (Fig. 3.11). The down shifted band of 4E-BP1[WT] after Torin1 treatment corresponded to the 4E-BP1[TA] band without Torin1 treatment, which confirmed that 4E-BP1[TA] is unphosphorylated and hence active. Torin1 treatment of 4E-BP1[TA] overexpressing cells sharpened the band and removed faint background bands, which migrated slower than unphosphorylated 4E-BP1. Presumably, this was due to endogenous wildtype 4E-BP1, which was still sensitive to mTOR inhibitors.
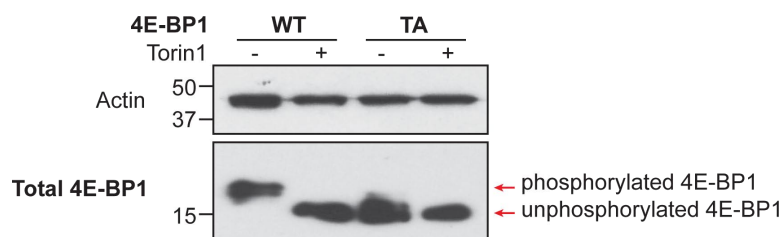
Figure 3.11: Phosphorylation state of 4E-BP1[TA]. T-REx HEK293 cells overexpressed 4E-BP1[WT] or 4E-BP1[TA] after treatment with 1 µg/ml tetracycline for 24 h. 4E-BP1[WT] was dephosphorylated by 250 nM Torin1 treatment for 2 h. 4E-BP1 was analysed by immunoblotting with total 4E-BP1 antibodies (n = 1). Actin served as loading control. The molecular weight is indicated on the left hand side in kDa.

Before the T-REx clones could be used for quantitative mass spectrometry, it was important to investigate the nature of induction of 4E-BP1 overexpression in these cells over time. Due to 4E-BP1's function as a translation modulator, it is very likely that its overexpression causes many downstream effects including inevitable secondary effects, possibly induced by transcriptional responses. This kind of secondary effects sought to be avoided in order to more accurately depict the direct effects of 4E-BP1 activity. Secondary effects result from the upregulation of other proteins in response to the upregulation of 4E-BP1 effectors and could induce self-amplifying cascades of proteome alterations. Lysing cells as soon as 4E-BP1 is sufficiently overexpressed may reduce the detection of overlying secondary effects in subsequent quantitative mass spectrometry experiments. T-REx HEK293 4E-BP1[WT] clone 5 and 4E-BP1[TA] clone 2 were activated by 1 µg/ml tetracycline for different time periods to investigate by immunoblotting when 4E-BP1 level was accumulated. The relative amount of 4E-BP1, normalised to loading control, was calculated. Three different immunoblots with three independent biological replicates per clone were pooled and displayed in a graph (Fig. 3.12). The values were fitted to nonlinear regression curves and a typical immunoblot for each clone is shown below the graphs as well. After analysing this data, it was found that 4E-BP1 began to get convincingly overexpressed 6 h after tetracycline treatment, before reaching a maximum after around 24 h. Hence, 6 h of tetracycline treatment was best for quantitative mass spectrometry analyses of 4E-BP1 downstream effects.
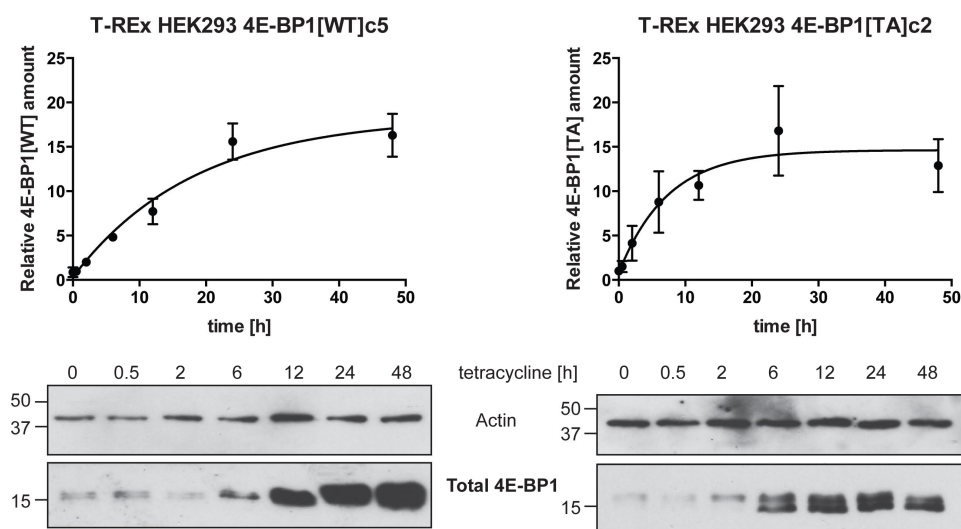
Figure 3.12: Time course of 4E-BP1 overexpression in T-REx HEK293 cells. T-REx HEK293 4E-BP1[WT] and 4E-BP1[TA] were treated with 1 μg/ml tetracycline over different times to induce 4E-BP1 overexpression. 4E-BP1 was analysed by immunoblotting with total 4E-BP1 antibodies. Actin served as loading control. Three immmunoblots of 4E-BP1[WT] and 4E-BP1[TA] were pooled together to calculate the graphs (n = 3). A typical immunoblot for every clone is displayed below each graph. The molecular weight is indicated on the left hand side in kDa. Data points in each graph were fitted by nonlinear regression. R^2[WT] 0.97, R^2[TA] 0.94. Data are presented as mean ± s.e.m.

3.3.5 Evaluating 4E-BP1 downstream effectors in T-REx HEK293 cells as potential indicators of 4E-BP1 activity

Although it is important to know the time course of 4E-BP1 overexpression in T-REx HEK293 cells, for calculating the optimal overexpression time for mass spectrometry experiments it would be good to know when overexpressed 4E-BP1 starts to have an effect on the proteome. This is a cyclical problem, because solving it requires to know the identity of 4E-BP1 downstream effectors, which is the aim of this study to begin with. Nonetheless, several publications revealed proteins, which are affected by 4E-BP1. However, these studies investigate the effect of 4E-BP1 on these target proteins mostly in a very specific context, e.g. in cancer, under hypoxia etc. Other 4E-BP1 targets, which may be more promising to this study have been identified in general studies of 4E-BP1 or in the context of neurodegenerative diseases. One investigation by Morita et al. (2013) in human MCF7 cells identified 4E-BPs as negative regulators of several mitochondrial proteins like TFAM, a mitochondrial transcription factor. They revealed that treat-

80

ing MCF7 cells with mTOR inhibitors like Torin1 downregulated TFAM in a 4E-BP1 dependent manner. Another study by Pierce et al. (2013) showed that feeding mTOR inhibitor rapamycin to AD mouse models increased the level of HSP90, a chaperone protein required to protect cells against stress and involved in protein degradation.

In an attempt to verify the action of 4E-BP1 in my cellular model, 4E-BP1 overexpression was induced in T-REx HEK293 cells and the effect on TFAM and HSP90 investigated with specific antibodies in immunoblots (Fig. 3.13A). As a further control and to make the experiments more consistent with the two published studies, the change of TFAM and HSP90 amount after treatment of normal HEK293 cells with mTOR inhibitors rapamycin, Torin1 and AZD8055 was also checked (Fig. 3.13B). Unfortunately, neither in T-REx HEK293 nor in normal HEK293 cells a change of TFAM or HSP90 level after 4E-BP1 overexpression or activation could be detected.
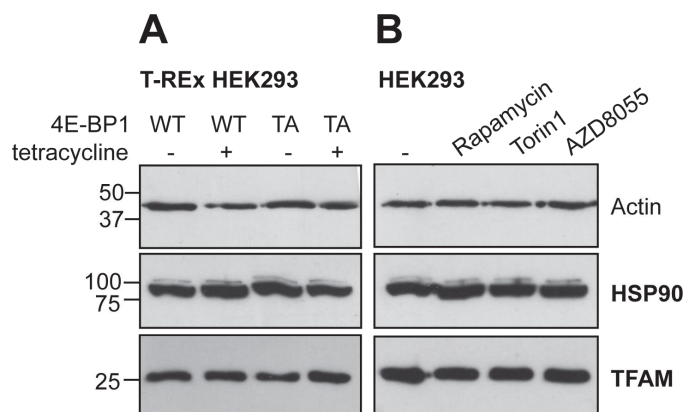
Figure 3.13: Effect of 4E-BP1 overexpression or activation on HSP90 and TFAM in T-REx HEK293 and normal HEK293 cells. T-REx HEK293 cell clones were treated with 1 µg/ml tetracycline for 24 h to induce 4E-BP1[WT] or 4E-BP1[TA] overexpression (A). HEK293 cells were treated for 2 h with 100 nM rapamycin, 250 nM Torin1 or 100 nM AZD8055. HSP90 and TFAM were analysed by immunoblotting with specific antibodies (n = 1). Actin served as loading control. The molecular weight is indicated on the left hand side in kDa.

In order to investigate whether the difference between my findings and previously published results may be partly due to different biological backgrounds, MCF7 cells were analysed side by side with HEK293 cells and treated with Torin1 and AZD8055. Immunoblots revealed that the effect of these mTOR inhibitors on 4E-BP1 phosphorylation state is similar in both cell lines, but the effect on TFAM amount is different. While 4E-BP1 dephosphorylation in HEK293 had no effect on TFAM, it was reduced in

Figure 3.14: **Effect of 4E-BP1 activation on HSP90 and TFAM in MCF7 and HEK293 cells.** MCF7 and HEK293 cells were treated for 2 h with 250 nM Torin1 or 100 nM AZD8055. Total 4E-BP1, Phospho-4E-BP1, HSP90 and TFAM were analysed by immunoblotting with specific antibodies (n = 1). Actin served as loading control. The molecular weight is indicated on the left hand side in kDa.
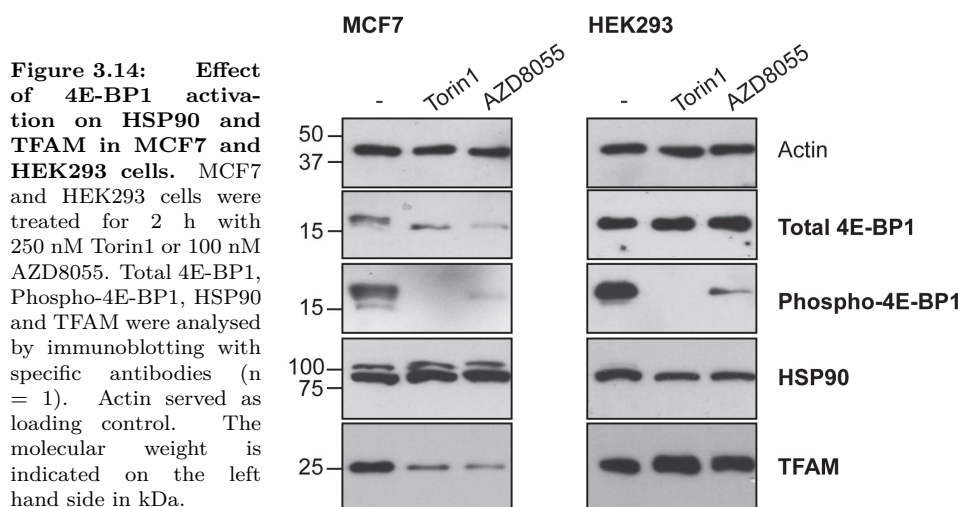
MCF7 cells (Fig. 3.14). This emphasised once again that the model system is very important for further conclusions and applications. MCF7 are human cancer cells and findings in this cellular context might not be applicable to a more physiological model systems so easily.

For this study, these results imply that the time course of 4E-BP1 overexpression described in the previous section remains the best indicator to assess a suitable time point for cell lysis and quantitative mass spectrometry.

3.4 Discussion

The aim of this chapter was to identify, develop and evaluate a human cellular model overexpressing 4E-BP1, which can be used for quantitative mass spectrometry to study the effects of 4E-BP1 activity on the cellular proteome. The T-REx HEK293 model is a very elegant model for this purpose. First of all, HEK293 cells is a human, non-cancer cell line. A common feature of cancer cell lines is exponential proliferation ignoring limiting signals, including contact inhibiton. Contact inhibiton is regulated by the mTOR pathway and 4E-BP1 (Azar et al., 2010) and a misregulated mTOR pathway may bias the effects on 4E-BP1 downstream effectors.

In this chapter was also revealed that different mTOR inhibitors act differently on 4E-BP1 in different cell lines, a phenomenon which has been reported before (Choo et al., 2008; Feldman et al., 2009; Huo et al., 2012;

Thoreen et al., 2009). Rapamycin binds mTOR together with FKBP12, but does not inhibit all functions of the mTORC1 complex. Next generation active-site-directed inhibitors, which compete with ATP for binding to the kinase domain like Torin1 and AZD8055 are much more potent and block not only mTORC1, but also the mTORC2 complex. The stronger inhibition of mTOR could be demonstrated here by dephosphorylation of 4E-BP1.

Compared to RPE1 cells, HEK293 cells are less physiological due to their hypotriploid genome. Furthermore, RPE1 are of neuronal origin, while HEK293 cells show many neuronal characteristics e.g. neuronal filaments, brain specific Hexokinase I and neuronal enolase, but lack in other characteristics e.g. nestin expression, a brain specific intermediate filament (Shaw et al., 2002). Due to their expression of neuronal and non-neuronal characteristics, HEK293 cells were described as early differentiating neurons. At least, many indications emphasised that RPE1 and HEK293 share the same developmental origin as ectodermal cells.

The difficulties which appear when using HEK293 rather then RPE1 cells are more than compensated by the advantages of the T-REx HEK293 cell system. It allows stable integration of 4E-BP1 into the genome and to use the very same cells with exactly the same genome for experiment or control depending on whether tetracycline is added to the medium or not. Due to the fact that control and experiment conditions are very congruent, biasing side effects will be avoided, which may interfere with the results otherwise. Leaky expression of the transgene may be a confounding issue in this model, but my analyses showed that no detectable leaky expression was present, which emphasised the robustness of the model. Furthermore, time course studies are possible with this model since 4E-BP1 expression can be controlled by timed addition of tetracyline. Theoretically, with this model one can study and compare the time depended effect of 4E-BP1 on the proteome depending on how long it is overexpressed.

Furthermore, this chapter revealed that endogenous 4E-BP1 amount is clearly dependent on the kind of cell line. While HEK293 and RPE1 cells showed about the same level of 4E-BP1 expression, it was clearly reduced in SH-SY5Y cells. On the one hand, this is contradicting the data released by the Human Proteome Atlas where they used a scoring system to quantify immunofluorescence of expressed 4E-BP1 among different cell lines by immunocytochemistry. On the other hand, the Human Proteome Atlas project

has revealed that many other human cancer cell lines have reduced 4E-BP1 expression levels. The advantage of my approach is that a scoring system was unnecessary. Instead, the protein amount was compared directly by blotting equal amounts of protein lysates on the same membrane. Furthermore, three different antibodies against different epitopes of the same protein were used here: total 4E-BP1, phospho-4E-BP1 and non-phospho-4E-BP1 antibodies. Among these antibodies, all my findings were consistent, which strengthens the conclusion that 4E-BP1 is indeed reduced in SH-SY5Y cells.

Another important aspect this chapter revealed is that 4E-BP1 downstream effectors can be very context and model dependent. The effect of 4E-BP1 on HSP90 and TFAM, reported by Pierce et al. (2013) in mouse models and by Morita et al. (2013) in human cancer MCF7 cells, could not be transferred to HEK293 cells. However, after repeating the exact procedure of the experiment in the same model described by Morita et al. (2013), their findings could be reproduced. This emphasised again that the effect of 4E-BP1 depends on the model system and the experimental set-up, e.g. whether one treats the model with mTOR inhibitors, knockdown or overexpress 4E-BP1.

In conclusion, a T-REx HEK293 cellular model was developed in this chapter, which was validated for the known regulation of 4E-BP1 and is ready to be used in quantitative mass spectrometry experiments.

Chapter 4

Development of an *in vivo Drosophila* model overexpressing d4E-BP

4.1 Background

4.1.1 *Drosophila* as an *in vivo* model

It is a very attractive and long pursued strategy to study proteins and their effects *in vitro*. The advantages are obvious: immortal cell lines can be amplified fast and easily and manipulations can be conducted comparably simple. However, *in vivo* models are also attractive and confer certain advantages over *in vitro* models. They allow studying the effect of genetic or external manipulations in a more complex system. Cultured cells are generally very homogenous in their gene expression, protein environment and in their response to different stimuli. Although this is one reason for the attractiveness of *in vitro* systems, it excludes several factors, which could be important to understand the impact of different regulators. One obvious difference of *in vivo* systems is their multicellularity. While in an *in vitro* system all cells are clonal copies of each other, cells specialise in multicellular organisms by activation and inactivation of different genes and interact with each other. Specialised cells form specific tissues, which are responsible for different tasks to keep the organism alive. This structure implies that different cells and tissues of one organism can respond differently to the

same stimulus and the accumulated responses account for the total response of the organism. Thus, *in vivo* model can give a much better indication on how a stimulus affects a living organism.

The fruit fly *Drosophila melanogaster* is a model, which has been studied for about a century. Hence, a lot of reference data has already been published about its genetic and molecular pathways, mechanisms of development and control of behaviour and can be consulted to assess the gained data of experiments. The available data revealed that gene sequences and function are highly conserved between flies and humans (Rubin et al., 2000). The *Drosophila* genome is completely sequenced and consists of approximately 13,600 genes (Adams et al., 2000). *Drosophila* is very easy to breed. They require no complex diet, but amplify quickly. At 25 °C, *Drosophila* has a generation time of approximately ten days to develop from an egg to an adult fly. A single pair of flies can produce hundreds of offspring, which guarantees the production of required number of individuals for every experiment. In comparison with other organisms, flies do not require much storage space and are easy to handle. Genetic manipulations can be achieved easily by homologous recombination of injected transgenes into the oocyte.

Despite its simplicity, *Drosophila* has many characteristics, which makes it attractive to investigate function of human organ systems or pathology of human diseases. In particular, *Drosophila* exhibits a simple, but well developed central nervous system with approximately 100,000 neurons, which allows studying neurodegenerative diseases like PD (Whitworth, 2011). 200 *Drosophila* neurons were characterised as dopaminergic neurons, which are predominantly affected by degeneration in PD. The function of the nervous system is highly conserved between *Drosophila* and humans, e.g. many identified PD risk genes are conserved in *Drosophila* and mutation of them leads to comparable locomotor deficits and loss of dopaminergic neurons. Among them are also *PINK1* (32 % sequence identity with fly homologue), *PARK2* (42 % sequence identity with fly homologue) and *LRRK2* (26 % sequence identity with fly homologue). The TOR pathways is also conserved in flies with its 4E-BP1 homologue Thor. Together, these characteristics make *Drosophila* a highly suitable model to study 4E-BP *in vivo* in the context of different pathophysiological conditions.

4.1.2 *Drosophila* genetics

Drosophila melanogaster carries a diploid chromosome set of 4 chromosomes. The first pair are gonosomes X or Y. In contrast to humans, the presence of the Y chromosome does not determine the sex, but the ratio of X chromosomes to autosomes. The Y is with about 40 Mbp much larger than the X chromosome with 22.4 Mbp. Despite its size, only very few protein coding genes have been identified on the Y chromosome (Bernardo Carvalho et al., 2009). The second and third chromosomes are the biggest with 44.1 Mbp and 52.4 Mbp, while the last chromosome is quite tiny with 1.35 Mbp. For this reason, the fourth chromosome is mostly ignored for transgenic applications, while these are normally carried out on the large chromosomes X, 2 or 3.

In nomenclature, wildtype chromosomes are designated by a "+", while mutations or transgenes are described by names or abbreviations. When more than one mutation or transgene is located on one chromosome, they are written in sequences separated by commas. If flies are heterozygous for a transgene or mutation, the transgenic chromosome is separated by a slash from its wildtype counterpart (e.g. *mutant/+*). In case flies are homozygous, the slash becomes obsolete (e.g. *mutant*). If more than one chromosome is mutated or modified by a transgene, the chromosomes are designated in the correct order from X to 4, separated by a semicolon (e.g. *mutant; transgene*).

4.1.3 The usage of balancer chromosomes

A special genetic tool commonly used in *Drosophila* are balancer chromosomes. Balancer chromosomes are the result of multiple artificial chromosome inversions. This prevents crossing over events during meiosis between the balancer chromosome and the matching functional chromosome. Furthermore, balancer chromosomes carry recessive lethal mutations, which means that balancer chromosomes are not homozygous viable. An exception are X chromosome balancers, which have to be homo- and hemizygous viable otherwise males would not inherit these balancers. The purpose of balancer chromosomes are that you can maintain a mutation or transgene stably on a chromosome and prevent genetic drift through recombination. In this way it is possible to maintain a transgene or mutation in a stock

without sequencing individual offspring of every generation. Sequencing individual flies without killing them is impossible, which is why the strategy to work with balancer chromosomes is so popular in *Drosophila*.

Balancers usually carry dominant and recessive visible mutations, which means that flies show a certain phenotype. By following the balancer phenotypes, it is possible to draw conclusion from the balanced partner chromosome and to select flies with a distinct genotype in this way. In this study, the balancer *CyO, TM6B* and *FM7c* were utilised. *Gla* and *If* also appear in this study, but are no balancer chromosomes, but mutated 2nd and 3rd chromosomes with a recessive phenotype, which are the partner chromosomes to maintain balancer fly stocks. *CyO* is a 2nd chromosome balancer and *TM6B* is a 3rd chromosome balancer, while *FM7c* balances the X chromosome. Most characteristic phenotypical effects of different balancer chromosomes are displayed in figure 4.1. *CyO* exhibit curled-up wings, *Gla* leads to smaller, "glassy" eyes, *If* to slit-shaped eyes, *TM6B* to increased numbers of humeral bristles and *FM7c* to kidney-shaped eyes in heterozygosis or slit-shaped eyes in homo- and hemizygosis.

All transgenes utilised in this study also had a phenotypic marker to trace them. They were all w^+, which means that they exhibited red or orange eyes in contrast to white eyed mutant background (w^-).
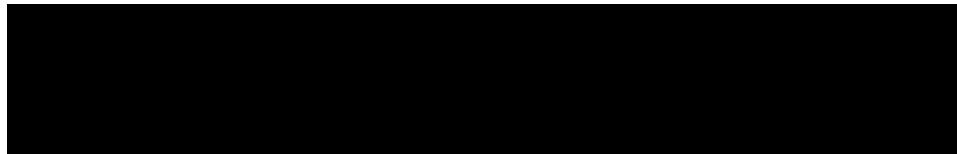
Figure 4.1: Sketch of typical phenotypic changes caused by mutated and balancer chromosomes. The phenotypes are displayed as they appear in flies carrying one copy of the indicated chromosome. *CyO*: curled-up wings *Gla*: smaller, "glassy" eyes *If*: slit-shaped eyes *TM6B*: increased numbers of humeral bristles *FM7c*: kidney shaped eyes. Adapted from Roote and Prokop (2013)

4.1.4 The UAS-GAL4 overexpression system

To overexpress transgenes in *Drosophila*, the UAS-GAL4 system was utilised in this study. It consists of two elements: the yeast transcription activator protein GAL4 and the upstream activation sequence (UAS) to which GAL4 specifically binds and initiate transgene transcription. The separation of these two elements allows controlling transgene expression depending on the kind of GAL4 element. Typically, GAL4 is using the promoter of an en-

dogenous gene, e.g. Actin-GAL4 uses the actin promoter. In this way, you can limit transgene overexpression to defined tissues, depending on the promoter activity of the GAL4 driver. In this study, the following *Drosophila* GAL4 lines were utilised: the ubiquitous GAL4 line da-GAL4, the muscle specific Dmef-GAL4 line, the preferentially muscle-expressed 24B-GAL4 line, the neuronal elav-GAL4 line and the hedgehog GAL4 line (hh-GAL4). These driver lines were crossed with the transgenic lines to initiate transgenic overexpression in the F1 generation. Driver inducing overexpression of certain transgenes are indicated by ">" between driver and transgene (e.g. *driver>transgene*).

4.2   Hypothesis and aims

Drosophila melanogaster is a very well known and over years extensively studied *in vivo* model. It is easy to handle and to breed. *Drosophila* was chosen as a model to overexpress wildtype (d4E-BP[WT]) or mutant (d4E-BP[TA]) *Drosophila* 4E-BP (d4E-BP) *in vivo* analogously to the cellular model described before (see chapter 3). In order to avoid misunderstandings, the term d4E-BP will be used to describe transgenic *Drosophila* 4E-BP overexpressed in flies, while Thor is describing endogenous 4E-BP of *Drosophila* in this study.

This model shall be used to study the effect of d4E-BP overexpression in a complex living organism to learn more about its effects beyond the knowledge gained by cellular models. In particular behavioural changes upon d4E-BP overexpression in an endogenous knockout background and PD mutants may give further evidence of the rescuing capability of d4E-BP[WT] and d4E-BP[TA] under these conditions.

The *Drosophila* model shall be designed in a way to make it applicable for quantitative mass spectrometry to identify translationally upregulated proteins upon d4E-BP overexpression. It is the aim to compare these results with the mass spectrometry results gained from the cellular model to identify similarities and differences between the *in vitro* and the *in vivo* model. These comparisons may give more information about the importance of 4E-BP downstream effectors in a whole organism.

The developed *Drosophila* model shall also be applicable for further studies to assess the impact of different d4E-BP effectors identified by mass

spectrometry in the future.

4.3 Design of transgenic lines

The design and strategy of making transgenic *Drosophila* lines for subsequent experiments was a very important part of this study. It required very careful considerations about what these lines should achieve and with which experimental protocols they have to be compatible.

Like for the cell model, two different strains were generated: a line overexpressing wildtype d4E-BP[WT] and a line overexpressing constitutively active d4E-BP[TA], carrying two point mutations at position 37 and 46. At these positions, threonine was replaced by alanine, which prevents phosphorylation and inactivation of d4E-BP. These phosphorylation sites are very well conserved among different species, although the protein sequence identity of human 4E-BP1 and d4E-BP is just 49 %. Both constructs were generated and kindly provided by Aurelio Teleman (DKFZ, Heidelberg, Germany).

A serious problem when dealing with d4E-BP is that no high quality antibody is available to detect the protein in immunoblots or immunofluorescence. Most commercial antibodies are optimised for humans and mice. In order to avoid later detection problems, d4E-BP was tagged with an N-terminal FLAG-tag (DYKDDDDK). 4E-BP has been successfully tagged several times in different model systems, e.g. with hemagglutinin (Gingras et al., 2001), glutathione S-transferase (Gingras et al., 2001), polyhistidine (Gingras et al., 1999), myc (Wang et al., 2003), GFP (Rong et al., 2008) or even FLAG (Hughes et al., 1999). 4E-BP remained always functional after attaching the tag. It was constantly tagged at the N-terminus, because the C-terminus was reported to bear multiple regulatory features for its function and phosphorylation (Wang et al., 2003).

For transgenesis, site-specific integration of *UAS-FLAG-d4E-BP* was favoured over a random integration for three reasons: 1) To raise comparability between wildtype and mutant *d4E-BP* lines. If both constructs are integrated in the same position then these lines differ just by their constructs without biasing background effects. 2) To avoid destroying important genes. Random integration may disrupt genes which causes a phenotype itself. A site-specific integration prevents unintentional background effects. 3) To

choose the optimal position for later recombinations. The transgenic lines may be recombined with other mutants to overexpress d4E-BP in a certain genetic background. If one consider possible recombinations for establishment in the future, a matching integration site can be chosen.

In this study, *d4E-BP* was integrated by attP site-specific recombination initiated by λ-integrase. Transgenic d4E-BP was planned to be overexpressed in endogenous d4E-BP knockout lines (*Thor²*) or parkin (*park²⁵*) or Pink1 (*Pink1^{B9}*) knockout lines as PD models. In the former case, the aim is to study how well transgenic d4E-BP can replace endogenous d4E-BP, while it is to study the rescuing capability in a disease model for the latter one. Transgenic d4E-BP should be integrated on the right arm of the second chromosome (cyto site 51C1 or 55C4, Fig. 4.2) as endogenous *Thor* is located on the left arm of the second chromosome (cyto site 23F3-23F6), while *park* is based on the left arm of the third chromosome (cyto site 78C2-78C2) and *Pink1* on the X chromosome (cyto site 6C6-6C6). The selected integration sites allowed easy recombinations with the described mutants.
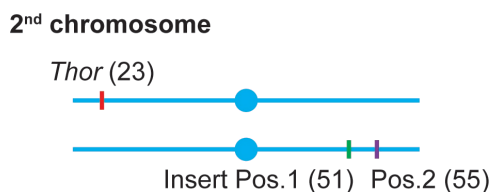
Figure 4.2: Sketch of 2nd chromosome pair of *Drosophila melanogaster*. The position of endogenous d4E-BP *Thor*, 23F3-23F6, is indicated on the left arm of the chromosome, while the integration sites of the transgenes in this study are located on the right arm of the chromosome in position 51C1 (Position 1) or in position 55C4 (Position 2). In both cases it is far apart from *Thor*, which allows the generation of recombinants with endogenous d4E-BP knockout lines (*Thor²*).

4.4 Generation of transgenic lines

In order to generate transgenic *Drosophila* lines overexpressing N-terminal FLAG-tagged d4E-BP[WT] or d4E-BP[TA], the provided *d4E-BP* constructs had to be cloned from pAT322 and pAT324 vectors into the pUAST.attB vector. This vector contains attB recognition sequences, which are required to initiate site-specific recombination with the attP element in the *Drosophila* genome. To achieve this, FLAG-d4E-BP 5'-3' primers were designed, which contained one *Eco*RI endonuclease recognition sequence followed by the FLAG-tag sequence. This primer together with the 3'-5' pAT322 primer were utilised to amplify d4E-BP constructs from the orig-

inal vector by PCR and to attach the FLAG-tag at the same time. The amplified constructs had a size of 478 bp (Fig. 4.3A). The PCR product were extracted, digested with *Eco*RI and *Xho*I and ligated into the target vector pUAST.attB.
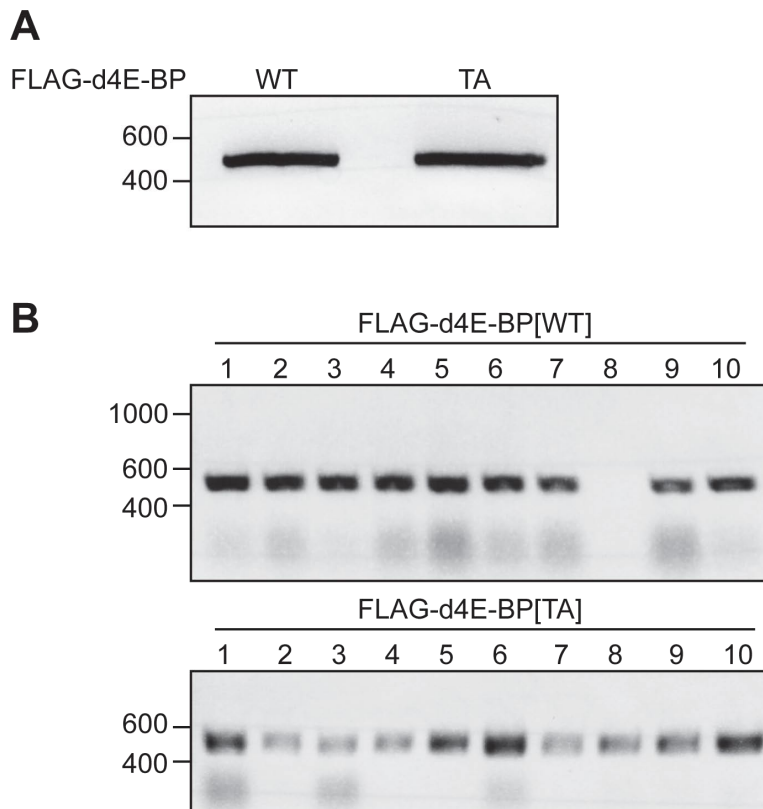
Figure 4.3: *FLAG-d4E-BP[WT]* and *FLAG-d4E-BP[TA]* PCR products in agarose gel. (A) *FLAG-d4E-BP* genes were amplified from pAT322/324 vectors by PCR and purified by gel electrophoresis. The calculated size of both PCR products is 478 bp. (B) Integration success of *FLAG-d4E-BP* genes into pUAST.attB vector was reviewed in ten transformed *E. coli* colonies per genotype (1 - 10). The calculated size of successfully integrate genes is 510 bp. DNA markers are indicated on the left hand side in bp.

The new *FLAG-4E-BP[WT/TA]* carrying plasmids were amplified in 10-β competent *E. coli* bacteria and the success confirmed in different bacteria colonies by PCR (Fig. 4.3B). The plasmid DNAs of *FLAG-4E-BP[WT]* colony no. 6 and *FLAG-d4E-BP[TA]* colony no. 10 were extracted and sent to the Core Genomic Facility at the Medical School of the University of Sheffield for sequencing to exclude the possibility that unintentional mutations within the transgenes have been acquired during the cloning process. For sequencing, the same pUAST 5'-3' and 3'-5' primers have been used as
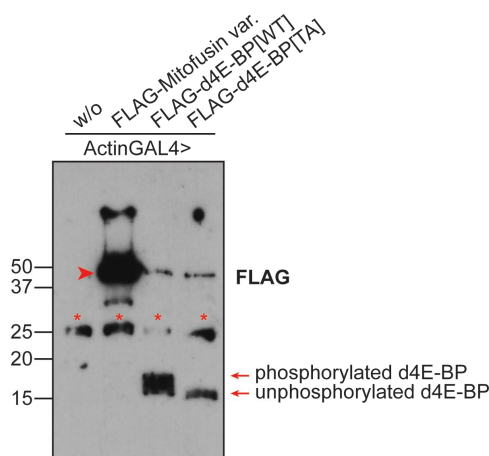
Figure 4.4: Functional test of *FLAG-d4E-BP[WT/TA]* plasmids. *Drosophila* S2R+ cells were co-transfected with *FLAG-d4E-BP[WT/TA]* and *Actin-GAL4*. Positive control was a FLAG-tagged mitofusin variant, highlighted by a red triangle in the blot. Cells were transfected with Actin-GAL4 only for negative control. Expression was analysed by immunoblotting of 50 µg proteins/lane from whole cell lysates and labelling with anti-FLAG antibodies (n = 1). Unspecific bands in all samples were indicated by asterisks. The molecular weight is indicated on the left hand side in kDa.

for previous PCRs. After confirming the genetic integrity, *E. coli* colonies were further amplified to gain plasmids for subsequent experiments.

To test whether the newly generated plasmids are functional, the constructs were overexpressed in the *Drosophila* S2R+ cell line. For this purpose, cells were co-transfected with *Actin-GAL4* and *FLAG-d4E-BP* carrying plasmids. The same UAS-GAL4 overexpression system as in flies was applied in these cells with Actin-GAL4 as driver for FLAG-d4E-BP overexpression. 72 h after transfection, 50 µg protein of lysed cells were separated on an SDS gel and immunoblotted subsequently using anti-FLAG antibodies. The blot clearly showed that FLAG-4E-BP[WT/TA] were expressed (Fig. 4.4). The size of the FLAG-d4E-BP protein was 14.1 kDa. Also, FLAG-d4E-BP[WT] emerged with a broader band on the membrane than FLAG-d4E-BP[TA], which corresponds to different phosphorylation states, while FLAG-d4E-BP[TA] is entirely unphosphorylated. As a positive control, a previously designed C-terminal FLAG-tagged mitofusin variant with a size of 41 kDa was utilised, while the negative control represents S2R+ cells transfected with the driver *Actin-GAL4* only.

After successfully testing the generated plasmids, they were posted to BestGene Inc. (USA) to make transformants. As host fly stock, BDSC stock 24482 was choosen. It is a FlyC31 strain and has an attP landing site on cyto site 51C1. After receiving five isolates of the transformants, the flies were crossed with second chromosome balancers *Gla/CyO* to generate a stable stock. Offspring of transgenic flies balanced with *CyO* were amplified and maintained for further analyses.

Transgene expression was analysed in a first approach by male transgenic

flies crossing with *da-GAL4* driver virgins to overexpress FLAG-d4E-BP ubiquitously within all fly tissues. The transcribed d4E-BP mRNA was quantified by qRT-PCR using the q-d4E-BP primer pair after reverse transcription of mRNA into cDNA. The overexpression of *d4E-BP* was quantified relative to the reference 18S ribosomal RNA.
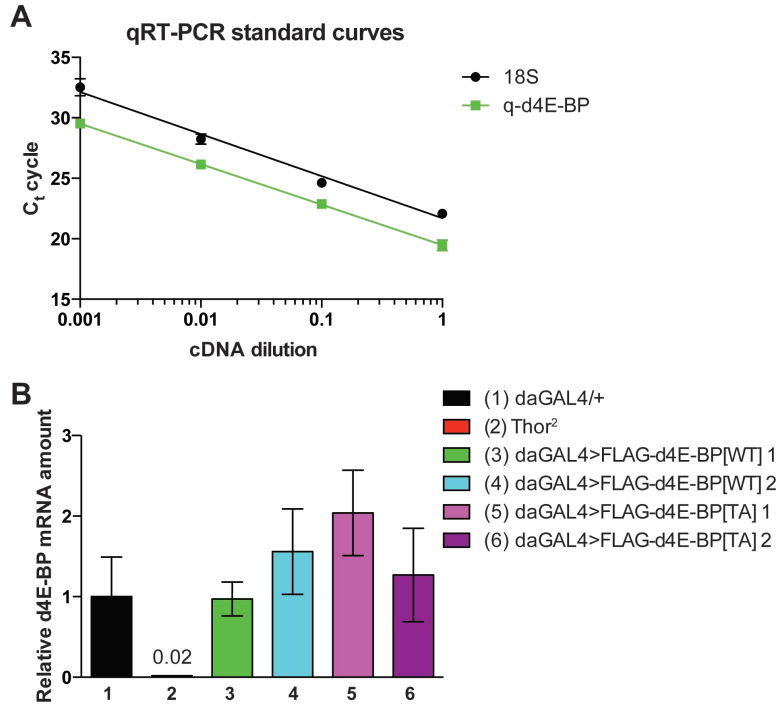
Figure 4.5: qRT-PCR of transgenic *Drosophila* lines overexpressing FLAG-d4E-BP[WT/TA]. (A) Threshold cycle (C_T) of primer pairs 18S and q-d4E-BP at different cDNA dilutions with constant primer concentration. The decadic logarithmic curves had slopes of -3.48 (R^2 0.98) for 18S and -3.35 (R^2 1) for q-d4E-BP. (B) Relative *d4E-BP* mRNA yield in *d4E-BP* transgenic flies. All values were normalised to the control *da-GAL4/+*. *Thor[2]* served as negative control. Error bars indicate standard deviation of three technical replicates.

The efficiency of both primers was determined with a *da-GAL4/+* cDNA dilution series of 1:10, 1:100 and 1:1000 from the standard concentration and qRT-PCRs were performed with constant primer concentrations. The average values of threshold cycles (C_T) for every cDNA dilution are displayed in figure 4.5A. Based on the slope of the C_T curves, the primer efficiencies were calculated with $E_{18S} = 93\,\%$ and $E_{q-d4E-BP} = 99\,\%$. Highly efficient primers would have efficiency values between 80 % and 105 %. Thus, values were completely in range and the primers could be utilised for qRT-PCR analyses.

The evaluated primers were used to study the new transgenic lines. Mea-

sured mRNA amount of two transgenic lines per genotype was normalised against mRNA yield of *da-GAL4/+*. *Thor²* served as negative control. The results show that *Thor²* is almost completely undetectable in the knockout, which emphasises the primer specificity (Fig. 4.5B). However, none of the two transgenic lines per genotype overexpressed *d4E-BP* at a convincing level. The strongest overexpression was detected for *d4E-BP[TA]* 1, but is only 2.04 times over control level. The expected overexpression level laid between 10 and 15 times over control. The reason for insufficient overexpression may be due to unsuccessful integration or ineffective transcription of transgenes.

4.5   Improvement of transgenic constructs

In order to tackle the problem of lacking transgenic d4E-BP overexpression, three different strategies were developed to improve the overexpression level (Fig. 4.6). The original constructs (o.c.) was led by an N-terminal FLAG-tag followed by d4E-BP[WT/TA]. In a first approach, a Kozak consensus sequence CAAAATG upstream of the FLAG-tag according to the sequence characterisation by Cavener (1987) was added (No. 2 in figure 4.6). A Kozak consensus sequence describes a short sequence of nucleotides 5' of the start codon, which are preferred for translation initiation at the ribosomes. Thus, it can improve translation and expression of transgenes. Cloning was performed using the previously designed constructs in the pUAST.attB vector as a template, Kozak-FLAG-d4E-BP and 3'-5' pUAST primers.
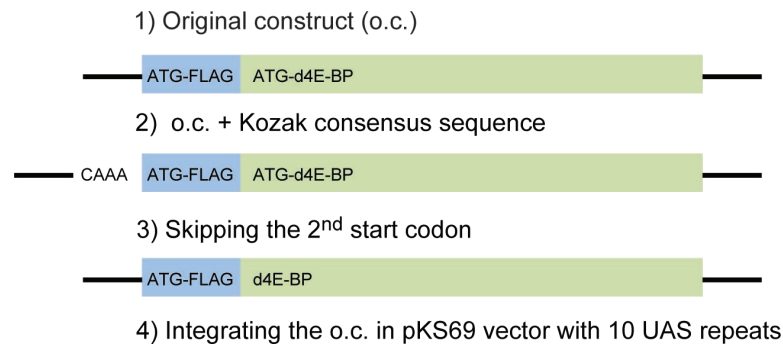
Figure 4.6: Scheme of different designs for FLAG-tagged *d4E-BP* transgenes. 1) The original construct (o.c.) has the FLAG-tag directly upstream of *d4E-BP*. 2) The second construct has the Kodak consensus sequence CAAAATG upstream of the FLAG-tag start codon. 3) The third construct lacks the start codon of *d4E-BP*, while the forth construct (4) matches the o.c., but is cloned in a different vector called pKS69.

In a second approach, a construct without the start codon of the d4E-BP transgenes was designed (No. 3 in figure 4.6). This design should avoid possible competitive and hindering effects of the FLAG-tag start codon and the closely downstream transgene start codon. Primers -2nd start-codon-d4E-BP and pAT322 were used to clone the construct of the transgenes into the pUAST.attB vector.
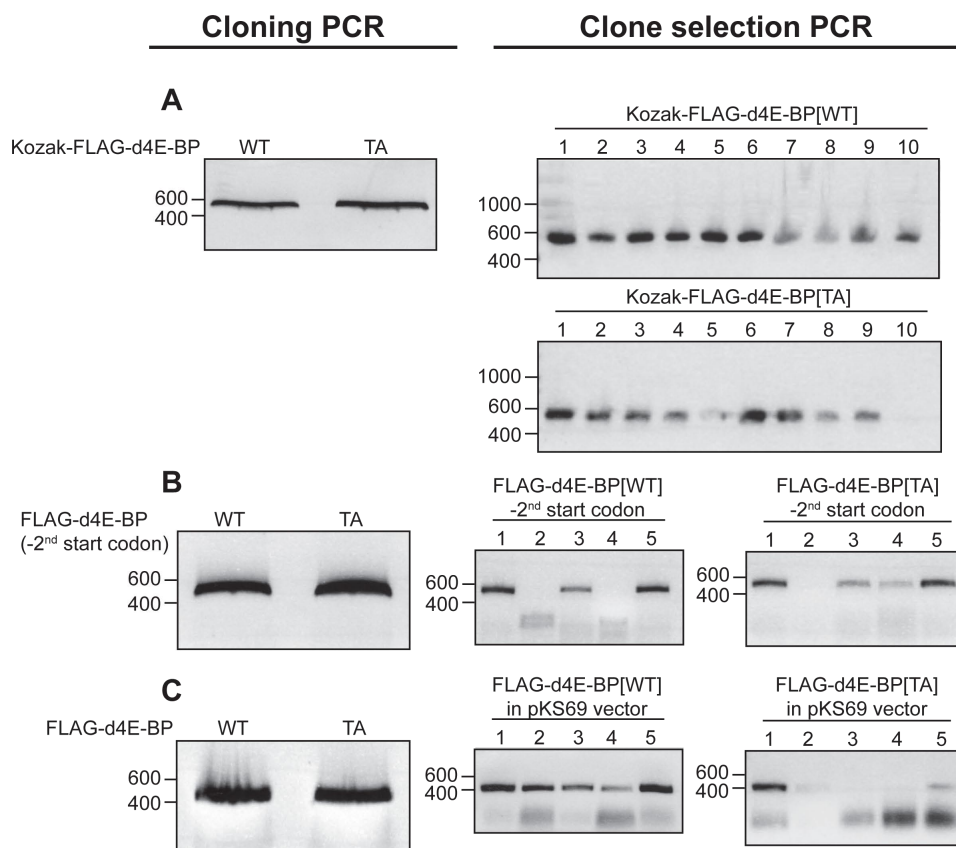
Figure 4.7: Different *FLAG-d4E-BP[WT]* and *FLAG-d4E-BP[TA]* constructs in agarose gel. (A) *Kozak-FLAG-d4E-BP[WT/TA]* were amplified from pAT322/324 vectors by cloning PCR and purified by gel electrophoresis. The calculated size of both PCR products is 482 bp. Integration success of *Kozak-FLAG-d4E-BP* genes into pUAST.attB vector was reviewed in ten transformed *E. coli* colonies per genotype (1 - 10) by clone selection PCR. The calculated size of successfully integrate genes is 514 bp. (B) The same strategy was utilised to clone and verify integration of *FLAG-d4E-BP[WT/TA]* constructs lacking the start codon of *d4E-BP*. The calculated size of cloning PCR products is 475 bp, while clone selection PCR gave products of 507 bp. (C) Also, the original constructs of *FLAG-d4E-BP[WT/TA]* described in section 4.4 were amplified and integration in pKS69 vector analysed by clone selection PCR. The cloning and clone selection PCR products had a size of 404 bp. DNA markers are indicated on the left hand side in bp.

In a last approach, the original constructs were cloned, as described in the previous chapter, into the pKS69 vector. For cloning PCR, FLAG-

d4E-BP and pKS69 primers were used to introduce a *Xba*I restriction site at the 5'-end of the construct. The pKS69 vector carries ten UAS repeats upstream of the transgene in contrast to five UAS repeats in pUAST.attB. The prolonged enhancer region allows more GAL4 proteins to bind, which may improve transgene transcription.

The different constructs were amplified by cloning PCR and the products are displayed in figure 4.7. After ligating the transgenes into their vectors using *Eco*RI and *Xho*I for constructs 2 and 3 or *Eco*RI and *Xba*I for construct 4 respectively, 10-β competent *E. coli* bacteria were transformed with them for amplification. Five or ten colonies were amplified for each construct and the clones were checked for successful integration by PCR using pUAST primers for constructs 2 and 3 (Fig. 4.7A and B) or FLAG-d4E-BP and pKS69 primers for construct 4 (Fig. 4.7C). In all cases clone 1 was amplified by Midi Prep and utilised for further tests.

After making the new constructs, the TA variants were utilised for co-transfection with *Actin-GAL4* into *Drosophila* S2R+ cells to test whether the genetic modifications had an effect on transgene expression. The cells were lysed 72 h after transfection, the proteins in the lysate quantified by Bradford assay and 50 µg protein per sample separated by SDS-gel electrophoresis before immunoblotting. However, labelling of the immunoblot membrane with anti-FLAG antibodies revealed that none of the new constructs substantially increased the expression of the transgene (Fig. 4.8).
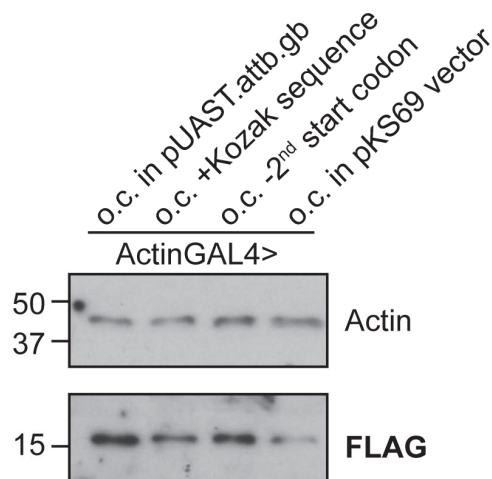
Figure 4.8: Functional test of different *FLAG-d4E-BP[TA]* constructs. *Drosophila* S2R+ cells were co-transfected either with the original construct (o.c.) *FLAG-d4E-BP[TA]* (o.c. in pUAST.attB), the construct with a 5' Kozak consensus sequence (o.c. +Kozak sequence), the construct lacking *d4E-BP*'s start codon (o.c. -2nd start codon) or the original construct in pKS69 instead of pUAST.attB vector (o.c. in pKS69 vector) and *Actin-GAL4*. Expression was analysed by immunoblotting of 50 µg proteins/lane from whole cell lysates and labelling with anti-FLAG antibodies (n = 1). Actin served as loading control. The molecular weight is indicated on the left hand side in kDa.

Thus, as it was impossible to improve the quality of the transgene itself, another way to improve the transgene expression in flies may be to decide

for a different integration site in the *Drosophila* genome. BDSC stock 8621 was chosen, which is a P{CaryP} strain and has an attP landing site on cyto site 55C4, close to to the previously tested integration at 51C1 (see section 4.4). The original transgenic *FLAG-d4E-BP[WT/TA]* constructs were sent to BestGene Inc. (USA) again to generate transformants. After receiving five isolates of them, the flies were crossed with second chromosome balancers *Gla/CyO* to generate a stable stock. Offspring of transgenic flies balanced with *CyO* were amplified and maintained for further analyses.

4.6 Detection of d4E-BP overexpression in transgenic lines

In order to test the functionality of the new transgenic flies carrying *FLAG-d4E-BP[WT/TA]* at position 55C4 on the second chromosome, overexpression of transgenes was induced by crossing *FLAG-d4E-BP[WT/TA]* males with *da-GAL4* virgins. The mRNA was quantified by qRT-PCR after reverse transcription into cDNA using 18S and q-d4E-BP primers (Fig. 4.9). The data clearly revealed that *d4E-BP* is overexpressed in all *d4E-BP* transgenic flies in contrast to previous flies with integration site 51C1 (compare figure 4.5B). This result was the first indication that the transgene was transcribed and changing the integration site resolved the problem of non-functional transgenic lines. The most samples showed similar overexpression
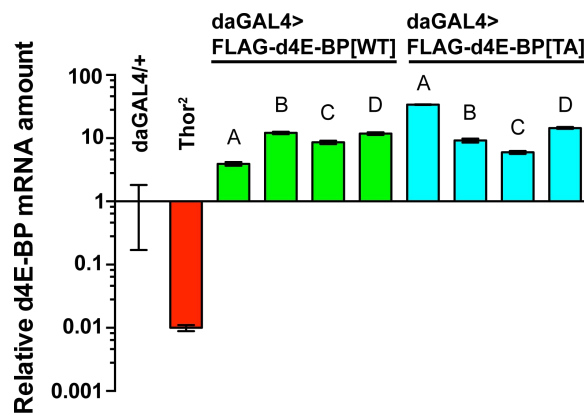
Figure 4.9: **qRT-PCR of transgenic *Drosophila* lines overexpressing *FLAG-d4E-BP[WT/TA]*.** Relative *d4E-BP* mRNA yield in four isolates per genotype of *d4E-BP* transgenic flies (A - D). All values were normalised to baseline control *da-GAL4/+*. *Thor²* served as negative control. Error bars indicate standard deviation of three technical replicates.

levels between ten and 15 times over control level. However, sample A of *d4E-BP[WT]* was clearly reduced compared to the others, while sample A of *d4E-BP[TA]* showed about double the amount than other samples. Higher levels of expression may be due to individual fluctuations in local chromatin architecture. The inconsistency of *d4E-BP[WT/TA]* samples A led to exclusion of these samples from further analysis.
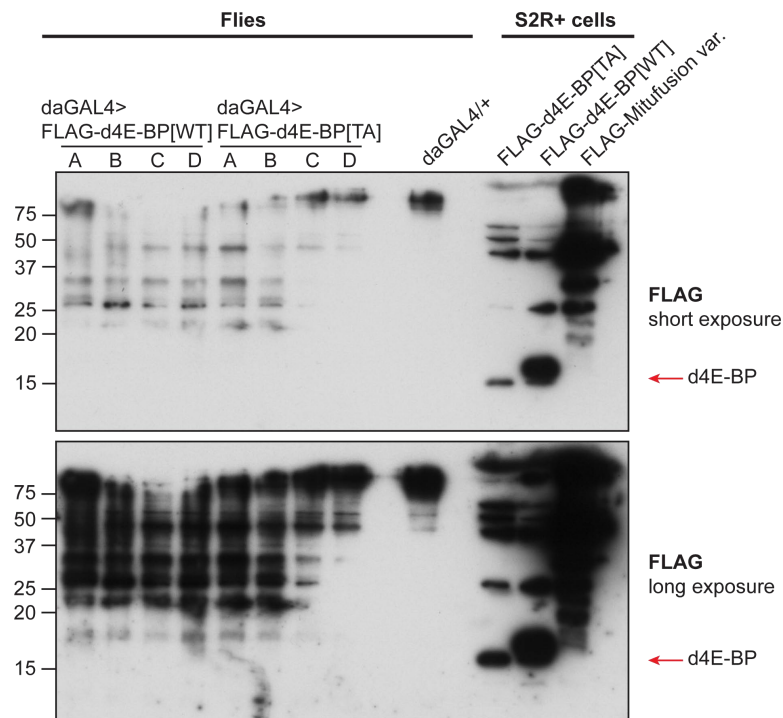
Figure 4.10: Immunoblot of transgenic flies. 50 µg of whole fly protein lysate per lane were blotted and labelled with anti-FLAG antibodies (n = 1). As positive controls, the same amount of transfected S2R+ cell lysate was loaded. Actin-GAL4 was driver for protein overexpression in S2R+ cells. FLAG-Mitofusin variant served as another positive control with a protein size of 41 kDa. FLAG-d4E-BP transgenic proteins have a size of 14.1 kDa. The same blot with long and short exposure is displayed. The molecular weight is indicated on the left hand side in kDa.

After confirming that new transgenic lines are functional, immmunblotting with *Drosophila* protein lysates of whole adult flies were performed utilising anti-FLAG antibodies to investigate translation of transgenic proteins. 50 µg proteins/lane were loaded on an SDS-Gel together with *da-GAL4/+* as negative control and the same amount of whole cell lysate from S2R+ cells transfected with the generated transgenic plasmids as positive control. A FLAG-tagged mitofusin variant of 41 kDa served as a further positive control. The results show that the transgenes could not be detected in any

of the four isolates per genotype, although there was a clear signal in the transfected S2R+ cells (Fig. 4.10). Even a very long exposure could not uncover specific bands of FLAG-d4E-BP in flies.

To determine whether the lacking FLAG-d4E-BP detection was due to technical problems or unforeseen biological issues, which prevent translation of transgenes, a second immunoblot was performed (Fig. 4.11). Instead of anti-FLAG antibodies, anti-Phospho-4E-BP1 antibodies were utilised to detect FLAG-d4E-BP[WT] or anti-Nonphospho-4E-BP1 antibodies for *FLAG-d4E-BP[TA]* transgenic lines. In all four isolates (A - D), signal bands of about 15 kDa were increased in almost all transgenic lines compared to the baseline control *da-GAL4/+*. Only isolate A of *FLAG-d4E-BP[WT]* lacked an overexpression signal. This result matched the outcome of qRT-PCR experiments, which confirmed a reduced overexpression of *FLAG-d4E-BP[WT]* of isolate A compared to isolates B - D (Fig. 4.9). Furthermore, isolates A of *FLAG-d4E-BP[TA]* showed stronger signal bands than the other isolates, which was also confirmed by qRT-PCR data. The bands disappeared completely in endogenous *Thor²* knockouts, which emphasised specific antibody binding. Nonetheless, the bands were not very "clean" and multiple bands appeared in all individual samples due to the fact that 4E-BP1 antibodies were not optimised for d4E-BP.

To further analyse whether the transgenic lines overexpressed FLAG-d4E-BP, transgenic recombinants with endogenous *Thor²* knockouts were made. This strategy should clear the background in immunoblots from endogenous d4E-BP and give a better answer to the question whether transgenic *FLAG-d4E-BP* is not only transcribed, but also translated. To generate recombinants, males of isolate C of *FLAG-d4E-BP[WT]* and isolate B of *FLAG-d4E-BP[TA]* were utilised (Fig. 4.9). These isolates were used for all subsequent experiments, if not indicated otherwise. Transgenic males were crossed with *Thor²* virgins. *FLAG-d4E-BP/Thor²* virgins of the F1 generation were subsequently crossed with *Gla/CyO* males. During this cross, recombinants should be generated by chromosomal crossover in prophase I of meiosis. Eight single males of the F2 generation with genotype *FLAG-d4E-BP, (Thor²)/CyO* were separated and mated with *Gla/CyO* virgins. Ten flies of the F3 generation from each individual stock were pooled together and their DNA used for PCR to check in which stocks recombinations had taken place. Gene spanning ext-Thor primers were designed for
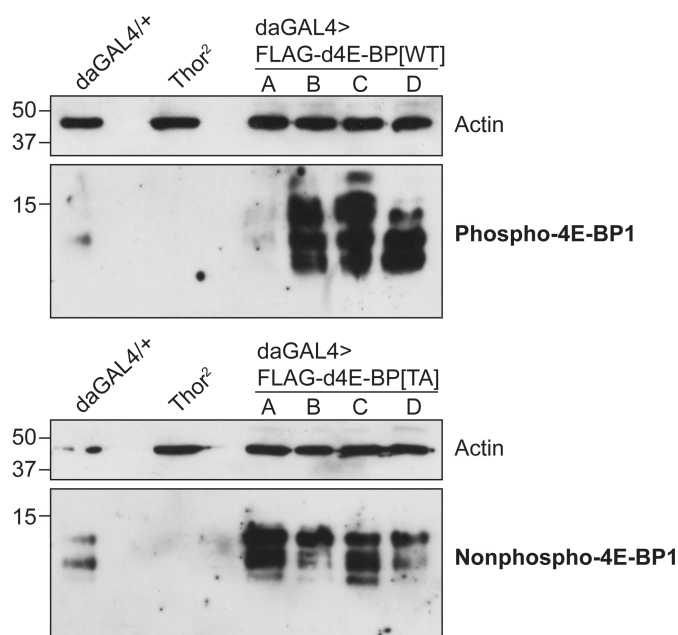
Figure 4.11: Immunoblot of transgenic flies. 50 μg of whole fly protein lysate per lane were blotted and labelled with anti-Phospho-4E-BP1 antibodies for four isolates *FLAG-d4E-BP[WT]* (A - D) or anti-Nonphospho-4E-BP1 for four replicates of *FLAG-d4E-BP[TA]* (A - D) (n = 1). *da-GAL4/+* was blotted to determine d4E-BP expression in wildtype, while the endogenous knockout *Thor²* is a negative control. Actin served as loading control. The molecular weight is indicated on the left hand side in kDa.

this purpose. The PCR results show positive recombination for recombinant stocks 1, 5 and 8 of *FLAG-d4E-BP[WT]* and stock 1, 4, 5 and 8 of *FLAG-d4E-BP[TA]* (Fig. 4.12A). Positive recombination is indicated by the appearance of 276 bp bands in the agarose gel, while endogenous wildtype *Thor* produces bands of 1.7 kbp. Stocks 5 of *d4E-BP[WT/TA]* were amplified and maintained for subsequent experiments.

In an initial experiment with generated recombinants, qRT-PCR was performed with and without driver da-GAL4 to investigate transgenic leak expression and functionality of transgenes in these new stocks. The results showed a bit more *d4E-BP* expression in transgenic flies without da-GAL4 driver compared to *Thor²*. However, the values are still 84 % (*FLAG-d4E-BP[WT]*) or 85 % (*FLAG-d4E-BP[TA]*) below wildtype level of *da-GAL4/+*. This indicated very little leak expression. Flies expressed 5.2 or 5.15 times more *d4E-BP* than wildtype controls, which approved functional transgenic overexpression in recombinants (Fig. 4.12B).

Next, protein lysates of recombinant 5 and also recombinant 8 of
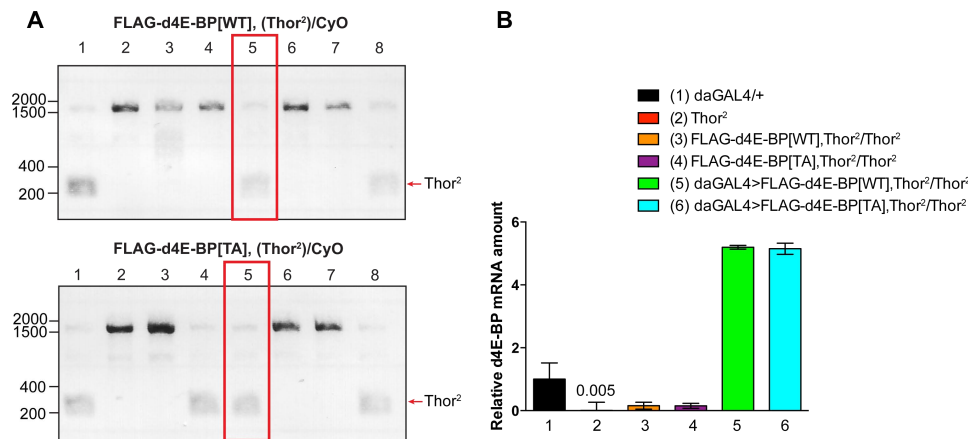
Figure 4.12: PCR and qRT-PCR of recombinant *Drosophila* lines *FLAG-d4E-BP[WT/TA], Thor²*. (A) PCR products of eight potential *d4E-BP[WT/TA], Thor²* recombinants in an agarose gel. Endogenous *Thor* knockout (*Thor²*) results in bands of 276 bp, while wildtype *Thor* produces bands of 1.7 kbp. Red framed stocks 5 were used for qRT-PCR. (B) Relative *d4E-BP* mRNA yield in recombinants of *FLAG-d4E-BP[WT/TA]* transgenic flies. All values were normalised to the wildtype control *da-GAL4/+*. *Thor²* served as negative control. Transgenic lines without driver da-GAL4 were measured to record transgenic leak expression, while it drove transgenic expression otherwise. Error bars indicate standard deviation of three technical replicates.

FLAG-d4E-BP[WT/TA], Thor² were separated on SDS-gels and blotted on PVDF membranes. The immunoblotting with anti-Phospho- and anti-Nonphospho-4E-BP1 antibodies revealed that multiple bands appeared only when transgenic overexpression was induced by da-GAL4 (Fig. 4.13). This showed that the expression was specific, but still produced multiple bands with anti-4E-BP1 antibodies. Furthermore, one could detect that anti-Phospho-4E-BP1 antibodies bound better to FLAG-d4E-BP[WT] than to FLAG-d4E-BP[TA]. However, the different phosphorylation state could not be confirmed clearly with anti-Nonphospho-4E-BP1 antibodies, although lower bands in recombinant 5 of *FLAG-4E-BP[TA]* showed stronger signals compared to *FLAG-d4E-BP[WT]*. Nonetheless, it was still questionable how well and specific these antibodies bind in *Drosophila*. Furthermore, the blots revealed that recombinant 8 of *FLAG-d4E-BP[TA]* was completely nonfunctional and is not overexpressing at all.

After continuing problems to detect the transgenes in immunoblots, a different strategy was developed to finally investigate transgenic translation without the poor anti-4E-BP1 antibodies in *Drosophila*. Instead of detecting denatured transgenic proteins, immunofluorescence experiments were performed *in situ* to visualise native proteins with anti-FLAG antibodies
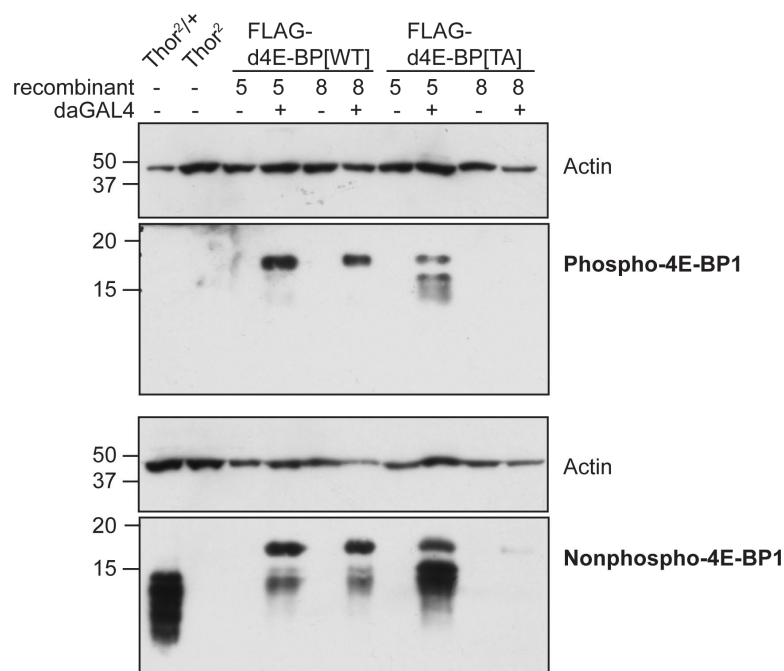
Figure 4.13: Immunoblot of recombinant *Drosophila* lines *FLAG-d4E-BP[WT/TA]*, *Thor²*. 50 μg of whole fly protein lysate per lane were blotted and labelled with anti-Phospho- or anti-Nonphospho-4E-BP1 antibodies. The blots derived from two separate SDS-PAGES of the same biological replicate (n = 1). A *Thor²* outcross was utilised as positive wildtype control, while homozygous *Thor²* served as negative control. Recombinants no. 5 and 8 of *FLAG-d4E-BP[WT/TA],Thor²* were analysed with and without da-GAL4 transgene driver. FLAG-d4E-BP transgenic proteins have a calculated size of 14.1 kDa. Actin served as loading control. The molecular weight is indicated on the left hand side in kDa.

in order to improve epitope binding. Transgenes were overexpressed by hedgehog-GAL4 driver (hh-GAL4) in *Drosophila* 3rd instar larvae. Hedgehog is a developmental gene, which is expressed in posterior cells of imaginal discs. These are structures which will develop into external features in adult flies, e.g. wings and legs . In this model, hh-GAL4 drove the expression of UAS-RFP. This allowed the exact determination of hh-GAL4 expression in the imaginal discs. Using immunofluorescence allowed determination of RFP and FLAG-d4E-BP[WT/TA] co-localisation. This was a very elegant approach, because it included a negative control in the very same sample. Indeed, the results showed a clear co-localisation of transgenes and RFP (Fig. 4.14). An outcross of *hh-GAL4/+* was utilised as an extra control to demonstrate that posterior binding of FLAG is specifically due to transgene expression in this area and not due to RFP expression.

After confirming transgene overexpression, genomic DNA of *FLAG-*

4E-BP[WT] isolate C and *FLAG-4E-BP[TA]* isolate B were sequenced at the Core Genomic Facility at the Medical School of the University of Sheffield along with pUAST primers. The results verified that the transgenes were completely intact, including the FLAG-tag and the two threonine to alanine point mutations at position 37 and 46 in FLAG-d4E-BP[TA]. The point mutations were indicated by a replacement of adenine by guanine in the codons ACG/GCG and ACT/GCT. Eventually, these results showed altogether that the transgenes were genetically intact, transcribed and translated. Thus, the transgenic *Drosophila* models could be used for further experiments.
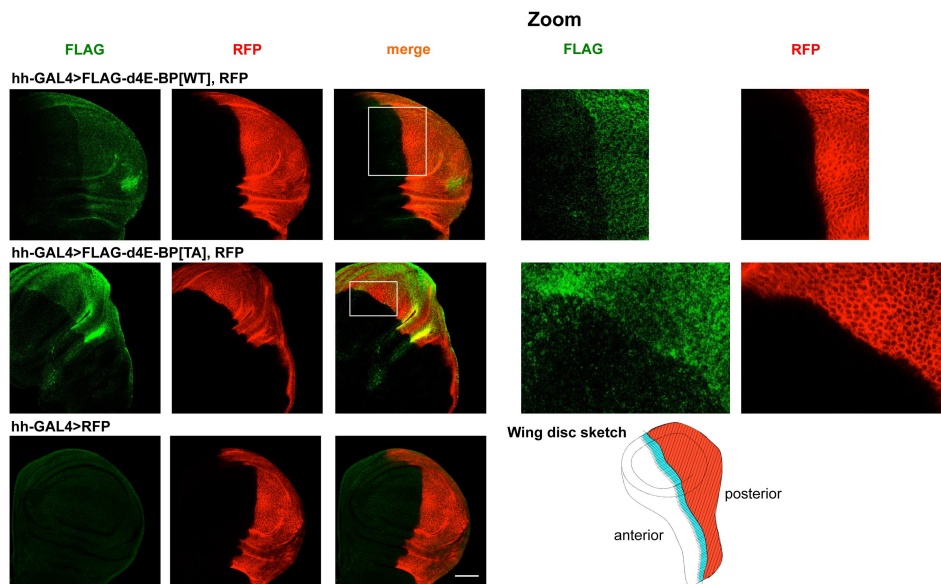
Figure 4.14: Immunofluorescence of FLAG-4E-BP[WT/TA] overexpressed by hh-GAL4 in the posterior wing imaginal disc part of *Drosophila* larvae. Wing imaginal discs from 3rd instar larvae were labelled with anti-FLAG (1:50). Hedgehog (hh) is only expressed in the posterior wing disc part as illustrated in the wing discs sketch. The hedgehog promoter is used to overexpress RFP. *hh-GAl4>RFP* served as negative control. The scale bar is 50 µm.

4.7 Evaluating the effect of d4E-BP overexpression in *Thor* knockout flies

After confirming that the transgenic lines overexpress FLAG-d4E-BP[WT/TA], it was important to investigate whether transgene overexpression caused a phenotype. To begin with, the focus laid on endogenous *Thor* knockout flies, *Thor²*, and their phenotype in motility

and lifespan. Tettweiler et al. (2005) have described that an incomplete deletion of *Thor*, *Thor¹*, shortens life span of *Drosophila*, while Bernal et al. (2004) have mentioned, but never shown, the same observation for *Thor²*. Motility evaluation is a further common straightforward strategy to determine the fitness of mutants.

As a first step, it was important to learn more about the phenotype of *Thor* knockouts. *Thor²* flies are homozygous viable and appear to be healthy and of normal size. Here, male and female *Thor²* flies were aged under standard conditions on standard diet and at 25 °C. The number of dead flies was counted everyday. Kaplan-Meier curves revealed that median lifespan of *Thor²* male and female flies were lower than in controls (Fig. 4.15). Controls were *Thor²* outcrosses with *w¹¹¹⁸*. Female *Thor²* flies lived a median life of 48.5 days compared to 67 days of controls, while male *Thor²* flies lived 30 days compared to 54 days of controls. These results demonstrated a very common aspect in nature that females live longer than males. Also, the effect of *Thor²* mutation appeared to affect males stronger than females, because the margin of median lifespan between mutants and controls was 18.5 days for females, but 24 days for males.
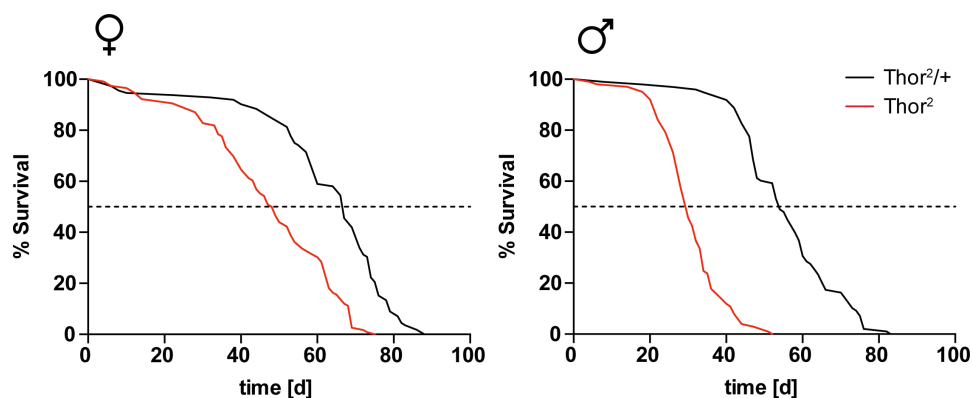
Figure 4.15: Lifespan of male and female *Drosophila* flies displayed in Kaplan-Meier curves. Female (♀) and male (♂) flies were maintained on standard food at 25 °C and surviving flies were counted every day. Median lifespan is indicated by dotted lines. $n \geq 98$

After investigating the differences between *Thor* knockouts and controls with respect to their lifespan, it should be studied whether knockouts also respond differently to stress, as 4E-BP has been described to be important for stress resistance. To achieve this, flies were fed with a 5 % sucrose solution instead of standard food. 5 mM paraquat was added to the solution.

Paraquat is a herbicide with redox activity, which leads to toxic superoxide production. Paraquat was previously linked to development of common symptoms of PD (Tanner et al., 2011). Feeding the toxin to flies reduced the median lifespan of control and mutant flies dramatically. Female and male controls had a median survival of 13 days, while it was reduced to nine days for *Thor²* females or seven days for *Thor²* males, respectively (Fig. 4.16). Flies not treated with paraquat survived the whole 15 days duration of the assay almost completely and independent of the genotype. Thus, it became clear that *Thor²* flies were also more sensitive to stress than controls, while again males exhibit a stronger phenotype than females. For this reason, only male flies were used for all subsequent behavioural experiments.
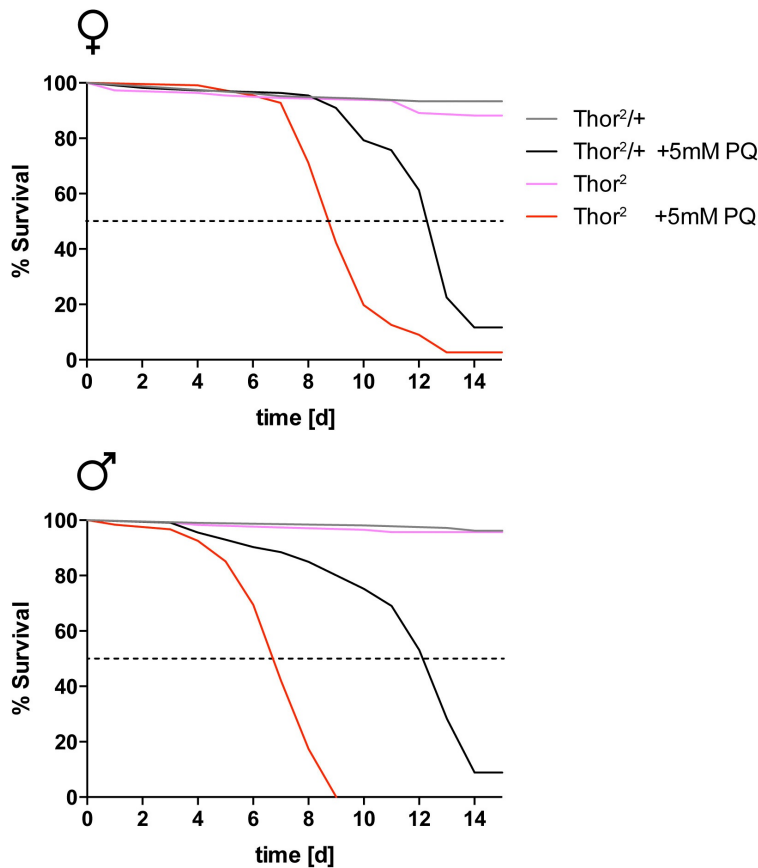
Figure 4.16: Survival of male and female *Drosophila* flies after feeding 5 mM paraquat displayed in Kaplan-Meier curves. Female (♀) and male (♂) flies were maintained on 5 % sucrose solution with or without 5 mM paraquat (PQ) at 25 °C. Surviving flies were counted every day. Median survival is indicated by dotted lines. n > 100

After knowing that *Thor* knockout flies have reduced lifespan and stress

resistance, it was interesting to determine whether overexpressing FLAG-d4E-BP[WT] or FLAG-d4E-BP[TA] can rescue this phenotype. Before doing this, it should be confirmed that the discovered phenotype was entirely due to *Thor* knockout and not to random mutations acquired over time in inbreed stocks. To do this, a different allelic combination with another endogenous *Thor* mutant strain, $Thor^{GS}$, was used. In contrast to $Thor^2$, this strain was not generated by excision of *Thor*, but by insertion of a P-element into the coding sequence of the gene. In the paraquat survival assay both stocks behaved similarly (Fig. 4.17A), which means that the $Thor^2$ phenotype under stress in this survival assay was entirely due to *Thor* and not biased by accumulated random mutations in the genetic background.
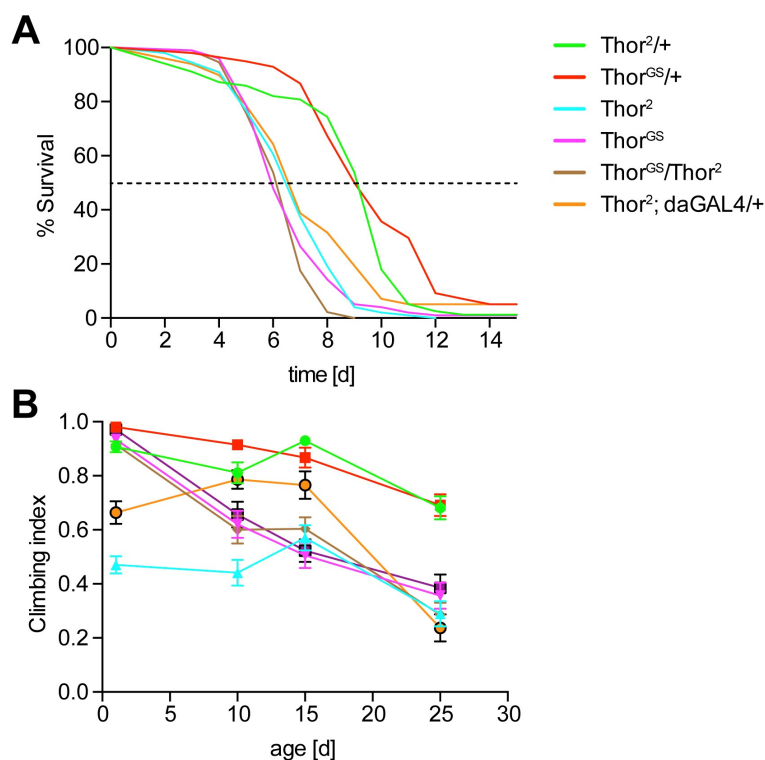
Figure 4.17: Stress resistance and motility of male *Drosophila Thor* knockout flies. (A) Male flies were fed with 5 % sucrose solution including 5 mM paraquat at 25 °C. Surviving flies were counted every day. Kaplan-Meier curves are displayed for every genotype and median survival is indicated by a dotted line. n > 75 (B) Male flies were aged on standard food at 25 °C for 1, 10, 15 and 25 days. Subsequent climbing assays were performed with aged flies and climbing index calculated. Error bars indicate s.e.m. $n \geq 35$

The same set of *Thor* knockout recombinations were utilised to investigate its motility phenotype. For this purpose, climbing assays with flies of

different age were performed and the climbing ability scored (Fig. 4.17B). Young *Thor²* and *Thor², da-GAL4/+* flies exhibited a reduced climbing performance compared to all other combinations, including *Thor²* and *Thor^GS* outcrosses as well as homozygous *Thor^GS* and *Thor²/Thor^GS* flies. These results raised the suspicion that *Thor²* accumulated some mutations, which resulted in reduced motility, but are not linked to *Thor* knockout. Ten days old flies showed the same picture, although the climbing ability of *Thor^GS* and *Thor²/Thor^GS* flies declined more than controls. The phenotypic difference between *Thor²* and *Thor^GS* disappeared in older flies. After 15 days, almost all *Thor* knockout combination exhibited the same climbing phenotype, while both controls performed better. Only *Thor², da-GAL4/+* did still surprisingly well after 15 days. Nevertheless, when utilising 25 days old flies all *Thor* knockout combinations grouped neatly together at a climbing index score of 0.3, while the controls group together at 0.7. These results revealed that aged *Thor* knockouts had a reduced motility, which is independent of random mutations. Whether younger flies also have a phenotype could not be clearly stated, because genetic background effects seemed to bias the results at this stage.

In order to test whether the generated transgenic *FLAG-d4E-BP* flies were able to rescue the reduced lifespan upon stress and reduced motility of aged endogenous *Thor* knockout flies, FLAG-d4E-BP[WT] and FLAG-d4E-BP[TA] were overexpressed in endogenous *Thor* knockout backgrounds using previously generated recombinants (see Fig. 4.12). These flies were fed with 5 mM paraquat as described for the previous assay above. Kaplan-Meier curves reveal that overexpressing FLAG-d4E-BP[WT] or FLAG-d4E-BP[TA] rescued the *Thor²* phenotype completely (Fig. 4.18A). *Thor²* outcrosses had a median survival of ten days, which was reduced to seven days in *Thor²* homozygous flies. Overexpressing FLAG-d4E-BP[WT] increased median survival to its base level of ten days, while overexpression of FLAG-d4E-BP[TA] even led to a median survival of eleven days.

The rescuing capability of transgenic FLAG-d4E-BP was also confirmed for motility (Fig. 4.18B). All flies were aged for 25 days before being utilised in a climbing assay. The results showed that the reduced climbing ability was rescued almost completely by FLAG-d4E-BP[WT] and FLAG-d4E-BP[TA]. In contrast to the survival assay, here it was not more beneficial for the phenotype to overexpress mutant d4E-BP instead of wildtype d4E-BP.

Survival and motility assays revealed that endogenous *Thor* knockout flies have a clear phenotype, despite they were homozygous viable. These phenotypes could be rescued by generated transgenic lines overexpressing FLAG-d4E-BP[WT/TA], which indicated that both lines were not only genetically, but also physiologically functional.
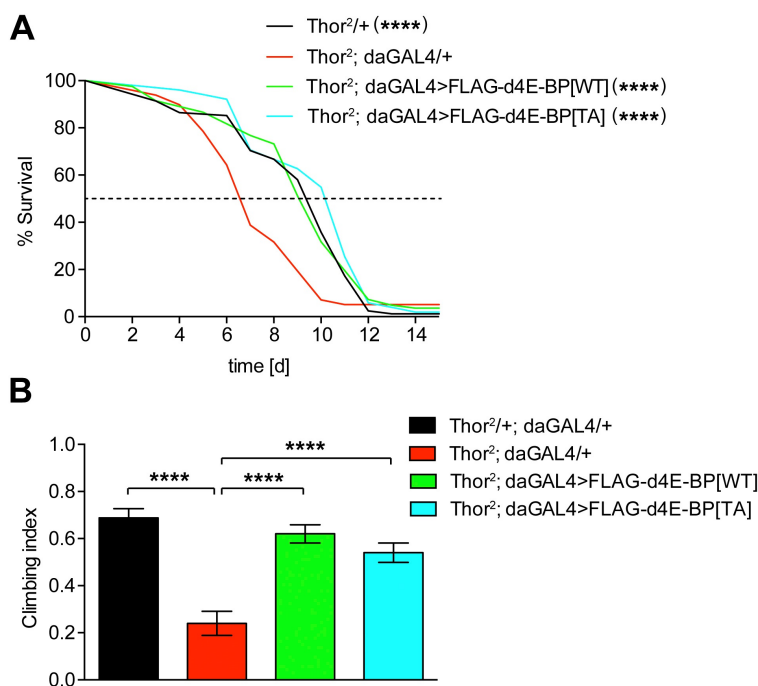
Figure 4.18: FLAG-d4E-BP[WT] and FLAG-d4E-BP[TA] overexpressing flies rescued reduced stress resistance and motility in endogenous *Thor* knockout *Drosophila* flies. (A) Male flies were fed with 5 % sucrose solution including 5 mM paraquat at 25 °C. Surviving flies were counted every day. Kaplan-Meier curves are displayed for every genotype and median survival is indicated by a dotted line. Significant survival improvement in comparison to knockout *Thor²*, *daGAL4/+* was determined by the log-rank test. (**** $P \leq 0.0001$) n > 50 (B) Male flies were aged on standard food at 25 °C for 25 days before climbing assay was performed. Error bars indicate s.e.m. Significance was determined by one-way ANOVA with Bonferroni correction. (**** $P \leq 0.0001$) n > 35

4.8 Evaluating the effect of d4E-BP overexpression in *park* and *Pink1* knockout flies

After confirming that transgenic FLAG-d4E-BP is functional and able to rescue the phenotype of endogenous *Thor* knockout flies, it was important to study whether it could also have a positive effect on other phenotypes. Tain et al. (2009) reported that transgenic overexpression of d4E-BP[WT] with muscle-specific 24B-GAL4 driver in PD *Drosophila* models rescued the

climbing ability of *park^{25}* and *Pink1^{B9}* mutants by regenerating muscle tissue structures.

For an initial test, the results gained by Tain et al. should be reproduced with the new generated transgenic fly strains. For this purpose, previously generated *24B-GAL4, park^{25}/TM6B* male flies were crossed with transgenic *FLAG-d4E-BP[WT/TA]/CyO; park^{25}/TM6B* virgins to get an F1 generation overexpressing FLAG-d4E-BP[WT/TA] driven by 24B-GAL4 in a homozygous *park* knockout background. As a control, virgins of the original strain utilised by Tain et al. were crossed with *24B-GAL4, park^{25}/TM6B* males. These males were outcrossed with *w^{1118}* virgins to get positive controls or with *park^{25}/TM6B* virgins for negative controls. F1 generations of these crosses were utilised to perform a climbing assay. The results revealed that homozygous *park* knockouts had a severely reduced climbing ability compared to controls, but overexpression of d4E-BP by utilising the transgenic line generated by Tain et al. could not rescue this phenotype significantly (Fig. 4.19A). Also FLAG-d4E-BP[TA] overexpressing flies were lacking a rescuing effect, while the rescue by FLAG-d4E-BP[WT] was statistically significant. Nevertheless, *FLAG-d4E-BP[WT]* lacked a biological substantial improving effect on climbing ability like the other two transgenic lines. However, the question remained why the rescuing effect reported by Tain et al. could not be reproduced, even by using the original transgenic line and the same driver. A possible explanation may be that fly inbreed stocks change over time due to accumulation of random mutations. Furthermore, fly behaviour could be affected by minor changes of room temperature, food composition or even plastic composition of climbing and stock tubes. In practice, it is very difficult to control all these factors, which may change fly behaviour.

Another important factor for the effect of overexpressed transgenes is the driver. 24B-GAL4 was utilised as a muscle specific driver, but was abandoned due to leaky expression in other tissues. Therefore, the experiments were repeated with da-GAL4, an ubiquitous driver, and elav-GAL4, a neuronal driver, with comparable results like with 24B-GAL4 (data not shown). In the end, Dmef-GAL4 was selected, a strong muscle-specific driver, for experimental repetition and a clear substantial and significant rescue of flies climbing ability by FLAG-d4E-BP[WT] and FLAG-d4E-BP[TA] in *park* knockouts was found (Fig. 4.19A). Positive and negative controls with the

appropriate driver were generated as described above. Thus, it can be concluded that transgenic overexpression of FLAG-d4E-BP[WT/TA] can rescue climbing deficits in *park* knockout flies, but the effect is dependent on the utilised driver.
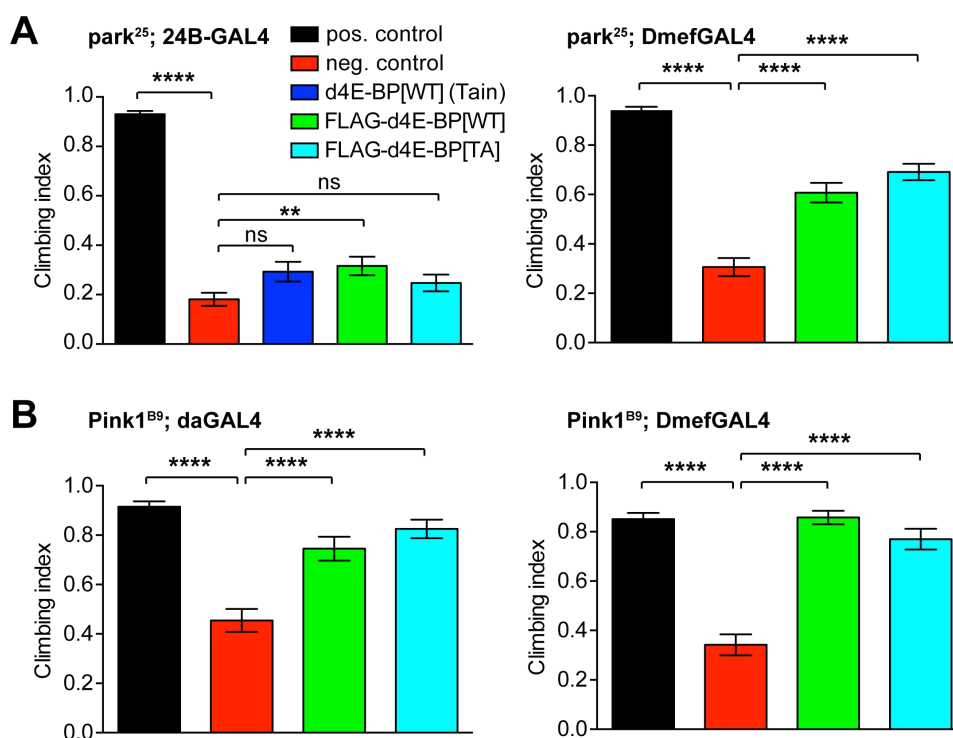
Figure 4.19: Rescuing effect on climbing ability by d4E-BP overexpression in *Drosophila park* and *Pink1* knockout models of PD. (A) Scored climbing ability of young *park* knockout flies ($park^{25}$) raised on standard food at 25 °C. (B) Scored climbing ability of young *Pink1* knockout flies ($Pink1^{B9}$) raised on standard food at 25 °C. Positive controls were outcrosses of the mutant with indicated driver to w^{1118}. Negative controls were homozygous mutants with indicated drivers. Error bars indicate ± s.e.m. Significance was determined by one-way ANOVA with Bonferroni correction (ns P > 0.05, ** P ≤ 0.01, **** P ≤ 0.0001). n > 50

As a next step, it was investigated whether climbing deficits of *Pink1* knockout flies can also be rescued by transgenic d4E-BP overexpression. Pink1 recruits parkin (*park*) to the mitochondria for mitochondrial autophagy and caused similar climbing deficits after knockout (Fig. 4.19B). *Pink1* is localised on the X chromosome, which is why only females were utilised as positive controls and only males for negative controls and transgenic overexpression of FLAG-d4E-BP. These experiments were performed with the ubiquitous da-GAL4 and the muscle specific Dmef-GAL4 driver and almost complete rescue could be achieved in both cases with FLAG-d4E-BP[WT] and FLAG-d4E-BP[TA]. Thus, it seems to be easier to rescue

climbing deficits caused by *Pink1* knockout with FLAG-d4E-BP than defects caused by *park²⁵*. This may be due to the fact that Pink1 acts upstream of parkin, which makes it easier to compensate the loss.

Tain et al. (2009) reported as well that *park* and *Thor* double knockout flies have a very reduced viability, which can be rescued by overexpression of d4E-BP. *park* and *Thor* single knockouts have no reduced viability on their own. *Thor²* is even homozygous viable, while *park²⁵* is also homozygous viable, but male sterile. For the viability assay, *Thor²/CyO; park²⁵, da-GAL4/TM6B* virgins were crossed with *FLAG-d4E-BP[WT/TA], Thor²/CyO; park²⁵/TM6B* male flies. For positive controls, virgins were crossed with *w¹¹¹⁸* or *Thor²/CyO; park²⁵/TM6B* males for negative controls. The theoretical proportion of the different genotypes was calculated according to the rules of Mendelian inheritance. Hence, the theoretical percentage for positive control *Thor²/+; park²⁵/+* flies was 25 % and 11 % for homozygous double knockouts with or without FLAG-d4E-BP[WT/TA] overexpression. These calculations considered that homozygous combinations of the same balancer chromosome are lethal. Three to four independent crossings per genotype were performed and the flies counted every day. Mean values were normalised to the positive control. The results confirmed a reduced viability for *Thor* and *park* double knockouts, but much less se-
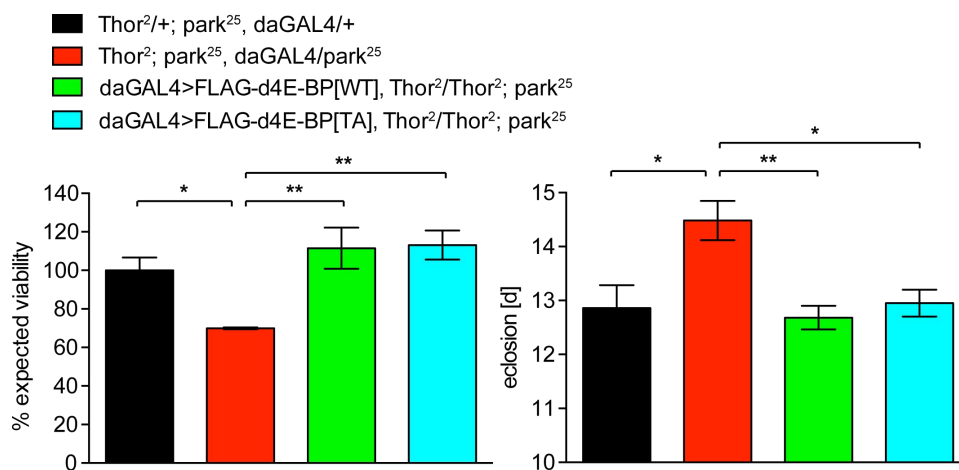
Figure 4.20: Viability and eclosion time of *Thor* and *park* double knockout flies. Viability analysis show percent of expected adults emerging from a cross of balanced heterozygote flies. Flies were raised on standard food at 25 °C. Viability was normalised to heterozygote positive control. Average eclosion time for all four genotypes is displayed. Error bars indicate ± s.e.m. Significance was determined by one-way ANOVA with Bonferroni correction (* $P \leq 0.05$, ** $P \leq 0.01$) n $\geq$ 3

vere than described by Tain et al. While Tain et al. reported a reduction by about 70 %, here the decline was only by about 30 % (Fig. 4.20). Nevertheless, both transgenic lines were able to rescue the reduced viability completely.

Futhermore, I noticed that double knockout flies eclosed much later from their pupae, so the average eclosion time was quantified. Normally, flies begin to eclose ten days after the eggs were laid. In Fig. 4.20 one can see that the eclosion time of double knockouts was significantly delayed by about 1.5 days, while transgenic overexpression of FLAG-d4E-BP[WT/TA] could rescue this phenotype as well. A delayed eclosion time is another indicator for impaired development, which could be rescued by d4E-BP overexpression.

4.9 Discussion

With this chapter, two aims should be achieved: the generation of a *Drosophila* model overexpressing FLAG-d4E-BP[WT/TA] for mass spectrometry experiments to identify upregulated proteins upon d4E-BP overexpression in flies and which can also be used to test the effect of d4E-BP downstream effectors for PD.

For this purpose, *FLAG-d4E-BP[WT/TA]* were integrated site-specifically into the *Drosophila* genome on the right arm of the second chromosome, far away from endogenous *Thor* on the left arm of the same chromosome. Although the initial transgene integration gave poor expression, this problem could be solved by changing the integration site. Successful integration was confirmed on DNA level by sequencing and expression was confirmed by qRT-PCR. However, it appeared to be more difficult to confirm translation of transgenes as anti-FLAG antibodies could detect the transgenes overexpressed in *Drosophila* S2R+ cells by immunoblotting, but not in extracts from flies. The alternative approach of utilising anti-4E-BP1 antibodies had only limited success. It could confirm that d4E-BP was expressed, because of specific appearance of bands in the immunoblot, but as these antibodies were optimised for human 4E-BP1, they produced multiple bands, which were difficult to interpret. The question why anti-FLAG antibodies did not detect the transgenes in flies remains not completely answered. I hypothesised that lower protein expression or higher protein

degradation in flies compared to S2R+ cells may explain the difficulties to dected the FLAG epitope with anti-FLAG antibodies. To overcome this problem, the method was changed in order to detect native FLAG-d4E-BP[WT/TA] with anti-FLAG antibodies by immunofluorescence microscopy in *Drosophila* wing discs. This strategy delivered the final confirmation that the transgenes were translated as required.

In order to test the functionality of transgenes, genetic recombinants of transgenes with *Thor²* were generated. Stress resistance tests with paraquat revealed that overexpression of transgenes in these recombinants rescued the reduced survival rate of *Thor* knockouts completely. Furthermore, *Thor²* climbing defects in aged flies were also rescued fully by both transgenes. These experiments confirmed that both transgenes were functional and able to replace endogenous *Thor*.

After verifying that *d4E-BP* transgenes were functional, it was tested whether these transgenes had also a beneficial effect for motility and viability of *Drosophila* models of PD as reported by Tain et al. (2009). Initial experiments utilising the original driver from Tain et al. could not reproduce these findings in climbing assays with *park* knockout flies. However, after utilising the strong muscle specific driver Dmef-GAL4, my transgenic lines were able to rescue the *park²⁵* significantly. It was much easier to rescue the climbing defects of *Pink1^{B9}*. Overexpression of transgenes with Dmef-GAL4 rescued the phenotype completely as well as overexpression with da-GAL4. This is not very surprising as *Pink1* acts upstream of *parkin* and a loss is easier to compensate in this way. These data revealed that overexpressing FLAG-d4E-BP[WT/TA] transgenes in *Drosophila* models of PD had a beneficial effect on their motility, but the magnitude was depending on the driver and not universally equal.

Further tests on the ability of *d4E-BP* transgenes to rescue the reduced viability of *Thor* and *park* double knockout flies revealed that both transgenes were able to compensate the loss of both genes completely. Furthermore, the extended eclosion time of double knockouts was also reduced to wildtype level by both transgenes.

Interestingly, these *in vivo* behavioural studies never found a clear difference between the effect of overexpressed wildtype FLAG-d4E-BP[WT] or FLAG-d4E-BP[TA]. It seems that overexpressing wildtype d4E-BP is sufficient to oversaturate the phosphorylation/dephosphorylation system of

d4E-BP. Thus, overexpressing entirely unphosphoryated d4E-BP has no further effect beyond wildtype d4E-BP as cap-dependent translation was already completely blocked by the dephosphorylated fraction of wildtype d4E-BP.

In summary, transgenic fly lines generated in this chapter were successfully tested for their capability to overexpress the transgenes, rescue the loss of endogenous *Thor* and exhibit a rescuing capability in *Drosophila* models of PD. Thus, they can next be used for quantitative mass spectrometry to study downstream effectors of d4E-BP. Different experimental approaches are possible: Transgenes can be overexpressed in a wildtype background, but also in an endogenous knockout background as it was possible to generate recombinants with *Thor²*. Furthermore, it would be possible to study the effect of d4E-BP overexpression in different tissues by using tissue specific drivers. Even temporal studies on the effects of d4E-BP are possible as inducible GAL4 systems have been developed (Osterwalder et al., 2001; Roman et al., 2001).

After identification of d4E-BP downstream effectors by mass spectrometry, these targets could be knocked down in *Drosophila* by cross breeding flies with specific RNAi lines. In this way, it would be possible to utilise the generated model to assess different d4E-BP downstream targets on their ability to contribute to the beneficial effect of d4E-BP in PD models. Overexpression of d4E-BP in PD *Drosophila* models while simultaneously knocking down d4E-BP downstream targets would reveal which downstream targets contribute to the rescuing capability of d4E-BP in PD models.

Thus, both aims of this chapter could be achieved: a *Drosophila* model to study d4E-BP downstream targets by mass spectrometry was successfully generated and it can also be utilised to assess the contribution of different downstream targets to the rescuing capability of d4E-BP in PD.

Chapter 5

Quantitative mass spectrometry investigations of 4E-BP1/d4E-BP downstream effectors in T-REx HEK293 cells and *Drosophila*

5.1 Hypothesis and aims

The intention of this part of the study was to utilise the previously generated cell and *Drosophila* models overexpressing 4E-BP1/FLAG-d4E-BP[WT/TA] to identify and quantify up- and downregulated proteins relative to non-overexpressing control conditions.

The aim was to quantify several thousand proteins in order to get a broad picture of the impact of 4E-BP1/d4E-BP overexpression on the proteome. In particular, it was important to identify upregulated proteins as it was hypothesised that these had the greatest potential to mediate cellular protective functions. These targets could be analysed for their potential positive impact on PD or, more generally, on viability and survival.

Furthermore, it was intended to compare quantitative data from *in*

vitro and *in vivo* experiments to find commonly upregulated proteins upon 4E-BP1/d4E-BP overexpression. This information could be used in the future to overexpress 4E-BP1/d4E-BP downstream effectors in *Drosophila* models of PD in order to evaluate their individual contribution to the rescuing effect of d4E-BP in PD models.

5.2 Background

5.2.1 Principle of quantitative mass spectrometry

Quantitative mass spectrometry of the whole proteome, as performed in this study, is based on relative quantification against a control. For this purpose, the same T-REx HEK293 cell clones were passaged and grown in light and heavy media (Fig. 5.1A). The media contained arginine and lysine amino acids with either ^{12}C and ^{14}N or ^{13}C and ^{15}N isotopes. As a result, proteins synthesised by cells in these media were either a bit heavier or lighter than their counterpart, but remained the same biological and chemical properties. Overexpression of 4E-BP1 was only initiated in heavy labelled cells for a defined time period before the cells were harvested and proteins extracted. In the case of sample preparation of *Drosophila*, larvae were fed with labelled food.
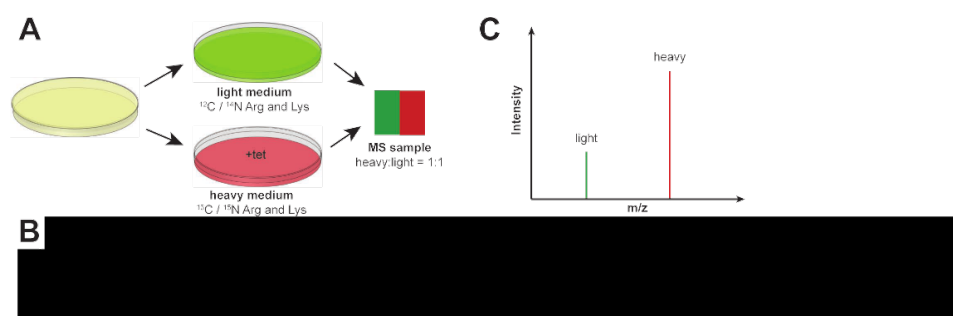
Figure 5.1: Principle of whole proteome quantitative mass spectrometry. (A) In order to label samples, cells are grown in light or heavy media to incorporate these isotopes. 4E-BP1 overexpression is only induced in the heavy medium by tetracycline (tet). The extracted proteins are united in a ratio of 1:1 for quantification. The different protein labels allows protein assignment to their growing condition and hence relative quantification. *Drosophila* samples are treated likewise and received differently labelled food. (B) The labelled protein samples, are fractioned, before peptides can be fractioned by HPLC and injected into the mass spectrometer via electrospray ionisation (ESI). The raw data is computer processed to assign measured spectra to different peptides and proteins. Fig. was adapted from Steen and Mann (2004). (C) Relative quantification is achieved by calculating the peak intensity ratio of the same peptides labelled with light or heavy isotopes.

The extracted proteins were fractionated to reduce complexity of the protein mix, and digested by proteases, most typically trypsin (Fig. 5.1B). The resulting peptides were further fractioned by HPLC and injected via electrospray ionisation into the mass spectrometer. The measured spectra were analysed and matched to an *in silico* digested protein database in order to identify peptides and proteins. Peptides were quantified by calculating the ratio of peak intensity between light and heavy labelled equivalents (Fig. 5.1C). Hence, quantification of proteins in this study was a relative quantification, which is only feasible if both partners of a peptide pair could be identified.

Three parameters determined mass spectrometry results: the sample preparation, the settings of the mass spectrometer and the software settings to analyse the data. There is no standard way to conduct mass spectrometry experiments due to the complexity of the proteome and diverse applications. Despite all diversity it became standard to reduce and alkylate cysteine residues in order to prevent the establishment of cysteine disulfid bonds (Sechi and Chait, 1998). Indefinite disulfid bond states would increase the diversity of peptides and reduce the likelihood of identifying cysteine containing peptides. The software settings can also define which modifications should be considered. Here, N-terminal acetylation and oxidation of peptide residues were considered as possible modification. The number of considered modifications have to be limited, because they reduce the number of identified peptides and proteins due to an complexity increase of the *in silico* peptide reference database. The number of identified proteins is also limited by the number of required peptides to identify a protein. In this study, one unique peptide was sufficient for a protein identification. A careful optimisation of the mass spectrometry settings is necessary for every application due to many parameters that can interfere with the mass spectrometry results.

5.2.2   Functionality of the mass spectrometer

Mass spectra of peptides are recorded by injecting charged peptide ions into the mass spectrometer (Fig. 5.2A). This ion cloud is focused and compressed in the high-pressure cell. A portion of the peptides is passed on to the C-Trap from where they are injected into the Orbitrap analyser. In the Orbitrap, charged ions are electrostatically trapped and started rotating around the

central electrode, while performing axial oscillation. This oscillation induces an image current into the second electrode in the outer half of the Orbitrap, which can be detected by a differential amplifier. Every single peptide will induce a sine current. Different peptides cause overlapping sine waves, which are separated by Fourier transformation. The gained so called MS^1 spectrum (Fig. 5.2B) contains information about the mass to charge ratio (m/z) of individual peptides and their abundance. The frequency of the sine wave is proportional to the m/z ratio, while the amplitude is proportional to peptide abundance.
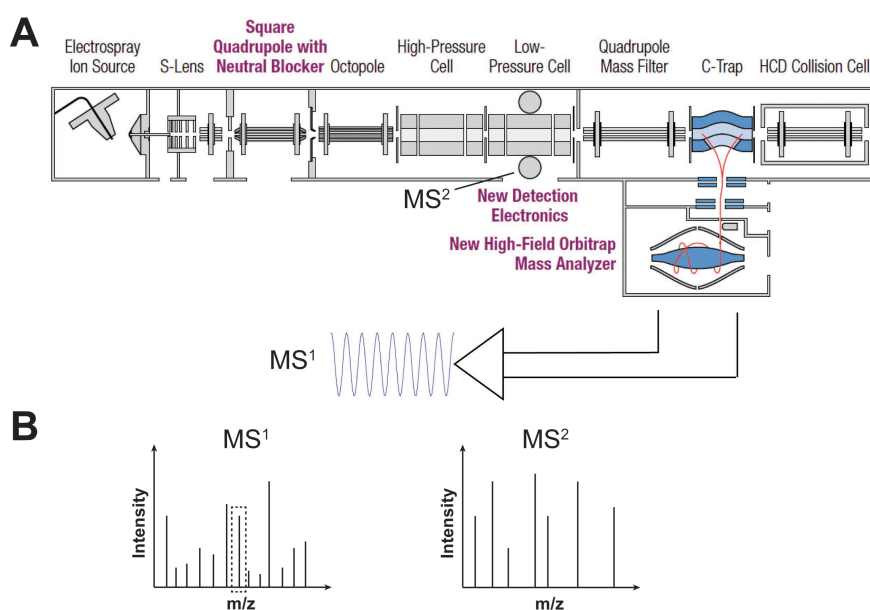
Figure 5.2: Composition of the mass spectrometer and gaining of mass spectra. (A) The schematic of an Orbitrap Elite mass spectrometer is displayed here, which has been used in this study. The peptide ions were injected by electrospray and passed through the whole machine till the C-Trap, where they were compressed and transferred into the Orbitrap analyser to gain the MS^1 spectrum. Detectors adjacent to the Low Pressure Cell gained the MS^2 spectra. (B) A single peak in a MS^1 spectrum represents a whole peptide (see e.g. highlighted peak), while all peaks in an associated MS^2 spectrum represent peptide fragments and amino acids of the same MS^1 peptide.

However, the gained information would be insufficient to match the peptides uniquely to their proteins. To achieve this, more information about the peptide composition and sequence are necessary. For this purpose, tandem mass spectrometry was performed. The information of the MS^1 spectrum were utilised to identify the most abundant peaks with distinct m/z ratios and to release previously stored peptides with the same m/z ratio selectively into the low pressure cell. In this cell, peptide ions were broken by collision

with an inert gas. Peptides brake preferentially at peptide bonds and the gained MS^2 spectra of the peptide fragments (Fig. 5.2B) were recorded to identify sequence characteristics of the peptide. These information allowed matching peptides to their proteins, while the MS^1 spectrum contributed information of the protein abundance.

5.3 *In vitro* mass spectrometry of T-REx HEK293

5.3.1 Label incorporation

Prior to any protein quantification experiments, it was important to confirm the relative incorporation efficiency of heavy isotopes into the proteins of T-REx HEK293 cell clones after twelve cell doublings. For this purpose, cells grown in heavy medium were lysed in Guanidine Lysis buffer, 1 µg protein digested by trypsin and the peptides injected straight into the mass spectrometer without prior protein fractionation. The peptides were analysed as all other following quantification samples. The only difference was that a heavy peptide without an identified light counterpart was quantified as 100 % labelled as it is expected that most of the proteins have incorporated heavy isotopes completely. In total, 609 proteins were analysed in the 4E-BP1[WT] and 550 proteins in the 4E-BP1[TA] sample. The results confirmed an average incorporation of 99.3 % in the 4E-BP1[WT] clone and 99.2 % in the 4E-BP1[TA] clone (Fig. 5.3). An average incorporation of 95 % was considered as completely labelled. Hence, both clones appeared to be sufficiently labelled and could be used for quantification experiments. It was unnecessary to test isotope incorporation of proteins of cells grown in light medium as the natural average occurrence of the isotopes ^{12}C and ^{14}N is 98.9 % and 99.6 % anyway.

Figure 5.3: Incorporation of heavy isotopes in proteins of T-REx HEK293 cell clones. The average isotope incorporation is displayed for every single analysed protein, ordered from highest to lowest incorporation. The dotted line indicates 95 % incorporation, which is considered as completely labelled.
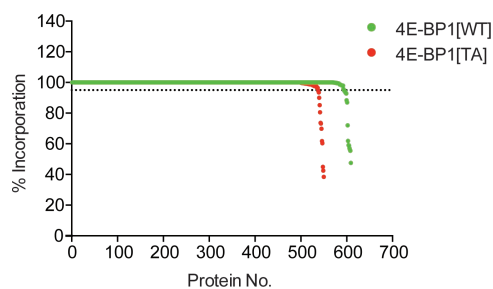
5.3.2 Optimisation of protein in-gel fractionation for mass spectrometry

The aim here was to quantify as many proteins as possible in order get the most detailed idea of the downstream effects of 4E-BP1. To achieve this, it was necessary to develop and optimise a mass spectrometry protocol to identify several thousand proteins, if possible. In a first step, 4E-BP1[TA] was overexpressed for 24 h in heavy labelled cells prior lysing cells grown in both media with Cell Lysis buffer, also used for lysing cells in preparation of immunoblotting. 37.5 µg protein from heavy and light media were combined and loaded together on an SDS gel. The gel was stained and the lane cut in 11 equal sized fractions. The fractions were trypsinised individually and the extracted peptides analysed on the mass spectrometer. At the same time, 50 µg heavy and light proteins were utilised for immunoblotting to confirm that 4E-BP1[TA] was only overexpressed in cells grown in heavy medium (Fig. 5.4A). The normalised heavy to light ratios of all quantified proteins are displayed in Fig. 5.4B. In total, 793 proteins were quantified. Here, proteins with more than 50 % abundance increase upon 4E-BP1[TA] overexpression were considered as upregulated, while proteins with 50 % decreased abundance were considered as downregulated. In this experiment, 18 proteins were up- and 17 downregulated (see whole list in the appendix, table A2 and A3).
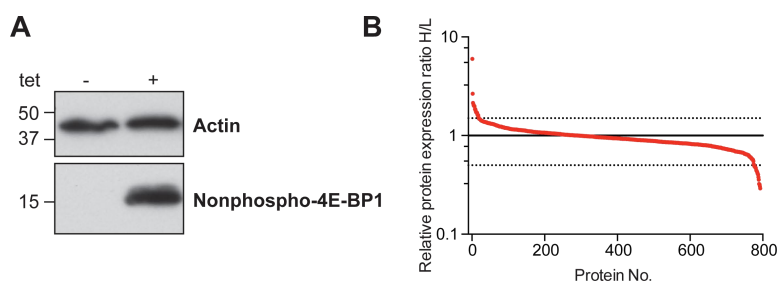
Figure 5.4: Effect of 24 h 4E-BP1[TA] overexpression on the proteome. (A) Immunoblotting of light (-) and heavy (+) proteins to confirm the overexpression of 4E-BP1[TA] by tetracycline (tet). Actin served as negative control and the molecular weight is indicated on the left hand side in kDa. (B) Normalised heavy to light ratio (H/L) of all quantified proteins. The upper dotted separates proteins, which were more than 50 % upregulated upon 4E-BP1[TA] overexpression, while the lower dotted line indicates proteins, which were more than 50 % downregulated.

In a first approach to increase the number of quantified proteins, the number of gel fractions was increased. This reduced the complexity of pep-

tides per mass spectrometry analysis and can improve the number of quantified peptides and proteins. In preparation, 4E-BP1[WT/TA] were overexpressed for 12 h in T-REx HEK293 cells growing in heavy medium and lysed as described before along with the same clones grown in light medium. The 4E-BP1 induction time was halved compared to the previous experiment in a first attempt to avoid secondary effects of 4E-BP1 overexpression on transcriptional level. 37.5 µg protein from heavy and light media were combined and separated on an SDS gel. The gel was stained and the lanes cut in 21 equal sized fractions (Fig. 5.5A), which almost doubled the number of fractions compared to the first experiment. The fractions were trypsinised individually and the extracted peptides analysed on the mass spectrometer. At the same time, 50 µg heavy and light proteins were utilised for
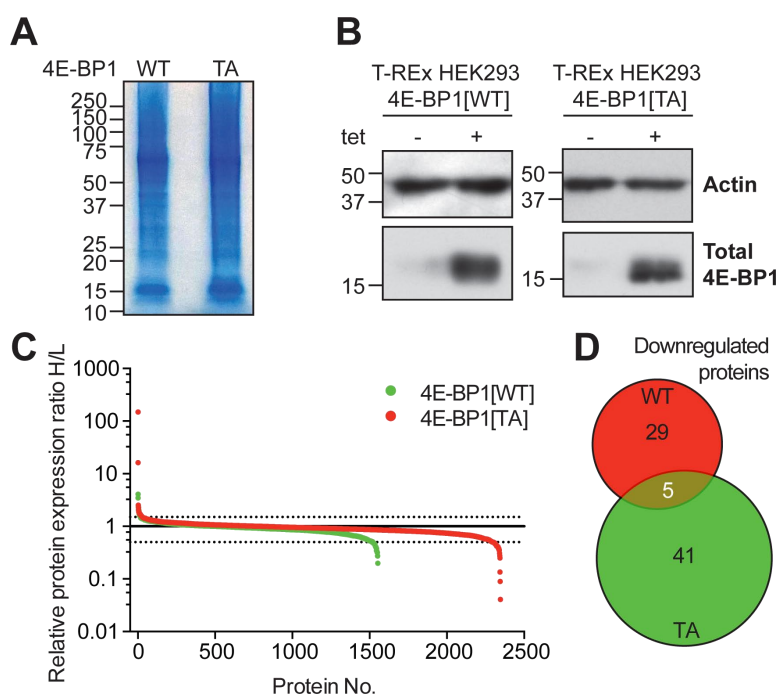
Figure 5.5: Effect of 12 h 4E-BP1[WT] or 4E-BP1[TA] overexpression on the proteome. (A) SDS gel of 75 µg protein per lane from cells overexpressing 4E-BP1[WT] or 4E-BP1[TA]. Samples are 1:1 mix of lysates from light and heavy media. The molecular weight is indicated at the left hand side in kDa. (B) Immunoblotting of light (-) and heavy (+) proteins to confirm the overexpression of 4E-BP1[WT] or 4E-BP1[TA] by tetracycline (tet). Actin served as negative control and the molecular weight is indicated on the left hand side in kDa. (C) Normalised heavy to light ratio (H/L) of all quantified proteins. The upper dotted separates proteins, which were more than 50 % upregulated upon 4E-BP1[WT/TA] overexpression, while the lower dotted line indicates proteins, which were more than 50 % downregulated. (D) VENN diagram of all proteins downregulated by 4E-BP1[WT] or 4E-BP1[TA] overexpression. Five proteins were downregulated in both samples.

immunoblotting to confirm that 4E-BP1[WT] and 4E-BP1[TA] were only overexpressed in cells grown in heavy medium (Fig. 5.5B). The normalised heavy to light ratios of all quantified proteins are displayed in Fig. 5.5C. In total, 1553 proteins were quantified in 4E-BP1[WT] overexpressing cells, while 2346 proteins were quantified in 4E-BP1[TA] overexpressing cells. This was a clear improvement compared to the previous quantification experiment. As described above, proteins with more than 50 % abundance increase upon 4E-BP1[WT/TA] overexpression were considered as upregulated, while proteins with 50 % decreased abundance were considered as downregulated. In this experiment, 16 proteins were up- and 34 downregulated upon 4E-BP1[WT] overexpression, while 29 proteins were up- and 46 downregulated upon 4E-BP1[TA] overexpression (see whole lists in the appendix, table A4, A5, A6, A7 and A8). 4E-BP1[WT] and 4E-BP1[TA] did not share upregulated proteins, but 5 commonly downregulated proteins (Fig. 5.5D). The 40S ribosomal protein RPS15, was downregulated upon 12 h 4E-BP1[WT] overexpression and 24 h 4E-BP1[TA] (compare with previous experiment above). This was the only common up- or downregulated protein of the first two quantitative experiments.

To increase the number of quantified proteins even further, a different approach was considered. Previous stainings of protein gels showed strong signals, but not very sharp protein bands. If the protein migration was hindered, it could have an effect on the number of identified proteins, because if proteins spread over a wider range, they could be found in more gel fractions, which dilutes them and makes quantification more difficult. Thus, an accurate protein separation was crucial. To improve it, the lysis buffer was replaced by MS Lysis buffer, which contained SDS as the only detergent. The previously used Cell Lysis buffer contained Triton X-100 and glycerol, two detergents, which may interfere with the SDS in the protein gel and are known to interfere with the mass spectrometry analysis, which may explain the reduced number of identified proteins. Indeed, SDS gel stainings revealed a better protein band resolution with the new lysis strategy (Fig. 5.6A). Furthermore, for these experiments the amount of loaded protein was reduced to 50 μg per lane in order to avoid imprecise protein fractionation due to gel overload. It was also taken into account that immunoblot experiments have revealed that 6 h of 4E-BP1 induction by tetracycline in T-REx HEK293 cells were sufficient to overexpress 4E-BP1

(see chapter 3, Fig. 3.12). For this reason, the induction time in heavy medium was reduced to 6 h. 50 µg heavy and light proteins were utilised for immunoblotting to confirm that 4E-BP1[WT] and 4E-BP1[TA] was only overexpressed in cells grown in heavy medium (Exp. 1 in Fig. 5.6B). At the same time, 25 µg protein from heavy and light media were combined and loaded together on an SDS gel. The gel was stained and the lanes cut in nine equal sized fractions to simplify the practical implementation of this first experiment with new lysis conditions. The fractions were trypsinised individually and the extracted peptides analysed on the mass spectrometer.
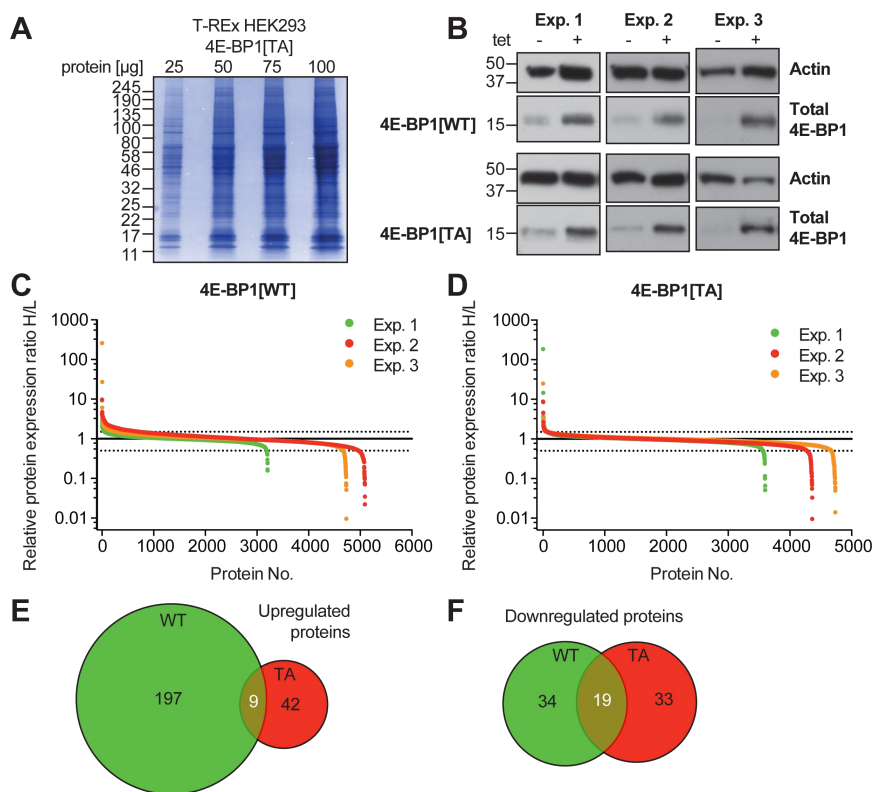
Figure 5.6: Effect of 6 h 4E-BP1[WT] or 4E-BP1[TA] overexpression on the proteome.
(A) Stained SDS gel of T-REx HEK293 4E-BP1[TA] clone. 25 µg, 50 µg, 75 µg or 100 µg protein were loaded per lane. The molecular weight is indicated at the left hand side in kDa. (B) Immunoblotting of light (-) and heavy (+) proteins to confirm the overexpression of 4E-BP1[WT] or 4E-BP1[TA] by tetracycline (tet) in all three experiments (Exp. 1 - 3) using total 4E-BP1 antibodies. Actin served as negative control and the molecular weight is indicated on the left hand side in kDa. (C) Normalised heavy to light ratio (H/L) of all quantified proteins after 4E-BP1[WT] or 4E-BP1[TA] overexpression (D) in all three experiments. The upper dotted separates proteins, which were more than 50 % upregulated upon 4E-BP1[WT/TA] overexpression, while the lower dotted line indicates proteins, which were more than 50 % downregulated. (E) VENN diagram of all proteins upregulated by 4E-BP1[WT] or 4E-BP1[TA] overexpression. Nine proteins were upregulated in both samples. (F) VENN diagram of all proteins downregulated by 4E-BP1[WT] or 4E-BP1[TA] overexpression. 19 proteins were downregulated in both samples.

124

The normalised heavy to light ratios of all quantified proteins are displayed in Fig. 5.6C and D. In total, 3207 proteins were quantified in 4E-BP1[WT] overexpressing cells, while 3599 proteins were quantified in cells overexpressing 4E-BP[TA]. Again, this was a much better coverage than in the experiments before, despite a lower number of fractions.

The experiment was repeated twice in the very same way, but the number of fractions was slightly increased to 14 fractions per sample. The immunoblots of experiment 2 and 3 are shown in Fig. 5.6B and the normalised heavy to light ratios of all quantified proteins are displayed in Fig. 5.6C and D. In experiment 2 and 3, 5091 and 4731 proteins were quantified for 4E-BP1[WT] overexpressing cells, while 4361 and 4736 proteins were quantified in 4E-BP1[TA] overexpressing cells, respectively. The separately recorded results of all three experiments were analysed for up- and downregulated proteins. Proteins with an abundance change of 50 % or more upon 4E-BP1[WT/TA] overexpression in one of three experiments and a confirmed abundance change of more than 40 % in another experiment were considered as up- or downregulated. By applying these criteria, 206 proteins were identified to be consistently upregulated in 4E-BP1[WT] overexpressing cells, while 51 proteins were upregulated in 4E-BP1[TA] overexpressing cells (Fig. 5.6E). They share 9 proteins, which were commonly upregulated by 4E-BP1[WT] and 4E-BP1[TA]. 53 proteins were downregulated upon 4E-BP1[WT] overexpression and 52 by 4E-BP1[TA] (Fig. 5.6F). 19 were downregulated by both. The whole list of proteins is displayed in the appendix, table A9 - A14.

The last experiments quantified several thousand proteins after only 6 h of 4E-BP1 overexpression. This is a solid data set to identify 4E-BP1 downstream effectors and the short 4E-BP1 induction time reduced the chance to detect secondary effects. Hence, these data shall be used for bioinformatic analyses in order to identify groups of proteins, which may explain the protective effect of 4E-BP1 activation in different models.

5.3.3 Bioinformatic analyses of upregulated hits

In order to identify upregulated proteins upon 4E-BP1 overexpression, which may contribute to its protective effect, the hits from quantitative mass spectrometry, which are summarised in Fig. 5.6, were analysed by different bioinformatic tools. In all cases, the aim was to identify proteins, which group

together according to their function or localisation and may be able to make contribution to the protective effect of 4E-BP1.

In a first attempt, proteins upregulated by 4E-BP1[WT/TA] were analysed utilising the PANTHER database (Protein Analysis through Evolutionary Relationships, http://www.pantherdb.org, Version 10). It classifies proteins according to their molecular function, biological process or other criteria, which is a result of human curation and bioinformatic algorithms. PANTHER classified the hits of 4E-BP1[WT] in nine groups according to their molecular function and in eight groups for 4E-BP1[TA] (Fig. 5.7A). However, the general distribution is similar in 4E-BP1[WT] and 4E-BP1[TA] hit groups. The most abundant groups were "binding" and "catalytic activity", which is not very surprising as these are very general terms, which apply to many proteins. For 4E-BP1[WT], PANTHER identified with glutathione peroxidase 8 (GPX8) one protein with "antioxidant activity" and five proteins with "protein binding transcription factor activity". These include THO complex subunit 2 (THOC2), SET and MYND domain-containing protein 5 (SMYD5), Pirin (PIR), splicing factor 1 (SF1) and MMS19 nucleotide excision repair protein homolog (MMS19). On the other hand the eukaryotic initiation factor 4A-III (EIF4A3) was identified for 4E-BP1[TA] in the category "translation regulator activity".
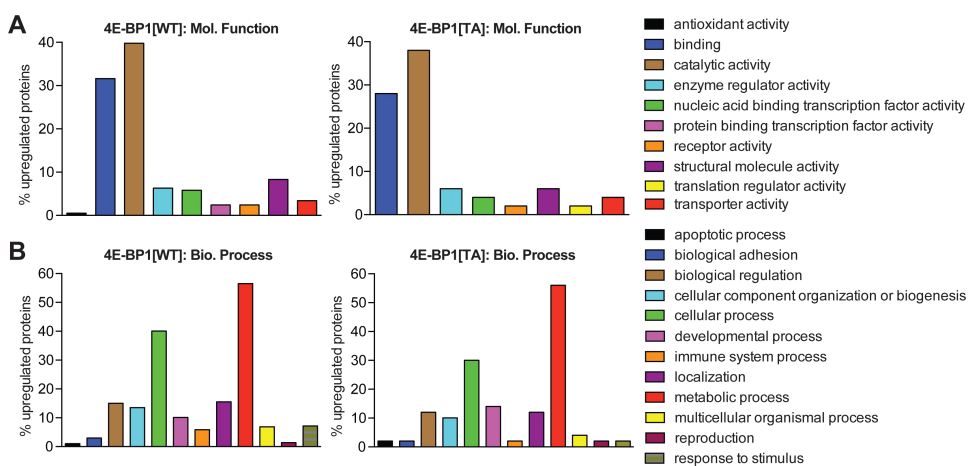
Figure 5.7: Classification of proteins upregulated by 4E-BP1[WT/TA] by PANTHER. (A) Upregulated proteins were classified according to the molecular process they contribute to or the biological process they are involved in (B).

When the hits were analysed with respect to involved biological processes, PANTHER grouped 4E-BP1[WT] and 4E-BP1[TA] hits in the same

twelve categories (Fig. 5.7B). The two most abundant groups were "cellular process" and "metabolic process", although more hits of 4E-BP1[WT] fit into the first category than hits of 4E-BP1[TA]. More 4E-BP1[WT] hits were also associated to the category "response to stimulus". Of these, seven proteins were classified into the subgroup "response to stress", including receptor-interacting serine/threonine-protein kinase 2 (RIPK2), CD97 antigen (CD97), glutathione peroxidase 8 (GPX8), dual specificity protein phosphatase 3 (DUSP3), heat shock 70 kDa protein 13 (HSPA13), autophagy-related protein 101 (ATG101) and tetratricopeptide repeat protein 4 (TTC4). The 4E-BP1[TA] hit in the "response to stimulus category" was interferon regulatory factor 3 (IRF3).

With respect to neurodegenerative diseases, it was also interesting to notice that PANTHER identified one 4E-BP1[WT] hit associated with the "AD - presenilin pathway", CD44 antigen (CD44), and five proteins associated the "Huntington disease". These were actin-related protein 2/3 complex subunit 1A (ARPC1A), calpain-2 catalytic subunit (CAPN2), cytoplasmic FMR1-interacting protein 1 (CYFIP1), Huntingtin-interacting protein 1-related protein (HIP1R) and tubulin β-2A chain (TUBB2A). All definitions of the category terms can be found in the appendix, table A21 and A22.

Another approach to determine groups of proteins was to use the STRING database (Search Tool for the Retrieval of Interacting Genes/Proteins, http://string-db.org, Version 10). The aim of the database is to find known and predicted protein-protein interactions, which includes physical and functional interactions. This could help to find proteins, which drive cells towards a certain fate, although the proteins do not have the same function or localisation. In this case, 4E-BP1[WT] and 4E-BP1[TA] were analysed separately, as for the PANTHER analysis, but also together in order to increase the chance to find interacting protein groups, which could not be connected because of missing links in the 4E-BP1[WT] or 4E-BP1[TA] cohort.

The first analysis of 4E-BP1[WT] hits revealed that a complex network of interactions exists between these proteins (Fig. 5.8). STRING confirmed that this network has significantly more interactions then statistically expected for a random group of proteins ($p < 0.0001$). The protein network does not have a single, but multiple centres. The CAD protein
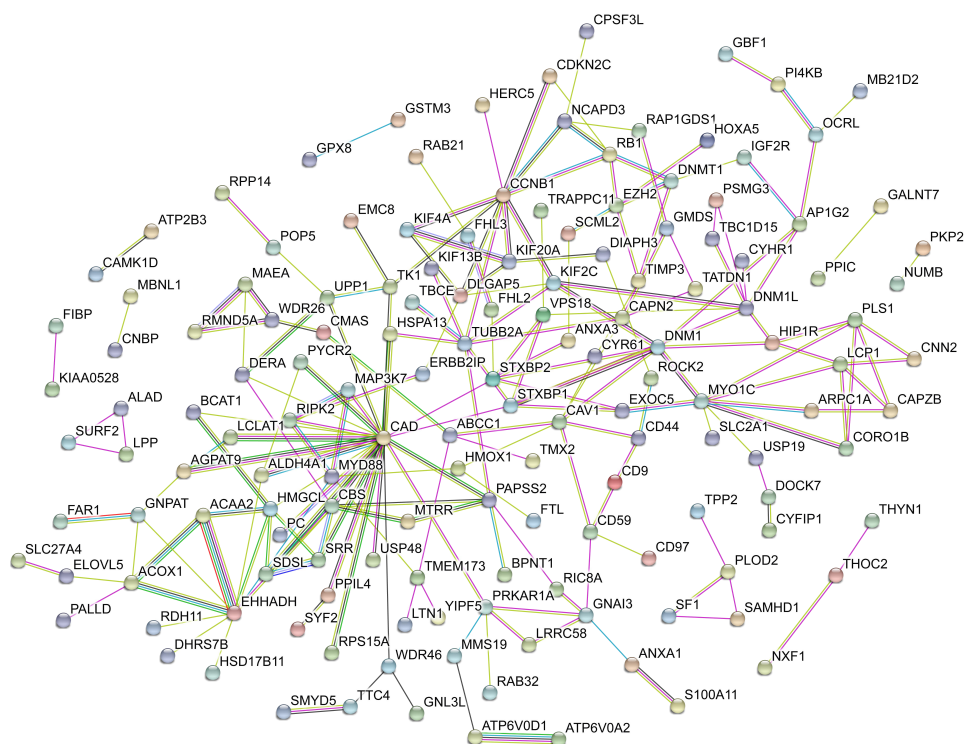
Figure 5.8: Protein interactions of hits upregulated by 4E-BP1[WT] overexpression determined by STRING. The colours of the connecting lines indicate the kind of interaction. Known interactions are turquoise or magenta. These interactions were extracted from curated databases or experimental determined. Predicted interactions are displayed green, red or blue. Interactions were predicted by gene neighbourhood, gene fusions or gene co-occurrences. Yellow, black and light blue lines indicate interactions predicted by textmining, co-expression or protein homology.

(CAD), tubulin β-2A chain (TUBB2A), dynamin-1-like protein (DNM1L), G2/mitotic-specific cyclin-B1 (CCNB1) and peroxisomal bifunctional enzyme (EHHADH) appear to be the central proteins with many links to others. CAD is a multi-functional enzyme encoding four enzymatic activities of the pyrimidine pathway. Its multifunctionality may be the reason why it interacts with many other proteins. TUBB2A was associated with Huntington's disease by PANTHER. It is a major constituent of microtubules and the cytoskeleton and thus involved in protein and organelle trafficking. An important reason why it has so many connections. DNM1L is involved in mitochondrial and peroxisomal division. Through its function in mitochondrial division, it ensures the survival of cells by suppressing oxidative damage. This could make this protein an interesting candidate for 4E-BP1's cellular protective capability. Among others, DNM1L is linked to the Huntingtin-

interacting protein 1-related protein (HIP1R), which is associated with the neurodegenerative Huntington's disease according to PANTHER. HIP1R is a component of clathrin-coated pits and vesicles that may link the endocytic machinery to the actin cytoskeleton. It may also promote cell survival by stabilizing receptor tyrosine kinases following ligand-induced endocytosis (Hyun et al., 2004). The other node protein CCNB1 is a proto-oncogene, which is linked to many proteins which are involved in chromatin and DNA architecture. It could be an indicator that the change on translational level is going to alter gene transcription, too. The last node protein in this cohort, EHHADH, is involved in the fatty acid β-oxidation, which is part of the lipid metabolism. It seems logical that extra energy sources would be mobilised in an event of cellular stress. The protein is linked with other enzymes of lipid metabolism, including the anti-apoptotic mitochondrial 3-ketoacyl-CoA thiolase (ACAA2) (Cao et al., 2008).

Some proteins, which have been associated with stress response by PANTHER also interact with the node proteins of STRING. One example is HSPA13, a heat shock protein, which is linked to CAD and TUBB2A. Another example is RIPK2, which interacts with CAD, too. RIPK2 can activate the transcription factor NF-κB, which leads to transcription of anti-apoptotic genes.

The STRING analysis of the upregulated proteins upon 4E-BP1[TA] overexpression appeared to be very different to the one of 4E-BP1[WT] (Fig. 5.9). One reason is that many more proteins were upregulated upon 4E-BP1[WT] overexpression, which makes is much easier to find connections between proteins. A smaller cohort makes it more likely to miss out on important links. For this reason, only few interactions were found for 4E-BP1[TA] hits. However, the number of interactions was significantly increased compared to a random group of proteins (p = 0.03). The analysis identified an interaction between nucleolin (NCL), prelamin-A/C (LMNA) and lamin-B1 (LMNB1). All three proteins are part of the nuclear lamina, which also interacts with chromatin and is involved in chromatin regulation and organisation. U3 small nucleolar ribonucleoprotein IMP4 (IMP4), protein SDA1 homolog (SDAD1) and the mitochondrial dimethyladenosine transferase 2 (TFB2M) are also proteins linked to ribosomal RNA processing. Pre-mRNA-splicing factor CWC22 homolog (CWC22) and eukaryotic initiation factor 4A-III (EIF4A3) are two proteins, which change protein

Figure 5.9: Protein interactions of hits upregulated by 4E-BP1[TA] overexpression determined by STRING. The colours of the connecting lines indicate the kind of interaction. Known interactions are turquoise or magenta. These interactions were extracted from curated databases or experimental determined. Predicted interactions are displayed green, red or blue. Interactions were predicted by gene neighbourhood, gene fusions or gene co-occurrences. Yellow, black and light blue lines indicate interactions predicted by textmining, co-expression or protein homology.
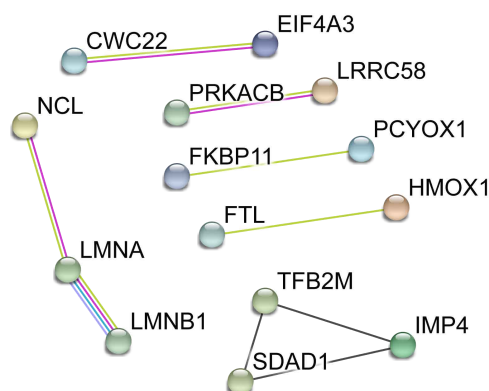
translation. Interestingly, eIF-4A is part of the translation initiation complex as well as eIF-4E, the binding partner of 4E-BP1. Its upregulation could be a compensatory effect due to 4E-BP1[TA] overexpression. This idea is supported by the upregulation of the peptidyl-prolyl cis-trans isomerase FKBP11 (FKBP11), which alters protein folding, but is also a negative modulator of the mTOR pathway. The protein is linked to another post-translational modifying enzyme prenylcysteine oxidase 1 (PCYOX1). The two proteins involved in ion homeostasis, heme oxygenase 1 (HMOX1) and ferritin light chain (FTL), are of particular interest, because they are among the nine proteins, which were found upregulated upon 4E-BP1[TA] as well as 4E-BP1[WT]. The same is the case for leucine-rich repeat-containing protein 58 (LRRC58), which was linked to the cAMP-dependent protein kinase catalytic subunit β (PRKACB), a protein involved in diverse cellular processes.

Finally, STRING analysis was also performed on all upregulated proteins of 4E-BP1[WT] or 4E-BP1[TA] (Fig. 5.10). Apparently, the network was even more complex (significance $p < 0.0001$), but some proteins upregulated by 4E-BP1[TA], found an interaction partner in this context. For instance, the mitochondrial trifunctional enzyme subunit β (HADHB) links to the other proteins involved in fatty acid β-oxidation or EIF4A3 groups together with other proteins involved in translation regulation. The glutathione S-transferase Mu 3 (GSTM3) is one of the proteins upregulated by 4E-BP1[WT] and 4E-BP1[TA]. STRING linked it to glutathione peroxidase 8 (GPX8), a protein with antioxidant activity and involved in stress response. Another commonly upregulated protein was four and a half LIM domains protein 2 (FHL2), which inhibits the transcriptional activity of

FOXO1 and its apoptotic function. It is linked via four and a half LIM domains protein 3 (FHL3) to N-chimaerin (CHN1), a protein involved in neurogenesis.

Figure 5.10: Protein interactions of hits upregulated by 4E-BP1[WT] or 4E-BP1[TA] determined by STRING. The colours of the connecting lines indicate the kind of interaction. Known interactions are turquoise or magenta. These interactions were extracted from curated databases or experimental determined. Predicted interactions are displayed green, red or blue. Interactions were predicted by gene neighbourhood, gene fusions or gene co-occurrences. Yellow, black and light blue lines indicate interactions predicted by textmining, co-expression or protein homology.

In a final bioinformatic investigation, a DAVID analysis was conducted. DAVID (Database for Annotation, Visualization and Integrated Discovery; https://david.ncifcrf.gov, Version 6.7) is a database, which provides a comprehensive set of functional annotation tools for investigators to understand biological meaning behind large list of genes. In contrast to PANTHER, it is not exclusively restricted to Gene Ontology (GO) term enrichment, but also utilises other annotation sources. The DAVID annotation system adapted the Fisher Exact test to measure gene enrichment of annotation

terms. Significant enrichment is expressed by p-value < 0.05.

When analysing proteins upregulated by 4E-BP1[WT], many impressions from the STRING analysis were confirmed (Table 5.1). Proteins associated with cytoskeleton and cytoskeleton organisation were enriched, which is why TUBB2A was one of the central node proteins in STRING with many other connections. Also motor proteins and proteins associated with protein transport and vesicle-mediated transport were enriched, which corresponds to the change in cytoskeletal organisation. Nucleotide binding proteins were also significantly enriched, which points to the change in protein transcription and translation. Furthermore, proteins with antioxidant activity were enriched. As seen in STRING, metabolic proteins were also significantly affected by 4E-BP1[WT], which were involved in fatty acid metabolism or more generally in carboxylic acid catabolism. These proteins may be crucial to mobilise energy reserves in order to cope with stress.

Table 5.1: Excerpt of significantly enriched annotation terms of upregulated proteins after 4E-BP1[WT] overexpression in T-REx HEK293 cells.

Annotation term	% of input genes	p-value
cytoskeleton organization	8.08	2.22E-04
nucleotide-binding	16.67	4.82E-04
vesicle-mediated transport	8.08	0.0037
oxidation reduction	8.08	0.0093
carboxylic acid catabolic process	3.03	0.0106
motor protein	3.03	0.0116
fatty acid metabolism	2.02	0.0257
protein transport	5.56	0.0284

When the proteins upregulated upon 4E-BP1[TA] were analysed, those involved in translation regulation via ribosome biogenesis or RNA processing were significantly overrepresented (Table 5.2), which fits with the impressions of the STRING analysis. As in the 4E-BP1[WT] cohort, proteins with antioxidant potential were significantly enriched. A link consists also between 4E-BP1[TA] overexpression and upregulation of proteins involved in fatty acid metabolism in mitochondria. The annotation term "fatty acid elongation in mitochondria" refers to the whole cycle of this pathway including the constructive and destructive part as the two proteins, which were associated with this term, PPT1 and HADHB, are involved in β-oxidation.

Interestingly, when analysing hits of 4E-BP1[WT] and 4E-BP1[TA] together by DAVID, many significant annotation terms involving mitochon-

dria appeared (data not shown). This was a major difference compared to separate analyses. Mitochondria are vital for cellular functions and these mitochondrial proteins could be involved in stress resistance induced by 4E-BP1.

Table 5.2: Excerpt of significantly enriched annotation terms of upregulated proteins after 4E-BP1[TA] overexpression in T-REx HEK293 cells.

Annotation term	% of input genes	p-value
ribosome biogenesis	8	0.0063
RNA processing	14	0.0065
fatty acid elongation in mitochondria	4	0.0280
oxidation reduction	12	0.0466

5.3.4 Bioinformatic analyses of downregulated hits

As the upregulated proteins upon 4E-BP1 overexpression were investigated bioinformatically, it was also interesting to analyse proteins, which were downregulated. It may shed light on the effect of 4E-BP1 on the proteome in general and may also help to assess the importance of upregulated protein groups, when other members of these groups may be downregulated by 4E-BP1.

Downregulated hits were analysed by the same databases as upregulated proteins. First, a PANTHER analysis was conducted. With respect to the molecular function of proteins, the results showed that the proteins grouped in fewer categories than their upregulated counterparts
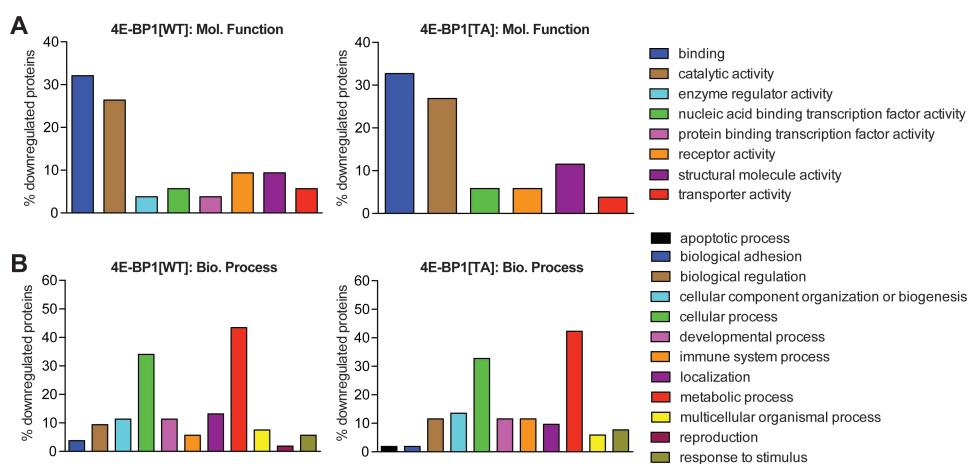
Figure 5.11: Classification of proteins downregulated by 4E-BP1[WT/TA] by PANTHER. (A) Downregulated proteins were classified according to the molecular process they contribute to or the biological process they are involved in (B).

(Fig. 5.11A). 4E-BP1[WT] hits clustered in eight groups and 4E-BP1[TA] hits grouped in six categories. The two most abundant groups were "binding" and "catalytic activity".

When analysing the results of PANTHER with respect to the biological processes the proteins were involved in, the two most abundant groups were again "cellular process" and "metabolic process", hits could be matched to ten further groups (Fig. 5.11B).

Figure 5.12: Protein interactions of hits downregulated by 4E-BP1[WT] determined by STRING. The colours of the connecting lines indicate the kind of interaction. Known interactions are turquoise or magenta. These interactions were extracted from curated databases or experimental determined. Predicted interactions are displayed green, red or blue. Interactions were predicted by gene neighbourhood, gene fusions or gene co-occurrences. Yellow, black and light blue lines indicate interactions predicted by textmining, co-expression or protein homology.
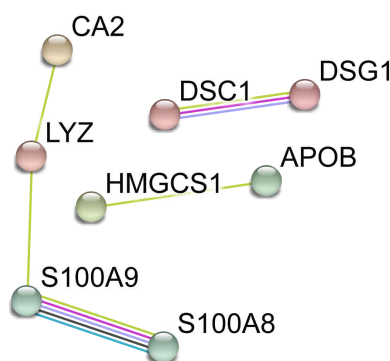
The downregulated proteins of 4E-BP1[WT] and 4E-BP1[TA] were also analysed by STRING, first independently and finally together. The number of connections was significantly increased compared to a random group of proteins for 4E-BP1[TA] and combined 4E-BP1[WT/TA] hits (4E-BP1[WT] only: p = 0.16, 4E-BP1[TA] only/4E-BP1[WT] and 4E-BP1[TA]: p < 0.0001). Still, STRING did not find many connections between the proteins downregulated upon 4E-BP1[WT] (Fig. 5.12). Immune response proteins were linked together, e.g. calprotectin. It is a complex of protein S100-A8 and A9 (S100A8, S100A9), which is a multifunctional complex with pro- and anti-apoptotic characteristics. The complex was commonly downregulated in 4E-BP1[WT] and 4E-BP1[TA] samples. Desmoglein-1 (DSG1) and Desmocollin-1 (DSC1) were two linked proteins involved in cell adhesion. These proteins were also among the downregulated proteins by 4E-BP1[TA]. Hydroxymethylglutaryl-CoA synthase (HMGCS1) and apolipoprotein B-100 (APOB) are connected, because they are involved in synthesis and transport of cholesterol.

Analysis of the 4E-BP1[TA] hits revealed that the S100A8/A9 axis was extended to connect with bis(5'-adenosyl)-triphosphatase (FHIT) (Fig. 5.13), a protein associated with pro-apoptotic potential and for this
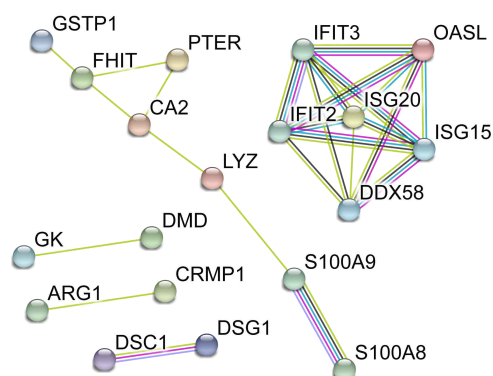
Figure 5.13: Protein interactions of hits downregulated by 4E-BP1[TA] determined by STRING. The colours of the connecting lines indicate the kind of interaction. Known interactions are turquoise or magenta. These interactions were extracted from curated databases or experimental determined. Predicted interactions are displayed green, red or blue. Interactions were predicted by gene neighbourhood, gene fusions or gene co-occurrences. Yellow, black and light blue lines indicate interactions predicted by textmining, co-expression or protein homology.

reason, a tumour suppressor gene (Barnes et al., 1996; Weiske et al., 2007). Its downregulation may promote cell survival. However, the major protein cluster of 4E-BP1[TA] is one of six proteins: probable ATP-dependent RNA helicase DDX58 (DDX58), interferon-induced protein with tetratricopeptide repeats 2 and 3 (IFIT2, IFIT3), the 2'-5'-oligoadenylate synthase-like protein (OASL) and ubiquitin-like protein ISG15 and ISG20 (ISG15, ISG20). All these proteins are involved in immune response, a group of proteins, which already found overrepresented in the PANTHER analysis.

When analysing 4E-BP1[WT] and 4E-BP1[TA] data together by STRING, not many new connections were identified (Fig. 5.14). Some connections, were extended, e.g. ABOB and HMGCS1 linked to the cluster of immune response proteins. Also, a connection between protein NDRG1 (NDRG1) and CD166 antigen (ALCAM) was revealed. NDRG1 is necessary for p53/TP53-mediated caspase activation and apoptosis (Stein et al., 2004), while ALCAM is another protein involved in immune response.

In a final step, the 4E-BP1[WT] and 4E-BP1[TA] hits were analysed by DAVID to investigate whether the proteins were significantly overrepresented in certain functional annotation groups. Interestingly, there was not much difference of the results between 4E-BP1[WT] and 4E-BP1[TA] (Table 5.3 and 5.4). In both cases, proteins involved in antimicrobial response and cytoskeleton organisation were significantly enriched. Apparently, when analysing both protein groups together, not many more new annotation became significantly enriched, which have not been identified before in separate analyses. One exception were proteins involved in ubiquitination. Several annotation terms describing this group of protein were found significantly enriched when analysing both cohorts of downregulated proteins together.
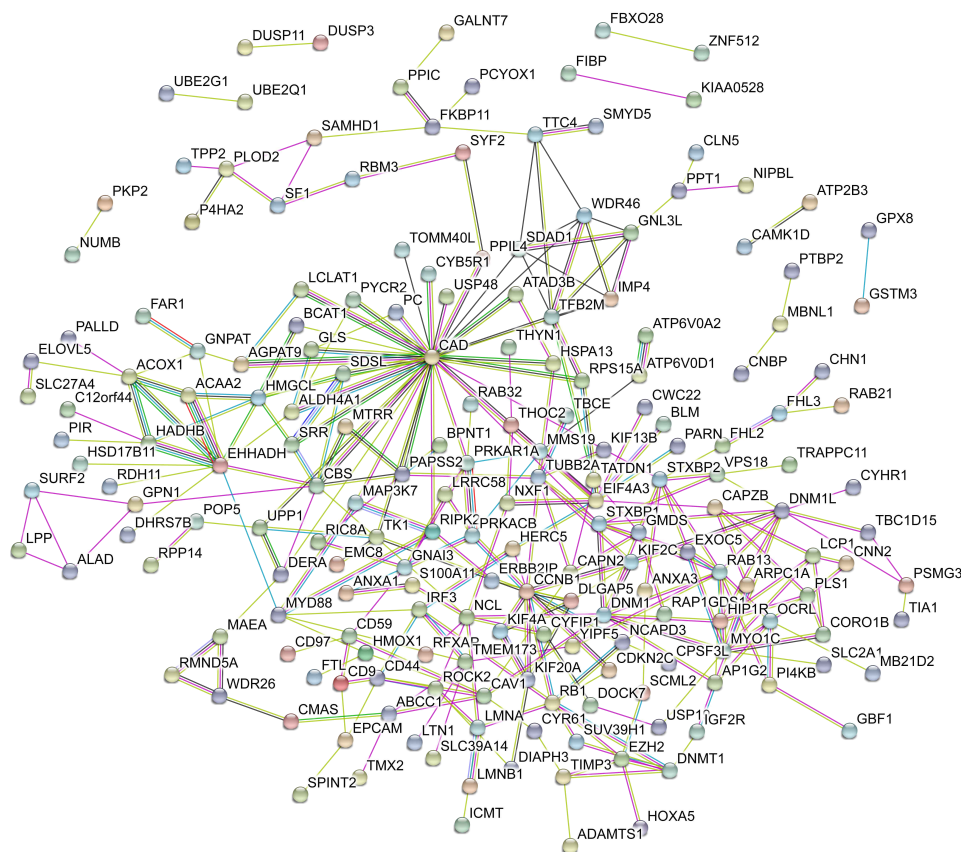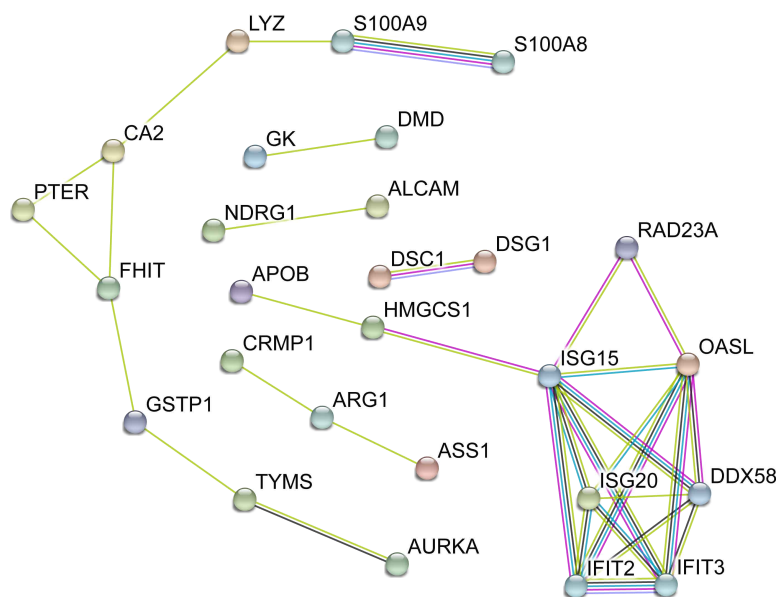
Figure 5.14:   Protein interactions of hits downregulated by 4E-BP1[WT] or 4E-BP1[TA] determined by STRING. The colours of the connecting lines indicate the kind of interaction. Known interactions are turquoise or magenta. These interactions were extracted from curated databases or experimental determined. Predicted interactions are displayed green, red or blue. Interactions were predicted by gene neighbourhood, gene fusions or gene co-occurrences. Yellow, black and light blue lines indicate interactions predicted by textmining, co-expression or protein homology.

Table 5.3: Excerpt of significantly enriched annotation terms of downregulated proteins after 4E-BP1[WT] overexpression in T-REx HEK293 cells.

Annotation term	% of input genes	p-value
antimicrobial	7.55	0.0009
cell motion	11.32	0.0125
cytoskeleton organization	9.43	0.039

Table 5.4: Excerpt of significantly enriched annotation terms of downregulated proteins after 4E-BP1[TA] overexpression in T-REx HEK293 cells.

Annotation term	% of input genes	p-value
antimicrobial	8	0.0008
cytoskeleton organization	10	0.036
response to virus	6	0.0393
cell motion	10	0.0469

5.4 *In vivo* mass spectrometry of *Drosophila*

5.4.1 Label incorporation

Equivalently to the T-REx HEK293 cells, *Drosophila* had to be labelled with amino acids of heavy isotopes to integrate them into their proteome. To achieve this, flies of the parental generation were mated on Sugar-Yeast-Agar (SYA) food, which contained yeast with Lys(6) as the sole amino acid source. In contrast, T-REx HEK293 cells were double labelled with Arg(10) and Lys(8). The F1 generation passed through the whole life cycle from an egg via a larva to an adult fly while consuming the labelled food. Only the heads of the F1 generation were subsequently utilised for mass spectrometry experiments to limit proteome complexity due to organ and tissue diversity.

Because of the fact that fly proteins were only single labelled, trypsin could not be used for digestion as it cleaves at the carboxyl side of arginine or lysine. Hence, Lys-C was utilised, which cleaves at the carboxyl side of lysine residues only. Initially, *UAS-lacZ* and *da-GAL4* flies were crossed to overexpress a protein in the F1 generation, which should not have an effect on the expression level of other proteins. This was supposed to serve as the quantification reference to FLAG-d4E-BP overexpressing flies raised
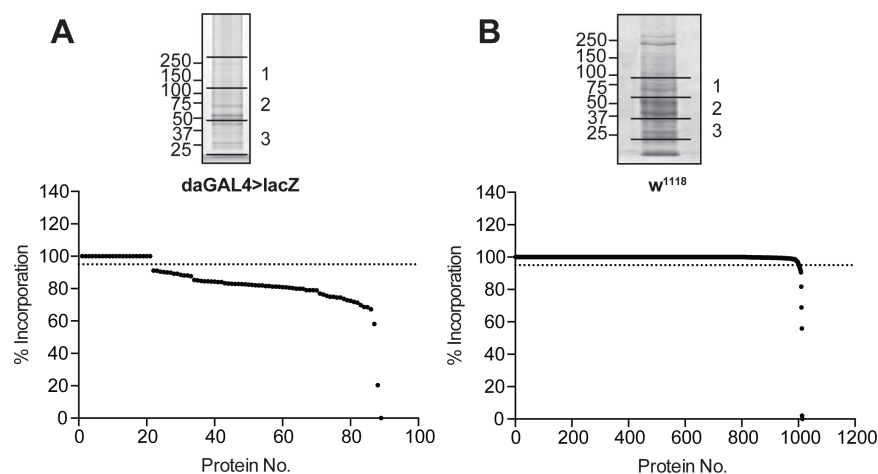
Figure 5.15: Incorporation of heavy isotopes in proteins of *Drosophila* flies. Coomassie stained SDS gels show the loaded fractions of extracted heavy labelled proteins from *da-GAL4>lacZ* (A) or *w1118* flies (B). The lines indicate where the samples were cut and fractionated for incorporation analyses by mass spectrometry. In the diagrams, the average isotope incorporation is displayed for every single analysed protein underneath their gels, ordered from highest to lowest incorporation. The dotted lines indicate 95 % incorporation, which is considered as completely labelled.

on light yeast to identify up- and downregulated proteins. The activation of the UAS-GAL4 system in the reference flies should reduce the number of randomly up- or downregulated proteins due to the activation of the overexpression system in experimental samples. 1 µg of extracted labelled proteins from fly heads were fractioned briefly by SDS gel electrophoresis (Fig. 5.15A). The lane was cut in three pieces, in-gel digested with Lys-C and the peptides extracted. Fraction 2 was utilised for initial incorporation tests. However, quantitative mass spectrometry revealed that the average incorporation was only 83.7 %, which was too little. Incomplete labelling reduces the chance to detect up- or downregulated proteins. It is possible that the other chemical components of the fly food may have become contaminated with a protein source, e.g. bacteria, which was incorporated by *Drosophila* or enzymatic reactions during protein preparations may have converted unlabelled proline to lysine. To avoid these problems, commercially available Lys(6) w^{1118} labelled fly heads were ordered. These flies correspond to the genetic background of FLAG-d4E-BP overexpressing flies and are an acceptable reference genotype. The extracted proteins were processed as described before and all three gel fractions were utilised for the incorporation analysis (Fig. 5.15B). This time the average label incorporation was 99.5 % and therefore clearly sufficient for quantitative experiments.

5.4.2   Mass spectrometry measurements of in-gel fractionated proteins

After confirming that the reference flies had incorporated the heavy labelled proteins, protein quantification *in vivo* could be performed. In preparation, *UAS-FLAG-d4E-BP[WT/TA]* transgenic flies were crossed with *da-GAL4* flies to overexpress the transgenes ubiquitously in the F1 generation. Parental flies were mated on fly food containing Lys(0) labelled yeast. Thus, flies overexpressing d4E-BP were labelled with the light isotopes, while the reference w^{1118} flies were labelled with the heavy isotopes. This was reciprocal to the experiments in T-REx HEK293 cells. To avoid confusion for the quantitative analysis, the heavy to light ratios of *Drosophila* proteins (H/L) were inverted so that they can be read like the quantifications from cells. This means that proteins with H/L ratio > 1 were upregulated, while they were downregulated with a value < 1.

The heads of flies raised on heavy and light food were harvested, lysed
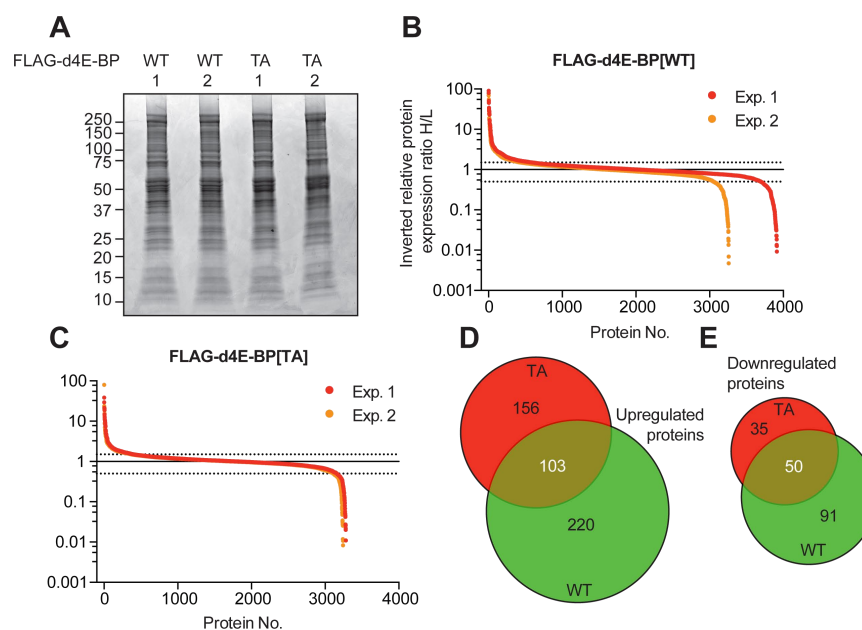
Figure 5.16: Effect of FLAG-d4E-BP[WT] or FLAG-d4E-BP[TA] overexpression on the *Drosophila* proteome. (A) Coomassie stained SDS gel of extracted proteins from fly heads. 50 µg protein (25 µg heavy + light labelled) were loaded per lane. The molecular weight is indicated at the left hand side in kDa. (B) Normalised inverted heavy to light ratio (H/L) of all quantified proteins after FLAG-d4E-BP[WT] or FLAG-d4E-BP[TA] overexpression (C) in biological duplicates (Exp. 1/2). The upper dotted line separates proteins, which were more than 50 % upregulated upon FLAG-d4E-BP[WT/TA] overexpression, while the lower dotted line indicates proteins, which were more than 50 % downregulated. (D) VENN diagram of all proteins upregulated by FLAG-d4E-BP[WT] or FLAG-d4E-BP[TA] overexpression. 103 proteins were upregulated in both samples. (E) VENN diagram of all proteins downregulated by FLAG-d4E-BP[WT] or FLAG-d4E-BP[TA] overexpression. 50 proteins were downregulated in both samples.

and their proteins extracted. From the same cross, two fractions of heads were harvested and lysed separately to gain protein material of two biological replicates. 25 µg heavy labelled proteins were combined with the same amount of light labelled proteins and separated by SDS gel electrophoresis (Fig. 5.16A). The gel was stained, the lanes cut into twelve equally sized fractions and digested with Lys-C. The peptides were extracted and analysed by quantitative mass spectrometry.

In *Drosophila* overexpressing FLAG-d4E-BP[WT], 3913 and 3259 proteins could be quantified in the first and second biological duplicate (Fig. 5.16B). The same criteria for up- and downregulated were applied as before in T-REx HEK293 cells. Proteins changed by more than 50 % in one of two experiments and a confirmed change of more than 40 % in the other experiment were considered as altered. By applying these criteria, 323 proteins were found upregulated upon FLAG-d4E-BP[WT] overexpression,

while 141 were downregulated (Fig. 5.16D and E, whole lists in the appendix table A15, A17, A18 and A20).

In flies overexpressing FLAG-d4E-BP[TA], 3281 and 3243 proteins could be quantified in both experiments (Fig. 5.16C). 259 proteins were up- and 85 proteins were downregulated (Fig. 5.16D and E, whole lists in the appendix table A16, A17, A19 and A20). Among the upregulated proteins were 103, which were upregulated by both d4E-BP[WT] and d4E-BP[TA], while 50 proteins were downregulated in both conditions (Fig. 5.16D and E, lists in the appendix table A17 and A20).

The mass spectrometry analysis of fly proteins also revealed that the annotation of fly proteins is clearly limited compared to human proteins. This became apparent by the fact that many identified peptides could only be matched to proteins, which have been described for other *Drosophila* species, but not for *Drosophila melanogaster* yet. To fill the gaps in the list of up- and downregulated fly proteins, the protein IDs were analysed by BLAST (Basic Local Alignment Search Tool) to identify *Drosophila melanogaster* proteins with a similar sequence. However, BLAST analysed hits were excluded for subsequent bioinformatic analyses as sequence similarities were sometimes limited. Conclusions about the function of these proteins could bias the analyses.

5.4.3 Bioinformatic analyses of upregulated hits

All hits of the *Drosophila* mass spectrometry experiments were analysed in the same way as *in vitro* hits by PANTHER, STRING and DAVID. The PANTHER analysis of upregulated proteins revealed that d4E-BP[WT] and d4E-BP[TA] hits grouped in nine categories according to the molecular process they are involved in (Fig. 5.17A). The two most prominent categories were "binding" and "catalytic activity", although approximately 10 % more d4E-BP[WT] proteins were associated with the latter group than d4E-BP[TA] proteins. Otherwise, the distribution pattern of d4E-BP1[WT] and d4E-BP1[TA] looked similar.

When it came to the biological process the proteins were involved in, PANTHER analysis showed that d4E-BP[WT] proteins clustered in ten categories, while d4E-BP[TA] protein assembled in twelve categories, with "biological adhesion" and "immune system process" in d4E-BP[TA] overexpressing samples only. The most abundant categories were "cellular process"

and "metabolic process". While the first one is similar in d4E-BP[WT] and d4E-BP[TA], about 10 % less proteins were involved in metabolic processes among the d4E-BP[TA] hits compared to d4E-BP[WT]. Both samples had comparable proportion of proteins, which were classified to be involved in "response to stimulus". Among them were seven proteins involved in stress response in the d4E-BP[WT] cohort and eight for d4E-BP[TA]. Four proteins are shared between both samples. These were serine/threonine-protein phosphatase 2B catalytic subunit 2 and 3 (Pp2B-14D, CanA-14F), CG9617 protein (Sgt1), a chaperone binding protein and GH12714p (PpD3), another serine/threonine-protein phosphatase. The other three candidates of d4E-BP[WT] were methionine-R-sulfoxide reductase B1 (SelR) and peptide methionine sulfoxide reductase (Eip71CD), which are both involved the regeneration of thioredoxin, as well as CG4019 (CG4019), a transmembrane glycerol channel. The four proteins upregulated by d4E-BP[TA] only were the thioester-containing protein 4, an endopeptidase inhibitor and the chaperones DnaJ protein homolog 1 (DnaJ-1), heat shock protein 22 (Hsp22) as well as FI21225p1 (unc-45).

Figure 5.17: Classification of proteins upregulated by FLAG-d4E-BP[WT/TA] by PANTHER. (A) Upregulated proteins were classified according to the molecular process they contribute to or the biological process they are involved in (B).

Furthermore, PANTHER found two proteins in the d4E-BP[TA] cohort, which were associated with AD, an actin variant (Act79B) and the transient-receptor-potential-like protein (trpl). Trpl is a calcium channel, which is activated by fatty acids and metabolic stress (Agam et al., 2000; Chyb et al., 1999). Act79B was also associated with Huntington's disease. Additionally,

PANTHER found asator, a serine/threonine kinase, to be linked to PD. In the d4E-BP[WT] protein cohort, PANTHER found nicastrin (nct), an essential subunit of the γ-secretase complex, to be involved in AD.

When analysing all proteins, which were upregulated by d4E-BP[WT] with STRING, many links and interactions were found between the proteins (Fig. 5.18). The number of connections was significantly increased compared to random groups of proteins (p < 0.0001). Several clusters of proteins were revealed, which are also connected with each other. The biggest cluster includes central proteins like acetyl-CoA carboxylase (ACC), acetyl-coenzyme A synthetase (AcCoAS) and the mitochondrial probable methylmalonate-semialdehyde dehydrogenase (CG17896). AcCoAS activates acetate for energy generation, while ACC contributes to the fatty acid metabolism as well as CG17896. Thus, this cluster consists of proteins

Figure 5.18: Protein interactions of hits upregulated by FLAG-d4E-BP[WT] determined by STRING. The colours of the connecting lines indicate the kind of interaction. Known interactions are turquoise or magenta. These interactions were extracted from curated databases or experimental determined. Predicted interactions are displayed green, red or blue. Interactions were predicted by gene neighbourhood, gene fusions or gene co-occurrences. Yellow, black and light blue lines indicate interactions predicted by textmining, co-expression or protein homology.

involved in metabolism. Another prominent cluster consists of different variants of glutathione *S*-transferases (GstE1, E5, E6, E7, D9), anti-apoptotic proteins that are involved in detoxification. A further cluster revealed the upregulation of proteins involved in translation, the eukaryotic translation initiation factors 4G and 5 (eIF4G, eIF5). This could be a compensating mechanism as d4E-BP is the binding partner of eIF-4E. Furthermore, proteins involved in transcription regulation were also upregulated as the inorganic pyrophosphatase (Nurf-38) or the ATP-dependent helicase brm (brm). Proteins defining the iron metabolism where upregulated, too. This is demonstrated e.g. the detection of transferrin 1 (Tsf1).
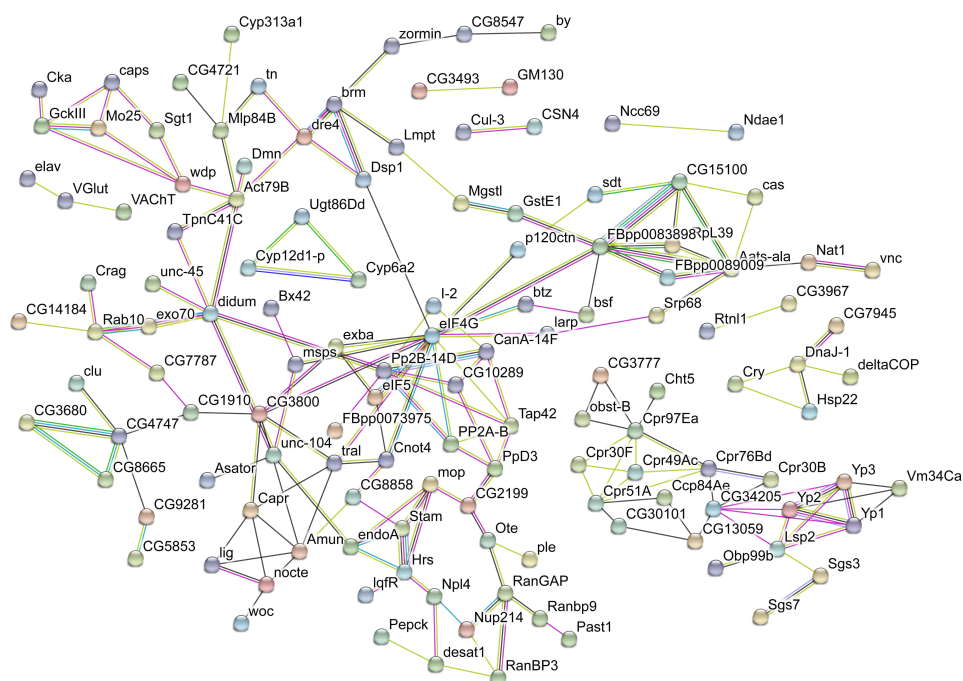
Figure 5.19: Protein interactions of hits upregulated by FLAG-d4E-BP[TA] determined by STRING. The colours of the connecting lines indicate the kind of interaction. Known interactions are turquoise or magenta. These interactions were extracted from curated databases or experimental determined. Predicted interactions are displayed green, red or blue. Interactions were predicted by gene neighbourhood, gene fusions or gene co-occurrences. Yellow, black and light blue lines indicate interactions predicted by textmining, co-expression or protein homology.

Similar to the *in vitro* experiments, the data revealed that many different pathways and groups of proteins were affected by d4E-BP[WT] overexpression. The protein network is less complex for d4E-BP[TA], but still reveals important protein clusters (p < 0.0001, Fig. 5.19). Again, proteins involved in translation modulation were upregulated. In this case, the cen-

tral proteins eIF-4G and eIF-5 were further linked to the bifunctional glutamate/proline-tRNA ligase (FBpp0083898), the alanine-tRNA ligase (Aatsala) and the mitochondrial 39S ribosomal protein L39 (mRpL39).

Proteins involved in protein transport and cell mobility were also upregulated. A central protein of this cluster is the motor protein dilute class unconventional myosin (didum), which is linked to the muscle protein troponin C (TpnC41C). Didum was also upregulated by d4E-BP[WT].

A small, but well connected cluster of proteins is involved in the synaptic vesicle cycle and neurotransmitter secretion at the neuromuscular junction. Among them was endophilin-A (endoA), the Jak pathway signal transduc-
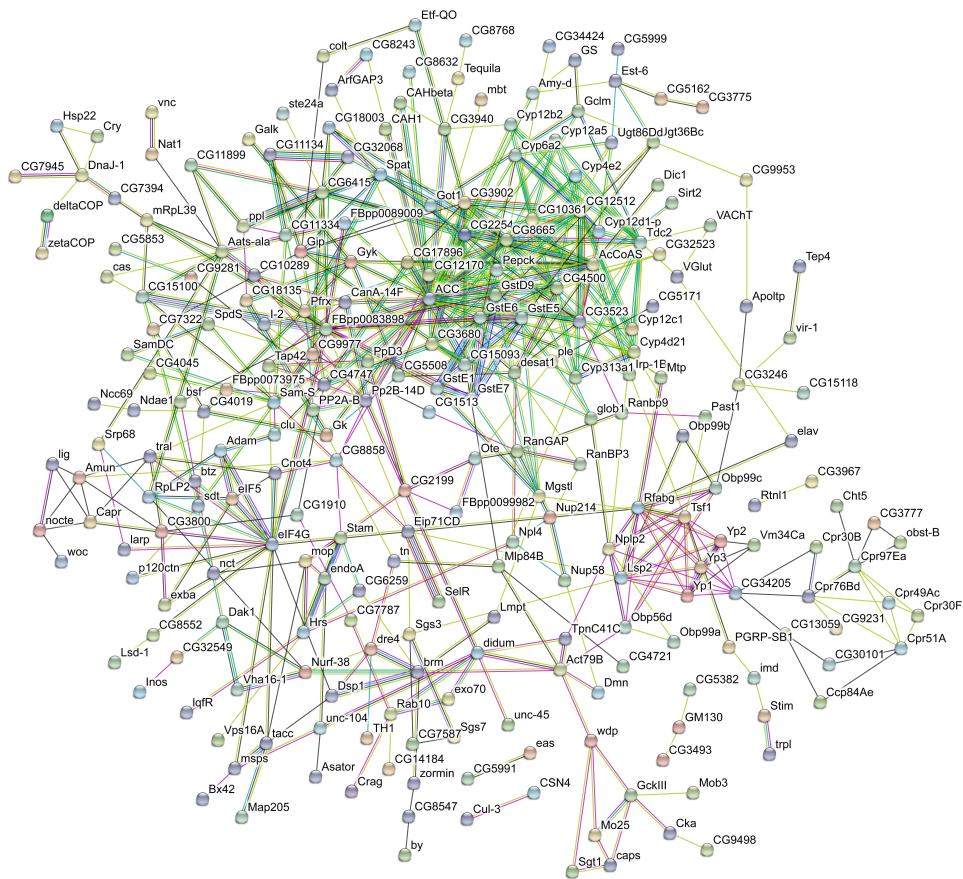
Figure 5.20: Protein interactions of hits upregulated by FLAG-d4E-BP[WT] or FLAG-d4E-BP[TA] determined by STRING. The colours of the connecting lines indicate the kind of interaction. Known interactions are turquoise or magenta. These interactions were extracted from curated databases or experimental determined. Predicted interactions are displayed green, red or blue. Interactions were predicted by gene neighbourhood, gene fusions or gene co-occurrences. Yellow, black and light blue lines indicate interactions predicted by textmining, co-expression or protein homology.

tion adaptor molecule (Stam) and the hepatocyte growth factor-regulated tyrosine kinase substrate (Hrs).

Interestingly, proteins with chaperone function clustered together in this STRING analysis, too. For instance, DnaJ-1 and Hsp22 belonged to them, which have been identified by PANTHER before.

When hits of d4E-BP1[WT] and d4E-BP1[TA] were analysed together, the sheer number of proteins and edges made a meaningful analysis difficult ($p < 0.0001$, Fig. 5.20). The same major clusters became apparent including proteins for translation regulation around eIF4G, proteins involved in cell mobility and iron metabolism around didum and Tsf1 as well as the very big cluster of lipid metabolism proteins around ACC. However, when the number of hits is so high, STRING is clearly overstrained and not the tool of choice.

DAVID is a much more convenient tool when it comes to large numbers of targets. When analysing d4E-BP[WT] hits, many annotation terms were significantly overrepresented, which have been confirmed by STRING or PANTHER before (Table 5.5). For example, proteins of lipid metabolism were among them, but also proteins of glutathione metabolism. Furthermore, proteins responsible for reduction of oxidation were enriched, e.g. the ubiquinol-cytochrome c reductase (UQCR-6.4). Other enriched protein groups were mitochondrial proteins as the translocase of the inner mitochondrial membrane subunit TIM14 (Tim14), proteins involved in iron metabolism and the neurotransmitter cycle like endoA.

Table 5.5: Excerpt of significantly enriched annotation terms of upregulated proteins after FLAG-d4E-BP[WT] overexpression in *Drosophila*.

Annotation term	% of input genes	p-value
glutathione metabolism	4.42	0.0001
oxidation reduction	11.24	0.0002
lipid metabolism	3.21	0.0006
glutathione transferase activity	2.41	0.0015
mitochondrion	8.84	0.0184
regulation of neurotransmitter levels	2.81	0.0275
neurotransmitter transport	2.81	0.0484
iron	3.21	0.0490

d4E-BP[TA] hits also had proteins enriched, which were involved in the neurotransmitter cycle and mitochondrial proteins (Table 5.6), e.g. the probable cytochrome P450 12d1 distal (Cyp12d1-d). Further enriched

groups were proteins involved in protein translation, like eIF-4G or protein folding, like HSP22.

When d4E-BP[WT] and d4E-BP[TA] hits were analysed together by DAVID, again annotation categories of proteins involved in lipid metabolism, the neurotransmitter cycle at the synapse and mitochondrial proteins were enriched. However, the analysis did not reveal groups, which have not been identified by the separate analyses before.

Table 5.6: Excerpt of significantly enriched annotation terms of upregulated proteins after FLAG-d4E-BP[TA] overexpression in *Drosophila*.

Annotation term	% of input genes	p-value
protein transport	6.58	0.0002
regulation of neurotransmitter levels	3.51	0.0023
neurotransmitter transport	3.51	0.0049
neurotransmitter secretion	3.07	0.0069
iron	3.95	0.0101
synaptic transmission	3.95	0.0133
translation initiation factor activity	2.19	0.0238
mitochondrion	3.51	0.0366
protein folding	2.63	0.0424

5.4.4   Bioinformatic analyses of downregulated hits

After the upregulated hits, also the downregulated hits were analysed by bioinformatic tools beginning with PANTHER. When the proteins were clustered according to their molecular function, d4E-BP[WT] hits grouped into
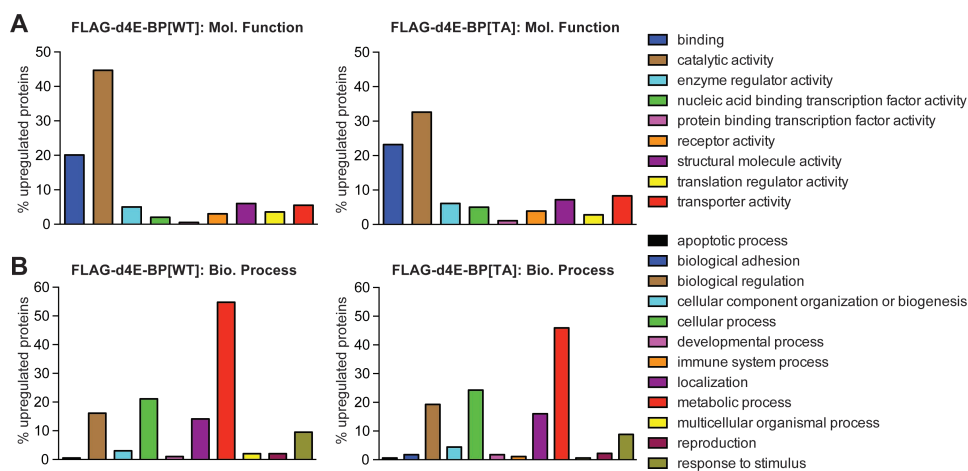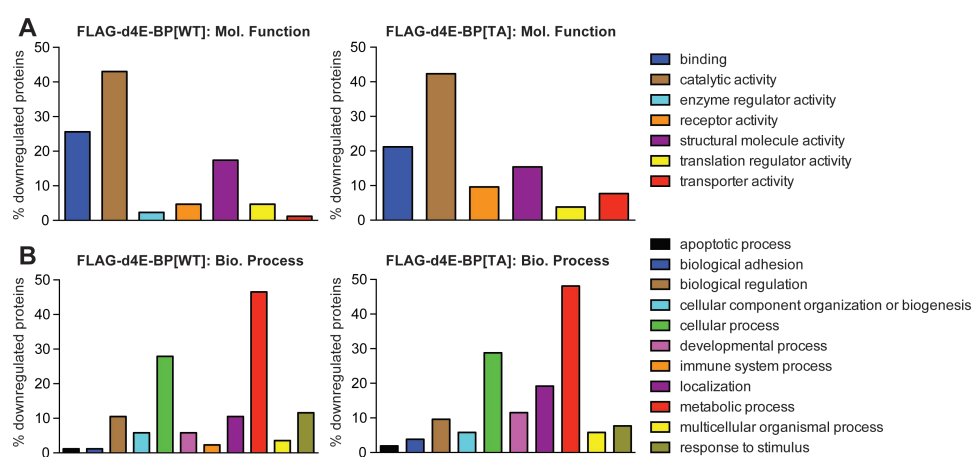

Figure 5.21: Classification of proteins downregulated by FLAG-d4E-BP[WT/TA] with PANTHER. (A) Downregulated proteins were classified according to the molecular process they contribute to or the biological process they are involved in (B).

seven and d4E-BP[TA] hits into six groups (Fig. 5.21). In contrast to the d4E-BP1[WT] cohort, among the d4E-BP[TA] hits were no proteins with enzyme regulatory activity. The two most abundant groups were "binding" and "catalytic activity".

The two most abundant biological processes that the downregulated proteins were involved in were "cellular process" and "metabolic process". The ratio of proteins involved in cellular processes was decreased among downregulated proteins. Two proteins in the d4E-BP[WT] cohort were involved
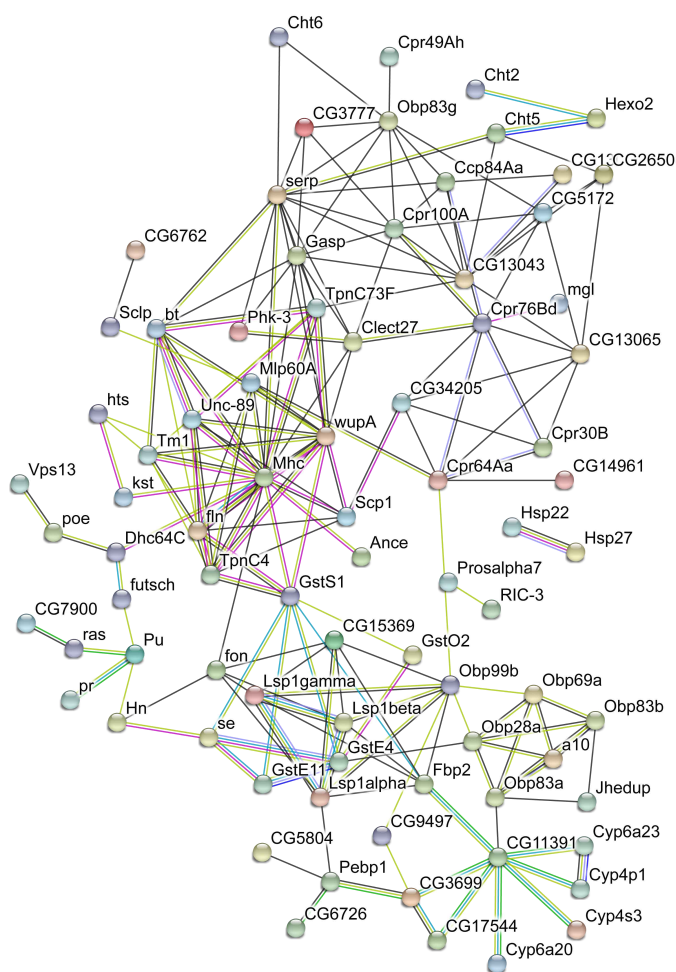
Figure 5.22: Protein interactions of hits downregulated by FLAG-d4E-BP[WT] determined by STRING. The colours of the connecting lines indicate the kind of interaction. Known interactions are turquoise or magenta. These interactions were extracted from curated databases or experimental determined. Predicted interactions are displayed green, red or blue. Interactions were predicted by gene neighbourhood, gene fusions or gene co-occurrences. Yellow, black and light blue lines indicate interactions predicted by textmining, co-expression or protein homology.

in stress response, the heat shock proteins 22 and 27 (Hsp22, Hsp27).

Some proteins associated with the development of neurodegenerative diseases were identified by PANTHER among the downregulated proteins. The proteasome subunit alpha type-3 (Prosalpha7) was downregulated in d4E-BP[WT] and d4E-BP[TA] and is linked to PD as well as the dynein heavy chain (Dhc64C), which is involved in retrograde movement of vesicles and organelles along microtubules and linked to Huntington's disease. An actin variant (Act88F) was downregulated by d4E-BP[TA] and is linked to AD, while another AD linked protein, megalin (mgl) was downregulated by d4E-BP[WT].

The downregulated hits were further analysed by STRING. The network of downregulated proteins by d4E-BP[WT] revealed a significantly enriched number of connections compared to a random group of proteins ($p < 0.0001$, Fig. 5.22). Central proteins of the biggest cluster were myosin heavy chain (Mhc) and troponin I (wupA), which are muscle proteins involved in cell mobility. On the other hand, other proteins of this groups were upregulated (see above). Many proteins involved in chitin setting were also downregulated, e.g. the cuticular protein 30B (Cpr30B), serpentine (serp) or gasp, but not much is known yet about the precise functions of these proteins. Noticeable is also the cluster of downregulated glutathione *S*-transferases E4, E11, O2 and S1 (GstE4, GstE11, GstO2, GstS1). Other variants were found upregulated by d4E-BP1[WT]. Furthermore, several cytochrome P450 variants were downregulated like 4p1, 6a20, 6a23 and 4s3 (Cyp4p1, Cyp6a20,
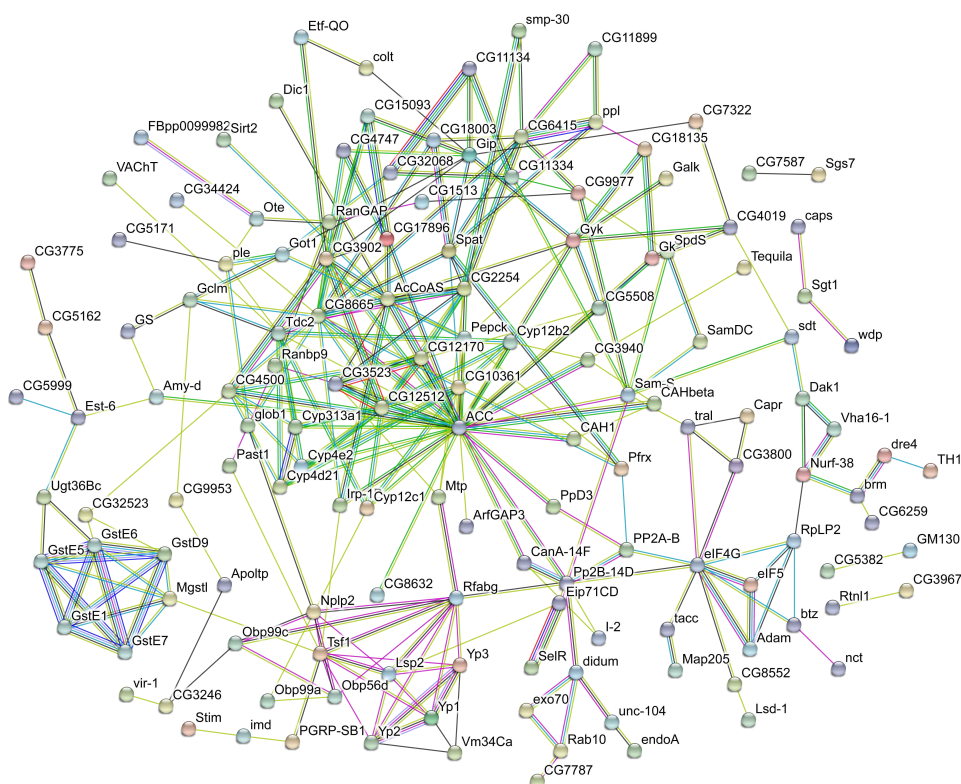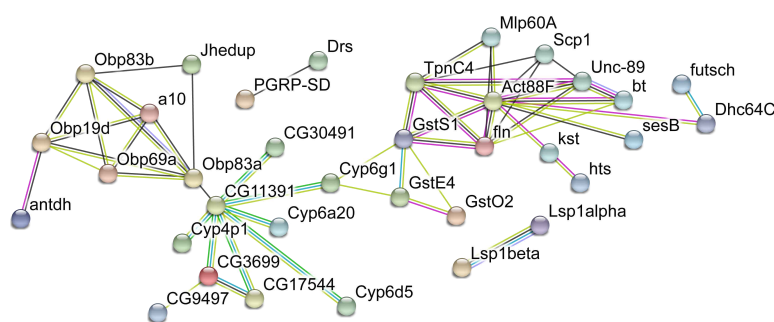

Figure 5.23: Protein interactions of hits downregulated by FLAG-d4E-BP[TA] determined by STRING. The colours of the connecting lines indicate the kind of interaction. Known interactions are turquoise or magenta. These interactions were extracted from curated databases or experimental determined. Predicted interactions are displayed green, red or blue. Interactions were predicted by gene neighbourhood, gene fusions or gene co-occurrences. Yellow, black and light blue lines indicate interactions predicted by textmining, co-expression or protein homology.

Cyp6a23, Cyp4s3).

The STRING analysis of proteins downregulated by d4E-BP[TA] revealed a similar pattern as for the wildtype counterpart (p < 0.0001, Fig. 5.23). The number of links between proteins were significantly enriched
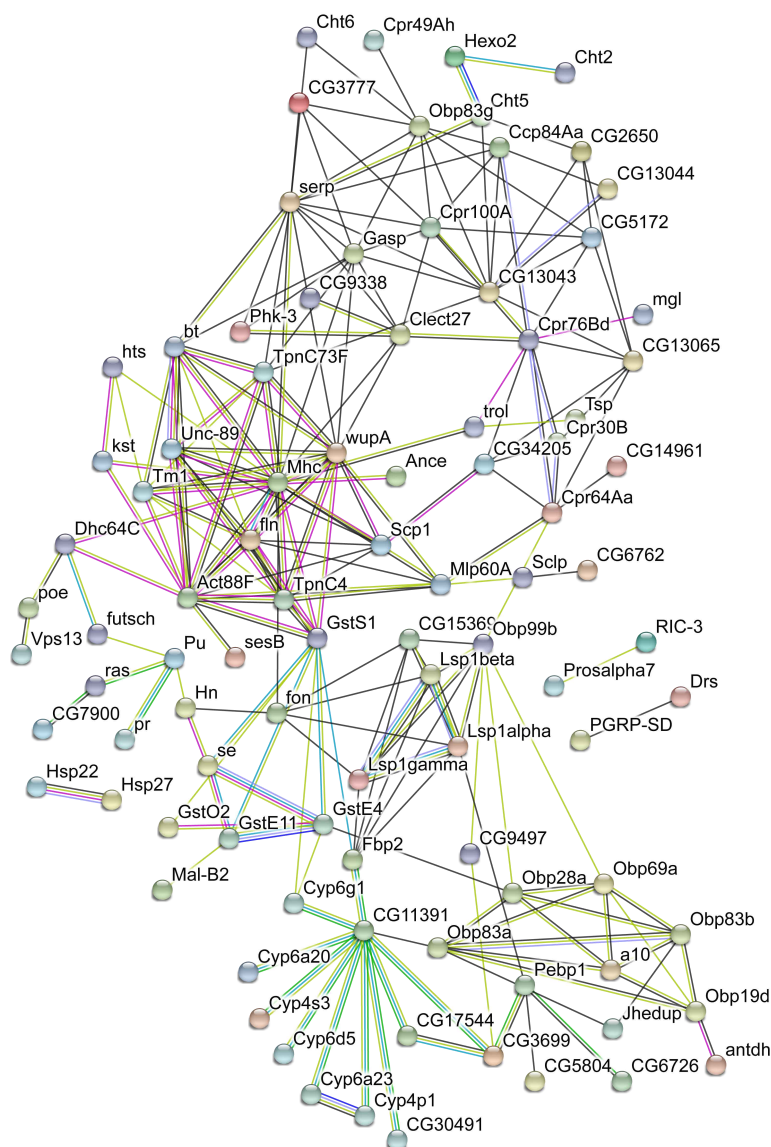
Figure 5.24: Protein interactions of hits downregulated by FLAG-d4E-BP[WT] or FLAG-d4E-BP[TA] determined by STRING. The colours of the connecting lines indicate the kind of interaction. Known interactions are turquoise or magenta. These interactions were extracted from curated databases or experimental determined. Predicted interactions are displayed green, red or blue. Interactions were predicted by gene neighbourhood, gene fusions or gene co-occurrences. Yellow, black and light blue lines indicate interactions predicted by textmining, co-expression or protein homology.

and the proteins grouped in three major clusters. One cluster involved protein responsible for olfactory perception including the central protein putative odorant-binding protein A10 (a10). As for d4E-BP[WT], several cytochrome P450 variants were downregulated as well as proteins involved in muscle contraction and cell mobility as an actin variant (Act88F) or troponin C (TpnC4).

As the patterns of downregulated proteins by d4E-BP[WT] and d4E-BP[TA] were very similar in the STRING analysis, it is no surprise that the analysis of both cohorts together did not reveal further protein clusters, but showed that the existing clusters were only supplemented by further proteins (p < 0.0001, Fig. 5.24).

Table 5.7: Excerpt of significantly enriched annotation terms of downregulated proteins after FLAG-d4E-BP[WT] overexpression in *Drosophila*.

Annotation term	% of input genes	p-value
insect pheromone/ odorant binding protein	5.41	0.0001
insect cuticle protein	7.21	0.0001
muscle protein	3.60	0.0003
glutathione transferase activity	4.50	0.0005
oxidation reduction	13.51	0.0005
sensory perception of chemical stimulus	6.31	0.0057
chitin metabolic process	4.50	0.0155
cytoskeleton	7.21	0.0311
cytochrome P450	3.60	0.0473

Table 5.8: Excerpt of significantly enriched annotation terms of downregulated proteins after FLAG-d4E-BP[TA] overexpression in *Drosophila*.

Annotation term	% of input genes	p-value
pheromone binding	8.06	0.0001
insect pheromone/odorant binding protein PhBP	6.45	0.0005
cytochrome P450	6.45	0.0105
oxidation reduction	16.13	0.0109
glutathione transferase activity	4.84	0.0185
skeletal myofibril assembly	3.23	0.0358

The DAVID analysis confirmed the results found by STRING. Significantly enriched proteins among the hits downregulated by d4E-BP[WT] were muscle and cytoskeletal proteins, different variants of cytochrome P450, proteins involved in the chitin metabolism or olfactory perception, but also proteins, which can reduce oxidation (Table 5.7). Among the latter are many glutathione transferases. Aside from cytoskeletal and chitin proteins, this

picture was confirmed by the analysis of hits d4E-BP[TA] (Table 5.8) and of both combined set of hits.

5.5   Comparison of upregulated mass spectrometry hits of *in vitro* and *in vivo* experiments

After analysing up- and downregulated mass spectrometry hits of T-REx HEK293 cells and *Drosophila* flies, it was important to compare upregulated proteins of these *in vitro* and *in vivo* experiments to investigate whether conserved targets exist, which were upregulated by 4E-BP1/d4E-BP. For this purpose, genes of upregulated *Drosophila* proteins were analysed with the Ensembl Biomart database (http://www.ensembl.org/biomart) to identify human homologues. The analysis revealed that homologues of twelve human proteins were upregulated *in vitro* and *in vivo* (Table 5.9). Additionally, homologues were identified, which matched to different variants of 22 human proteins of the same protein family. One example is the ras-related protein Rab-13 (RAB13), which was found upregulated in cells by 4E-BP1[TA]. The gene found upregulated in flies was homologous to RAB10. However, as both proteins are involved in similar biological processes and are key regulators of intracellular membrane trafficking, there were still listed here.

Compared with the whole number of hits in all experiments, the number of overlapping homologues was not very high, but the identified proteins cover a huge variety of biological functions, which have been shown to be enriched in the previous bioinformatic analyses. Among these proteins was four and a half LIM domains protein 2 (FHL2), an interlink between different pathway to alter gene transcription. This protein was upregulated in all quantitative 4E-BP1/d4E-BP[WT/TA] experiments. Proteins involved in transcriptional regulation were identified by bioinformatic analyses.

Another examples was fatty acyl-CoA reductase 1 (FAR1), a protein involved in the lipid metabolism, which was upregulated by 4E-BP1[WT] and d4E-BP[WT/TA]. The mitochondrial pyruvate carboxylase (PC) was upregulated by 4E-BP1[WT] and d4E-BP[WT]. It is an example of the several upregulated mitochondrial proteins identified in all experiments. As a compensatory response, translation initiating proteins were also upregulated. EIF4-A3 was found in 4E-BP1[TA], while eIF-4G was found in d4E-BP[WT/TA] overexpressing flies. Both proteins are part of the com-

plex to initiate cap-dependent translation.

Table 5.9: List of human genes and their homologues in *Drosophila*, which were translationally upregulated by 4E-BP1/d4E-BP *in vitro* and *in vivo*. If the *Drosophila* gene was identified by BLAST, then this was indicated in the column. The third column indicates the name of the human homolgue of the *Drosophila* gene in column two. The last two columns show, whether the human and *Drosophila* proteins were found upregulated by 4E-BP1/d4E-BP[WT] and/or 4E-BP1/d4E-BP[TA].

Human Gene	*Drosophila* Gene	Human Homologues	Found *in vitro*	Found *in vivo*
ALDH4A1	CG8665	ALDH1L1/2	WT	WT, TA
ANXA1/3	Blast: AnxB9	ANXA7	WT	TA
ATP6V0A2/ D1	Vha16-1	ATP6V0C	WT	TA
CNBP	CG3800	CNBP	WT	WT, TA
CSRP1	Mlp84B	CSRP1	WT	TA
CYB5R1	zetaCOP; CG5946	CYB5R1	TA	WT
DHRS11	Blast: CG40485, CG8757	DHRS11	WT	WT, TA
DLGAP5	Blast: vlc	DLGAP1-4	WT	TA
EIF4A3	eIF4G	EIF4G1/3	TA	WT, TA
ETNK1	eas	ETNK1	WT	WT
EXOC5	exo70	EXOC7	WT	WT, TA
FAR1	CG5065	FAR1	WT	WT, TA
FHL2	CG34325	FHL2	WT, TA	WT, TA
FHL3	CG34325	FHL3	WT	WT, TA
FKBP11	CG14715	FKBP2	TA	WT, TA
HSPA13	Hsp22	HSPB1/2/3/8	WT	TA
IPO8	Ranbp9	IPO9	WT	WT, TA
KIF2C/ 4A/ 13B/ 20A	unc-104	KIF1A/B	WT	WT, TA
METTL2B	CG4045	METTL1	WT	TA
MYO1C	didum	MYO5A/B/C	WT	WT, TA
PALLD	zormin	PALLD	WT	TA
PC	PCB	PC	WT	WT
PKP2	p120ctn	PKP2	WT	TA
RAB13	Rab10	RAB10	TA	WT, TA
RAB21/32	Rab10	RAB10	WT	WT, TA
RAP1GDS1	vimar	RAP1GDS1	WT	TA
SLC25A24	colt	SLC25A20	TA	WT
TTC4	CG14105	TTC36	WT	WT

5.6   Discussion

The results of this chapter demonstrated that the generated *in vitro* and *in vivo* models could be utilised successfully for quantitative mass spectrometry of the proteome. In the end, several thousand proteins were quanti-

fied. However, the optimisation of the mass spectrometry protocol in T-REx HEK293 cells emphasised how important a sophisticated protocol optimisation is to get the best possible result for the desired question, application and model. The increase of protein fractionation improved the coverage of quantified proteins, but other factors had important influence as well. After changing the lysis protocol, the number of proteins could be increased further even with a lower number of fractions.

In this case, the aim was to quantify proteins of all different cell compartments in order to get an overview as complete as possible of translational changes caused by 4E-BP1/d4E-BP. This aim was achieved as nuclear, mitochondrial, membrane and cytosolic proteins were identified.

Surprisingly, in T-REx HEK293 many more proteins were upregulated upon 4E-BP1[WT] overexpression than 4E-BP1[TA]. As 4E-BP1[TA] is the permanently active form, one should expect that it has a more substantial effect on the proteome. However, it has to be considered that active 4E-BP1 is an negative regulator of cap-dependent translation, the most effective and predominant form of translation. When 4E-BP1[WT] was overexpressed, one could imagine that cap-dependent translation was not as tightly turned off as by 4E-BP1[TA], while unbalacing the sensitive system of protein translation at the same time. This could mean that some proteins were upregulated by 4E-BP1[WT] as a response to its overexpression, but independently of IRES mediated protein translation. Huo et al. (2012) tested the effect of different mTOR inhibitors on translational changes of proteins. Their supplementary data revealed that more proteins were overexpressed in response to the partial mTOR inhibitor rapamycin, while the more potent mTOR inhibitors upregulated fewer proteins. Although these experiments cannot be compared directly due to its different experimental approaches, it demonstrates that incomplete suppression of cap-dependent translation may overexpress more proteins than a stronger inhibition.

The same effect as in cells was observed in flies as well, although it was less distinct. The reason may be that some proteins were just upregulated as an immediate response to 4E-BP1[WT] overexpression and returned to normal levels after some time. While 4E-BP1[WT] in cells was only overexpressed for 6 h, in flies overexpressed occured during the whole period of their development from an egg to an adult fly. Interestingly, d4E-BP[WT] also downregulated more proteins (141) than d4E-BP[TA] (85). This im-

pression may be due to the technique used to quantify proteins. Quantitative mass spectrometry used in this study was a relative quantification method depending on the detection of both, heavy and light, peptide partners. If a protein was downregulated by d4E-BP[TA] so much that it was below detection level, the peptide would not be quantified any more. That may be a reason why fewer downregulated proteins were detected upon d4E-BP[TA] overexpression. In cells, the number of downregulated proteins upon 4E-BP1[WT] or 4E-BP1[TA] overexpression was almost comparable. This may be due to the circumstance that 6 h overexpression was too short to allow the degradation of proteins below detectable levels.

When comparing the identity of proteins upregulated in cells and flies, it was apparent that many overlaps were detectable, but also some differences. Typically in cells and in flies, proteins involved in regulating the DNA architecture and altering transcription were upregulated. This demonstrates that beyond the effect on translational level, 4E-BP also has an indirect effect on transcription. Another common group of upregulated proteins were involved in lipid metabolism. Also in this case one can find examples in all samples of cells and flies. Furthermore, mitochondrial proteins were enriched among the upregulated proteins in cells and flies. 4E-BP1[WT] overexpressing cells and d4E-BP[WT/TA] overexpressing flies revealed a number of proteins, which were classified as stress response proteins by PANTHER, while 4E-BP1[TA] overexpressing cells lacked these proteins. However, it does not mean that overexpressed proteins by 4E-BP1[TA] were not responsible for stress resistance. 4E-BP1[TA] overexpressing cells had enriched proteins for iron homeostasis, which was also found in d4E-BP[WT] overexpressing cells. Free iron can drive cells into apoptosis and proteins involved in its homeostasis may have a protective effect. Often, proteins involved in translation initiation were also upregulated, as it was the case for 4E-BP1[TA] overexpressing cells and d4E-BP[WT/TA] overexpressing flies. This may be seen as a compensatory response to 4E-BP overexpression or an adaptation to the promotion of cap-independent translation. In contrast to cells, *Drosophila* models exhibited many upregulated proteins involved in the neurotransmitter cycle, while d4E-BP[TA] overexpressing flies also enriched chaperones and other proteins involved in protein folding.

It became apparent that flies and cells downregulated different proteins. In cells, downregulated proteins were mostly involved in immune response

154

and ubiquitination. This makes sense as immune proteins are waste of energy under cellular stress, while ubiquitination would degrade many proteins, which may be required for stress resistance. Downregulated *Drosophila* proteins were involved in developmental processes, olfactory perception and chitin production; proteins which may not be as important under stress. However, muscle proteins and proteins involved in cell mobility were also downregulated, while many of them were upregulated as well. This up- and downregulation of different candidates of the same protein group may emphasise the alteration of cell cytoskeleton and protein transportation under stress. Furthermore, it highlights the fact that selecting potential target hits, which are responsible for the protective effect of 4E-BP1 is not trivial as it is insufficient to identify upregulated protein groups upon 4E-BP1 overexpression, because other proteins of the same group may be downregulated. Instead, it is important to identify individual candidates for which cytoprotective potential was confirmed in other studies before.

Chapter 6

Evaluation of 4E-BP1 downstream effectors regarding their anti-apoptotic potential *in vitro*

6.1 Hypothesis and aims

Quantitative mass spectrometry experiments in T-REx HEK293 cells and *Drosophila* have identified many proteins whose abundance was affected by 4E-BP1/d4E-BP. It was hypothesised that these hits may contribute to the cell-protective action of 4E-BP1. I next sought to assess them for their ability to contribute to the cell protective potential of 4E-BP1/d4E-BP under stress. Ideally, potential candidates could be tested in previously evaluated *Drosophila* models of PD. However, the generation and testing of new transgenic flies is time and resources consuming. Hence, potential candidates should be tested in an *in vitro* siRNA knockdown assay to isolate promising hits, which could be used for later *in vivo* investigations. The idea was that mRNA knockdown of 4E-BP1 effectors should partly abolish the protection against stress induced by 4E-BP1, if these targets contributed to this effect.

The aim of this part of the study was to develop, test and evaluate

an *in vitro* system, which can be used to test the cellular protective effect of 4E-BP1 downstream effectors. From the long list of upregulated mass spectrometry hits upon 4E-BP1[WT/TA] overexpression, 15 suitable candidates with cellular protecting potential would be selected and tested to filter promising candidates for later investigations in *Drosophila* PD models.

6.2 Selection of candidates for further investigations

The candidates for *in vitro* cell protective investigations were selected from the lists of upregulated protein upon 4E-BP1[WT/TA] (Table A9, A11 and A13). Five candidates were chosen from each group - upregulated upon 4E-BP1[WT] overexpression, upregulated upon 4E-BP1[TA] overexpression and upregulated in both.

From the list of commonly upregulated proteins by 4E-BP1[WT] and 4E-BP1[TA], the following five proteins were selected: heme oxygenase 1 (HMOX1), ferritin light chain (FTL), glutathione *S*-transferase Mu 3 (GSTM3) and four and a half LIM domains protein 2 (FHL2) and myomesin-1 (MYOM1). HMOX1 is a protein previously identified to be initiated by oxidative stress, also by tissues which are not involved in heme degradation (Keyse and Tyrrell, 1989; Yachie et al., 1999; Gozzelino et al., 2010). Heme sensitises cells to undergo apoptosis, while heme catabolites like CO have anti-apoptotic properties. Thus, it was speculated that HMOX1 is involved in a general response to oxidative stress. Furthermore, it was found that HMOX1 as well as TMX2, another protein upregulated by 4E-BP1[WT/TA], are part of the mitochondria-associated membrane, a domain of the endoplasmic reticulum that mediates the exchange of ions, lipids and metabolites between the endoplasmic reticulum and mitochondria (Lynes et al., 2012).

FTL stores iron in a non-toxic form. On the other hand, it has been demonstrated that loss of function mutations of FTL causes neurodegeneration (Baraibar et al., 2008, 2012; Barbeito et al., 2009; Vidal et al., 2008).

GSTM3 is a glutathione transferase, which may be involved in the detoxification of both endogenous compounds and xenobiotics at the blood-brain barrier (Campbell et al., 1990). It is part of the antioxidant response and reduced in some PD patients (Chanas et al., 2002; Gui et al., 2016).

FHL2 is an interlink between different pathways to upregulate transcription as it negatively regulates FOXO1 apoptotic activity (Yang et al., 2005), an upregulated transcription factor in PD (Dumitriu et al., 2012).

Finally, MYOM1 is a muscular protein, but also involved in parkin mediated autophagy of mitochondria (Orvedahl et al., 2011). The mechanism can be impaired in PD.

Chosen candidates from the list of upregulated proteins by 4E-BP1[TA] only were mitochondrial trifunctional enzyme subunit β (HADHB), mitochondrial import receptor subunit TOM40B (TOMM40L), nucleolysin TIA-1 isoform p40 (TIA1), Δ24-sterol reductase (DHCR24) and palmitoyl-protein thioesterase 1 (PPT1). HADHB is involved in fatty acid β-oxidation to mobilise energy storages. It was described previously as a protein involved in stress response (Magdeldin et al., 2015). TOMM40L is a channel forming protein importing protein precursors into mitochondria. It is involved in shuttling of Pink1 in the process of Parkin-mediated mitophagy and thus also associated with PD (Gottschalk et al., 2014). TIA1 mediates the formation of stress granules, a composition of chaperones and RNAs (Gilks et al., 2004). The formation of these granules is triggered by stress, but their function remains controversial. It was proposed that they may protect certain RNAs from damage or hold them for later translation or sequestration, depending on the needs of the cell. DHCR24 catalyses sterol intermediates for steroid production. It has been reported to protect cells from oxidative stress by reducing caspase 3 activity (Greeve et al., 2000). The expression can be reduced in AD and it has been demonstrated that overexpression is neuroprotective (Greeve et al., 2000; Peri, 2016). PPT1 is involved in lysosomal protein degradation. It has been shown to be a negative regulator of apoptotic processes (Cho and Dawson, 2000). Deficiency of PPT1 causes infantile neuronal ceroid lipofuscinosis, a neurodegenerative lysosomal storage disease, with PD-like motor disorders in mice (Dearborn et al., 2015).

The candidates from the 4E-BP1[WT] hit list were protein CYR61 (CYR61), serpin B6 (SERPINB6), heat shock 70 kDa protein 13 (HSPA13), V-type proton ATPase 116 kDa subunit a isoform 2 (ATP6V0A2) and the mitochondrial pyruvate carboxylase (PC). CYR61 encodes for a secreted protein with proto-oncogenic potential, which is in involved in matrix remodelling. It is among the few cellular proteins, which have been described

cap-independent translating (Johannes et al., 1999). SERPINB6 is an inhibitor of different proteases and it was proposed that it may play an important role in the protection against leakage of lysosomal content during stress and that loss of this protection results in cell death (Sirmaci et al., 2010). HSPA13 is a chaperone, a protein of stress response, which contributes to re-folding misfolded protein. ATP6V0A2 is a subunit of a lysosomal proton pump, which is crucial for their acidification and deacidification of the cytoplasm. Loss of function leads to impaired vesicular trafficking and increased apoptosis (Hucthagowder et al., 2009). As a last candidate gene PC was chosen. It is a central metabolic protein catalysis the carboxylation of pyruvate to oxaloacetate, which can be degraded in the Krebs cycle and be utilised for gluconeogenesis, lipogenesis or neurotransmitter synthesis. In the nervous system, it accounts for a significant fraction of glucose oxidation. In mice models of AD, the activity of PC was found to be reduced (Tiwari and Patel, 2014).

The candidates chosen for initial follow-up experiments represent the functional huge variety of proteins affected by 4E-BP1. This selection was intended to help narrow down the kind of 4E-BP1 downstream targets, which contribute to its cellular protective effect.

6.3   Establishing an *in vitro* system to test selected candidates

In preparation of developing an *in vitro* system to evaluate the contribution of different selected candidates on the protective effect of 4E-BP1, it was necessary to find a way to stress cells and rescue them by 4E-BP1 overexpression. In a first attempt, the paraquat experiment from flies was adapted for *in vitro* experiments. 4E-BP1[TA] T-REx HEK293 cell clones were treated with 50 µM, 150 µM and 500 µM for 24 h after initiation of 4E-BP1[TA] overexpression by tetracycline and the results were compared to cells treated the same way without 4E-BP1[TA] overexpression. Two different systems were tested to measure cell viability: an absorbance assay, measuring the cell number by the activity of dehydrogenases and a luminescence system detecting total ATP.

The assays were performed in parallel and the results revealed that the differences between both assays were marginal (Fig. 6.1). 50 µM paraquat

reduced viability to approximately 90 % with or without 4E-BP1[TA] over-expression in both assays, but an increase of 15 % viability was detectable with 150 µM paraquat after 4E-BP1[TA] overexpression in the absorbance assay, although with this conditions there was no difference in the luminescence assay. After 500 µM paraquat treatment, the viability increased by 18 % in the absorbance assay and 16 % in the luminescence assay with 4E-BP1[TA] overexpression compared to controls. For all future assays in this study, the luminescence assay was utilised as its measured values were a bit less variable with a lower standard deviation.
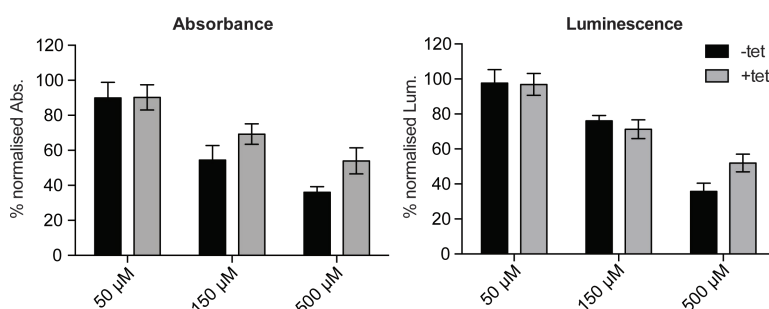
Figure 6.1: Cell viability after 24 h paraquat, detected with a absorbance or luminescence assay. 4E-BP1[TA] overexpression in T-REx HEK293 cells was induced by 1 µg/ml tetracycline in cell medium, but not in controls (+/- tet). 50 µM, 150 µM or 500 µM paraquat were added later and the viability detected with absorbent or luminescent dyes. All values were normalised to control cells without paraquat treatment. Error bars indicate standard deviation of four to six technical replicates.

Since 4E-BP1[TA] could partially rescue cells from death induced by paraquat, the next step was to optimise the protocol. Next, two other toxins were tested: rotenone and sodium azide. While paraquat's mechanism of toxicity is to be reduced by an electron donor, like NADPH, before being oxidised, which produces reactive and destructive superoxides radicals, the mechanism of rotenone and sodium azide is more specifically linked to the mitochondria. Rotenone is an inhibitor of the electron transfer from iron-sulfur centres in complex I of the electron transport chain to ubiquinone. Sodium azide acts similar to CO and blocks the oxygen binding site of complex IV irreversibly. 4E-BP1[WT] and 4E-BP1[TA] overexpressing T-REx HEK293 cells were treated with these two chemicals in different concentration for 24 h or 48 h (Fig. 6.2). As the data revealed, the rescuing capability after 24 h rotenone treatment was better with 4E-BP1[WT] at lower concentrations of rotenone, while 4E-BP1[TA] rescuing capability was better at higher toxin concentrations (Fig. 6.2A). When analysing the rescuing

capability of 4E-BP1 overexpression after 48 h rotenone treatment, the impression consolidated that 4E-BP1[TA] rescues better with increasing cell stress. While 4E-BP1[WT] overexpression never made a significant difference, 4E-BP1[TA] overexpression always improved cell viability, which became significant with 37 % cell viability improvement with 10 μM rotenone.

The finding that 4E-BP1[WT] rescues better at lower concentration of cell toxins was consistent with sodium azide as well (Fig. 6.2B). After 48 h of sodium azide treatment, neither 4E-BP1[WT] nor 4E-BP1[TA] were able to improve cell viability significantly, although 4E-BP1[TA] showed a clear difference to controls, while 4E-BP1[WT] did not exhibit any detectable effect.

All together, these results revealed that under certain conditions, 4E-BP1[TA] was better to rescue cell stress induced by rotenone and sodium azide than by paraquat. The maximum increase of cell viability was 37 % with rotenone and 36 % with sodium azide, but only 15 % in paraquat ex-
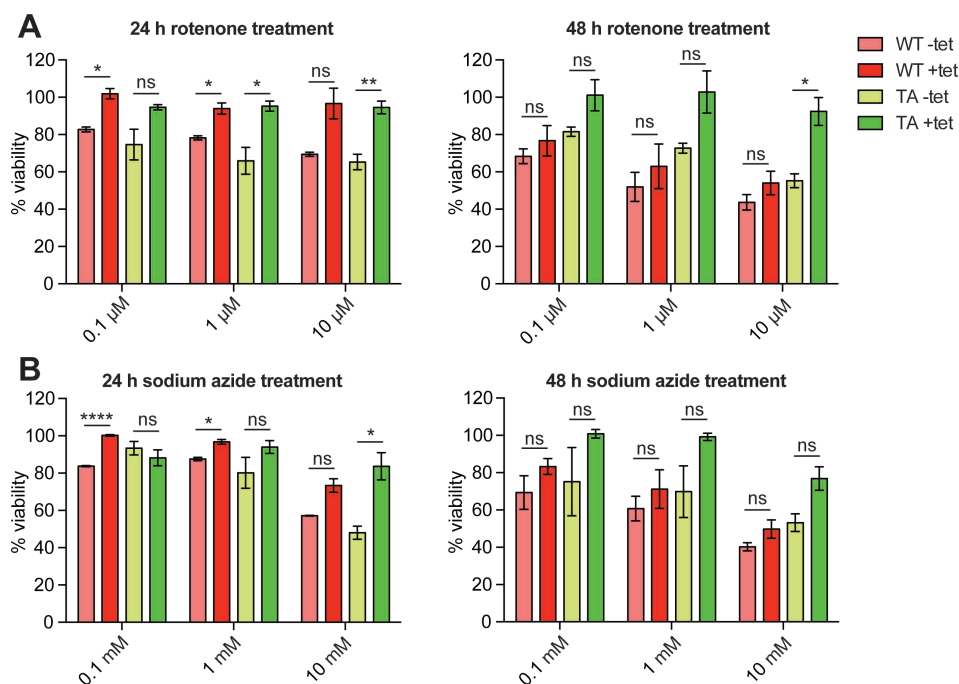
Figure 6.2: Cell viability after 24 h of 48 h rotenone or sodium azide treatment in cells overexpressing 4E-BP1[WT] or 4E-BP1[TA]. 4E-BP1[WT/TA] overexpression in T-REx HEK293 cells was induced by 1 μg/ml tetracycline in cell medium, but not in controls (+/- tet). Rotenone (A) or sodium azide (B) were added later and the viability detected. All values were normalised to control cells without toxin treatment. Error bars indicate ± s.e.m. Significance was determined by two-tailed Student's t-test with Welch's correction (ns P > 0.05, * P ≤ 0.05, ** P ≤ 0.01, **** P ≤ 0.0001). n ≥ 3

Figure 6.3: Phosphorylation state of endogenous 4E-BP1 of HEK293 cells after paraquat, rotenone or sodium azide toxification. Cells were treated with 500 µM paraquat (PQ), 10 µM rotenone, 10 mM sodium azide (azide) or no toxin (w/o) for 2 h. The proteins of these cells were analysed by immunoblotting with total, phospho- and nonphospho-4E-BP1 antibodies. The blots derived from three separate SDS-PAGES of the same biological replicate (n = 1). Actin served as loading control. The molecular weight is indicated on the left hand side in kDa.

periments. Hence, the condition of 48 h 10 µM rotenone toxification after 4E-BP1[TA] overexpression was chosen to test 4E-BP1 downstream effectors on their capability to contribute to its protective effect. Thus, the viability assays confirmed a difference in rescuing capability of 4E-BP1 after toxification with rotenone, sodium azide or paraquat.

It was relevant to determine whether the differences were also matched by the capability of these toxins to provoke 4E-BP1 activation. To investigate this question, HEK293 cells were incubated with paraquat, rotenone and sodium azide for 2 h and the extracted proteins were utilised for immunoblotting in order to analyse the status of endogenous 4E-BP1 phosphorylation. Indeed rotenone and sodium azide activated 4E-BP1 much more than paraquat (Fig. 6.3). This was confirmed by all three 4E-BP1 antibodies. While the signal strengths of phospho-4E-BP1 decreased and of nonphospho-4E-BP1 increased after rotenone and sodium azide treatment, they remained constant after paraquat treatment compared to controls.

The reason for the different response of 4E-BP1 to toxin treatment may be linked to the different modes of action. While paraquat produces superoxides nonspecifically everywhere in the cell, rotenone and sodium azide are very specific inhibitors of mitochondrial proteins. It is also possible that paraquat has a slower kinetic than the other toxins and that its effect on 4E-BP1 may become manifest later. However, if the place of toxin action is crucial for effectiveness of 4E-BP1 rescue capability, this may emphasise the

importance of mitochondrial proteins, which were seen to be upregulated by 4E-BP1. To test this hypothesis, a recently developed compound described as mitochondrial paraquat (mitoPQ) was tested. It is chemically modified to target the compound to the mitochondria specifically where it has been shown to be predominantly active (Robb et al., 2015). Interestingly, Robb
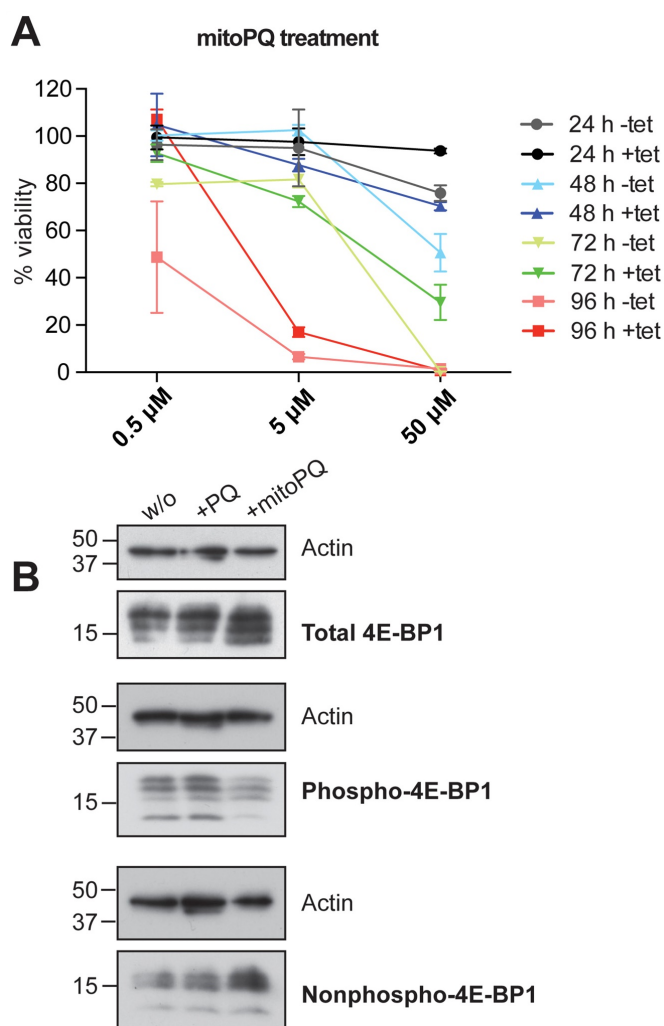
Figure 6.4: Cell viability and endogenous 4E-BP1 phosphorylation state of HEK293 cells after mitochondrial paraquat treatment. (A) 4E-BP1[TA] overexpression in T-REx HEK293 cells was induced by 1 µg/ml tetracycline in cell medium, but not in controls (+/- tet). Mitochondrial paraquat (mitoPQ) was added later and the viability detected. All values were normalised to control cells without toxin treatment. Error bars indicate standard deviation of six technical replicates. (B) Cells were treated with 500 µM paraquat (PQ) or 50 µM mitoPQ or no toxin (w/o) for 2 h. The proteins of these cells were analysed by immunoblotting with total, phospho- and nonphospho-4E-BP1 antibodies. The blots derived from three separate SDS-PAGES of the same biological replicate (n = 1). Actin served as loading control. The molecular weight is indicated on the left hand side in kDa.

et al. also found that targeting paraquat to mitochondria amplified the potency of the toxin. Here, mitoPQ was tested in cell viability assays. The viability after 4E-BP1[TA] overexpression revealed that the rescuing capability of 4E-BP1[TA], but also the reduction of cell viability was very little after 24 h (Fig. 6.4A). After 48 h mitoPQ treatment, the effect remained the same, but the rescuing effect became more apparent after 72 h mitoPQ treatment. After 96 h toxification, the rescuing effect was at 51 % at 0.5 µM mitoPQ treatment, at 10 % with 5 µM mitoPQ, but undetectable with 50 µM as all cells died completely, independently of their 4E-BP1 overexpression status.

These results confirmed a better rescuing capability for mitoPQ than for normal paraquat under certain conditions, but it is very difficult to compare two different compounds correctly, when dose, potency and timings were different. However, the immunoblot revealed that mitoPQ activated endogenous 4E-BP1 of HEK293 cells a bit more than normal paraquat, but the effect was milder than with rotenone or sodium azide (Fig. 6.4B). Nonetheless, these data emphasised that mitochondrial proteins may contribute to the cellular protective potential of 4E-BP1.

6.4 siRNA knockdown of candidate genes in cell toxicity test system

After an *in vitro* assay was established to evaluate the effect of 4E-BP1 overexpression on the cell viability, this assay could be utilised to investigate the contribution of the previously selected 4E-BP1 downstream effector to the improvement of cell viability by 4E-BP1 under stress. For this purpose, specific siRNAs were used to knock down mRNAs of selected downstream effectors, while 4E-BP1[TA] was overexpressed in T-REx HEK293 cells and the reduction of viability improvement after rotenone treatment was measured. Five of the tested targets were found upregulated by 4E-BP1[WT], but were still tested in a 4E-BP1[TA] assay. The reason was that 4E-BP1[TA] exhibited stronger rescuing capabilities, which makes it easier to detect differences.
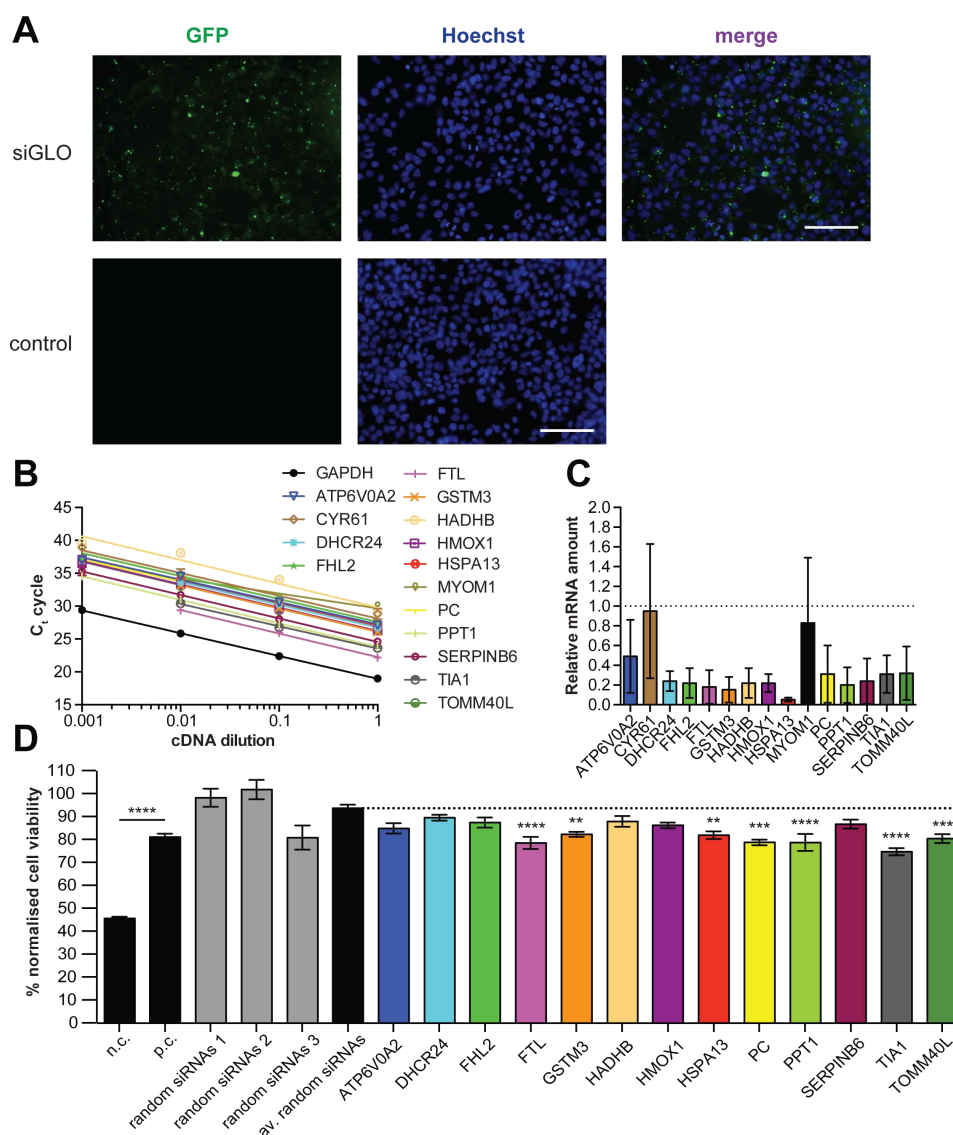
Figure 6.5: siRNA knockdown of 4E-BP1 downstream effectors in T-REx HEK293 cells. (A) T-REx HEK293 4E-BP1[TA] cells were transfected with green fluorescent siRNAs to check the efficiency of the transfection protocol. Controls were not transfected. Cells were stained with Hoechst (blue). The scale bar is 100 µm. (B) Threshold cycle (C_t) of 4E-BP1 effector and *GAPDH* primer pairs at different cDNA dilutions with constant primer concentration. Primer efficiencies (E) were calculated: *GAPDH*: 94 %; *ATP6V0A2*: E = 97 %; *CYR61*: E = 94 %; *DHCR24*: E = 94 %; *FHL2*: 93 %; *FTL*: E = 90 %; *GSTM3*: E = 92 %; *HADHB*: E = 89 %; *HMOX1*: E = 92 %; *HSPA13*: E = 95 %; *MYOM1*: 177 %; *PC*: E = 99 %; *PPT1*: E = 90 %; *SERPINB6*: E = 90 %; *TIA1*: E = 97 %; *TOMM40L*: E = 91 %. (C) Relative mRNA yield after siRNA knockdown. All values were normalised to the controls without siRNA knockdown. The reference gene was *GAPDH*. The dotted line indicates the RNA level without siRNA knockdown. Error bars indicate standard deviation of three technical replicates. (D) 4E-BP1[TA] overexpression in T-REx HEK293 cells was induced by 1 µg/ml tetracycline in cell medium (p.c.), but not in controls (n.c.). 10 µM rotenone were added later. The viability was detected 48 h after rotenone treatment. All values were normalised to control cells without rotenone treatment. The dotted line indicates the average value of cells transfected with random siRNAs. The viability of cells transfected with specific siRNAs were compared to this value. Error bars indicate $\pm$ s.e.m. Significance was determined by one-way ANOVA with Bonferroni correction (** P $\leq$ 0.01, *** P $\leq$ 0.001, **** P $\leq$ 0.0001). n $\geq$ 3

165

In an initial test, T-REx HEK293 cells were transfected with green fluorescent siRNA to test the efficiency of the transfection protocol. The results showed that siRNAs were incorporated by the cells (Fig. 6.5A). The fluorescent siRNAs co-localised very well with the Hoechst staining of cell nuclei, while no fluorescence signal was detected from areas were no cells grew. Thus, the transfection protocol was considered as suitable for this experiment.

Next, the siRNA knockdown efficiencies were tested. For this purpose, T-REx HEK293 cells were transfected with siRNAs and their RNAs were harvested, transcribed to cDNA and utilised for qRT-PCR. In preparation of qRT-PCR experiments, the utilised primers were tested in cDNA dilution series (Fig. 6.5B). cDNA of control cells was diluted 1:2, 1:10, 1:100 and 1:1000. With some primers, no signal was detectable after 1:1000 dilution or the results became inconsistent. In this case, all calculations were performed with the three higher dilutions. Based on the slope of the dilution curves, the primer efficiency was calculated. All primer pairs had a good efficiency between 80 % and 100 % aside of *MYOM1* with 177 %. A too high efficiency could point to unspecific amplification of side products by these primers.

However, as the repetition of this experiment with an alternative primer pair did not improve the efficiency, the primers were used for subsequent qRT-PCR anyway.

qRT-PCR experiments of siRNA knockdown revealed that most siRNAs reduced the RNA yield of their targets clearly (Fig. 6.5C). The two exceptions were *CYR61* and *MYOM1*. Due to the described problem with *MYOM1* primers, it was not entirely clear whether the knockdown failed or whether the primer overestimated the mRNA amount.

CYR61 and *MYOM1* siRNAs were excluded from the viability analysis as their knockdown could not be confirmed by qRT-PCR. All other siRNAs were utilised to transfected T-REx HEK293 overexpressing 4E-BP1[TA] before 10 µM rotenone was applied. Aside from specific siRNAs, control cells were transfected with three different random siRNAs. The average viability of these controls was used as a reference to assess the effect of specific mRNA knockdown. The results revealed that seven out of 13 siRNAs reduced the cell viability rescue by 4E-BP1 significantly, although each individual contribution was little (Fig. 6.5D). *FTL*, *GSTM3*, *HSPA13*, *PC*, *PPT1*, *TIA1* and *TOMM40L* showed a significant contribution to the protective effect of

4E-BP1[TA]. However, one has to consider as well that the viability of two of three random siRNA controls were higher than without any siRNA (p.c.). If the statistic analyses would have been calculated against the positive control without siRNA transfection (p.c.), none of the samples would have been significantly different.

6.5 Discussion

The results of this chapter have revealed that it was possible to develop an *in vitro* assay, which was able to mimic the protective potential of d4E-BP in *Drosophila* under stress. The rescuing capability of 4E-BP1 depended on the utilised toxin. The effect was smaller with paraquat than with rotenone or sodium azide. The better potency of mitoPQ to activate endogenous 4E-BP1 of HEK293 cells and the fact that the rescuing capability of 4E-BP1[TA] was stronger than with normal paraquat emphasised the possibility that mitochondrial proteins may contribute to the effect of 4E-BP1. Two mitochondrial linked proteins, *PC* and *TOMM40L*, were described to contribute significantly to the protective effect of 4E-BP1 in this assay.

Nonetheless, when the *in vitro* viability assay was applied for evaluating 4E-BP1 downstream targets, it seems questionable whether it is reliable enough to give credible results. It was surprising that two of three random siRNA controls showed better cell viability than controls without any siRNAs. If this was due to the variability of the assay, the results for specific siRNAs may not be authoritative. One problem of this assay may be that the potential 4E-BP1 downstream targets were knocked down to investigate how much this abolishes the protective effect of 4E-BP1[TA]. However, this means that two contradicting mechanisms were applied on the cells at the same time. While 4E-BP1[TA] increased translation of certain targets, the mRNAs of the very same targets were knocked down. These contradicting mechanisms may caused unforeseen effects, which may have biased the result. In order to improve the assay in the future, it would be better to transiently transfect and overexpress 4E-BP1 downstream targets in HEK293 to investigate whether overexpression of downstream targets may be able to mimic the protective effect of 4E-BP1[TA] overexpression.

The 4E-BP1 downstream effectors, which were found to contribute significantly to the protective effect in this assay, were part of all three co-

horts. *HSPA13* and *PC* were upregulated upon 4E-BP1[WT] overexpression, *PPT1*, *TIA1* and *TOMM40L* belonged to the 4E-BP1[TA] cohort and *FTL* and *GSTM3* were upregulated by both.

The best approach to investigate whether the hits characterised in this assay really contribute to the protective effect of d4E-BP in *Drosophila* PD models would be to generate new transgenic flies to overexpress *Drosophila* homolgoues of significant hits from this assay in *Drosophila* models of PD. Subsequent behavioural experiments should elucidate whether they also have an impact *in vivo*.

Chapter 7

Discussion

7.1 Results summary

In this study, an *in vitro* cellular model and an *in vivo Drosophila* model overexpressing human 4E-BP1[WT/TA] or FLAG-d4E-BP[WT/TA] respectively were designed and generated. Both models were successfully utilised for quantitative proteomics to determine the effect of 4E-BP overexpression. A selection of upregulated hits by 4E-BP1 were tested in an *in vitro* stress test assay.

I opted to use an inducible, non-cancer T-REx HEK293 cell model as an *in vitro* system to overexpress 4E-BP1[WT/TA] in order to avoid biasing effects of malregulated mTOR in many cancer cell lines and to control the overexpression of 4E-BP1, which allowed the application of the same cells without 4E-BP1 overexpression as a reference. The overexpression was exponentially time dependent before it reached a saturation point after approximately 24 h. A clear overexpression was detectable after approximately 6 h. Due to the inducibility of 4E-BP1 overexpression, the same cells could be utilised as negative controls in quantitative mass spectrometry experiments. Analyses also confirmed that the effect on 4E-BP1 downstream effectors is very cell and assay dependent. Observations of TFAM downregulation by mTOR inhibition in MCF7 published by Morita et al. (2013) could be reproduced in this very model, but this was not observed in HEK293 cells.

Likewise in *Drosophila* models, overexpression of FLAG-d4E-BP[WT/TA] was confirmed. Different behavioural assays investigated the effect of d4E-BP overexpression and revealed that both transgenes

were able to extend lifespan of *Thor* knockout mutants and their stress resistance as well as the locomotor activity in PD models and aged *Thor* knockout mutants. Furthermore, overexpression of the transgenes improved the viability of *Thor* and *park* double knockout mutants.

Quantitative proteomics in the generated *in vitro* and *in vivo* models successfully quantified thousand of proteins. The nature of up- and down-regulated proteins upon 4E-BP overexpression was very diverse. However, common motifs were found among the quantified hits. For example, proteins involved in lipid metabolism and mitochondrial proteins were significantly enriched proteins in cells and flies. Furthermore, *Drosophila* revealed up-regulated proteins involved in neurotransmitter metabolism, transport and release. With respect to the downregulated proteins, proteomics experiments in cells revealed that many immune system responsive proteins were among the downregulated hits, while in flies most downregulated proteins were involved in developmental processes, olfactory perception and chitin synthesis. As far as I know, this is the first high-throughput study, which paid attention to up- as well as downregulated proteins upon 4E-BP over-expression or activation. Hence, it was possible to reveal also contradictory effects of 4E-BP overexpression as seen by the up- and downregulation of different candidates responsible for cell mobility and cell movement, which emphasised a change of the cell skeleton and protein transportation under stress.

The development of an *in vitro* assay to test the ability of individual mass spectrometry hits on their contribution to 4E-BP1's cellular protective potential revealed that this potential depended on the utilised drug to stress cells. Indeed, paraquat seemed to activate 4E-BP1 insufficiently, while rotenone and sodium azide provoked a much stronger activation of 4E-BP1. In contrast, *Drosophila* overexpressing d4E-BP improved their resistance to paraquat, which may be due to a different 4E-BP response of different tissues to paraquat or a general difference of these two utilised *in vitro* and *in vivo* models. In the subsequent siRNA knockdown assay with 15 selected candidates, seven candidates were found to contribute to 4E-BP1 protective potential, but the robustness of the assay itself remains doubtful.

7.2 Mass spectrometry hits of 4E-BP sensitive proteins

7.2.1 Confirmation of previously identified cap-independent translating hits

For some decades, different studies tried to identify proteins, which can be synthesised cap-independently. Here, many new potential candidates were identified by blocking cap-dependent translation. Notably, the confirmed number of cellular IRES translating mRNA is still very little also because of the experimental expenditure to verify them experimentally. In some cases, previously IRES confirmed mRNAs were still rejected later, because the previously applied experimental procedure did not come up to standards, which were established because of new information about IRES characteristics (Dumas et al., 2003; Han and Zhang, 2002; Han et al., 2003; Vergé et al., 2004; Wang et al., 2005). Thompson (2012) has reviewed several state of the art approaches to evaluate IRES activity. The most common method is cloning of a suspected IRES sequence in a DNA bicistronic reporter assay where the first cistron is translated cap-dependently, while the second second cistron is translated by the suspected IRES sequence. Both cistrons are easily quantifiable proteins, e.g. luciferases. However, further controls are necessary to confirm an IRES activity of the suspected sequence and to rule out translation due to ribosomal readthrough and synthesis of a two cistron fusion protein, alternative RNA splicing or cryptic DNA promoters (Kozak, 2003). The homepage http://www.iresite.org lists 115 cellular IRES mRNAs at the moment, but points out that characterisation is an ongoing process, which may lead also to the removal of some previously accepted IRES mRNAs.

Two of the proteins upregulated by 4E-BP1 in this study were confirmed to be IRES translated. One was the RNA-binding protein 3 (RBM3), which was upregulated by 4E-BP1[TA]. Chappell et al. (2001) and Baranick et al. (2008) found that this cold stress-induced mRNA is translated by IRES in mice. Recently, it was found to prevent cell death by protection from stress induced by misfolded proteins (Zhu et al., 2016). Furthermore, it was described to be neuroprotective in AD mice models (Peretti et al., 2015). It may be another target to be considered to contribute to 4E-BP1's cellular

protective effect.

The second upregulated protein with confirmed IRES activity was CYR61. It was described to be involved in many processes including cell adhesion, but it also seems to have a pro-apoptotic capacity by induction of endoplasmic reticulum stress (Borkham-Kamphorst et al., 2016). This effect would rather exclude this candidate from further investigations on whether it may contribute to 4E-BP1's protective potential.

Altogether, these findings emphasised the fact that too little is known about IRES translated mRNAs and the references available so far are still too fragmentary to have a solid base for IRES translated mRNA identification in high-throughput experiments.

7.2.2 Similarities with previous high-throughput mTOR pathway studies

Several studies have attempted to investigate downstream effectors of 4E-BP1 and the mTOR pathway in recent years. However, the precise aim, strategies and hypotheses were different compared to this study, but also among each other. Mostly, these studies were more focused on proteins with reduced biosynthesis rate after cap-dependent translation inhibition by 4E-BP1 activation. However, supplementary data published along with these studies also included upregulated proteins upon 4E-BP1 activation. Here, these data were utilised to assess my data set of upregulated proteins upon 4E-BP1[WT/TA] overexpression and to identify similarities. For this purpose, my data was compared to data published by Huo et al. (2012), Thoreen et al. (2012) and Zid et al. (2009). For this analysis, the definition whether a protein was upregulated was adopted from each individual study.

Huo et al. (2012) analysed the effects of different mTOR inhibitors on protein synthesis. For this purpose, they treated human cancer HeLa cells with the allosteric mTOR inhibitor rapamycin or active-site-directed inhibitors PP242 and AZD8055, before proteins were analysed by quantitative mass spectrometry. Together, in all experiments with these three different mTOR inhibitors they found 82 proteins, which were upregulated by at least one of these mTOR inhibitors. Nine of them matched to variants of protein families, which were found upregulated in my study. For example, the peptidyl-prolyl cis-trans isomerases FKBP10 and FKBP3 were identified by Huo et al., while FKBP11 was upregulated by 4E-BP1[TA] in my

study. The differences between the proteins are not completely revealed yet, but they all have a protein folding capacity and FKBP10 and FKBP11 have been described to be able to reduce misfolded protein stress (Lu et al., 2008; Ramadori et al., 2015). Another example is the mitochondrial protein TOMM22 which is part of the translocase of the outer membrane. TOMM40L, which this study found was upregulated by 4E-BP1[TA] overexpression forms a channel with TOMM22 and other subunits to import protein precursors into the mitochondria. Huo et al. also found ANXA6 was upregulated upon mTOR inhibition, while in this study ANXA1 and ANXA3 were upregulated by overexpressed 4E-BP1[WT]. Different annexin variants have been described to be proto-oncogenic in several studies (Baine et al., 2011; Boudhraa et al., 2014; Chen et al., 2001; Han et al., 2014; Tong et al., 2015), but they are not very well characterised yet. It is known that they associate with components the cytoskeleton or with proteins that mediate interactions with the extracellular matrix (Moss and Morgan, 2004). SERPINH1 was also upregulated by mTOR inhibition, while SERPINB6 was found upregulated by overexpressed 4E-BP1[WT] in this study. Both variants were described to contribute to stress resistance, but through different pathways. SERPINH1 is also known as heat shock protein 47 and involved in the maturation of collagen while protecting cells from misfolded protein stress (Kawasaki et al., 2015). SERPINB6 may play an important role in the protection against leakage of lysosomal content during stress (Sirmaci et al., 2010). However, SERPINB6 was among the candidates tested in the *in vitro* cell stress assay with rotenone here and did not exhibit a significant contribution to the protective potential of 4E-BP1[TA]. Also, the 40S ribosomal proteins RPS7/8/19 were found upregulated by Huo et al., while RPS15A was upregulated by overexpressed 4E-BP1[WT] in this study. This may highlight the demand for other ribosomal proteins, which promote cap-independent translation.

Thoreen et al. (2012) have investigated the regulation of mRNA translation by mTORC1 in murine embryonic fibroblasts. They treated cells with the mTOR inhibitor Torin1 and downstream effects were quantified by ribosome profiling, a technique which considers the ribosomal associated mRNAs as an indicator of currently translating mRNAs. The disadvantage in comparison to mass spectrometry techniques is that it neglects accumulation and degradation of proteins over time and only gives evidence of the trans-

latome at a defined moment. Thoreen et al. identified 199 mRNAs to be upregulated upon mTOR inhibition. Considering the human homologues of these hits, twelve genes were matched to related variants of the same protein family found in this study. Four candidates identified by Thoreen et al. were confirmed in this study. Among them were ADAMTS1, VEZF1, USP48 and VPS18. ADAMTS1 was found upregulated upon 4E-BP1[TA] overexpression here and is described as aggrecan cleaving metalloprotease, which is also upregulated in mouse stress models (Kurumaji and Nishikawa, 2012). Very little is known about VEZF1, but it was speculated that it may be a transcription factor. UPS48 is a not very well characterised ubiquitin hydrolase, while VPS18 is a vacuolar sorting protein. Although there is not much known about it, another member of this vacuolar protein sorting family, VPS35, was associated as a PD risk gene (Vilariño-Güell et al., 2011; Zimprich et al., 2011) and linked to mitochondrial homeostasis (Braschi et al., 2010; Malik et al., 2015; Tang et al., 2015; Wang et al., 2016b). Additionally, Thoreen et al. found TIMM10 upregulated, another component involved in the transfer of protein precursors into the mitochondrion like TOMM40L found in this study. RAB22A and RAB23 were also upregulated in the investigation by Thoreen et al., while in this study RAB13/21/32 were upregulated by 4E-BP1. The different Ras-related proteins regulate vesicular trafficking pathways (Barnekow et al., 2009). Motor proteins were commonly upregulated in both studies. Thoreen et al. identified kinesin-like protein KIF1C, while in this investigation KIF2C/4A/13B/20A were found. Oxidoreductases were commonly upregulated as well. DHRS9 in the study by Thoreen et al. and DHRS7B/11 in this investigation were identified. They transfer electrons using NAD^+ or $NADP^+$ as electron acceptor, which is crucial for many metabolic processes. Different V-type proton ATPases were also upregulated. Thoreen et al. found ATP6V1G1, while here ATP6V0A2/D1 were identified. These proton pumps are crucial for the acidification of lysosomes and contrary deacidification of the cell plasma. This makes them crucial for the maintenance of the intracellular pH and thus for the survival of cells.

Zid et al. (2009) studied the effect of 4E-BP in a different context. They restricted the diet of *Drosophila*, which inhibited TOR and activated *Drosophila* 4E-BP homologue Thor. Again, the response on the translational landscape was monitored by ribosomal profiling. In their study, 201

genes were translationally upregulated. The human homologues of the fly genes were compared with the list of proteins upregulated by 4E-BP1 in this study. Two genes were found in both studies to be upregulated and related variants of the same protein family were identified in three cases. CSPR1, a transcriptional co-factor and calponin 2 (CNN2), a protein involved in muscle contraction regulation and cytoskeletal organisation are described as upregulated by 4E-BP1[WT] in this investigation and in the study by Zid et al. The elongation of very long chain fatty acids portein 5 (ELOVL5), the heat shock protein HSPA13 and again TOMM40L were found upregulated in this study by 4E-BP1[WT/TA], while Zid et al. described ELOVL1/7, HSPB and TIMM10 as upregulated in *Drosophila*. These are representatives of proteins involved in fat metabolism, stress resistance and mitochondrial proteins. HSPA13 was tested for its contribution to the rescuing effect of 4E-BP1[TA] after rotenone treatment and was found to make a significant contribution, which could further emphasise the importance of heat shock proteins for the effect of 4E-BP1. When comparing the gene list published by Zid et al. with the list of upregulated proteins in flies gained in this study, three further overlapping hits were found: CG14495, CG4646 and TpnC41C. The function of the first two is still unknown and no homologue or identifiable structure was found. The latter is a troponin C isoform, a further protein involved in muscle contraction, which was found upregulated in flies overexpressing d4E-BP[TA] here. This is surprising given that only fly heads were used in this study. However, studies in chicken have revealed that troponin C isoforms are expressed in non-muscular tissues as well, in particular in the brain and it was suggested that it may have other functions aside from muscle contractions (Berezowsky and Bag, 1992).

It was interesting to notice that subunits of the mitochondrial import complex were upregulated in all discussed studies here: TOMM40L in this study, TOMM22 in Huo et al. and TIMM10 in Thoreen et al. and Zid et al. This suggests that this protein transportation system is increased in abundance and is probably increasing mitochondrial activity under different stressors. Otherwise, the targets commonly found in the discussed studies were very diverse as the whole protein downstream spectrum of 4E-BP1 in this study.

7.2.3 Promotion of antioxidant response by 4E-BP

The regulation of oxidative stress is a crucial factor for cellular survival. This kind of stress is induced by the production of reactive oxygen and nitrogen species (ROS/RNS) like superoxide, hydroxyl radicals or peroxynitrite. These radicals are produced by many metabolic processes, e.g. in the mitochondria or at the endoplasmic reticulum. ROS/RNS have potential to oxidise and damage proteins, lipids and DNA. Therefore, a functional defensive system to catch and eliminate ROS and RNS is crucial. The imbalance of the ROS/RNS protection system is associated with the development of many diseases including PD (Hwang, 2013). Interestingly, among the nine proteins which were commonly upregulated by 4E-BP1[WT/TA] in T-REx HEK293 cells at least three were part of the antioxidant NFE2L2/ARE pathway. NFE2L2, also known as NRF2, is a transcription factor (Nuclear factor erythroid 2-related factor 2) that binds to the antioxidant responsive element (ARE) on the DNA to initiate transcription of antioxidant genes in response to oxidative stress (Fig. 7.1). Three of these target genes found upregulated upon 4E-BP1[WT/TA] overexpression in this study were: GSTM3, HMOX1 and FTL. GSTM3 is a glutathione *S*-transferase, which catalyse the conjugation of different toxic substances to glutathione for detoxification. HMOX1 and FTL are both involved in the $Fe(II)$ homeostasis. HMOX1 is a heme oxygenase, which breaks down heme molecules and releases $Fe(II)$, while FTL is the light chain of the ferritin complex, which oxidises $Fe(II)$ to $Fe(III)$. An imbalance in these proteins would increase free $Fe(II)$ ions and promote the production of hydroxyl radicals. Aside from these three proteins, TMX2 was also upregulated by 4E-BP1[WT/TA]. TMX2 is a theoredoxin related variant and although it was not described as an NFE2L2 target yet, other thioredoxin variants are known to be regulated by NFE2L2. Thioredoxins facilitate the reduction of other proteins and are key players to repair damage caused by ROS/RNS. GPX8 was also found to be upregulated by 4E-BP1[WT]. GPX8 is a glutathione peroxidase involved in the functional regulation of glutathione like GSTM3.

The upregulation of so many different components of one pathway highlights the possibility that the different proteins are not only transcriptionally, but also translationally connected via cap-independent translation. This would allow a much faster response to ROS/RNS caused stress. The NFE2L2/ARE pathway and its targets were found to be impaired in PD

patients and may play a crucial for the pathogenesis (Gui et al., 2016).
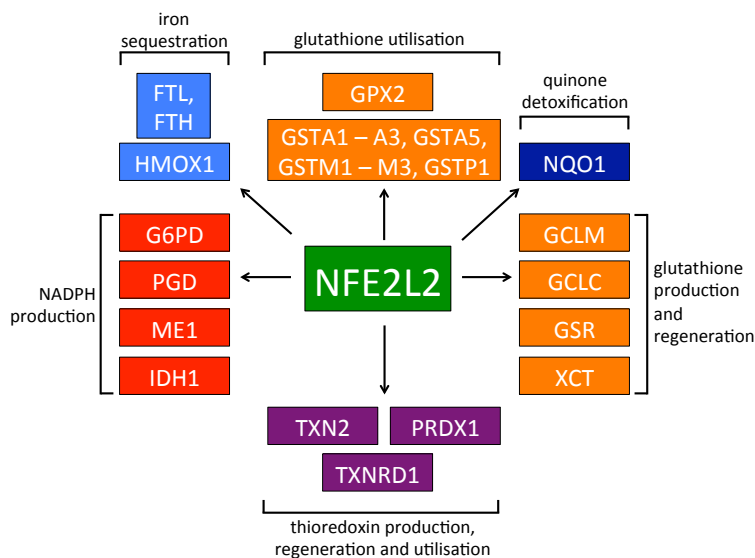
Figure 7.1: Target genes of NFE2L2 with antioxidant activity. NFE2L2 is a transcription factors, which is a master regulator for many antioxidant proteins including proteins which are involved in gluthatione (GSH) production, regeneration and utilisation, but also proteins responsible for iron sequestration, thioredoxin production, regeneration and utilisation as well as NADPH production. NADPH is required to regenerate GSH and thioredoxin after they have reduced ROS.

7.2.4 Impact of 4E-BP dependent upregulation of mitochondrial proteins

This study found that mitochondrial proteins are significantly enriched among the upregulated proteins *in vitro* and *in vivo*. One tested candidate, TOMM40L, was found to contribute to the protective effect of 4E-BP1[TA] in the rotenone cell toxicity assay. However, the question remains whether upregulation of mitochondrial proteins in general contributes to the protective effect of 4E-BP. Mitochondria are important for cell survival as they are key players for energy generation and initiation of apoptosis. The regulation of mitochondria protein translation by the mTOR pathway is still under intensive investigation as several partly contradicting studies of the past years showed. Zid et al. (2009) have demonstrated that mitochondrial proteins are significantly upregulated in their dietary restricted *Drosophila* model and that this change is Thor dependent. In contrast, Morita et al. (2013) have reported that ATP synthase subunits and the mitochondrial transcription factor A (TFAM) are downregulated when mTOR is pharma-

cologically inhibited in breast cancer MCF7 cells. Again, it was claimed that this downregulation was driven by 4E-BP1 activation. In this study, it was demonstrated that the effect of different mTOR inhibitors on TFAM was reproducible in MCF7 but not in HEK293 cells (see chapter 3, Fig. 3.14). Mass spectrometry experiments of T-REx HEK293 cells confirmed that TFAM was not affected by 4E-BP1 overexpression. Hence, this demonstrates that the described effect on TFAM is dependent on the cell context. As already discussed in the introduction, this seems to be a common characteristic of 4E-BP as contradictory effects were reported in different contexts. For instance, many studies suggested a neuroprotective effect of 4E-BP in PD (Crews et al., 2010; Imai et al., 2008; Tain et al., 2009), while others claimed the opposite effect (Malagelada et al., 2006; Xu et al., 2014). It is likely that mitochondrial proteins are regulated differently and thus candidates have to be analysed individually on their contribution to the protective effect of 4E-BP.

Recently, Gehrke et al. (2015) described that PINK1 and parkin, mitochondrial proteins previously known for their role in mitochondrial autophagy, bind and promote respiratory chain component mRNA translation at the mitochondria outer membrane in cooperation with the above described mitochondrial protein import complex (TOM) by removing translation repressors in *Drosophila* and mammalian cells. While binding of the mRNA cap structure seems to be crucial for this localised translation initiation, eIF-4E was ruled out to be involved in the process, while other initiation factors like eIF-4A and eIF-4G participated. The mRNA specific binding was abrogated by mutated PINK1, which makes it possible that PINK1 binds the cap structure itself. Technically, this new mechanism would not be cap-independent, but eIF-4E independent, which means that it could be promoted by eIF-4E binding to 4E-BP1. The fact that *PINK1* and *PARK2* are PD risk genes emphasises even more the importance of potential translation impairments in PD.

7.2.5 Impact of 4E-BP dependent upregulation of lipid metabolism proteins

In T-REx HEK293 cells overexpressing 4E-BP1[WT/TA] and in *Drosophila* overexpressing FLAG-d4E-BP[WT], many upregulated proteins function in lipid or fatty acid metabolism. Two candidates were tested for their ability

to contribute to the protective effect of 4E-BP1[TA] after rotenone treatment, but neither HADHB nor DHCR24 showed a significant effect in the assay. Nonetheless, there are good reasons that other candidates may be important for cell survival under stress. Studies in *Drosophila* demonstrated that 4E-BP prevents a too rapid fat depot degradation under metabolic stress and acts as a metabolic brake (Teleman et al., 2005). In line with this study, a recent investigation in a cellular model of hepatic steatosis, a metabolic disease characterised by fat accumulation in liver cells, found that the sterol regulatory element-binding protein-1 (SREBP-1), a transcription factor and master regulator for different lipogenic proteins, is upregulated via cap-independent translation (Siculella et al., 2016). Furthermore, the cap-dependent translation of SREBP-1 is also promoted by serum starvation and stress induced by misfolded proteins (Damiano et al., 2010). Interestingly, Ivatt et al. (2014) have identified SREBP-1 as a link between lipogenesis, mitochondrial autophagy and sporadic PD. They suggested that lipogenesis is crucial for the membrane composition of mitochondria and the recruitment of PINK1 for mitochondrial autophagy and that impaired lipogenesis may contribute to PD even if *PINK1* or *PARK2* are genetically intact. Again, these links suggest that the lipid metabolism hits, which were identified in this study may be cellular protective indeed, also for PD.

7.2.6 Impact of 4E-BP dependent upregulation of neurotransmitter level regulating proteins

In this study, proteomic analysis of *Drosophila* revealed that d4E-BP1[WT/TA] upregulates different proteins which are involved in neurotransmitter transport and release, e.g. exocyst complex component 7 (Exo70), a protein involved in intracellular vesicle targeting and docking, or the calcium-dependent secretion activator (Caps), a protein involved in calcium dependent neurotransmitter and neuropeptide release. This highlights the possibility that 4E-BP may have a beneficial effect for neuronal plasticity, which may contribute to the improved motor functions in *Drosophila* PD models. So far, the published evidence for an impact of 4E-BP on neurotransmitter level is limited. Nonetheless, studies in murine hippocampal slices revealed that 4E-BP2 knockout led to enhanced metabotropic glutamate receptor-dependent long term depression (LTD) (Banko et al., 2006). LTD is a reduction of neuronal efficacy mainly due to

a decrease in postsynaptic receptor density, but also reduced presynaptic neurotransmitter release.   These knockout mice also exhibited impaired spatial learning and memory as well as conditioned fear-associated memory deficits (Banko et al., 2005).   Another study in *Drosophila* revealed that d4E-BP postsynaptic overexpression is able to compensate the reduction of the bouton number caused by dLRRK overexpression (Lee et al., 2010). Boutons are specialised areas of the nerve terminal that contain neurotransmitters enclosed in many synaptic vesicles at the neuromuscular junction. The data on neurotransmitter release change by 4E-BP is still incomplete, but studies like the ones discussed above suggested a contribution of 4E-BP to the balance of synaptic functions.

7.2.7   Impact of 4E-BP dependent downregulation of immune responsive proteins

This study revealed that proteins involved in antimicrobial or viral response were significantly enriched among the proteins downregulated by 4E-BP1[WT/TA] in T-REx HEK293 cells, but not in *Drosophila*. For instance, S100-A8/A9, two proteins that can induce neutrophils and cell apoptosis and are a very well studied effectors of innate immune response and act against bacterial and fungal infections. The ubiquitin-like proteins ISG15/20 are two further examples of the innate immune response with anti-bacterial and anti-viral properties. Investigations in mice have previously shown that 4E-BP1/2 double knockouts have a lower viral threshold to initiate an immune response and suppress viral replication much more effectively than wildtype controls (Colina et al., 2008).   Furthermore, a neuronal *in vitro* model of herpes simplex virus-1 revealed that active 4E-BP1 is able to reactivate viral replication (Kobayashi et al., 2012).   These findings seem logical as many viruses capture their host translation system to translate their own proteins cap-independently.   If the viral response would require cap-independent translation, viral defensive would promote viral translation involuntarily. Thus, promotion of cap-dependent translation upon viral infections seem more sensible.

However, studies in *Drosophila* described the opposite situation.   *Thor* knockouts appeared immune compromised and exhibited a shorter survival after bacterial infections, while Thor was upregulated after bacterial infections in wildype controls (Bernal and Kimbrell, 2000). Also infections with

the yeast *Candida albicans* upregulated Thor in *Drosophila* cells, while the survival was reduced in *Thor* knockouts (Levitin et al., 2007). The contradictory results of these studies could be due to different models and may illustrate a difference of 4E-BP function between mammals and insects, but also the kind of infection may explain the different results. Licursi et al. (2012) developed a cellular model to study the change of viral IRES-mediated translation of different virus upon different stressors. They found that only IRES-mediated translation of mRNAs from encephalomyocarditis virus and foot-and-mouth disease virus were upregulated during amino acid starvation, while translation of other viral mRNAs from hepatitis C virus or human rhinovirus did not change. The translational upregulation of the mRNA of these two viruses was promoted by 4E-BP1, which emphasises that the kind of infection seems to important for the effect caused by 4E-BP. Nonetheless, these data do not exclude the option of functional differences between mammalian and *Drosophila* 4E-BP with respect to immune response, but give enough evidence to support the findings of this study in T-REx HEK293 cells.

7.3 Future perspectives

This study has demonstrated that downstream targets of 4E-BP can be investigated using quantitative mass spectrometry high-throughput technologies in *in vitro* and *in vivo* models. The identified hits could be validated by other studies and highlighted the importance of different groups of translationally upregulated proteins to overcome cell stress, which may have relevance for PD. Antioxidant, mitochondrial and lipid metabolic proteins were enriched in mass spectrometry analyses and have a confirmed impact on cellular survival under stress. Antioxidant proteins have the ability to reduce ROS/RNS and save cellular components from their oxidative-destructive potential, while mitochondrial proteins contribute to the homeostasis of mitochondria, the major energy generator in the cells, but also important for the initiation of apoptosis. Lipid metabolic proteins can alter the lipid composition of different organelle membranes, which can have an important impact for the functionality of cell organelles.

In order to confirm the precise contribution of the protective effect of 4E-BP, further investigations will be necessary. In this section, some strate-

gies shall be discussed, which could maximise the knowledge gained with the developed model systems.

7.3.1   Further applications for the utilised model systems to gain a deeper insight into the downstream effectors of 4E-BP

The *in vitro* and *in vivo* models for this study were carefully designed and generated, but their full potential has not been tapped yet. Further experiments using the same models may enlighten more facts about the downstream effects of 4E-BP. For instance, the cellular model was designed as an inducible system to control 4E-BP1 overexpression time dependently. This characteristic was exploited to determine the best time to harvest cells in order to prevent secondary effects. However, in further experiments cells could be harvested at different time points after 4E-BP1 induction for quantitative mass spectrometry to follow how different proteins accumulate over time and also to differentiate better between primary and secondary effects of 4E-BP1 overexpression. This kind of investigation could also help to distinguish between real targets with a certain impact on the cells and indirect effects, which were upregulated temporarily in response to a change of the whole cell protein metabolism.

The *in vivo Drosophila* model is temporally and spatially inducible via the GAL4/UAS method, but the extent of control was not fully exploited here. In this study da-GAL4, a ubiquitous driver was used and only fly heads were analysed. Tissue specific drivers would allow to study different effects on the proteomics upon overexpression of d4E-BP in different tissues, e.g. muscles or the nervous system. Drug-inducible GAL4 lines are also available (Osterwalder et al., 2001). In this case, gene expression can be temporally controlled by addition of an activating drug in the fly food. An inducible model would allow to use the very same flies without d4E-BP induction as negative control equivalently to the inducible cellular model. This would eliminate background effects due to different genotypes in experimental and control flies and would guarantee that all measured proteomic differences are due to d4E-BP for sure.

7.3.2 Alternative mass spectrometry methods to detect more 4E-BP sensitive proteins

The mass spectrometry of classic SILAC labelled proteins *in vivo* and *in vitro* identified many upregulated proteins upon 4E-BP overexpression, but the problem of a undefined threshold of upregulated proteins remained. In this study, proteins with an abundance increase of more than 50 % were considered as upregulated. However, this definition could prevent the detection of subtly upregulated proteins. Several strategies are possible to overcome this problem and to identify also slightly upregulated proteins. One method is pulsed SILAC (pSILAC) labelling (Schwanhausser et al., 2009) (Fig. 7.2). Instead of labelling cells with light and heavy isotopes only, they would be labelled with three isotope sets: light (e.g. Arg(0)/Lys(0)), medium-heavy (e.g. Arg(6)/Lys(4)) and heavy (e.g. Arg(10), Lys(8)). Before the experiments, all cells would be labelled with light medium for several cell doublings to make sure the medium was completely incorporated. Subsequently, cells would be split into two separate dishes and treated with medium-heavy or heavy medium for the duration of the experiment. The heavy medium would also contain tetracycline to induce 4E-BP1 overexpression. After the experiment, equal amounts of cell lysate from medium-heavy and heavy medium would be united and used for mass spectrometry. All proteins labelled with light isotopes could be excluded, because they were synthesised before the experiment began. These proteins define the threshold. The ratio medium-heavy/heavy defines the upregulation of proteins. Although this technique has the advantage that it can remove the background of proteins synthesised before 4E-BP1 was overexpressed and is thus more sensitive, it also deals with a higher rate of protein and peptide complexity as three sets of isotopes are required. This may reduce the number of total identified proteins.

In order to overcome this problem of increasing complexity, BONLAC (bioorthogonal noncanonical and stable isotope labelling with amino acids in cell culture) could be applied for labelling (Zhang et al., 2014). In principal, it is a modified pSILAC strategy (Fig. 7.2). Additional to the medium-heavy and heavy media, newly synthesised proteins were labelled with L-azidohomoalaine (AHA) at the beginning of the experiment. The azide moiety from AHA allows labelled proteins to be covalently conjugated to alkyne-labelled beads. In this way, newly synthesised proteins after 4E-BP1

overexpression could be purified prior to mass spectrometry experiments in order to reduce the background and complexity.

The described strategies could be applied for *in vivo* experiments as well, but no report has tested BONLAC *in vivo* yet. Quantitative mass spectrometry is a very prospering field at the moment and it is to expect that better technologies will become available in the next years.
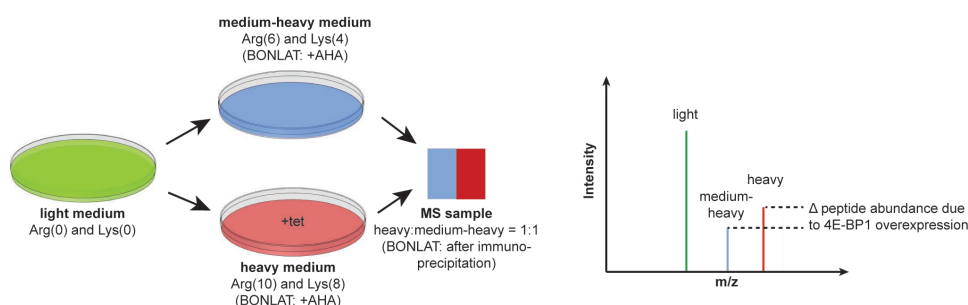
Figure 7.2: Principal of proteomics with pSILAC or BONLAT *in vitro*. For pSI-LAC experiments, T-REx HEK293 cells are grown in light medium for several cell doublings and subsequently split in two different petri dishes with medium-heavy or heavy media. 4E-BP1 over-expression would be induced by tetracycline (tet) in heavy medium. Cells from both media would be lysed at a defined time point and the proteins united for mass spectrometry experiments. The ratio of medium-heavy to heavy proteins defines the effect of 4E-BP1 overexpression on the protein. Light proteins indicate the background before the experiment started. BONLAT helps to remove this background by adding AHA to medium-heavy and heavy media. Incorporated azide can be targeted by immunoprecipitation and all non-targeted proteins would be removed.

7.3.3   Further experiments to investigate the cellular protective potential of identified proteins

Although many potential cellular protecting proteins upon 4E-BP overexpression could be identified in this study, the evaluation of the individual contribution of different candidates *in vitro* and *in vivo* is not completed. The siRNA knockdown assay of selected candidates was a promising strategy to evaluate their contribution fast. However, further tests are necessary to get a better understanding of the cellular protective contribution of selected targets. In a first approach, identified 4E-BP downstream targets could be transiently overexpressed in HEK293 and the effect on survival capability investigated in a rotenone assay. *Drosophila* homologues of hits from this assay should be overexpressed in fly models of PD or *Thor* knockouts to explore whether these targets can improve their phenotype.

The evaluation of 4E-BP1 downstream targets could help in the future to identify new targets for the treatment of many neurodegenerative and

other apoptotic diseases.

Bibliography

Adams, M. D., Celniker, S. E., Holt, R. A., Evans, C. A., et al. The genome sequence of Drosophila melanogaster. *Science*, 287(5461):2185–2195, Mar 2000.

Agam, K., von Campenhausen, M., Levy, S., Ben-Ami, H. C., et al. Metabolic stress reversibly activates the Drosophila light-sensitive channels TRP and TRPL in vivo. *J Neurosci*, 20(15):5748–5755, Aug 2000.

Allard, E. K., Grujic, M., Fisone, G., and Kristensson, K. Prion formation correlates with activation of translation-regulating protein 4E-BP and neuronal transcription factor Elk1. *Neurobiol Dis*, 58:116–22, 2013.

Altmann, M., Schmitz, N., Berset, C., and Trachsel, H. A novel inhibitor of cap-dependent translation initiation in yeast: p20 competes with eIF4G for binding to eIF4E. *EMBO J*, 16(5):1114–1121, Mar 1997.

An, W. L., Cowburn, R. F., Li, L., Braak, H., et al. Up-regulation of phosphorylated/activated p70 S6 kinase and its relationship to neurofibrillary pathology in Alzheimer's disease. *Am J Pathol*, 163(2):591–607, 2003.

Avdulov, S., Li, S., Michalek, V., Burrichter, D., et al. Activation of translation complex eIF4F is essential for the genesis and maintenance of the malignant phenotype in human mammary epithelial cells. *Cancer Cell*, 5(6):553–63, 2004.

Azar, R., Susini, C., Bousquet, C., and Pyronnet, S. Control of contact-inhibition by 4E-BP1 upregulation. *Cell Cycle*, 9(7):1241–1245, Apr 2010.

Baine, M. J., Chakraborty, S., Smith, L. M., Mallya, K., et al. Transcriptional profiling of peripheral blood mononuclear cells in pancreatic cancer

patients identifies novel genes with potential diagnostic utility. *PLoS One*, 6(2):e17014, 2011.

Baird, S. D., Lewis, S. M., Turcotte, M., and Holcik, M. A search for structurally similar cellular internal ribosome entry sites. *Nucleic Acids Res*, 35(14):4664–4677, 2007.

Banko, J. L., Poulin, F., Hou, L., DeMaria, C. T., Sonenberg, N., and Klann, E. The translation repressor 4E-BP2 is critical for eIF4F complex formation, synaptic plasticity, and memory in the hippocampus. *J Neurosci*, 25 (42):9581–9590, Oct 2005.

Banko, J. L., Hou, L., Poulin, F., Sonenberg, N., and Klann, E. Regulation of eukaryotic initiation factor 4E by converging signaling pathways during metabotropic glutamate receptor-dependent long-term depression. *J Neurosci*, 26(8):2167–2173, Feb 2006.

Baraibar, M. A., Barbeito, A. G., Muhoberac, B. B., and Vidal, R. Iron-mediated aggregation and a localized structural change characterize ferritin from a mutant light chain polypeptide that causes neurodegeneration. *J Biol Chem*, 283(46):31679–31689, Nov 2008.

Baraibar, M. A., Barbeito, A. G., Muhoberac, B. B., and Vidal, R. A mutant light-chain ferritin that causes neurodegeneration has enhanced propensity toward oxidative damage. *Free Radic Biol Med*, 52(9):1692–1697, May 2012.

Baranick, B. T., Lemp, N. A., Nagashima, J., Hiraoka, K., Kasahara, N., and Logg, C. R. Splicing mediates the activity of four putative cellular internal ribosome entry sites. *Proc Natl Acad Sci U S A*, 105(12):4733–4738, Mar 2008.

Barbeito, A. G., Garringer, H. J., Baraibar, M. A., Gao, X., et al. Abnormal iron metabolism and oxidative stress in mice expressing a mutant form of the ferritin light polypeptide gene. *J Neurochem*, 109(4):1067–1078, May 2009.

Barnekow, A., Thyrock, A., and Kessler, D. Chapter 5: rab proteins and their interaction partners. *Int Rev Cell Mol Biol*, 274:235–274, 2009.

Barnes, L. D., Garrison, P. N., Siprashvili, Z., Guranowski, A., et al. Fhit, a putative tumor suppressor in humans, is a dinucleoside 5',5"'-P1,P3-triphosphate hydrolase. *Biochemistry*, 35(36):11529–11535, Sep 1996.

Battelli, C. and Cho, D. C. mTOR inhibitors in renal cell carcinoma. *Therapy*, 8(4):359–367, Jul 2011.

Beaudoin, M. E., Poirel, V.-J., and Krushel, L. A. Regulating amyloid precursor protein synthesis through an internal ribosomal entry site. *Nucleic Acids Res*, 36(21):6835–6847, Dec 2008.

Berezowsky, C. and Bag, J. Slow troponin C is present in both muscle and nonmuscle cells. *Biochem Cell Biol*, 70(8):691–697, Aug 1992.

Bernal, A. and Kimbrell, D. A. Drosophila Thor participates in host immune defense and connects a translational regulator with innate immunity. *Proc Natl Acad Sci U S A*, 97(11):6019–6024, May 2000.

Bernal, A., Schoenfeld, R., Kleinhesselink, K., and Kimbrell, D. A. Loss of Thor, the single 4E-BP gene of Drosophila, does not result in lethality. *Drosophila Information Service*, 87:81–84, 2004.

Bernardo Carvalho, A., Koerich, L. B., and Clark, A. G. Origin and evolution of Y chromosomes: Drosophila tales. *Trends Genet*, 25(6):270–277, Jun 2009.

Beugnet, A., Wang, X., and Proud, C. G. Target of rapamycin (TOR)-signaling and RAIP motifs play distinct roles in the mammalian TOR-dependent phosphorylation of initiation factor 4E-binding protein 1. *J Biol Chem*, 278(42):40717–22, 2003.

Bjedov, I., Toivonen, J. M., Kerr, F., Slack, C., et al. Mechanisms of life span extension by rapamycin in the fruit fly Drosophila melanogaster. *Cell Metab*, 11(1):35–46, Jan 2010.

Borkham-Kamphorst, E., Steffen, B. T., Van de Leur, E., Haas, U., et al. CCN1/CYR61 overexpression in hepatic stellate cells induces ER stress-related apoptosis. *Cell Signal*, 28(1):34–42, Jan 2016.

Boudhraa, Z., Rondepierre, F., Ouchchane, L., Kintossou, R., et al. Annexin A1 in primary tumors promotes melanoma dissemination. *Clin Exp Metastasis*, 31(7):749–760, Oct 2014.

Braschi, E., Goyon, V., Zunino, R., Mohanty, A., Xu, L., and McBride, H. M. Vps35 mediates vesicle transport between the mitochondria and peroxisomes. *Curr Biol*, 20(14):1310–1315, Jul 2010.

Braunstein, S., Karpisheva, K., Pola, C., Goldberg, J., et al. A hypoxia-controlled cap-dependent to cap-independent translation switch in breast cancer. *Mol Cell*, 28(3):501–512, Nov 2007.

Brown, E. J., Albers, M. W., Shin, T. B., Ichikawa, K., et al. A mammalian protein targeted by G1-arresting rapamycin-receptor complex. *Nature*, 369(6483):756–8, 1994.

Brunn, G. J., Williams, J., Sabers, C., Wiederrecht, G., Lawrence, J., Jr, and Abraham, R. T. Direct inhibition of the signaling functions of the mammalian target of rapamycin by the phosphoinositide 3-kinase inhibitors, wortmannin and LY294002. *EMBO J*, 15(19):5256–5267, Oct 1996.

Burnett, P. E., Barrow, R. K., Cohen, N. A., Snyder, S. H., and Sabatini, D. M. RAFT1 phosphorylation of the translational regulators p70 S6 kinase and 4E-BP1. *Proc Natl Acad Sci U S A*, 95(4):1432–7, 1998.

Buttgereit, F. and Brand, M. D. A hierarchy of ATP-consuming processes in mammalian cells. *Biochem J*, 312 (Pt 1):163–167, Nov 1995.

Campbell, D. S. and Holt, C. E. Chemotropic responses of retinal growth cones mediated by rapid local protein synthesis and degradation. *Neuron*, 32(6):1013–26, 2001.

Campbell, E., Takahashi, Y., Abramovitz, M., Peretz, M., and Listowsky, I. A distinct human testis and brain mu-class glutathione S-transferase. Molecular cloning and characterization of a form present even in individuals lacking hepatic type mu isoenzymes. *J Biol Chem*, 265(16):9188–9193, Jun 1990.

189

Cao, W., Liu, N., Tang, S., Bao, L., et al. Acetyl-Coenzyme A acyltransferase 2 attenuates the apoptotic effects of BNIP3 in two human cell lines. *Biochim Biophys Acta*, 1780(6):873–880, Jun 2008.

Casadio, A., Martin, K. C., Giustetto, M., Zhu, H., et al. A transient, neuron-wide form of CREB-mediated long-term facilitation can be stabilized at specific synapses by local protein synthesis. *Cell*, 99(2):221–37, 1999.

Castro, A. F., Rebhun, J. F., Clark, G. J., and Quilliam, L. A. Rheb binds tuberous sclerosis complex 2 (TSC2) and promotes S6 kinase activation in a rapamycin- and farnesylation-dependent manner. *J Biol Chem*, 278 (35):32493–32496, Aug 2003.

Cavener, D. R. Comparison of the consensus sequence flanking translational start sites in Drosophila and vertebrates. *Nucleic Acids Res*, 15(4): 1353–1361, Feb 1987.

Chanas, S. A., Jiang, Q., McMahon, M., McWalter, G. K., et al. Loss of the Nrf2 transcription factor causes a marked reduction in constitutive and inducible expression of the glutathione S-transferase Gsta1, Gsta2, Gstm1, Gstm2, Gstm3 and Gstm4 genes in the livers of male and female mice. *Biochem J*, 365(Pt 2):405–416, Jul 2002.

Chano, T., Okabe, H., and Hulette, C. M. RB1CC1 insufficiency causes neuronal atrophy through mTOR signaling alteration and involved in the pathology of Alzheimer's diseases. *Brain Res*, 1168:97–105, 2007.

Chao, M.-W., Wang, L.-T., Lai, C.-Y., Yang, X.-M., et al. eIF4E binding protein 1 expression is associated with clinical survival outcomes in colorectal cancer. *Oncotarget*, 6(27):24092–24104, Sep 2015.

Chappell, S. A., Owens, G. C., and Mauro, V. P. A 5' Leader of Rbm3, a Cold Stress-induced mRNA, Mediates Internal Initiation of Translation with Increased Efficiency under Conditions of Mild Hypothermia. *J Biol Chem*, 276(40):36917–36922, Oct 2001.

Cheatham, B., Vlahos, C. J., Cheatham, L., Wang, L., Blenis, J., and Kahn, C. R. Phosphatidylinositol 3-kinase activation is required for insulin stimulation of pp70 S6 kinase, DNA synthesis, and glucose transporter translocation. *Mol Cell Biol*, 14(7):4902–4911, Jul 1994.

Chen, J. S., Coustan-Smith, E., Suzuki, T., Neale, G. A., et al. Identification of novel markers for monitoring minimal residual disease in acute lymphoblastic leukemia. *Blood*, 97(7):2115–2120, Apr 2001.

Cheng, L. Y., Bailey, A. P., Leevers, S. J., Ragan, T. J., Driscoll, P. C., and Gould, A. P. Anaplastic lymphoma kinase spares organ growth during nutrient restriction in Drosophila. *Cell*, 146(3):435–47, 2011.

Chiu, M. I., Katz, H., and Berlin, V. RAPT1, a mammalian homolog of yeast Tor, interacts with the FKBP12/rapamycin complex. *Proc Natl Acad Sci U S A*, 91(26):12574–8, 1994.

Cho, S. and Dawson, G. Palmitoyl protein thioesterase 1 protects against apoptosis mediated by Ras-Akt-caspase pathway in neuroblastoma cells. *J Neurochem*, 74(4):1478–1488, Apr 2000.

Choi, K. M., McMahon, L. P., and Lawrence, J., J. C. Two motifs in the translational repressor PHAS-I required for efficient phosphorylation by mammalian target of rapamycin and for recognition by raptor. *J Biol Chem*, 278(22):19667–73, 2003.

Choo, A. Y., Yoon, S.-O., Kim, S. G., Roux, P. P., and Blenis, J. Rapamycin differentially inhibits S6Ks and 4E-BP1 to mediate cell-type-specific repression of mRNA translation. *Proc Natl Acad Sci U S A*, 105 (45):17414–17419, Nov 2008.

Chung, J., Grammer, T. C., Lemon, K. P., Kazlauskas, A., and Blenis, J. PDGF- and insulin-dependent pp70S6k activation mediated by phosphatidylinositol-3-OH kinase. *Nature*, 370(6484):71–75, Jul 1994.

Chyb, S., Raghu, P., and Hardie, R. C. Polyunsaturated fatty acids activate the Drosophila light-sensitive channels TRP and TRPL. *Nature*, 397 (6716):255–259, Jan 1999.

Clamp, M., Fry, B., Kamal, M., Xie, X., et al. Distinguishing protein-coding and noncoding genes in the human genome. *Proc Natl Acad Sci U S A*, 104(49):19428–19433, Dec 2007.

Clark, I. E., Wyckoff, D., and Gavis, E. R. Synthesis of the posterior determinant Nanos is spatially restricted by a novel cotranslational regulatory mechanism. *Curr Biol*, 10(20):1311–4, 2000.

Coldwell, M. J., Mitchell, S. A., Stoneley, M., MacFarlane, M., and Willis, A. E. Initiation of Apaf-1 translation by internal ribosome entry. *Oncogene*, 19(7):899–905, 2000.

Colina, R., Costa-Mattioli, M., Dowling, R. J. O., Jaramillo, M., et al. Translational control of the innate immune response through IRF-7. *Nature*, 452(7185):323–328, Mar 2008.

Cox, J. and Mann, M. Quantitative, high-resolution proteomics for data-driven systems biology. *Annu Rev Biochem*, 80:273–299, 2011.

Crews, L., Spencer, B., Desplats, P., Patrick, C., et al. Selective molecular alterations in the autophagy pathway in patients with Lewy body disease and in models of alpha-synucleinopathy. *PLoS One*, 5(2):e9313, 2010.

Damiano, F., Alemanno, S., Gnoni, G. V., and Siculella, L. Translational control of the sterol-regulatory transcription factor SREBP-1 mRNA in response to serum starvation or ER stress is mediated by an internal ribosome entry site. *Biochem J*, 429(3):603–612, Aug 2010.

De Benedetti, A. and Rhoads, R. E. Overexpression of eukaryotic protein synthesis initiation factor 4E in HeLa cells results in aberrant growth and morphology. *Proc Natl Acad Sci U S A*, 87(21):8212–8216, Nov 1990.

de Godoy, L. M. F., Olsen, J. V., Cox, J., Nielsen, M. L., et al. Comprehensive mass-spectrometry-based proteome quantification of haploid versus diploid yeast. *Nature*, 455(7217):1251–1254, Oct 2008.

Dearborn, J. T., Harmon, S. K., Fowler, S. C., O'Malley, K. L., et al. Comprehensive functional characterization of murine infantile Batten disease including Parkinson-like behavior and dopaminergic markers. *Sci Rep*, 5: 12752, 2015.

Demontis, F. and Perrimon, N. FOXO/4E-BP signaling in Drosophila muscles regulates organism-wide proteostasis during aging. *Cell*, 143(5): 813–825, Nov 2010.

Dmitriev, S. E., Terenin, I. M., Andreev, D. E., Ivanov, P. A., et al. GTP-independent tRNA delivery to the ribosomal P-site by a novel eukaryotic translation factor. *J Biol Chem*, 285(35):26779–26787, Aug 2010.

Dowling, R. J. O., Topisirovic, I., Alain, T., Bidinosti, M., et al. mTORC1-mediated cell proliferation, but not cell growth, controlled by the 4E-BPs. *Science*, 328(5982):1172–1176, May 2010.

Downward, J. Targeting RAS signalling pathways in cancer therapy. *Nat Rev Cancer*, 3(1):11–22, Jan 2003.

Dumas, E., Staedel, C., Colombat, M., Reigadas, S., et al. A promoter activity is present in the DNA sequence corresponding to the hepatitis C virus 5' UTR. *Nucleic Acids Res*, 31(4):1275–1281, Feb 2003.

Dumitriu, A., Latourelle, J. C., Hadzi, T. C., Pankratz, N., et al. Gene expression profiles in Parkinson disease prefrontal cortex implicate FOXO1 and genes under its transcriptional regulation. *PLoS Genet*, 8(6):e1002794, Jun 2012.

Fadden, P., Haystead, T. A., and Lawrence, J., J. C. Identification of phosphorylation sites in the translational regulator, PHAS-I, that are controlled by insulin and rapamycin in rat adipocytes. *J Biol Chem*, 272(15): 10240–7, 1997.

Fagerberg, L., Strömberg, S., El-Obeid, A., Gry, M., et al. Large-scale protein profiling in human cell lines using antibody-based proteomics. *J Proteome Res*, 10(9):4066–4075, Sep 2011.

Fang, Y., Vilella-Bach, M., Bachmann, R., Flanigan, A., and Chen, J. Phosphatidic acid-mediated mitogenic activation of mTOR signaling. *Science*, 294(5548):1942–1945, Nov 2001.

Fang, Y., Park, I.-H., Wu, A.-L., Du, G., et al. PLD1 regulates mTOR signaling and mediates Cdc42 activation of S6K1. *Curr Biol*, 13(23): 2037–2044, Dec 2003.

Feldman, M. E., Apsel, B., Uotila, A., Loewith, R., et al. Active-site inhibitors of mTOR target rapamycin-resistant outputs of mTORC1 and mTORC2. *PLoS biology*, 7(2):e38, 2009.

Feng, Z., Zhang, H., Levine, A. J., and Jin, S. The coordinate regulation of the p53 and mTOR pathways in cells. *Proc Natl Acad Sci U S A*, 102 (23):8204–8209, Jun 2005.

Fox, C. J., Hammerman, P. S., Cinalli, R. M., Master, S. R., Chodosh, L. A., and Thompson, C. B. The serine/threonine kinase Pim-2 is a transcriptionally regulated apoptotic inhibitor. *Genes Dev*, 17(15):1841–1854, Aug 2003.

Fredens, J., Engholm-Keller, K., Giessing, A., Pultz, D., et al. Quantitative proteomics by amino acid labeling in C. elegans. *Nat Methods*, 8(10): 845–847, 2011.

Fukuyo, A., In, Y., Ishida, T., and Tomoo, K. Structural scaffold for eIF4E binding selectivity of 4E-BP isoforms: crystal structure of eIF4E binding region of 4E-BP2 and its comparison with that of 4E-BP1. *J Pept Sci*, 17 (9):650–7, 2011.

Gao, X., Zhang, Y., Arrazola, P., Hino, O., et al. Tsc tumour suppressor proteins antagonize amino-acid-TOR signalling. *Nat Cell Biol*, 4(9): 699–704, Sep 2002.

Garami, A., Zwartkruis, F. J. T., Nobukuni, T., Joaquin, M., et al. Insulin activation of Rheb, a mediator of mTOR/S6K/4E-BP signaling, is inhibited by TSC1 and 2. *Mol Cell*, 11(6):1457–1466, Jun 2003.

Gebauer, F. and Hentze, M. W. Molecular mechanisms of translational control. *Nat Rev Mol Cell Biol*, 5(10):827–35, 2004.

Gehrke, S., Wu, Z., Klinkenberg, M., Sun, Y., et al. PINK1 and Parkin control localized translation of respiratory chain component mRNAs on mitochondria outer membrane. *Cell Metab*, 21(1):95–108, Jan 2015.

Gilbert, W. V. Alternative ways to think about cellular internal ribosome entry. *J Biol Chem*, 285(38):29033–29038, Sep 2010.

Gilks, N., Kedersha, N., Ayodele, M., Shen, L., et al. Stress granule assembly is mediated by prion-like aggregation of TIA-1. *Mol Biol Cell*, 15(12): 5383–5398, Dec 2004.

Gingras, A. C., Kennedy, S. G., O'Leary, M. A., Sonenberg, N., and Hay, N. 4E-BP1, a repressor of mRNA translation, is phosphorylated and inactivated by the Akt(PKB) signaling pathway. *Genes Dev*, 12(4):502–513, Feb 1998.

Gingras, A. C., Gygi, S. P., Raught, B., Polakiewicz, R. D., et al. Regulation of 4E-BP1 phosphorylation: a novel two-step mechanism. *Genes Dev*, 13 (11):1422–37, 1999.

Gingras, A. C., Raught, B., Gygi, S. P., Niedzwiecka, A., et al. Hierarchical phosphorylation of the translation inhibitor 4E-BP1. *Genes Dev*, 15(21): 2852–64, 2001.

Gottschalk, W. K., Lutz, M. W., He, Y. T., Saunders, A. M., et al. The Broad Impact of TOM40 on Neurodegenerative Diseases in Aging. *J Parkinsons Dis Alzheimers Dis*, 1(1), Nov 2014.

Gozzelino, R., Jeney, V., and Soares, M. P. Mechanisms of cell protection by heme oxygenase-1. *Annu Rev Pharmacol Toxicol*, 50:323–354, 2010.

Graff, J. R., Boghaert, E. R., De Benedetti, A., Tudor, D. L., et al. Reduction of translation initiation factor 4E decreases the malignancy of ras-transformed cloned rat embryo fibroblasts. *Int J Cancer*, 60(2):255–263, Jan 1995.

Greenberg, V. L. and Zimmer, S. G. Paclitaxel induces the phosphorylation of the eukaryotic translation initiation factor 4E-binding protein 1 through a Cdk1-dependent mechanism. *Oncogene*, 24(30):4851–4860, Jul 2005.

Greene, J. C., Whitworth, A. J., Kuo, I., Andrews, L. A., Feany, M. B., and Pallanck, L. J. Mitochondrial pathology and apoptotic muscle degeneration in Drosophila parkin mutants. *Proc Natl Acad Sci U S A*, 100(7): 4078–4083, Apr 2003.

Greeve, I., Hermans-Borgmeyer, I., Brellinger, C., Kasper, D., et al. The human DIMINUTO/DWARF1 homolog seladin-1 confers resistance to Alzheimer's disease-associated neurodegeneration and oxidative stress. *J Neurosci*, 20(19):7345–7352, Oct 2000.

Griffin, R. J., Moloney, A., Kelliher, M., Johnston, J. A., et al. Activation of Akt/PKB, increased phosphorylation of Akt substrates and loss and altered distribution of Akt and PTEN are features of Alzheimer's disease pathology. *J Neurochem*, 93(1):105–17, 2005.

Guan, L., Song, K., Pysz, M. A., Curry, K. J., et al. Protein kinase C-mediated down-regulation of cyclin D1 involves activation of the translational repressor 4E-BP1 via a phosphoinositide 3-kinase/Akt-independent, protein phosphatase 2A-dependent mechanism in intestinal epithelial cells. *J Biol Chem*, 282(19):14213–25, 2007.

Gui, Y., Zhang, L., Lv, W., Zhang, W., Zhao, J., and Hu, X. NFE2L2 variations reduce antioxidant response in patients with Parkinson disease. *Oncotarget*, 7(10):10756–10764, Mar 2016.

Gwinn, D. M., Shackelford, D. B., Egan, D. F., Mihaylova, M. M., et al. AMPK phosphorylation of raptor mediates a metabolic checkpoint. *Mol Cell*, 30(2):214–226, Apr 2008.

Gygi, S. P., Rist, B., Gerber, S. A., Turecek, F., Gelb, M. H., and Aebersold, R. Quantitative analysis of complex protein mixtures using isotope-coded affinity tags. *Nat Biotechnol*, 17(10):994–999, Oct 1999.

Han, B. and Zhang, J.-T. Regulation of gene expression by internal ribosome entry sites or cryptic promoters: the eIF4G story. *Mol Cell Biol*, 22(21):7372–7384, Nov 2002.

Han, B., Dong, Z., and Zhang, J.-T. Tight control of platelet-derived growth factor B/c-sis expression by interplay between the 5'-untranslated region sequence and the major upstream promoter. *J Biol Chem*, 278(47):46983–46993, Nov 2003.

Han, G., Tian, Y., Duan, B., Sheng, H., Gao, H., and Huang, J. Association of nuclear annexin A1 with prognosis of patients with esophageal squamous cell carcinoma. *Int J Clin Exp Pathol*, 7(2):751–759, 2014.

Harding, H. P., Zhang, Y., Bertolotti, A., Zeng, H., and Ron, D. Perk is essential for translational regulation and cell survival during the unfolded protein response. *Mol Cell*, 5(5):897–904, 2000.

Harrison, D. E., Strong, R., Sharp, Z. D., Nelson, J. F., et al. Rapamycin fed late in life extends lifespan in genetically heterogeneous mice. *Nature*, 460(7253):392–5, 2009.

Heesom, K. J. and Denton, R. M. Dissociation of the eukaryotic initiation factor-4E/4E-BP1 complex involves phosphorylation of 4E-BP1 by an mTOR-associated kinase. *FEBS Lett*, 457(3):489–93, 1999.

Heesom, K. J., Avison, M. B., Diggle, T. A., and Denton, R. M. Insulin-stimulated kinase from rat fat cells that phosphorylates initiation factor 4E-binding protein 1 on the rapamycin-insensitive site (serine-111). *Biochem J*, 336 (Pt 1):39–48, Nov 1998.

Heesom, K. J., Gampel, A., Mellor, H., and Denton, R. M. Cell cycle-dependent phosphorylation of the translational repressor eIF-4E binding protein-1 (4E-BP1). *Curr Biol*, 11(17):1374–1379, Sep 2001.

Helliwell, S. B., Wagner, P., Kunz, J., Deuter-Reinhard, M., Henriquez, R., and Hall, M. N. TOR1 and TOR2 are structurally and functionally similar but not identical phosphatidylinositol kinase homologues in yeast. *Mol Biol Cell*, 5(1):105–18, 1994.

Hertz, M. I., Landry, D. M., Willis, A. E., Luo, G., and Thompson, S. R. Ribosomal protein S25 dependency reveals a common mechanism for diverse internal ribosome entry sites and ribosome shunting. *Mol Cell Biol*, 33(5):1016–1026, Mar 2013.

Holcik, M. and Sonenberg, N. Translational control in stress and apoptosis. *Nat Rev Mol Cell Biol*, 6(4):318–27, 2005.

Holcik, M., Lefebvre, C., Yeh, C., Chow, T., and Korneluk, R. G. A new internal-ribosome-entry-site motif potentiates XIAP-mediated cytoprotection. *Nat Cell Biol*, 1(3):190–2, 1999.

Holcik, M., Sonenberg, N., and Korneluk, R. G. Internal ribosome initiation of translation and the control of cell death. *Trends Genet*, 16(10):469–73, 2000a.

Holcik, M., Yeh, C., Korneluk, R. G., and Chow, T. Translational upregulation of X-linked inhibitor of apoptosis (XIAP) increases resistance to radiation induced cell death. *Oncogene*, 19(36):4174–7, 2000b.

Hsieh, A. C., Liu, Y., Edlind, M. P., Ingolia, N. T., et al. The translational landscape of mTOR signalling steers cancer initiation and metastasis. *Nature*, 485(7396):55–61, 2012.

Hsieh, A. C., Costa, M., Zollo, O., Davis, C., et al. Genetic dissection of the oncogenic mTOR pathway reveals druggable addiction to translational control via 4EBP-eIF4E. *Cancer Cell*, 17(3):249–261, Mar 2010.

Hucthagowder, V., Morava, E., Kornak, U., Lefeber, D. J., et al. Loss-of-function mutations in ATP6V0A2 impair vesicular trafficking, tropoelastin secretion and cell survival. *Hum Mol Genet*, 18(12):2149–2165, Jun 2009.

Hughes, J. M., Ptushkina, M., Karim, M. M., Koloteva, N., von der Haar, T., and McCarthy, J. E. Translational repression by human 4E-BP1 in yeast specifically requires human eIF4E as target. *The Journal of biological chemistry*, 274(6):3261–4, 1999.

Huo, Y., Iadevaia, V., Yao, Z., Kelly, I., et al. Stable isotope-labelling analysis of the impact of inhibition of the mammalian target of rapamycin on protein synthesis. *Biochem J*, 444(1):141–51, 2012.

Hwang, O. Role of oxidative stress in Parkinson's disease. *Exp Neurobiol*, 22(1):11–17, Mar 2013.

Hyun, T. S., Rao, D. S., Saint-Dic, D., Michael, L. E., et al. HIP1 and HIP1r stabilize receptor tyrosine kinases and bind 3-phosphoinositides via epsin N-terminal homology domains. *J Biol Chem*, 279(14):14294–14306, Apr 2004.

Im, E., von Lintig, F. C., Chen, J., Zhuang, S., et al. Rheb is in a high activation state and inhibits B-Raf kinase in mammalian cells. *Oncogene*, 21(41):6356–65, 2002.

Imai, Y., Gehrke, S., Wang, H. Q., Takahashi, R., et al. Phosphorylation of 4E-BP by LRRK2 affects the maintenance of dopaminergic neurons in Drosophila. *EMBO J*, 27(18):2432–43, 2008.

Inoki, K., Li, Y., Zhu, T., Wu, J., and Guan, K.-L. TSC2 is phosphorylated and inhibited by Akt and suppresses mTOR signalling. *Nat Cell Biol*, 4 (9):648–657, Sep 2002.

Inoki, K., Zhu, T., and Guan, K.-L. TSC2 mediates cellular energy response to control cell growth and survival. *Cell*, 115(5):577–590, Nov 2003.

Ivatt, R. M., Sanchez-Martinez, A., Godena, V. K., Brown, S., Ziviani, E., and Whitworth, A. J. Genome-wide RNAi screen identifies the Parkinson disease GWAS risk locus SREBF1 as a regulator of mitophagy. *Proc Natl Acad Sci U S A*, 111(23):8494–8499, Jun 2014.

Jaeschke, A., Hartkamp, J., Saitoh, M., Roworth, W., et al. Tuberous sclerosis complex tumor suppressor-mediated S6 kinase inhibition by phosphatidylinositide-3-OH kinase is mTOR independent. *J Cell Biol*, 159(2):217–224, Oct 2002.

Janzen, C., Sen, S., Cuevas, J., Reddy, S. T., and Chaudhuri, G. Protein phosphatase 2A promotes endothelial survival via stabilization of translational inhibitor 4E-BP1 following exposure to tumor necrosis factor-α. *Arterioscler Thromb Vasc Biol*, 31(11):2586–2594, Nov 2011.

Johannes, G., Carter, M. S., Eisen, M. B., Brown, P. O., and Sarnow, P. Identification of eukaryotic mRNAs that are translated at reduced cap binding complex eIF4F concentrations using a cDNA microarray. *Proc Natl Acad Sci U S A*, 96(23):13118–23, 1999.

Jones, A. C., Shyamsundar, M. M., Thomas, M. W., Maynard, J., et al. Comprehensive mutation analysis of TSC1 and TSC2-and phenotypic correlations in 150 families with tuberous sclerosis. *Am J Hum Genet*, 64(5): 1305–1315, May 1999.

Kaeberlein, M., Powers, R. W., 3rd, Steffen, K. K., Westman, E. A., et al. Regulation of yeast replicative life span by TOR and Sch9 in response to nutrients. *Science*, 310(5751):1193–1196, Nov 2005.

Kandel, E. R. The molecular biology of memory storage: a dialogue between genes and synapses. *Science*, 294(5544):1030–8, 2001.

Kapahi, P., Zid, B. M., Harper, T., Koslover, D., Sapin, V., and Benzer, S. Regulation of lifespan in Drosophila by modulation of genes in the TOR signaling pathway. *Curr Biol*, 14(10):885–890, May 2004.

Karlsson, E., Waltersson, M. A., Bostner, J., Pérez-Tenorio, G., et al. High-resolution genomic analysis of the 11q13 amplicon in breast cancers identifies synergy with 8p12 amplification, involving the mTOR targets S6K2 and 4EBP1. *Genes Chromosomes Cancer*, 50(10):775–787, Oct 2011.

Karlsson, E., Pérez-Tenorio, G., Amin, R., Bostner, J., et al. The mTOR effectors 4EBP1 and S6K2 are frequently coexpressed, and associated with a poor prognosis and endocrine resistance in breast cancer: a retrospective study including patients from the randomised Stockholm tamoxifen trials. *Breast Cancer Res*, 15(5):R96, 2013.

Kawasaki, K., Ushioda, R., Ito, S., Ikeda, K., Masago, Y., and Nagata, K. Deletion of the collagen-specific molecular chaperone Hsp47 causes endoplasmic reticulum stress-mediated apoptosis of hepatic stellate cells. *J Biol Chem*, 290(6):3639–3646, Feb 2015.

Keyse, S. M. and Tyrrell, R. M. Heme oxygenase is the major 32-kDa stress protein induced in human skin fibroblasts by UVA radiation, hydrogen peroxide, and sodium arsenite. *Proc Natl Acad Sci U S A*, 86(1):99–103, Jan 1989.

Kim, D. H., Sarbassov, D. D., Ali, S. M., Latek, R. R., et al. GbetaL, a positive regulator of the rapamycin-sensitive pathway required for the nutrient-sensitive interaction between raptor and mTOR. *Mol Cell*, 11(4): 895–904, 2003.

Kim, D.-H., Sarbassov, D. D., Ali, S. M., King, J. E., et al. mTOR interacts with raptor to form a nutrient-sensitive complex that signals to the cell growth machinery. *Cell*, 110(2):163–175, Jul 2002.

Kim, J. H., Park, S. M., Park, J. H., Keum, S. J., and Jang, S. K. eIF2A mediates translation of hepatitis C viral mRNA under stress conditions. *EMBO J*, 30(12):2454–2464, Jun 2011.

Kimura, N., Tokunaga, C., Dalal, S., Richardson, C., et al. A possible linkage between AMP-activated protein kinase (AMPK) and mammalian target of rapamycin (mTOR) signalling pathway. *Genes Cells*, 8(1):65–79, Jan 2003.

Kobayashi, M., Wilson, A. C., Chao, M. V., and Mohr, I. Control of viral latency in neurons by axonal mTOR signaling and the 4E-BP translation repressor. *Genes Dev*, 26(14):1527–1532, Jul 2012.

Komar, A. A. and Hatzoglou, M. Internal ribosome entry sites in cellular mRNAs: mystery of their existence. *J Biol Chem*, 280(25):23425–23428, Jun 2005.

Komar, A. A. and Hatzoglou, M. Cellular IRES-mediated translation: the war of ITAFs in pathophysiological states. *Cell Cycle*, 10(2):229–240, Jan 2011.

Komar, A. A., Mazumder, B., and Merrick, W. C. A new framework for understanding IRES-mediated translation. *Gene*, 502(2):75–86, Jul 2012.

Kozak, M. Alternative ways to think about mRNA sequences and proteins that appear to promote internal initiation of translation. *Gene*, 318:1–23, Oct 2003.

Kozak, M. A second look at cellular mRNA sequences said to function as internal ribosome entry sites. *Nucleic Acids Res*, 33(20):6593–6602, 2005.

Krüger, M., Moser, M., Ussar, S., Thievessen, I., et al. SILAC mouse for quantitative proteomics uncovers kindlin-3 as an essential factor for red blood cell function. *Cell*, 134(2):353–364, Jul 2008.

Kunz, J., Henriquez, R., Schneider, U., Deuter-Reinhard, M., Movva, N. R., and Hall, M. N. Target of rapamycin in yeast, TOR2, is an essential phosphatidylinositol kinase homolog required for G1 progression. *Cell*, 73 (3):585–96, 1993.

Kurumaji, A. and Nishikawa, T. An anxiogenic drug, FG 7142, induced an increase in mRNA of Btg2 and Adamts1 in the hippocampus of adult mice. *Behav Brain Funct*, 8:43, 2012.

Lai, C.-Y., Pan, S.-L., Yang, X.-M., Chang, L.-H., et al. Depletion of 4E-BP1 and regulation of autophagy lead to YXM110-induced anticancer effects. *Carcinogenesis*, 34(9):2050–2060, Sep 2013.

Larance, M., Bailly, A. P., Pourkarimi, E., Hay, R. T., et al. Stable-isotope labeling with amino acids in nematodes. *Nat Methods*, 8(10):849–851, 2011.

Law, B. K. Rapamycin: an anti-cancer immunosuppressant? *Crit Rev Oncol Hematol*, 56(1):47–60, Oct 2005.

Lazaris-Karatzas, A., Montine, K. S., and Sonenberg, N. Malignant transformation by a eukaryotic initiation factor subunit that binds to mRNA 5' cap. *Nature*, 345(6275):544–547, Jun 1990.

Lee, S., Liu, H.-P., Lin, W.-Y., Guo, H., and Lu, B. LRRK2 kinase regulates synaptic morphology through distinct substrates at the presynaptic and postsynaptic compartments of the Drosophila neuromuscular junction. *J Neurosci*, 30(50):16959–16969, Dec 2010.

Levitin, A., Marcil, A., Tettweiler, G., Laforest, M. J., et al. Drosophila melanogaster Thor and response to Candida albicans infection. *Eukaryot Cell*, 6(4):658–663, Apr 2007.

Lewis, S. M. and Holcik, M. For IRES trans-acting factors, it is all about location. *Oncogene*, 27(8):1033–1035, Feb 2008.

Licursi, M., Komatsu, Y., Pongnopparat, T., and Hirasawa, K. Promotion of viral internal ribosomal entry site-mediated translation under amino acid starvation. *J Gen Virol*, 93(Pt 5):951–962, May 2012.

Lin, W., Wadlington, N. L., Chen, L., Zhuang, X., Brorson, J. R., and Kang, U. J. Loss of PINK1 attenuates HIF-1alpha induction by preventing 4E-BP1-dependent switch in protein translation under hypoxia. *J Neurosci*, 34(8):3079–89, 2014a.

Lin, Y.-C., Boone, M., Meuris, L., Lemmens, I., et al. Genome dynamics of the human embryonic kidney 293 lineage in response to cell biology manipulations. *Nat Commun*, 5:4767, 2014b.

Liu, G., Zhang, Y., Bode, A. M., Ma, W.-Y., and Dong, Z. Phosphorylation of 4E-BP1 is mediated by the p38/MSK1 pathway in response to UVB irradiation. *J Biol Chem*, 277(11):8810–8816, Mar 2002.

Liu, J., Stevens, P. D., Eshleman, N. E., and Gao, T. Protein phosphatase PPM1G regulates protein translation and cell growth by dephosphorylating 4E binding protein 1 (4E-BP1). *J Biol Chem*, 288(32):23225–33, 2013.

Liu, Q., Chang, J. W., Wang, J., Kang, S. A., et al. Discovery of 1-(4-(4-propionylpiperazin-1-yl)-3-(trifluoromethyl)phenyl)-9-(quinolin-3-yl)benz o[h][1,6]naphthyridin-2(1H)-one as a highly potent, selective mammalian target of rapamycin (mTOR) inhibitor for the treatment of cancer. *Journal of medicinal chemistry*, 53(19):7146–55, 2010.

Liu, Q. Blocking IRES-mediated translation pathway as a new method to treat Alzheimer's disease. *Journal of Medical Hypotheses and Ideas*, 9(1): 57 – 60, 2015. ISSN 2251-7294.

Livak, K. J. and Schmittgen, T. D. Analysis of relative gene expression data using real-time quantitative PCR and the 2(-Delta Delta C(T)) Method. *Methods*, 25(4):402–408, Dec 2001.

Lu, H., Yang, Y., Allister, E. M., Wijesekara, N., and Wheeler, M. B. The identification of potential factors associated with the development of type 2 diabetes: a quantitative proteomics approach. *Mol Cell Proteomics*, 7 (8):1434–1451, Aug 2008.

Lynch, M., Fitzgerald, C., Johnston, K. A., Wang, S., and Schmidt, E. V. Activated eIF4E-binding protein slows G1 progression and blocks transformation by c-myc without inhibiting cell growth. *J Biol Chem*, 279(5): 3327–39, 2004.

Lynes, E. M., Bui, M., Yap, M. C., Benson, M. D., et al. Palmitoylated TMX and calnexin target to the mitochondria-associated membrane. *EMBO J*, 31(2):457–470, Jan 2012.

Magdeldin, S., Blaser, R. E., Yamamoto, T., and Yates, J. R., 3rd. Behavioral and proteomic analysis of stress response in zebrafish (Danio rerio). *J Proteome Res*, 14(2):943–952, Feb 2015.

Malagelada, C., Ryu, E. J., Biswas, S. C., Jackson-Lewis, V., and Greene, L. A. RTP801 is elevated in Parkinson brain substantia nigral neurons and mediates death in cellular models of Parkinson's disease by a mechanism involving mammalian target of rapamycin inactivation. *J Neurosci*, 26 (39):9996–10005, Sep 2006.

Malik, B. R., Godena, V. K., and Whitworth, A. J. VPS35 pathogenic mutations confer no dominant toxicity but partial loss of function in Drosophila and genetically interact with parkin. *Hum Mol Genet*, 24(21):6106–6117, Nov 2015.

Manning, B. D., Tee, A. R., Logsdon, M. N., Blenis, J., and Cantley, L. C. Identification of the tuberous sclerosis complex-2 tumor suppressor gene

product tuberin as a target of the phosphoinositide 3-kinase/akt pathway. *Mol Cell*, 10(1):151–162, Jul 2002.

Marcotrigiano, J., Lomakin, I. B., Sonenberg, N., Pestova, T. V., Hellen, C. U., and Burley, S. K. A conserved HEAT domain within eIF4G directs assembly of the translation initiation machinery. *Mol Cell*, 7(1):193–203, Jan 2001.

Martineau, Y., Azar, R., Bousquet, C., and Pyronnet, S. Anti-oncogenic potential of the eIF4E-binding proteins. *Oncogene*, 32(6):671–677, Feb 2013.

Mèndez, R., Myers, M., Jr, White, M. F., and Rhoads, R. E. Stimulation of protein synthesis, eukaryotic translation initiation factor 4E phosphorylation, and PHAS-I phosphorylation by insulin requires insulin receptor substrate 1 and phosphatidylinositol 3-kinase. *Mol Cell Biol*, 16(6): 2857–2864, Jun 1996.

Merrick, W. C. Mechanism and regulation of eukaryotic protein synthesis. *Microbiol Rev*, 56(2):291–315, Jun 1992.

Merrick, W. C. Cap-dependent and cap-independent translation in eukaryotic systems. *Gene*, 332:1–11, May 2004.

Miller, R. A., Harrison, D. E., Astle, C. M., Baur, J. A., et al. Rapamycin, but not resveratrol or simvastatin, extends life span of genetically heterogeneous mice. *J Gerontol A Biol Sci Med Sci*, 66(2):191–201, Feb 2011.

Miron, M., Verdú, J., Lachance, P. E., Birnbaum, M. J., Lasko, P. F., and Sonenberg, N. The translational inhibitor 4E-BP is an effector of PI(3)K/Akt signalling and cell growth in Drosophila. *Nat Cell Biol*, 3(6): 596–601, Jun 2001.

Moore, D. J., West, A. B., Dawson, V. L., and Dawson, T. M. Molecular pathophysiology of Parkinson's disease. *Annu Rev Neurosci*, 28:57–87, 2005.

Morita, M., Gravel, S. P., Chenard, V., Sikstrom, K., et al. mTORC1 controls mitochondrial activity and biogenesis through 4E-BP-dependent translational regulation. *Cell Metab*, 18(5):698–711, 2013.

Moss, S. E. and Morgan, R. O. The annexins. *Genome Biol*, 5(4):219, 2004.

Musa, J., Orth, M. F., Dallmayer, M., Baldauf, M., et al. Eukaryotic initiation factor 4E-binding protein 1 (4E-BP1): a master regulator of mRNA translation involved in tumorigenesis. *Oncogene*, Feb 2016.

Nakamura, A., Sato, K., and Hanyu-Nakamura, K. Drosophila cup is an eIF4E binding protein that associates with Bruno and regulates oskar mRNA translation in oogenesis. *Dev Cell*, 6(1):69–78, 2004.

Nanbru, C., Lafon, I., Audigier, S., Gensac, M. C., et al. Alternative translation of the proto-oncogene c-myc by an internal ribosome entry site. *J Biol Chem*, 272(51):32061–32066, Dec 1997.

Nelson, M. R., Leidal, A. M., and Smibert, C. A. Drosophila Cup is an eIF4E-binding protein that functions in Smaug-mediated translational repression. *EMBO J*, 23(1):150–9, 2004.

Nojima, H., Tokunaga, C., Eguchi, S., Oshiro, N., et al. The mammalian target of rapamycin (mTOR) partner, raptor, binds the mTOR substrates p70 S6 kinase and 4E-BP1 through their TOR signaling (TOS) motif. *J Biol Chem*, 278(18):15461–4, 2003.

Oda, Y., Huang, K., Cross, F. R., Cowburn, D., and Chait, B. T. Accurate quantitation of protein expression and site-specific phosphorylation. *Proc Natl Acad Sci U S A*, 96(12):6591–6596, Jun 1999.

Orvedahl, A., Sumpter, R., Jr, Xiao, G., Ng, A., et al. Image-based genome-wide siRNA screen identifies selective autophagy factors. *Nature*, 480 (7375):113–117, Dec 2011.

Osterwalder, T., Yoon, K. S., White, B. H., and Keshishian, H. A conditional tissue-specific transgene expression system using inducible GAL4. *Proc Natl Acad Sci U S A*, 98(22):12596–12601, Oct 2001.

Ottone, C., Galasso, A., Gemei, M., Pisa, V., et al. Diminution of eIF4E activity suppresses parkin mutant phenotypes. *Gene*, 470(1-2):12–19, Jan 2011.

Pasa-Tolic, L., Jensen, P. K., Anderson, G. A., Lipton, M. S., et al. High Throughput Proteome-Wide Precision Measurements of Protein Expres-

sion Using Mass Spectrometry. *Journal of the American Chemical Society*, 121(34):7949–7950, 1999.

Pause, A., Belsham, G. J., Gingras, A. C., Donze, O., et al. Insulin-dependent stimulation of protein synthesis by phosphorylation of a regulator of 5'-cap function. *Nature*, 371(6500):762–7, 1994.

Peretti, D., Bastide, A., Radford, H., Verity, N., et al. RBM3 mediates structural plasticity and protective effects of cooling in neurodegeneration. *Nature*, 518(7538):236–239, Feb 2015.

Peri, A. Neuroprotective effects of estrogens: the role of cholesterol. *J Endocrinol Invest*, 39(1):11–18, Jan 2016.

Pestova, T. V., Shatsky, I. N., Fletcher, S. P., Jackson, R. J., and Hellen, C. U. A prokaryotic-like mode of cytoplasmic eukaryotic ribosome binding to the initiation codon during internal translation initiation of hepatitis C and classical swine fever virus RNAs. *Genes Dev*, 12(1):67–83, Jan 1998.

Pestova, T. V., Kolupaeva, V. G., Lomakin, I. B., Pilipenko, E. V., et al. Molecular mechanisms of translation initiation in eukaryotes. *Proc Natl Acad Sci U S A*, 98(13):7029–36, 2001.

Pestova, T. V., de Breyne, S., Pisarev, A. V., Abaeva, I. S., and Hellen, C. U. T. eIF2-dependent and eIF2-independent modes of initiation on the CSFV IRES: a common role of domain II. *EMBO J*, 27(7):1060–1072, Apr 2008.

Peter, D., Igreja, C., Weber, R., Wohlbold, L., et al. Molecular architecture of 4E-BP translational inhibitors bound to eIF4E. *Mol Cell*, 57(6): 1074–1087, Mar 2015.

Peterson, R. T., Desai, B. N., Hardwick, J. S., and Schreiber, S. L. Protein phosphatase 2A interacts with the 70-kDa S6 kinase and is activated by inhibition of FKBP12-rapamycinassociated protein. *Proc Natl Acad Sci U S A*, 96(8):4438–42, 1999.

Pham, F. H., Sugden, P. H., and Clerk, A. Regulation of protein kinase B and 4E-BP1 by oxidative stress in cardiac myocytes. *Circ Res*, 86(12): 1252–8, 2000.

Pierce, A., Podlutskaya, N., Halloran, J. J., Hussong, S. A., et al. Overexpression of heat shock factor 1 phenocopies the effect of chronic inhibition of TOR by rapamycin and is sufficient to ameliorate Alzheimer's-like deficits in mice modeling the disease. *J Neurochem*, 124(6):880–893, Mar 2013.

Qin, X., Jiang, B., and Zhang, Y. 4E-BP1, a multifactor regulated multifunctional protein. *Cell Cycle*, 15(6):781–786, 2016.

Qu, Y., Zhao, R., Wang, H., Chang, K., et al. Phosphorylated 4EBP1 is associated with tumor progression and poor prognosis in Xp11.2 translocation renal cell carcinoma. *Sci Rep*, 6:23594, 2016.

Ramadori, G., Konstantinidou, G., Venkateswaran, N., Biscotti, T., et al. Diet-induced unresolved ER stress hinders KRAS-driven lung tumorigenesis. *Cell Metab*, 21(1):117–125, Jan 2015.

Ray, M. E., Yang, Z. Q., Albertson, D., Kleer, C. G., et al. Genomic and expression analysis of the 8p11-12 amplicon in human breast cancer cell lines. *Cancer Res*, 64(1):40–47, Jan 2004.

Ray, P. S., Grover, R., and Das, S. Two internal ribosome entry sites mediate the translation of p53 isoforms. *EMBO Rep*, 7(4):404–410, Apr 2006.

Robb, E. L., Gawel, J. M., Aksentijević, D., Cochemé, H. M., et al. Selective superoxide generation within mitochondria by the targeted redox cycler MitoParaquat. *Free Radic Biol Med*, 89:883–894, Dec 2015.

Robert, F., Kapp, L. D., Khan, S. N., Acker, M. G., et al. Initiation of protein synthesis by hepatitis C virus is refractory to reduced eIF2.GTP.Met-tRNA(i)(Met) ternary complex availability. *Mol Biol Cell*, 17(11):4632–4644, Nov 2006.

Roman, G., Endo, K., Zong, L., and Davis, R. L. P[Switch], a system for spatial and temporal control of gene expression in Drosophila melanogaster. *Proc Natl Acad Sci U S A*, 98(22):12602–12607, Oct 2001.

Rong, L., Livingstone, M., Sukarieh, R., Petroulakis, E., et al. Control of eIF4E cellular localization by eIF4E-binding proteins, 4E-BPs. *RNA*, 14 (7):1318–27, 2008.

Roote, J. and Prokop, A. How to design a genetic mating scheme: a basic training package for Drosophila genetics. *G3 (Bethesda)*, 3(2):353–358, Feb 2013.

Rubin, G. M., Yandell, M. D., Wortman, J. R., Gabor Miklos, G. L., et al. Comparative genomics of the eukaryotes. *Science*, 287(5461):2204–2215, Mar 2000.

Ruoff, R., Katsara, O., and Kolupaeva, V. Cell type-specific control of protein synthesis and proliferation by FGF-dependent signaling to the translation repressor 4E-BP. *Proc Natl Acad Sci U S A*, 113(27):7545–7550, Jul 2016.

Sabatini, D. M., Erdjument-Bromage, H., Lui, M., Tempst, P., and Snyder, S. H. RAFT1: a mammalian protein that binds to FKBP12 in a rapamycin-dependent fashion and is homologous to yeast TORs. *Cell*, 78 (1):35–43, 1994.

Saffran, H. A. and Smiley, J. R. The XIAP IRES activates 3' cistron expression by inducing production of monocistronic mRNA in the betagal/CAT bicistronic reporter system. *RNA*, 15(11):1980–1985, Nov 2009.

Sarbassov, D. D., Ali, S. M., Sengupta, S., Sheen, J.-H., et al. Prolonged rapamycin treatment inhibits mTORC2 assembly and Akt/PKB. *Mol Cell*, 22(2):159–168, Apr 2006.

Schalm, S. S., Fingar, D. C., Sabatini, D. M., and Blenis, J. TOS motif-mediated raptor binding regulates 4E-BP1 multisite phosphorylation and function. *Curr Biol*, 13(10):797–806, 2003.

Schwanhausser, B., Gossen, M., Dittmar, G., and Selbach, M. Global analysis of cellular protein translation by pulsed SILAC. *Proteomics*, 9(1): 205–9, 2009.

Sechi, S. and Chait, B. T. Modification of cysteine residues by alkylation. A tool in peptide mapping and protein identification. *Anal Chem*, 70(24): 5150–5158, Dec 1998.

Shang, Y. C., Chong, Z. Z., Wang, S., and Maiese, K. Prevention of beta-amyloid degeneration of microglia by erythropoietin depends on Wnt1,

the PI 3-K/mTOR pathway, Bad, and Bcl-xL. *Aging (Albany NY)*, 4(3): 187–201, 2012.

Sharma, P. M., Egawa, K., Huang, Y., Martin, J. L., et al. Inhibition of phosphatidylinositol 3-kinase activity by adenovirus-mediated gene transfer and its effect on insulin action. *J Biol Chem*, 273(29):18528–18537, Jul 1998.

Shatsky, I. N., Dmitriev, S. E., Terenin, I. M., and Andreev, D. E. Cap- and IRES-independent scanning mechanism of translation initiation as an alternative to the concept of cellular IRESs. *Mol Cells*, 30(4):285–293, Oct 2010.

Shaw, G., Morse, S., Ararat, M., and Graham, F. L. Preferential transformation of human neuronal cells by human adenoviruses and the origin of HEK 293 cells. *FASEB journal : official publication of the Federation of American Societies for Experimental Biology*, 16(8):869–71, 2002.

She, Q.-B., Halilovic, E., Ye, Q., Zhen, W., et al. 4E-BP1 is a key effector of the oncogenic activation of the AKT and ERK signaling pathways that integrates their function in tumors. *Cancer Cell*, 18(1):39–51, Jul 2010.

Shin, S., Wolgamott, L., Tcherkezian, J., Vallabhapurapu, S., et al. Glycogen synthase kinase-3β positively regulates protein synthesis and cell proliferation through the regulation of translation initiation factor 4E-binding protein 1. *Oncogene*, 33(13):1690–1699, Mar 2014a.

Shin, S., Wolgamott, L., Roux, P. P., and Yoon, S.-O. Casein kinase 1ϵ promotes cell proliferation by regulating mRNA translation. *Cancer Res*, 74(1):201–211, Jan 2014b.

Siculella, L., Tocci, R., Rochira, A., Testini, M., Gnoni, A., and Damiano, F. Lipid accumulation stimulates the cap-independent translation of SREBP-1a mRNA by promoting hnRNP A1 binding to its 5'-UTR in a cellular model of hepatic steatosis. *Biochim Biophys Acta*, 1861(5):471–481, May 2016.

Sirmaci, A., Erbek, S., Price, J., Huang, M., et al. A truncating mutation in SERPINB6 is associated with autosomal-recessive nonsyndromic sensorineural hearing loss. *Am J Hum Genet*, 86(5):797–804, May 2010.

209

Sonenberg, N. and Dever, T. E. Eukaryotic translation initiation factors and regulators. *Curr Opin Struct Biol*, 13(1):56–63, 2003.

Spilman, P., Podlutskaya, N., Hart, M. J., Debnath, J., et al. Inhibition of mTOR by rapamycin abolishes cognitive deficits and reduces amyloid-beta levels in a mouse model of Alzheimer's disease. *PLoS One*, 5(4):e9979, 2010.

Stebbins-Boaz, B., Cao, Q., de Moor, C. H., Mendez, R., and Richter, J. D. Maskin is a CPEB-associated factor that transiently interacts with eIF-4E. *Mol Cell*, 4(6):1017–27, 1999.

Steen, H. and Mann, M. The ABC's (and XYZ's) of peptide sequencing. *Nat Rev Mol Cell Biol*, 5(9):699–711, Sep 2004.

Stein, S., Thomas, E. K., Herzog, B., Westfall, M. D., et al. NDRG1 is necessary for p53-dependent apoptosis. *J Biol Chem*, 279(47):48930–48940, Nov 2004.

Steward, O. mRNA localization in neurons: a multipurpose mechanism? *Neuron*, 18(1):9–12, 1997.

Stoneley, M., Paulin, F. E., Le Quesne, J. P., Chappell, S. A., and Willis, A. E. C-Myc 5' untranslated region contains an internal ribosome entry segment. *Oncogene*, 16(3):423–428, Jan 1998.

Sury, M. D., Chen, J. X., and Selbach, M. The SILAC fly allows for accurate protein quantification in vivo. *Mol Cell Proteomics*, 9(10):2173–83, 2010.

Tain, L. S., Mortiboys, H., Tao, R. N., Ziviani, E., Bandmann, O., and Whitworth, A. J. Rapamycin activation of 4E-BP prevents parkinsonian dopaminergic neuron loss. *Nature neuroscience*, 12(9):1129–35, 2009.

Tang, F.-L., Liu, W., Hu, J.-X., Erion, J. R., et al. VPS35 Deficiency or Mutation Causes Dopaminergic Neuronal Loss by Impairing Mitochondrial Fusion and Function. *Cell Rep*, 12(10):1631–1643, Sep 2015.

Tang, S. J., Reis, G., Kang, H., Gingras, A. C., Sonenberg, N., and Schuman, E. M. A rapamycin-sensitive signaling pathway contributes to long-term synaptic plasticity in the hippocampus. *Proc Natl Acad Sci U S A*, 99(1): 467–72, 2002.

Tanner, C. M., Kamel, F., Ross, G. W., Hoppin, J. A., et al. Rotenone, paraquat, and Parkinson's disease. *Environ Health Perspect*, 119(6): 866–872, Jun 2011.

Taymans, J.-M., Nkiliza, A., and Chartier-Harlin, M.-C. Deregulation of protein translation control, a potential game-changing hypothesis for Parkinson's disease pathogenesis. *Trends Mol Med*, 21(8):466–472, Aug 2015.

Tee, A. R., Fingar, D. C., Manning, B. D., Kwiatkowski, D. J., Cantley, L. C., and Blenis, J. Tuberous sclerosis complex-1 and -2 gene products function together to inhibit mammalian target of rapamycin (mTOR)-mediated downstream signaling. *Proc Natl Acad Sci U S A*, 99(21):13571–13576, Oct 2002.

Tee, A. R., Manning, B. D., Roux, P. P., Cantley, L. C., and Blenis, J. Tuberous sclerosis complex gene products, Tuberin and Hamartin, control mTOR signaling by acting as a GTPase-activating protein complex toward Rheb. *Curr Biol*, 13(15):1259–1268, Aug 2003.

Teleman, A. A., Chen, Y. W., and Cohen, S. M. 4E-BP functions as a metabolic brake used under stress conditions but not during normal growth. *Genes Dev*, 19(16):1844–8, 2005.

Tettweiler, G., Miron, M., Jenkins, M., Sonenberg, N., and Lasko, P. F. Starvation and oxidative stress resistance in Drosophila are mediated through the eIF4E-binding protein, d4E-BP. *Genes Dev*, 19(16):1840–3, 2005.

Thakor, N. and Holcik, M. IRES-mediated translation of cellular messenger RNA operates in eIF2α- independent manner during stress. *Nucleic Acids Res*, 40(2):541–552, Jan 2012.

Thompson, S. R. So you want to know if your message has an IRES? *Wiley Interdiscip Rev RNA*, 3(5):697–705, 2012.

Thoreen, C. C., Kang, S. A., Chang, J. W., Liu, Q., et al. An ATP-competitive mammalian target of rapamycin inhibitor reveals rapamycin-resistant functions of mTORC1. *J Biol Chem*, 284(12):8023–32, 2009.

Thoreen, C. C., Chantranupong, L., Keys, H. R., Wang, T., Gray, N. S., and Sabatini, D. M. A unifying model for mTORC1-mediated regulation of mRNA translation. *Nature*, 485(7396):109–13, 2012.

Tiwari, V. and Patel, A. B. Pyruvate carboxylase and pentose phosphate fluxes are reduced in AβPP-PS1 mouse model of Alzheimer's disease: a ^{13}C NMR study. *J Alzheimers Dis*, 41(2):387–399, 2014.

Tomoo, K., Matsushita, Y., Fujisaki, H., Abiko, F., et al. Structural basis for mRNA Cap-Binding regulation of eukaryotic initiation factor 4E by 4E-binding protein, studied by spectroscopic, X-ray crystal structural, and molecular dynamics simulation methods. *Biochim Biophys Acta*, 1753(2): 191–208, Dec 2005.

Tong, M., Fung, T.-M., Luk, S. T., Ng, K.-Y., et al. ANXA3/JNK Signaling Promotes Self-Renewal and Tumor Growth, and Its Blockade Provides a Therapeutic Target for Hepatocellular Carcinoma. *Stem Cell Reports*, 5 (1):45–59, Jul 2015.

Trancikova, A., Mamais, A., Webber, P. J., Stafa, K., et al. Phosphorylation of 4E-BP1 in the mammalian brain is not altered by LRRK2 expression or pathogenic mutations. *PLoS One*, 7(10):e47784, 2012.

Tsukumo, Y., Alain, T., Fonseca, B. D., Nadon, R., and Sonenberg, N. Translation control during prolonged mTORC1 inhibition mediated by 4E-BP3. *Nat Commun*, 7:11776, 2016.

Ueki, K., Algenstaedt, P., Mauvais-Jarvis, F., and Kahn, C. R. Positive and negative regulation of phosphoinositide 3-kinase-dependent signaling pathways by three different gene products of the p85alpha regulatory subunit. *Mol Cell Biol*, 20(21):8035–8046, Nov 2000.

Uhlen, M., Oksvold, P., Fagerberg, L., Lundberg, E., et al. Towards a knowledge-based Human Protein Atlas. *Nat Biotechnol*, 28(12):1248–1250, Dec 2010.

Ventoso, I., Sanz, M. A., Molina, S., Berlanga, J. J., Carrasco, L., and Esteban, M. Translational resistance of late alphavirus mRNA to eIF2alpha phosphorylation: a strategy to overcome the antiviral effect of protein kinase PKR. *Genes Dev*, 20(1):87–100, Jan 2006.

Vergé, V., Vonlanthen, M., Masson, J.-M., Trachsel, H., and Altmann, M. Localization of a promoter in the putative internal ribosome entry site of the Saccharomyces cerevisiae TIF4631 gene. *RNA*, 10(2):277–286, Feb 2004.

Vidal, R., Miravalle, L., Gao, X., Barbeito, A. G., et al. Expression of a mutant form of the ferritin light chain gene induces neurodegeneration and iron overload in transgenic mice. *J Neurosci*, 28(1):60–67, Jan 2008.

Vilariño-Güell, C., Wider, C., Ross, O. A., Dachsel, J. C., et al. VPS35 mutations in Parkinson disease. *Am J Hum Genet*, 89(1):162–167, Jul 2011.

Vivanco, I. and Sawyers, C. L. The phosphatidylinositol 3-Kinase AKT pathway in human cancer. *Nat Rev Cancer*, 2(7):489–501, 2002.

von Manteuffel, S. R., Gingras, A. C., Ming, X. F., Sonenberg, N., and Thomas, G. 4E-BP1 phosphorylation is mediated by the FRAP-p70s6k pathway and is independent of mitogen-activated protein kinase. *Proc Natl Acad Sci U S A*, 93(9):4076–4080, Apr 1996.

Walters, B. and Thompson, S. R. Cap-Independent Translational Control of Carcinogenesis. *Front Oncol*, 6:128, 2016.

Wang, R., Ganesan, S., and Zheng, X. F. S. Yin and yang of 4E-BP1 in cancer. *Cell Cycle*, 15(11):1401–1402, Jun 2016a.

Wang, W., Wang, X., Fujioka, H., Hoppel, C., et al. Parkinson's disease-associated mutant VPS35 causes mitochondrial dysfunction by recycling DLP1 complexes. *Nat Med*, 22(1):54–63, Jan 2016b.

Wang, X., Li, W., Parra, J.-L., Beugnet, A., and Proud, C. G. The C terminus of initiation factor 4E-binding protein 1 contains multiple regulatory features that influence its function and phosphorylation. *Mol Cell Biol*, 23(5):1546–1557, Mar 2003.

Wang, Z., Weaver, M., and Magnuson, N. S. Cryptic promoter activity in the DNA sequence corresponding to the pim-1 5'-UTR. *Nucleic Acids Res*, 33(7):2248–2258, 2005.

Warnakulasuriyarachchi, D., Cerquozzi, S., Cheung, H. H., and Holcik, M. Translational induction of the inhibitor of apoptosis protein HIAP2 during endoplasmic reticulum stress attenuates cell death and is mediated via an inducible internal ribosome entry site element. *J Biol Chem*, 279(17): 17148–57, 2004.

Weiske, J., Albring, K. F., and Huber, O. The tumor suppressor Fhit acts as a repressor of beta-catenin transcriptional activity. *Proc Natl Acad Sci U S A*, 104(51):20344–20349, Dec 2007.

Wells, S. E., Hillner, P. E., Vale, R. D., and Sachs, A. B. Circularization of mRNA by eukaryotic translation initiation factors. *Mol Cell*, 2(1):135–40, 1998.

Whitworth, A. J. Drosophila models of Parkinson's disease. *Adv Genet*, 73: 1–50, 2011.

Wilhelm, J. E., Hilton, M., Amos, Q., and Henzel, W. J. Cup is an eIF4E binding protein required for both the translational repression of oskar and the recruitment of Barentsz. *J Cell Biol*, 163(6):1197–204, 2003.

Wilson, J. E., Pestova, T. V., Hellen, C. U., and Sarnow, P. Initiation of protein synthesis from the A site of the ribosome. *Cell*, 102(4):511–520, Aug 2000.

Wullschleger, S., Loewith, R., and Hall, M. N. TOR signaling in growth and metabolism. *Cell*, 124(3):471–484, Feb 2006.

Xia, X. and Holcik, M. Strong eukaryotic IRESs have weak secondary structure. *PLoS One*, 4(1):e4136, 2009.

Xu, Y., Liu, C., Chen, S., Ye, Y., et al. Activation of AMPK and inactivation of Akt result in suppression of mTOR-mediated S6K1 and 4E-BP1 pathways leading to neuronal cell death in in vitro models of Parkinson's disease. *Cell Signal*, 26(8):1680–1689, Aug 2014.

Yachie, A., Niida, Y., Wada, T., Igarashi, N., et al. Oxidative stress causes enhanced endothelial cell injury in human heme oxygenase-1 deficiency. *J Clin Invest*, 103(1):129–135, Jan 1999.

Yang, D. Q. and Kastan, M. B. Participation of ATM in insulin signalling through phosphorylation of eIF-4E-binding protein 1. *Nat Cell Biol*, 2 (12):893–898, Dec 2000.

Yang, Y., Hou, H., Haller, E. M., Nicosia, S. V., and Bai, W. Suppression of FOXO1 activity by FHL2 through SIRT1-mediated deacetylation. *EMBO J*, 24(5):1021–1032, Mar 2005.

Yang, Z. and Klionsky, D. J. Mammalian autophagy: core molecular machinery and signaling regulation. *Curr. Opin. Cell Biol.*, 22(2):124–131, 2010.

Zhang, G., Bowling, H., Hom, N., Kirshenbaum, K., et al. In-depth quantitative proteomic analysis of de novo protein synthesis induced by brain-derived neurotrophic factor. *J Proteome Res*, 13(12):5707–5714, Dec 2014.

Zhu, X., Zelmer, A., Kapfhammer, J. P., and Wellmann, S. Cold-inducible RBM3 inhibits PERK phosphorylation through cooperation with NF90 to protect cells from endoplasmic reticulum stress. *FASEB J*, 30(2):624–634, Feb 2016.

Zid, B. M., Rogers, A. N., Katewa, S. D., Vargas, M. A., et al. 4E-BP extends lifespan upon dietary restriction by enhancing mitochondrial activity in Drosophila. *Cell*, 139(1):149–60, 2009.

Zimprich, A., Benet-Pagès, A., Struhal, W., Graf, E., et al. A mutation in VPS35, encoding a subunit of the retromer complex, causes late-onset Parkinson disease. *Am J Hum Genet*, 89(1):168–175, Jul 2011.

Appendix

Abbreviations

4E-BP	Eukaryotic initiation factor 4E binding protein
AD	Alzheimer's disease
ATP	Adenosine tri-phosphate
BSA	Bovine serum albumin
CNS	Central nervous system
CT	Threshold cycle
ddH$_2$O	Double-distilled water
DMEM	Dulbecco's modified eagle medium
DMSO	Dimethyl sulfoxide
DTT	Dithiothreitol
EDTA	Ethylenediaminetetraacetic acid
EGTA	Ethylene glycol-bis(-aminoethyl ether)-N,N,N',N'-tetraacetic acid
FBS	Fetal bovine serum
FDR	False discovery rate
HEK293	Human embryonic kidney 293 cells
HeLa	Henrietta Lacks cells
IAM	Iodoacetamide
LB	Luria-Bertani agar
LC	Liquid chromatography
LTD	Long term depression
MCF7	Michigan cancer foundation-7 cells
mitoPQ	Mitochondrial paraquat
MS	Mass spectrometry
PBS	Phosphate buffered saline
PCR	Polymerase chain reaction
PD	Parkinson's disease
PFA	Paraformaldehyde
PQ	Paraquat
qRT-PCR	Quantitative real-time PCR
RIPA	Radioimmunoprecipitation buffer
RNS	Reactive nitrogen species
ROS	Reactive oxygen species
RPE1	Retinal pigmented epithelial cells
S2R+	Schneider 2 receptor plus cells
SDS	Sodium dodecyl sulfate

SILAC	Stable isotope labelling by amino acids in cell culture
siRNA	Small interfering RNA
TA	Thr to Ala point mutations at position 37 and 46
TBE	Tris-Borate-EDTA buffer
TCEP	Tris(2-carboxyethyl)phosphine
tet	Tetracycline
TOR	Target of rapamycin
Tris	2-Amino-2-hydroxymethyl-propane-1.3-diol
WT	Wildtype

List of up- and downregulated proteins in quantitative mass spectrometry experiments of T-REx HEK293 cells

Table A2: List of upregulated proteins after 24 h 4E-BP1[TA] overexpression in T-REx HEK293 cells. 4E-BP1 was overexpressed in cells grown in heavy medium only. The normalised ratio of proteins from cells grown in light and heavy medium is indicated (H/L).

Gene name	Protein name	H/L ratio
ATP5H	ATP synthase subunit d, mitochondrial	5.9926
PRPSAP2	Phosphoribosyl pyrophosphate synthase-associated protein 2	2.6587
STAG2	Cohesin subunit SA-2	2.1408
PDHA1; PDHA2	Pyruvate dehydrogenase E1 component subunit alpha, mitochondrial	2.0643
NRD1	Nardilysin	2.0085
XPOT	Exportin-T	2.0058
VIM	Vimentin	1.9874
RSL1D1	Ribosomal L1 domain-containing protein 1	1.8538
HADHB	Trifunctional enzyme subunit beta, mitochondrial; 3-ketoacyl-CoA thiolase	1.8534
PSMC2	26S protease regulatory subunit 7	1.7967
EIF3L	Eukaryotic translation initiation factor 3 subunit L	1.7404
HIST1H2BN; HIST1H2BL; HIST1H2BM; HIST1H2BH; HIST2H2BF; HIST1H2BC; HIST1H2BD; H2BFS; HIST1H2BK; HIST3H2BB; HIST2H2BE; HIST1H2BB; HIST1H2BO; HIST1H2BJ	Histone H2B	1.7144
EIF3J	Eukaryotic translation initiation factor 3 subunit J	1.707
SNX2	Sorting nexin-2	1.7013
HIST1H4A	Histone H4	1.6368
SNRPA	U1 small nuclear ribonucleoprotein A	1.6055
EIF4A3	Eukaryotic initiation factor 4A-III	1.6046

Gene name	Protein name	H/L ratio
HIST2H2AC; HIST2H2AA3; HIST1H2AJ; HIST1H2AH; H2AFJ; HIST1H2AD; HIST1H2AG; HIST1H2AC; HIST3H2A; HIST1H2AB	Histone H2A	1.5289

Table A3: List of downregulated proteins after 24 h 4E-BP1[TA] overexpression in T-REx HEK293 cells. 4E-BP1 was overexpressed in cells grown in heavy medium only. The normalised ratio of proteins from cells grown in light and heavy medium is indicated (H/L).

Gene name	Protein name	H/L ratio
CSRP2	Cysteine and glycine-rich protein 2	0.48896
RPS15	40S ribosomal protein S15	0.48287
EIF3G	Eukaryotic translation initiation factor 3 subunit G	0.48225
RALY	RNA-binding protein Raly	0.47026
RBM25	RNA-binding protein 25	0.46798
UBQLN2	Ubiquilin-2	0.4441
DDRGK1	DDRGK domain-containing protein 1	0.43722
ACP1	Low molecular weight phosphotyrosine protein phosphatase	0.433
CDC42	Cell division control protein 42 homolog	0.42301
CDC37	Hsp90 co-chaperone Cdc37	0.41089
RPL36	60S ribosomal protein L36	0.40167
STX18	Syntaxin-18	0.37816
PPP4R2	Serine/threonine-protein phosphatase 4 regulatory subunit 2	0.35671
TJP1	Tight junction protein ZO-1	0.32315
CHORDC1	Cysteine and histidine-rich domain-containing protein 1	0.31918
MAPRE1	Microtubule-associated protein RP/EB family member 1	0.30457
PSMC1	26S protease regulatory subunit 4	0.29094

Table A4: List of upregulated proteins after 12 h 4E-BP1[WT] overexpression in T-REx HEK293 cells. 4E-BP1 was overexpressed in cells grown in heavy medium only. The normalised ratio of proteins from cells grown in light and heavy medium is indicated (H/L).

Gene name	Protein name	H/L ratio
TSPAN3	Tetraspanin-3	4.0659
SYNE1	Nesprin-1	3.4757
NOL7	Nucleolar protein 7	2.3353
NSMCE4A	Non-structural maintenance of chromosomes element 4 homolog A	2.3253
POLDIP2	Polymerase delta-interacting protein 2	2.0669
RBM26	RNA-binding protein 26	2.0439
RPL37A	60S ribosomal protein L37a	1.9525
CASC3	Protein CASC3	1.9364
PRRC1	Protein PRRC1	1.7374

Gene name	Protein name	H/L ratio
GNL2	Nucleolar GTP-binding protein 2	1.7045
CYC1	Cytochrome c1, heme protein, mitochondrial	1.6619
RBM15	Putative RNA-binding protein 15	1.5997
RPP25L	Ribonuclease P protein subunit p25-like protein	1.5806
PIH1D1	PIH1 domain-containing protein 1	1.5679
TMEM258	Transmembrane protein 258	1.5658
GTF2F1	General transcription factor IIF subunit 1	1.5401

Table A5: List of downregulated proteins after 12 h 4E-BP1[WT] overexpression in T-REx HEK293 cells. 4E-BP1 was overexpressed in cells grown in heavy medium only. The normalised ratio of proteins from cells grown in light and heavy medium is indicated (H/L).

Gene name	Protein name	H/L ratio
MTX1	Metaxin-1	0.49123
DDX47	Probable ATP-dependent RNA helicase DDX47	0.49035
DDX6	Probable ATP-dependent RNA helicase DDX6	0.48968
UBE2N	Ubiquitin-conjugating enzyme E2 N	0.48851
FUS	RNA-binding protein FUS	0.48556
WDR36	WD repeat-containing protein 36	0.48203
SNRPG	Small nuclear ribonucleoprotein G; Small nuclear ribonucleoprotein G-like protein	0.48168
DDT; DDTL	D-dopachrome decarboxylase; D-dopachrome decarboxylase-like protein	0.47243
SNRPD1	Small nuclear ribonucleoprotein Sm D1	0.47192
LIN28B	Protein lin-28 homolog B	0.4683
UBE2D3; UBE2D2	Ubiquitin-conjugating enzyme E2 D3; Ubiquitin-conjugating enzyme E2 D2	0.46265
INCENP	Inner centromere protein	0.45768
PHPT1	14 kDa phosphohistidine phosphatase	0.45424
TOMM22	Mitochondrial import receptor subunit TOM22 homolog	0.44749
ZYX	Zyxin	0.43846
LRRFIP1	Leucine-rich repeat flightless-interacting protein 1	0.43212
C11orf58; SMAP	Small acidic protein	0.41472
XRCC1	DNA repair protein XRCC1	0.41442
SRRM1	Serine/arginine repetitive matrix protein 1	0.4083
ZNF428	Zinc finger protein 428	0.40723
RPS15	40S ribosomal protein S15	0.40139
PIN1	Peptidyl-prolyl cis-trans isomerase NIMA-interacting 1	0.39321
GSN	Gelsolin	0.38914
SMN1	Survival motor neuron protein	0.333
BRD2; DKFZp313H139	Bromodomain-containing protein 2	0.32131
ZC3H18	Zinc finger CCCH domain-containing protein 18	0.31641
GBE1	1,4-alpha-glucan-branching enzyme	0.27469

Gene name	Protein name	H/L ratio
HMGA1	High mobility group protein HMG-I/ HMG-Y	0.27271
ARPC2	Actin-related protein 2/3 complex subunit 2	0.19877

Table A6: List of upregulated proteins after 12 h 4E-BP1[TA] overexpression in T-REx HEK293 cells. 4E-BP1 was overexpressed in cells grown in heavy medium only. The normalised ratio of proteins from cells grown in light and heavy medium is indicated (H/L).

Gene name	Protein name	H/L ratio
URGCP	Up-regulator of cell proliferation	148.82
EXOC2	Exocyst complex component 2	16.248
DCAF13	DDB1- and CUL4-associated factor 13	2.515
CDO1	Cysteine dioxygenase type 1	2.2594
NIPBL	Nipped-B-like protein	2.044
IMP4	U3 small nucleolar ribonucleoprotein IMP4	1.8954
IFIT5	Interferon-induced protein with tetratricopeptide repeats 5	1.8599
PFDN1	Prefoldin subunit 1	1.8519
FAM169A	Soluble lamin-associated protein of 75 kDa	1.8325
DHRS7B	Dehydrogenase/reductase SDR family member 7B	1.7495
C1orf131	Uncharacterized protein C1orf131	1.7482
SRP9	Signal recognition particle 9 kDa protein	1.728
RPS19BP1	Active regulator of SIRT1	1.7231
HIBCH	3-hydroxyisobutyryl-CoA hydrolase, mitochondrial	1.7183
FER1L4	Fer-1-like protein 4	1.7183
AP3S1	AP-3 complex subunit sigma-1	1.7099
VPS4B	Vacuolar protein sorting-associated protein 4B	1.6504
PRAMEF8; PRAMEF24	PRAME family member 8; Putative PRAME family member 24	1.6234
CNTROB	Centrobin	1.6212
DHRS4	Dehydrogenase/reductase SDR family member 4	1.6054
SKP2	S-phase kinase-associated protein 2	1.6027
CCDC58	Coiled-coil domain-containing protein 58	1.594
PHKA1	Phosphorylase b kinase regulatory subunit alpha, skeletal muscle isoform	1.5852
HOXA9	Homeobox protein Hox-A9	1.5469
ANXA4	Annexin A4; Annexin	1.5428
FCF1	rRNA-processing protein FCF1 homolog	1.5348
BMS1	Ribosome biogenesis protein BMS1 homolog	1.52
HIST1H2BO; HIST2H2BE; HIST1H2BB	Histone H2B type 1-O; Histone H2B type 2-E; Histone H2B type 1-B	1.5174
NLE1	Notchless protein homolog 1	1.502

Table A7: List of downregulated proteins after 12 h 4E-BP1[TA] overexpression in T-REx HEK293 cells. 4E-BP1 was overexpressed in cells grown in heavy medium only. The normalised ratio of proteins from cells grown in light and heavy medium is indicated (H/L).

Gene name	Protein name	H/L ratio
CCNK	Cyclin-K	0.49985
CAST	Calpastatin	0.49758
CDC20	Cell division cycle protein 20 homolog	0.49541
ATP6AP2	Renin receptor	0.49352
SCAF4	Splicing factor, arginine/serine-rich 15	0.49132
C6orf120	UPF0669 protein C6orf120	0.49072
GNPDA1	Glucosamine-6-phosphate isomerase 1	0.48923
MAP1S	Microtubule-associated protein 1S; MAP1S heavy chain; MAP1S light chain	0.48878
ASB6	Ankyrin repeat and SOCS box protein 6	0.48572
CIZ1	Cip1-interacting zinc finger protein	0.47114
FTL	Ferritin light chain	0.46911
SYNJ2BP	Synaptojanin-2-binding protein	0.46788
SELENBP1	Selenium-binding protein 1	0.46684
HNRNPC	Heterogeneous nuclear ribonucleoproteins C1/C2	0.46191
UBE2A	Ubiquitin-conjugating enzyme E2 A	0.45858
TIMM17A	Mitochondrial import inner membrane translocase subunit Tim17-A	0.4535
TJP2	Tight junction protein ZO-2	0.45176
NXN	Nucleoredoxin	0.44059
TPP1	Tripeptidyl-peptidase 1	0.43254
TPX2; HCA90	Targeting protein for Xklp2	0.43007
UBE2E1	Ubiquitin-conjugating enzyme E2 E1	0.42919
RABL6	Rab-like protein 6	0.4199
GRSF1	G-rich sequence factor 1	0.41951
LRRC41	Leucine-rich repeat-containing protein 41	0.41911
ORMDL1; ORMDL2	ORM1-like protein 1; ORM1-like protein 2	0.4181
PPP1R10	Serine/threonine-protein phosphatase 1 regulatory subunit 10	0.4179
PDLIM5	PDZ and LIM domain protein 5	0.41313
C5orf22	UPF0489 protein C5orf22	0.40939
ASCC2	Activating signal cointegrator 1 complex subunit 2	0.40755
UBE2L3	Ubiquitin-conjugating enzyme E2 L3	0.40645
C7orf50	Uncharacterized protein C7orf50	0.4008
TYMS	Thymidylate synthase	0.37366
SQSTM1	Sequestosome-1	0.36737
MRPL40	39S ribosomal protein L40, mitochondrial	0.35207
C19orf43	Uncharacterized protein C19orf43	0.30961
MFF	Mitochondrial fission factor	0.30682
GMFB	Glia maturation factor beta	0.27602
RPL39P5; RPL39	Putative 60S ribosomal protein L39-like 5; 60S ribosomal protein L39	0.25028
TMEM230	Transmembrane protein 230	0.13523
CBPA6	Carboxypeptidase A6	0.089466

Gene name	Protein name	H/L ratio
RBP4	Retinol-binding protein 4; Plasma retinol-binding protein(1-182); Plasma retinol-binding protein(1-181); Plasma retinol-binding protein(1-179); Plasma retinol-binding protein(1-176)	0.040713

Table A8: List of commonly downregulated proteins after 12 h 4E-BP1[WT] or 4E-BP1[TA] overexpression in T-REx HEK293 cells. 4E-BP1 was overexpressed in cells grown in heavy medium only. The normalised ratio of proteins from cells grown in light and heavy medium is indicated (H/L).

Gene name	Protein name	H/L ratio [WT]	H/L ratio [TA]
ACTBL2	Beta-actin-like protein 2	0.37654	0.37255
HIST1H1D	Histone H1.3	0.32253	0.41456
HIST1H1E	Histone H1.4	0.344	0.38078
HTATSF1	HIV Tat-specific factor 1	0.34154	0.38467
TBX3	T-box transcription factor TBX3	0.48305	0.3545

Table A9: List of upregulated proteins after 6 h 4E-BP1[WT] overexpression in T-REx HEK293 cells. 4E-BP1 was overexpressed in cells grown in heavy medium only. The normalised ratio of proteins from cells grown in light and heavy medium is indicated (H/L) for experiment 1, 2 and 3. Proteins, which could not be identified in one sample were indicated as NA.

Gene name	Protein name	H/L ratio Exp. 1	H/L ratio Exp. 2	H/L ratio Exp. 3
ABCC1	Multidrug resistance-associated protein 1	NA	1.5103	1.5093
ACAA2	3-ketoacyl-CoA thiolase, mitochondrial	1.3025	1.7849	1.8466
ACOX1	Peroxisomal acyl-coenzyme A oxidase 1	0.95252	1.8532	1.7803
AGPAT9	Glycerol-3-phosphate acyl-transferase 3	NA	1.7323	3.2993
AIFM2	Apoptosis-inducing factor 2	NA	1.7829	1.7017
ALAD	Delta-aminolevulinic acid dehydratase	NA	1.7472	2.0589
ALDH4A1	Delta-1-pyrroline-5-carboxylate dehydrogenase, mitochondrial	1.3584	1.6598	1.4706
ANXA1	Annexin A1	0.61787	3.5371	6.0745
ANXA3	Annexin A3; Annexin	0.93051	1.7325	2.8603
AP1G2	AP-1 complex subunit gamma-like 2	0.97087	1.5248	1.576
ARPC1A	Actin-related protein 2/3 complex subunit 1A	1.1692	1.8254	1.7248

Gene name	Protein name	H/L ratio Exp. 1	H/L ratio Exp. 2	H/L ratio Exp. 3
ASRGL1	Isoaspartyl peptidase/L-asparaginase; Isoaspartyl peptidase/L-asparaginase alpha chain; Isoaspartyl peptidase/L-asparaginase beta chain	1.5909	1.9723	1.7891
ATG101	Autophagy-related protein 101	NA	1.7376	1.4412
ATP2B4; ATP2B3	Plasma membrane calcium-transporting ATPase 4; Plasma membrane calcium-transporting ATPase 3	NA	2.3279	1.8172
ATP6V0A2	V-type proton ATPase 116 kDa subunit a isoform 2	0.78251	1.71	1.8715
ATP6V0D1	V-type proton ATPase subunit d 1	NA	1.6708	1.5677
BAZ1B	Tyrosine-protein kinase BAZ1B	0.95487	2.1223	1.4336
BCAT1	Branched-chain-amino-acid aminotransferase, cytosolic	NA	2.0934	1.5882
BLM	Bloom syndrome protein	NA	2.1451	1.4154
BPNT1	3(2),5-bisphosphate nucleotidase 1	1.5396	1.7132	1.3231
BTAF1	TATA-binding protein-associated factor 172	0.91635	2.3798	1.4127
C10orf32	UPF0693 protein C10orf32	NA	1.6609	1.7326
C2CD5	C2 domain-containing protein 5	NA	2.0469	2.5049
C6orf211	UPF0364 protein C6orf211	NA	2.086	1.7192
CAD	CAD protein; Glutamine-dependent carbamoyl-phosphate synthase; Aspartate carbamoyltransferase; Dihydroorotase	1.4771	1.6192	1.2007
CAMK1D	Calcium/calmodulin-dependent protein kinase type 1D	NA	1.4611	1.9545
CAND2	Cullin-associated NEDD8-dissociated protein 2	NA	2.0084	1.5215
CAPN2	Calpain-2 catalytic subunit	1.2387	2.2527	1.6812
CAPZB	F-actin-capping protein subunit beta	1.3258	2.0891	1.4821
CAV1	Caveolin-1; Caveolin	NA	1.7881	2.0539
CBS	Cystathionine beta-synthase	1.2705	2.4455	1.4429
CCNB1	G2/mitotic-specific cyclin-B1	NA	1.4862	1.7042
CD44	CD44 antigen	0.79552	2.1128	2.8222
CD59V	CD59 glycoprotein	0.91797	1.8443	1.8303
CD9	CD9 antigen	NA	1.8522	2.0543

Appendix

Gene name	Protein name	H/L ratio Exp. 1	H/L ratio Exp. 2	H/L ratio Exp. 3
CD97	CD97 antigen; CD97 antigen subunit alpha; CD97 antigen subunit beta	NA	2.1766	1.5397
CDKN2C	Cyclin-dependent kinase 4 inhibitor C	NA	1.4255	1.5119
CHAC2	Cation transport regulator-like protein 2	1.1794	1.7348	1.4109
CLN5	Ceroid-lipofuscinosis neuronal protein 5	NA	1.4352	1.6709
CMAS	N-acylneuraminate cytidylyltransferase	0.97538	1.9579	1.5753
CNBP	Cellular nucleic acid-binding protein	1.0111	1.8571	1.4854
CNN2	Calponin-2	1.1278	1.4741	2.005
CORO1B	Coronin-1B; Coronin	0.96403	1.42	1.7915
CPSF3L	Integrator complex subunit 11	NA	1.986	1.4536
CSRP1	Cysteine and glycine-rich protein 1	NA	2.0151	3.1047
CYB561D2	Cytochrome b561 domain-containing protein 2	0.79264	3.0801	2.7762
CYFIP1	Cytoplasmic FMR1-interacting protein 1	1.1155	2.2833	1.4171
CYHR1	Cysteine and histidine-rich protein 1	NA	1.6485	2.303
CYR61	Protein CYR61	NA	2.7003	3.8274
DERA	Putative deoxyribose-phosphate aldolase	1.1176	1.5902	1.7452
DHRS11	Dehydrogenase/reductase SDR family member 11	0.85067	1.6618	1.591
DHRS7B	Dehydrogenase/reductase SDR family member 7B	NA	1.6233	1.9032
DIAPH3	Protein diaphanous homolog 3	0.81637	2.8798	1.868
DLGAP5	Disks large-associated protein 5	1.0096	2.0041	1.4132
DNM1	Dynamin-1	NA	2.1155	1.5292
DNM1L	Dynamin-1-like protein	0.88488	1.6895	1.5999
DNMT1	DNA (cytosine-5)-methyltransferase 1	0.70252	3.1239	1.6958
DOCK7	Dedicator of cytokinesis protein 7	1.0348	2.071	1.5259
DUSP3	Dual specificity protein phosphatase 3	1.0947	1.6465	1.8509
EHHADH	Peroxisomal bifunctional enzyme; Enoyl-CoA hydratase/3,2-trans-enoyl-CoA isomerase; 3-hydroxyacyl-CoA dehydrogenase	NA	1.6422	2.3835
ELOVL5	Elongation of very long chain fatty acids protein 5	NA	1.5083	2.1717

Appendix

Gene name	Protein name	H/L ratio Exp. 1	H/L ratio Exp. 2	H/L ratio Exp. 3
EMC8	ER membrane protein complex subunit 8	0.88801	1.527	1.6709
ERBB2IP	Protein LAP2	NA	1.8604	1.5626
ETNK1	Ethanolamine kinase 1	NA	1.7944	4.3709
EXOC5	Exocyst complex component 5	0.82955	1.9489	1.5139
EZH2	Histone-lysine N-methyltransferase EZH2	0.8118	2.2329	1.8593
FAM118B	Protein FAM118B	NA	1.7472	2.0257
FAM91A1	Protein FAM91A1	0.89682	1.6413	1.4227
FAR1	Fatty acyl-CoA reductase 1	NA	1.8204	1.4851
FHL3	Four and a half LIM domains protein 3	NA	1.4054	1.6022
FIBP	Acidic fibroblast growth factor intracellular-binding protein	NA	1.5696	1.7395
GALNT7	N-acetylgalactosaminyl-transferase 7	NA	2.0875	1.4192
GBF1	Golgi-specific brefeldin A-resistance guanine nucleotide exchange factor 1	0.98757	1.5764	1.7431
GIT2	ARF GTPase-activating protein GIT2	NA	1.6405	1.6185
GMDS	GDP-mannose 4,6 dehydratase	1.1204	3.1615	2.7541
GNAI3	Guanine nucleotide-binding protein G(k) subunit alpha	1.0892	1.8317	1.4657
GNL3L	Guanine nucleotide-binding protein-like 3-like protein	0.81983	2.5095	1.4298
GNPAT	Dihydroxyacetone phosphate acyltransferase	NA	2.0192	1.747
GPR180	Integral membrane protein GPR180	1.2155	1.5758	2.0287
GPX8	Probable glutathione peroxidase 8; Glutathione peroxidase	0.79661	2.0856	2.1098
HEATR3	HEAT repeat-containing protein 3	0.91338	1.7932	1.4898
HERC5	E3 ISG15–protein ligase HERC5	NA	1.7375	1.4026
HIP1R	Huntingtin-interacting protein 1-related protein	NA	1.5497	1.5449
HMGCL	Hydroxymethylglutaryl-CoA lyase, mitochondrial	NA	1.4906	1.5236
HOXA5	Homeobox protein Hox-A5	0.90477	1.4211	1.63
HSD17B11	Estradiol 17-beta-dehydrogenase 11	NA	1.5464	1.5433
HSPA13	Heat shock 70 kDa protein 13	NA	1.5613	1.9798
ICMT	Protein-S-isoprenylcysteine O-methyltransferase	NA	3.4241	3.1

Gene name	Protein name	H/L ratio Exp. 1	H/L ratio Exp. 2	H/L ratio Exp. 3
IGF2R	Cation-independent mannose-6-phosphate receptor	0.9935	1.544	1.5214
INF2	Inverted formin-2	1.878	1.8511	0.92536
IPO8	Importin-8	0.7919	1.5062	1.5444
IRGQ	Immunity-related GTPase family Q protein	0.75557	1.4571	1.5722
KIF13B	Kinesin-like protein KIF13B	1.1036	1.4503	1.5822
KIF20A	Kinesin-like protein KIF20A	0.97146	4.1214	1.4853
KIF2C	Kinesin-like protein KIF2C	1.4599	1.5445	1.1599
KIF4A	Chromosome-associated kinesin KIF4A	0.97732	2.939	1.6832
LCLAT1	Lysocardiolipin acyltransferase 1	1.3099	1.4438	1.5204
LCP1	Plastin-2	0.98125	1.647	1.5779
LPP	Lipoma-preferred partner	0.98275	1.6245	1.508
LTN1	E3 ubiquitin-protein ligase listerin	0.79528	3.5362	1.7719
MAEA	Macrophage erythroblast attacher	NA	1.7264	1.4491
MAP3K7; DK-FZp586F0420	Mitogen-activated protein kinase kinase kinase 7	NA	1.7343	1.5635
MB21D2	Protein MB21D2	NA	2.1594	1.4387
MBNL1; MBLL; MBNL2	Muscleblind-like protein 1; Muscleblind-like protein 2	1.1186	1.6451	1.4324
METTL2B	Methyltransferase-like protein 2B	1.6419	1.5252	0.7991
MIOS	WD repeat-containing protein mio	NA	1.4199	1.6269
MMS19	MMS19 nucleotide excision repair protein homolog	0.85814	2.1556	1.5532
MTRR	Methionine synthase reductase	0.82741	4.7372	1.6222
MYD88	Myeloid differentiation primary response protein MyD88	NA	1.4564	1.5548
MYO1C	Unconventional myosin-Ic	1.2105	1.5943	1.5587
NAPRT	Nicotinate phosphoribosyltransferase	NA	1.5159	1.5067
NCAPD3	Condensin-2 complex subunit D3	NA	2.3938	1.6958
NEK3	Serine/threonine-protein kinase Nek3	NA	1.644	1.7593
NEK7	Serine/threonine-protein kinase Nek7	NA	1.7093	1.4865
NEU1	Sialidase-1	NA	2.0305	1.7482
NIPBL	Nipped-B-like protein	0.92438	1.811	1.439
NPC2	Epididymal secretory protein E1	0.84011	1.4717	1.5646
NUMB	Protein numb homolog	NA	1.9546	1.5337
NXF1	Nuclear RNA export factor 1	1.2819	1.6781	1.4621

Appendix

Gene name	Protein name	H/L ratio Exp. 1	H/L ratio Exp. 2	H/L ratio Exp. 3
OCIAD2	OCIA domain-containing protein 2	0.90343	1.7161	2.2668
OCRL	Inositol polyphosphate 5-phosphatase OCRL-1	1.06	2.0222	1.4015
PALLD	Palladin	0.9023	1.5477	1.6531
PAPSS2	Bifunctional 3-phosphoadenosine 5-phosphosulfate synthase 2; Sulfate adenylyltransferase; Adenylyl-sulfate kinase	1.0451	1.5027	1.5436
PARN	Poly(A)-specific ribonuclease PARN	0.82001	1.5362	1.5989
PC	Pyruvate carboxylase, mitochondrial	NA	1.4263	1.7517
PCM1	Pericentriolar material 1 protein	0.78286	3.2816	1.4745
PI4KB	Phosphatidylinositol 4-kinase beta	1.0902	1.5344	2.0258
PIR	Pirin	NA	2.0022	2.7118
PKP2	Plakophilin-2	1.0515	1.7649	1.4684
PLEKHF1	Pleckstrin homology domain-containing family F member 1	NA	1.6528	1.4774
PLOD2	Procollagen-lysine,2-oxoglutarate 5-dioxygenase 2	0.83057	2.2478	1.5613
PLS1	Plastin-1	NA	1.7927	1.5307
POP5	Ribonuclease P/MRP protein subunit POP5	NA	1.8897	1.4755
PPIC	Peptidyl-prolyl cis-trans isomerase C	NA	1.7076	1.988
PPIL4	Peptidyl-prolyl cis-trans isomerase-like 4	NA	1.9034	1.4984
PRKAR1A	cAMP-dependent protein kinase type I-alpha regulatory subunit; cAMP-dependent protein kinase type I-alpha regulatory subunit, N-terminally processed	NA	1.4621	1.7873
PSMG3	Proteasome assembly chaperone 3	0.98396	1.689	1.5447
PYCR2	Pyrroline-5-carboxylate reductase 2	0.88764	1.5707	1.4138
RAB21	Ras-related protein Rab-21	1.0046	1.5359	1.7361
RAB32	Ras-related protein Rab-32	0.96918	1.431	2.151
RAP1GDS1	Rap1 GTPase-GDP dissociation stimulator 1	1.1577	1.7004	1.4552
RB1	Retinoblastoma-associated protein	NA	1.5893	1.4671
RDH11	Retinol dehydrogenase 11	0.89609	1.6542	1.4243
RFXAP	Regulatory factor X-associated protein	NA	1.5218	1.5009

Gene name	Protein name	H/L ratio Exp. 1	H/L ratio Exp. 2	H/L ratio Exp. 3
RIC8A	Synembryn-A	0.95354	1.5207	1.5708
RIPK2	Receptor-interacting serine/threonine-protein kinase 2	NA	2.3408	1.5988
RMND5A	Protein RMD5 homolog A	NA	2.0098	1.5918
ROCK2	Rho-associated protein kinase 2	NA	1.5116	1.6235
RPP14	Ribonuclease P protein subunit p14	0.91354	1.6213	1.5369
RPS15A	40S ribosomal protein S15a	0.88825	1.5316	1.5141
S100A11	Protein S100-A11; Protein S100-A11, N-terminally processed	NA	1.6428	1.6527
SAMHD1	Deoxynucleoside triphosphate triphosphohydrolase SAMHD1	1.0493	3.0473	1.4258
SCML2	Sex comb on midleg-like protein 2	0.82812	1.8565	1.4458
SCRN1	Secernin-1	0.82247	1.7339	1.5212
SDSL	Serine dehydratase-like	NA	1.6486	1.8136
SELENBP1	Selenium-binding protein 1	1.929	1.3532	1.5219
SERPINB6	Serpin B6	1.0489	1.4083	2.2803
SF1	Splicing factor 1	0.80507	1.4995	1.6425
SLC27A4	Long-chain fatty acid transport protein 4	NA	2.6607	2.1311
SLC2A1	Solute carrier family 2, facilitated glucose transporter member 1	NA	3.7747	3.0796
SMYD5	SET and MYND domain-containing protein 5	1.8111	0.87661	1.4129
SPINT2	Kunitz-type protease inhibitor 2	NA	2.6141	2.1305
SRR	Serine racemase	NA	1.6833	1.6263
STXBP1	Syntaxin-binding protein 1	1.0706	1.5583	1.6453
STXBP2; ZNF14	Syntaxin-binding protein 2	NA	1.4955	1.7388
SURF2	Surfeit locus protein 2	NA	1.9904	1.5417
SYF2	Pre-mRNA-splicing factor SYF2	NA	1.9399	1.6284
TATDN1	Putative deoxyribonuclease TATDN1	NA	1.8799	1.4667
TBC1D15	TBC1 domain family member 15	1.2997	2.0531	1.5804
TBCE	Tubulin-specific chaperone E	1.4851	1.694	1.2843
TES	Testin	0.98055	1.5618	1.7778
THOC2	THO complex subunit 2	0.95756	2.5251	1.8001
THYN1	Thymocyte nuclear protein 1	0.94536	1.6438	1.4186
TIGAR	Fructose-2,6-bisphosphatase TIGAR	0.77143	1.8561	1.5925
TIMP3	Metalloproteinase inhibitor 3	NA	1.4252	1.5431

Gene name	Protein name	H/L ratio Exp. 1	H/L ratio Exp. 2	H/L ratio Exp. 3
TK1	Thymidine kinase, cytosolic; Thymidine kinase	0.75825	1.9103	1.4705
TMEM147	Transmembrane protein 147	NA	2.1157	1.7823
TMEM160	Transmembrane protein 160	NA	1.5447	1.5563
TMEM173	Stimulator of interferon genes protein	NA	1.469	1.9245
TPMT	Thiopurine S-methyltransferase	1.0857	1.4552	1.5145
TPP2	Tripeptidyl-peptidase 2	0.88678	1.8683	1.4469
TRAPPC11	Trafficking protein particle complex subunit 11	NA	2.2302	1.8277
TTC4	Tetratricopeptide repeat protein 4	1.0852	2.1437	1.4228
TTC5	Tetratricopeptide repeat protein 5	NA	1.4476	1.5221
TUBB2A	Tubulin beta-2A chain	NA	2.3806	2.5448
UBE2G1	Ubiquitin-conjugating enzyme E2 G1; Ubiquitin-conjugating enzyme E2 G1, N-terminally processed	NA	1.4272	1.5889
UPP1	Uridine phosphorylase 1	NA	1.4949	1.7578
USP19	Ubiquitin carboxyl-terminal hydrolase	1.0375	1.5558	1.4466
USP48	Ubiquitin carboxyl-terminal hydrolase 48	1.5845	1.5738	1.2553
VEZF1	Vascular endothelial zinc finger 1	NA	1.5916	1.4533
VPS18	Vacuolar protein sorting-associated protein 18 homolog	0.96489	2.5202	1.6713
WDR26	WD repeat-containing protein 26	1.5737	1.7789	1.388
WDR46	WD repeat-containing protein 46	1.178	1.9301	1.5477
YIPF5	Protein YIPF5	1.4215	1.4821	2.1757
ZCCHC11	Terminal uridylyltransferase 4	1.4561	2.509	NA
ZNF512	Zinc finger protein 512	1.4012	1.6212	1.0193
ZNF787	Zinc finger protein 787	1.2536	1.5613	1.4619

Table A10: List of downregulated proteins after 6 h 4E-BP1[WT] overexpression in T-REx HEK293 cells. 4E-BP1 was overexpressed in cells grown in heavy medium only. The normalised ratio of proteins from cells grown in light and heavy medium is indicated (H/L) for experiment 1, 2 and 3. Proteins, which could not be identified in one sample were indicated as NA.

Gene name	Protein name	H/L ratio Exp. 1	H/L ratio Exp. 2	H/L ratio Exp. 3
ALKBH2	Alpha-ketoglutarate-dependent dioxygenase alkB homolog 2	NA	0.43872	0.50958

Gene name	Protein name	H/L ratio Exp. 1	H/L ratio Exp. 2	H/L ratio Exp. 3
ARHGAP8; LOC553158; PRR5-ARHGAP8	Rho GTPase-activating protein 8	NA	0.45622	0.58167
ASS1	Argininosuccinate synthase	1.2149	0.42701	0.49546
ATP5B		NA	0.50045	0.49561
B3GAT3	Galactosylgalactosylxylosylprotein 3-beta-glucuronosyltransferase 3	0.58019	0.89641	0.48342
BRI3BP	BRI3-binding protein	0.46507	0.5355	0.69375
CECR5	Cat eye syndrome critical region protein 5	1.1021	0.52729	0.4996
CHMP4C	Charged multivesicular body protein 4c	NA	0.36666	0.56507
CHTF8	Chromosome transmission fidelity protein 8 homolog isoform 2	NA	0.38629	0.53921
DERL2	Derlin-2	NA	0.37492	0.39809
EPPK1	Epiplakin	0.76118	0.49405	0.50138
GOLGA5	Golgin subfamily A member 5	0.59874	0.49495	1.0987
HBB	Hemoglobin subunit beta;LVV-hemorphin-7;Spinorphin	0.51553	NA	0.23831
HCFC1	Host cell factor 1;HCF N-terminal chain 1;HCF N-terminal chain 2;HCF N-terminal chain 3;HCF N-terminal chain 4;HCF N-terminal chain 5;HCF N-terminal chain 6;HCF C-terminal chain 1;HCF C-terminal chain 2;HCF C-terminal chain 3;HCF C-terminal chain 4;HCF C-terminal chain 5;HCF C-terminal chain 6	0.98559	0.18465	0.36122
HEBP2	Heme-binding protein 2	1.1146	0.4414	0.57098
HMGCS1	Hydroxymethylglutaryl-CoA synthase, cytoplasmic	1.1082	0.57076	0.46721
KHDRBS3	KH domain-containing, RNA-binding, signal transduction-associated protein 3	NA	0.33256	0.56568
LSM14B	Protein LSM14 homolog B	NA	0.36815	0.45728
NDUFA3	NADH dehydrogenase [ubiquinone] 1 alpha subcomplex subunit 3	NA	0.57971	0.49807

Gene name	Protein name	H/L ratio Exp. 1	H/L ratio Exp. 2	H/L ratio Exp. 3
NDUFB1	NADH dehydrogenase [ubiquinone] 1 beta subcomplex subunit 1	NA	0.42611	0.49564
NIT2	Omega-amidase NIT2	1.1156	0.4764	0.54861
OGFR	Opioid growth factor receptor	0.9068	0.38176	0.31023
PHACTR2	Phosphatase and actin regulator;Phosphatase and actin regulator 2	NA	0.439	0.59754
PM20D2	Peptidase M20 domain-containing protein 2	NA	0.46575	0.534
RAB22A; RAB31	Ras-related protein Rab-22A	1.0449	0.49661	0.47478
RAD23A	UV excision repair protein RAD23 homolog A	NA	0.49855	0.52231
RLTPR	Leucine-rich repeat-containing protein 16C	NA	0.28723	0.57335
SLMO2	Protein slowmo homolog 2	NA	0.46084	0.30464
SPCS1	Signal peptidase complex subunit 1	NA	0.47645	0.49512
STX16; STX16-NPEPL1	Syntaxin-16	NA	0.45933	0.52304
TPD52L2	tumour protein D54	0.96506	0.48996	0.49945
TYMS	Thymidylate synthase	0.57558	0.458	0.60965
YTHDF1	YTH domain-containing family protein 1	NA	0.29826	0.5573

Table A11: List of upregulated proteins after 6 h 4E-BP1[TA] overexpression in T-REx HEK293 cells. 4E-BP1 was overexpressed in cells grown in heavy medium only. The normalised ratio of proteins from cells grown in light and heavy medium is indicated (H/L) for experiment 1, 2 and 3. Proteins, which could not be identified in one sample were indicated as NA.

Gene name	Protein name	H/L ratio Exp. 1	H/L ratio Exp. 2	H/L ratio Exp. 3
ADAMTS1	A disintegrin and metalloproteinase with thrombospondin motifs 1	2.5986	1.1301	2.332
ATAD3B	ATPase family AAA domain-containing protein 3B	NA	1.5863	1.5269
CHN1	N-chimaerin	NA	2.121	1.7942
CWC22	Pre-mRNA-splicing factor CWC22 homolog	1.012	1.5296	1.5088
CYB5R1	NADH-cytochrome b5 reductase 1	NA	1.5203	1.5321
DUSP11	RNA/RNP complex-1-interacting phosphatase	NA	1.511	1.8733
EIF4A3	Eukaryotic initiation factor 4A-III;Eukaryotic initiation factor 4A-III, N-terminally processed	1.0453	1.5183	1.4074

Appendix

Gene name	Protein name	H/L ratio Exp. 1	H/L ratio Exp. 2	H/L ratio Exp. 3
EPCAM	Epithelial cell adhesion molecule	NA	1.4206	1.735
FAM105A	Inactive ubiquitin thioesterase FAM105A	NA	1.7968	2.068
FBXO28	F-box only protein 28	NA	1.5142	1.5478
FKBP11	Peptidyl-prolyl cis-trans isomerase; Peptidyl-prolyl cis-trans isomerase FKBP11	1.1562	1.7946	1.8905
GLS	Glutaminase kidney isoform, mitochondrial	NA	1.4813	1.593
GPATCH4	G patch domain-containing protein 4	NA	1.5623	1.6423
GPN1	GPN-loop GTPase 1	0.8425	1.8083	2.7733
HADHB	Trifunctional enzyme subunit beta, mitochondrial; 3-ketoacyl-CoA thiolase	0.98439	1.5769	1.4952
HS2ST1	Heparan sulfate 2-O-sulfotransferase 1	1.3681	1.6222	1.4717
IMP4	U3 small nucleolar ribonucleoprotein IMP4	0.67085	1.4193	1.5261
IRF3	Interferon regulatory factor 3	2.1237	1.5315	0.77176
LMNA	Prelamin-A/C; Lamin-A/C	0.91339	1.9547	1.8141
LMNB1	Lamin-B1	0.78388	1.6933	1.6802
MIER1	Mesoderm induction early response protein 1	NA	1.6	1.9067
Nbla03646; DHCR24	Delta(24)-sterol reductase	2.0822	1.326	1.5533
NCL	Nucleolin	0.88379	1.5099	1.4726
P4HA2	Prolyl 4-hydroxylase subunit alpha-2	1.0756	1.5447	1.4221
PCYOX1	Prenylcysteine oxidase 1	1.0136	1.5558	1.5929
PPT1	Palmitoyl-protein thioesterase 1	1.0401	1.4463	1.5175
PRCC	Proline-rich protein PRCC	NA	1.6464	1.5184
PRKACB	cAMP-dependent protein kinase catalytic subunit beta	NA	1.5115	1.4603
PTBP2	Polypyrimidine tract-binding protein 2	1.0531	1.9207	1.7393
PXMP2	Peroxisomal membrane protein 2	NA	1.5935	1.5339
RAB13	Ras-related protein Rab-13	0.84585	1.4379	1.5431
RBM3	RNA-binding protein 3	1.6563	1.1518	1.463
RBMXL1	RNA binding motif protein, X-linked-like-1	NA	1.5197	2.6168
SDAD1	Protein SDA1 homolog	1.8799	0.9318	1.4486
SLC25A24	Calcium-binding mitochondrial carrier protein SCaMC-1	1.2729	1.5415	1.5029

Gene name	Protein name	H/L ratio Exp. 1	H/L ratio Exp. 2	H/L ratio Exp. 3
SLC39A14	Zinc transporter ZIP14	1.819	0.9922	1.4518
SULT1A4; SULT1A3	Sulfotransferase 1A4; Sulfotransferase 1A3	NA	1.961	1.9083
SUV39H1	Histone-lysine N-methyltransferase SUV39H1	NA	1.4393	1.816
TFB2M	Dimethyladenosine transferase 2, mitochondrial	NA	1.8923	2.2303
TIA1	Nucleolysin TIA-1 isoform p40	NA	1.6019	1.5839
TOMM40L	Mitochondrial import receptor subunit TOM40B	NA	1.4891	1.5969
UBE2Q1	Ubiquitin-conjugating enzyme E2 Q1	NA	1.5006	1.5371

Table A12: List of downregulated proteins after 6 h 4E-BP1[TA] overexpression in T-REx HEK293 cells. 4E-BP1 was overexpressed in cells grown in heavy medium only. The normalised ratio of proteins from cells grown in light and heavy medium is indicated (H/L) for experiment 1, 2 and 3. Proteins, which could not be identified in one sample were indicated as NA.

Gene name	Protein name	H/L ratio Exp. 1	H/L ratio Exp. 2	H/L ratio Exp. 3
ARG1	Arginase-1	NA	0.25487	0.075274
ATAT1	Alpha-tubulin N-acetyltransferase 1	0.47431	0.63471	0.51999
AURKA	Aurora kinase A	0.47206	0.66902	0.54932
AZGP1	Zinc-alpha-2-glycoprotein	NA	0.1318	0.28154
CASP14	Caspase-14; Caspase-14 subunit p19; Caspase-14 subunit p10	NA	0.43032	0.2091
CDSN	Corneodesmosin	NA	0.032877	0.076716
CRMP1	Dihydropyrimidinase-related protein 1	NA	0.50106	0.33313
DDX58	Probable ATP-dependent RNA helicase DDX58	NA	0.39245	0.41175
FAM92A1	Protein FAM92A1	NA	0.54433	0.47074
FBXW4	F-box/WD repeat-containing protein 4	NA	0.52396	0.40153
FHIT	Bis(5-adenosyl)-triphosphatase	0.23621	0.51389	0.69821
GK; GK3P	Glycerol kinase; Putative glycerol kinase 3	0.70359	0.34479	0.45161
GSTP1	Glutathione S-transferase P	NA	0.40904	0.32854
IFIT2	Interferon-induced protein with tetratricopeptide repeats 2	NA	0.28103	0.23381
IFIT3	Interferon-induced protein with tetratricopeptide repeats 3	NA	0.4291	0.30968

Gene name	Protein name	H/L ratio Exp. 1	H/L ratio Exp. 2	H/L ratio Exp. 3
ISG15	Ubiquitin-like protein ISG15	0.39962	0.38758	0.24383
ISG20	Interferon-stimulated gene 20 kDa protein	NA	0.38725	0.30242
LACRT; AXIN2	Extracellular glycoprotein lacritin	NA	0.14753	0.25776
MCC	Colorectal mutant cancer protein	0.48154	0.37478	0.44422
MICALL1	MICAL-like protein 1	0.75911	0.53018	0.46611
NACC1	Nucleus accumbens-associated protein 1	NA	0.46007	0.56458
NDRG1	Protein NDRG1	0.72285	0.39969	0.36663
OASL	2-5-oligoadenylate synthase-like protein	NA	0.15053	0.2045
PEX7	Peroxisomal targeting signal 2 receptor	NA	0.48099	0.43611
PIGR	Polymeric immunoglobulin receptor; Secretory component	NA	0.15698	0.082005
PPP1R14B	Protein phosphatase 1 regulatory subunit 14B	NA	0.48357	0.54905
PTER	Phosphotriesterase-related protein	0.49459	0.77659	0.58205
PTGR2	Prostaglandin reductase 2	NA	0.4782	0.50655
RAB11FIP1	Rab11 family-interacting protein 1	0.79253	0.45402	0.40143
SMG8	Protein SMG8	0.85354	0.44128	0.57666
TAP1	Antigen peptide transporter 1	0.42108	0.43165	0.58001
TMOD2	Tropomodulin-2	NA	0.48205	0.55209
ZNF8	Zinc finger protein 8	NA	0.50412	0.49553

Table A13: List of upregulated proteins after 6 h 4E-BP1[WT] or 4E-BP1[TA] overexpression in T-REx HEK293 cells. 4E-BP1 was overexpressed in cells grown in heavy medium only. The normalised ratio of proteins from cells grown in light and heavy medium is indicated (H/L) for experiment 1, 2 and 3. Proteins, which could not be identified in one sample were indicated as NA.

Gene name	Protein name	H/L ratio WT Exp. 1	H/L ratio WT Exp. 2	H/L ratio WT Exp. 3	H/L ratio TA Exp. 1	H/L ratio TA Exp. 2	H/L ratio TA Exp. 3
FHL2	Four and a half LIM domains protein 2	1.1285	1.8936	2.092	1.6281	1.5583	1.602
FTL	Ferritin light chain	1.0288	1.5188	1.7724	1.771	2.0113	1.5501
GSTM3	Glutathione S-transferase Mu 3	1.8455	2.0885	1.4589	1.1542	1.5618	1.5256

Gene name	Protein name	H/L ratio WT Exp. 1	H/L ratio WT Exp. 2	H/L ratio WT Exp. 3	H/L ratio TA Exp. 1	H/L ratio TA Exp. 2	H/L ratio TA Exp. 3
HMOX1	Heme oxygenase 1	NA	1.6315	1.512	NA	1.805	2.1563
LMAN2L	VIP36-like protein	NA	1.4487	1.6838	1.6221	1.4654	1.4761
LRRC58	Leucine-rich repeat-containing protein 58	NA	1.5981	1.5261	NA	1.9937	1.6925
MBOAT7	Lysophospholipid acyltransferase 7	1.0957	1.899	2.2091	0.75278	1.4872	1.6059
MYOM1	Myomesin-1	2.7286	9.7667	27.125	14.574	8.4772	24.981
TMX2	Thioredoxin-related transmembrane protein 2	NA	2.0748	1.523	1.8272	1.4341	1.7454

Table A14: List of downregulated proteins after 6 h 4E-BP1[WT] or 4E-BP1[TA] overexpression in T-REx HEK293 cells. 4E-BP1 was overexpressed in cells grown in heavy medium only. The normalised ratio of proteins from cells grown in light and heavy medium is indicated (H/L) for experiment 1, 2 and 3. Proteins, which could not be identified in one sample were indicated as NA.

Gene name	Protein name	H/L ratio WT Exp. 1	H/L ratio WT Exp. 2	H/L ratio WT Exp. 3	H/L ratio TA Exp. 1	H/L ratio TA Exp. 2	H/L ratio TA Exp. 3
APOB	Apolipoprotein B-100; Apolipoprotein B-48	NA	0.27379	0.14677	NA	0.17712	0.10096
CA2	Carbonic anhydrase 2	0.50726	0.28652	0.34512	0.33988	0.41045	0.37204
CCBL1	Kynurenine–oxoglutarate transaminase 1	NA	0.36671	0.52375	NA	0.40665	0.48698
CISD1	CDGSH iron-sulfur domain-containing protein 1	0.74016	0.33036	0.2342	0.45389	NA	0.53852
COL6A1	Collagen alpha-1(VI) chain	NA	0.18843	0.56467	NA	0.21911	0.22322

Appendix

Gene name	Protein name	H/L ratio WT Exp. 1	H/L ratio WT Exp. 2	H/L ratio WT Exp. 3	H/L ratio TA Exp. 1	H/L ratio TA Exp. 2	H/L ratio TA Exp. 3
DCD	Dermcidin; Survival-promoting peptide; DCD-1	0.24106	0.073132	0.12668	0.25841	0.091491	0.17268
DMD	Dystrophin	NA	0.022287	0.0096571	0.066006	0.0095516	0.01402
DSC1	Desmocollin-1	NA	0.07652	0.13871	NA	0.13737	0.13693
DSG1	Desmoglein-1	NA	0.19382	0.49489	NA	0.38912	0.28892
FSCN1	Fascin	0.75674	0.38455	0.32782	0.32138	0.55407	0.46173
IGHA1	Ig alpha-1 chain C region	NA	0.33539	0.066305	NA	0.069237	0.23548
IRS4	Insulin receptor substrate 4	0.88091	0.42679	0.39897	0.39538	0.47136	0.4903
KRT2	Keratin, type II cytoskeletal 2 epidermal	NA	0.41306	0.41032	NA	0.30902	0.56577
LYZ	Lysozyme C	NA	0.11212	0.16491	NA	0.055534	0.15144
MACROD1	O-acetyl-ADP-ribose deacetylase MACROD1	1.8496	0.31135	0.35709	0.41872	NA	0.50808
PRKG1	cGMP-dependent protein kinase 1	NA	0.57879	0.47964	0.50174	0.4014	0.60787
S100A8	Protein S100-A8; Protein S100-A8, N-terminally processed	0.29682	0.11077	0.319	0.2494	0.1407	0.25221
S100A9	Protein S100-A9	NA	0.071064	0.12496	NA	0.14803	0.076486
SALL3; SALL1	Sal-like protein 3; Sal-like protein 1	NA	0.03482	0.075351	NA	0.078804	0.059321

List of up- and downregulated proteins in quantitative mass spectrometry experiments of *Drosophila*

Table A15: List of upregulated proteins after FLAG-d4E-BP[WT] overexpression in *Drosophila*. FLAG-d4E-BP[WT] was overexpressed in flies raised on light food only. The inverted normalised ratio of proteins from flies raised on light and heavy food is indicated (H/L) for experiment 1 and 2. Major protein IDs, which could not be matched with *Drosophila melanogaster* genes were analysed with BLAST and the result listed in the gene name column along with % sequence identity in brackets. If no result was detectable, the protein IDs were listed instead of a gene name.

Gene name/ Protein IDs	Protein name	H/L ratio WT Exp. 1	H/L ratio WT Exp. 2
Est-6		90.22829381	77.43532766
l(3)03670		45.2447659	18.86542897
K8WM60; K8WMC4; K8WKY2		34.21025612	14.98688866
GstE5		32.18434047	24.14117514
Obp99c		28.11357466	17.52049949
B4R0Y1; B4HZK0; B4PL58; B3P805		16.93594988	1.426859221
Blast: CG40485 (80.6)		13.67876428	6.698820062
RpLP2	60S acidic ribosomal protein P2	11.02693549	7.297670436
Blast: Est-6 (95.6)		9.287639661	8.276088083
GIP	Copia protein; Copia VLP protein; Copia protease	7.346458811	7.399188228
CG32795; EG:BACN33B1.2	Transmembrane protein 120 homolog	6.846501631	2.753077075
CG5999		6.725399646	10.2070991
A0A098ATW5		5.840099706	5.834985214
Blast: CG42486 (97.3)		4.562042858	4.849661323
Q4EB93; M9WVJ5; C0R2L5; C0FAB6; A0A098ASB7		4.489740308	4.035185509
nct	Nicastrin	3.912362366	3.244013897
Tim14	Mitochondrial import inner membrane translocase subunit TIM14	3.894991014	1.874238435
Q4EAW9; M9X0D5; C0R2Y1; A0A098ASE0		3.789745585	3.79809239
A0A098ATZ6; Q4EC67; C0R3V5; C0F897; M9WWW1		3.67161045	2.161695025
CG42336		3.632664173	3.725365559
Vps16A		3.538821516	28.74884319
Tequila		3.511111958	2.218869777
M9WZY9; C0R3P2; C0F912; A0A098ATV9		3.509141201	3.804162832
Blast: GlyRS (88.8)		3.448155891	3.185118394
Eip71CD	Peptide methionine sulfoxide reductase	3.435954662	2.6937482

Gene name/ Protein IDs	Protein name	H/L ratio WT Exp. 1	H/L ratio WT Exp. 2
Cyp12c1	Probable cytochrome P450 12c1, mitochondrial	3.189793433	3.394433919
A0A098ASM2; M9X1H4; C0F9Z5; M9WNY1; Q4EBZ8; C0R4K8		3.185321514	3.422313681
M9WW10; A0A098ASH2		3.184409783	3.118276806
Q4EBL3; C0R2W8; C0FAA1; A0A098ARW4; M9X0A1		3.144258868	2.858368658
Blast: FASN (98.8)		3.128421709	2.839456874
C0F940; A0A098ARU9; Q5GQ91; Q5GQ89; Q4EB62; M9WUE5; C0R2V4		3.099621379	3.201433405
CG31436		3.028375286	3.107809342
Amy-d; Amy-p	Alpha-amylase B; Alpha-amylase A	3.00860561	3.344593785
CG4577		2.924745313	2.951157668
C0R3Q2; C0F9Z9; A0A098ATW3; M9WZZ8		2.893183843	1.64698521
CG18135		2.885169344	2.7552763
CG14495		2.847867451	2.482190772
Blast: CG5010 (99.1)		2.742430387	2.704749528
Q4EB11; M9WU64; C0R2L6; C0FAB5; A0A098ATG4		2.725760869	2.670440981
BG: DS00941.11		2.702264699	2.781409182
alpha-Man-I		2.701388246	1.760222618
CG1943		2.684346669	4.425170369
Cyp4d21	Probable cytochrome P450 4d21	2.683483468	2.614856907
Q4E9N6; M9WSA6; C0R2Z5; A0A098AR91; C0F8P9		2.67186849	2.607698363
CG3775		2.647324415	2.919367837
CG7587		2.634559934	2.585449275
CG9953		2.626533527	2.839295489
Blast: CG5973 (92.9)		2.534533091	2.471882214
CG15739		2.528893006	2.197222545
Q4ECB1; M9X1P4; C0R4S2; A0A098ATR4		2.525953358	2.925858501
imd		2.509347027	2.67780703
CG12001	Uncharacterized protein CG12001	2.496505353	1.878145848
CG5508; BcDNA.GH07066		2.496505353	2.480343617
CG3902		2.480589481	2.506077447

Appendix

Gene name/ Protein IDs	Protein name	H/L ratio WT Exp. 1	H/L ratio WT Exp. 2
Iris		2.471882214	2.457969476
CG3523		2.450859871	2.578714401
CG43402		2.445226318	2.786213863
Blast: CLIP-190 (94.4)		2.410973845	3.16565931
glob1		2.383789757	2.442717456
A7XUH0; A0A098AR47		2.353273497	2.34758273
Blast: CG9953 (97.8)		2.349016749	2.480713282
CG8552		2.344445919	1.492782419
A0A098ATR1; Q4ECB5; M9X1N8; C0R4R7; C0F9K3		2.333830847	2.174952661
CG34424		2.325040747	2.411264644
Got1		2.319701225	2.324067547
CG14105	Tetratricopeptide repeat protein 36 homolog	2.299695742	2.723460608
Q0QAS4		2.269839046	3.152982145
ppl	Glycine cleavage system H protein, mitochondrial	2.249009882	1.474100003
Cpr11B; CG2555		2.248302255	1.875082015
Blast: CG7834 (95.7)		2.237536164	1.450747155
K8WNQ1; K8WTR1		2.236585639	2.122510955
CG13335		2.136432891	1.975894064
Obp56d	General odorant-binding protein 56d	2.125489305	2.222667277
Rfabg	Apolipophorins; Apolipophorin-2; Apolipophorin-1	2.120710955	1.973593132
Blast: CG31221 (91.3)		2.104909199	1.75460137
Blast: CG8642 (48.9)		2.103226172	2.26598137
rab3-GEF; Rab3-GEF	MAP kinase-activating death domain protein	2.097887042	1.946130965
CG3246		2.052461272	1.793046496
CG4500	Long-chain-fatty-acid–CoA ligase bubblegum-like	2.035168153	1.921229678
CG6910		2.008516064	2.12210641
Reg-2	Rhythmically expressed gene 2 protein	2.003727055	2.02101776
CG3792	Mannose-P-dolichol utilization defect 1 protein homolog	2.001882086	1.69932194
CG4716		1.990841961	1.949165781
ArfGAP3		1.98807144	1.716355141
PGRP-SB1	Peptidoglycan-recognition protein SB1	1.978317661	2.111976819
Tdc2		1.977339779	1.665445334
Vrp1		1.95637292	1.428428575
CG3940		1.930203824	1.730942379

Gene name/ Protein IDs	Protein name	H/L ratio WT Exp. 1	H/L ratio WT Exp. 2
SelR-RH; SelR	Methionine-R-sulfoxide reductase B1	1.924076019	1.493428947
CG12512		1.911351479	1.828588181
CG8398		1.908797687	2.07800914
A0A034VSK2; A0A034VNA1		1.90501598	1.924409198
Ccp84Ag		1.903674077	2.861231044
Mob3	MOB kinase activator-like 3	1.883487684	1.491491029
CG5599		1.882919863	1.952476657
M9WRG2		1.880406275	2.561343953
vir-1		1.875996583	1.820167475
Blast: Rfabg (88.7)		1.861504237	1.864836697
CG7322		1.853705552	1.743435873
LKR; BEST:CK02318		1.848804786	1.71541293
CG9231	UPF0389 protein CG9231	1.848292132	1.604235229
EG: 100G10.4		1.838032657	1.720903858
Smp-30		1.834761449	1.861573398
Ugt36Bc		1.829223806	1.595939874
CG18003; CG30019; CG18003		1.80694601	2.010293293
Obp99a	General odorant-binding protein 99a	1.801639421	1.870697257
Gyk		1.791825817	1.762331836
Blast: ptr (56.2)		1.790959359	1.683870161
CAHbeta		1.781737373	1.853842912
CG6415	Aminomethyl-transferase	1.781007387	1.658952639
CG11334	Methylthioribose-1-phosphate isomerase	1.769754937	1.426024927
stmA	Protein EFR3 homolog cmp44E	1.766316283	1.629540264
B2L9U4; B2L9S9		1.759045865	1.642144065
CG2233		1.758334561	1.830395614
CG3091		1.758303604	1.529309174
CG10184		1.745901418	1.425211965
Est-6	Esterase-6	1.734635452	1.574183475
CG8632		1.733703274	1.873501198
CAH1		1.732802104	1.794784463
Mtp		1.729505498	1.783325928
CG11899	Probable phosphoserine aminotransferase	1.728698174	1.607742768
crp		1.726578944	1.919643752
GstE7		1.723484232	1.75223406
Apoltp; CG15828		1.722623121	1.623956513
CG6144		1.720785174	1.514004612
Blast: Adh (98.1)		1.719424418	1.988704192
Sirt2	NAD-dependent protein deacetylase Sirt2	1.713707871	1.414247088

Appendix

Gene name/ Protein IDs	Protein name	H/L ratio WT Exp. 1	H/L ratio WT Exp. 2
CG32500	NFU1 iron-sulfur cluster scaffold homolog, mito-chondrial	1.710571371	1.644006838
Gclm		1.705146151	1.880123198
CG2254		1.702069798	1.626677325
SpdS		1.693853027	1.78084876
O61691; O61689; Q9U8N8; A0A097ZNU6; Q9TW68		1.690845687	1.467351392
CG15093	Probable 3-hydroxyisobutyrate dehydrogenase, mito-chondrial	1.685573222	1.855700775
Blast: Acsl (99)		1.685459429	1.646903702
Inos	Inositol-3-phosphate synthase	1.684863248	1.627339318
eas	Ethanolamine kinase	1.682340463	1.698860038
CG18501		1.677430275	1.609709665
Ude		1.669867115	1.412469289
CG10932		1.665140254	1.52837419
Blast: CG7886 (49.8)		1.664696874	1.482162059
AcCoAS	Acetyl-coenzyme A syn-thetase	1.66251044	1.70695071
Nup58	Probable nucleoporin Nup58	1.660136767	2.261521952
CG1513	Oxysterol-binding pro-tein	1.657275441	1.417554989
CG5162		1.655875838	1.770914549
CG12170	3-oxoacyl-[acyl-carrier-protein] synthase	1.653220548	1.420535219
CG31221		1.651500378	1.617207052
tacc		1.649402844	1.903674077
SamDC	S-adenosylmethionine decarboxylase proenzyme; S-adenosylmethionine de-carboxylase proenzyme; S-adenosylmethionine decarboxylase al-pha chain; S-adenosylmethionine decarboxylase beta chain	1.644006838	1.683246774
CG9399		1.630895676	1.475818699
CG17837		1.627259797	1.420656433
CG17032		1.624352337	1.796299608
Adh		1.623692909	1.815903704
Map205	205 kDa microtubule-associated protein	1.62353479	1.491624605

Gene name/ Protein IDs	Protein name	H/L ratio WT Exp. 1	H/L ratio WT Exp. 2
Blast: PCB (92.7)		1.616971891	1.420575589
CG15717		1.609398954	1.735900192
Blast: CG9686 (75.9)		1.606116118	1.63676829
flower; fwe	Calcium channel flower	1.604981869	1.469399817
CG6067		1.604544165	1.70843789
Blast: Rfabg (74.9)		1.604132153	1.42017213
CG4594		1.602461394	1.486325711
ogre	Innexin inx1	1.602024932	1.825217258
CG32068	1,2-dihydroxy-3-keto-5-methylthio-pentene dioxygenase	1.600768297	1.758272647
sky; CG9339		1.596474932	1.99517169
CG9498		1.594006707	1.564773996
dnd		1.587856019	1.47547032
GstE6		1.58677261	1.519710689
Gk		1.585288594	1.527440413
GstD9		1.583882485	1.582754283
CG2915		1.582754283	1.671346429
Cyp4e2	Cytochrome P450 4e2	1.579429345	1.584986992
Blast: Adh (91.4)		1.578930752	1.50242638
CG6259	Charged multivesicular body protein 5	1.576292534	1.603591972
CG5171		1.567717596	1.714707027
ACC		1.564406678	1.844439925
Etf-QO		1.563672736	1.411910852
raps		1.560013809	1.446759182
CG9675		1.559575828	1.420010798
Spat		1.559162395	1.73307225
CG5382	Zinc finger protein-like 1 homolog	1.558797799	1.517151439
zetaCOP; CG5946		1.557414	1.705989775
CG2118		1.557389819	1.627233404
Blast: Rfabg (88.7)		1.55734135	1.488183883
cv-d		1.555911821	1.641793636
bocksbeutel		1.555330847	1.501478899
CG2200	Probable alpha-aspartyl dipeptidase	1.554436303	1.507068194
CG6984		1.553373867	1.700506711
CG17896; EG:171D11.1	Probable methylmalonate-semialdehyde dehydrogenase [acylating], mitochondrial	1.551638631	1.456961445
Galk		1.547484544	1.647229417
GS		1.544186922	1.64674115
CG6983		1.541592224	1.48612699
Tsf1		1.541069685	1.55860343
Blast: Adh (84.8)		1.537090063	1.483195323
CG5171		1.536688449	1.416009456

Gene name/ Protein IDs	Protein name	H/L ratio WT Exp. 1	H/L ratio WT Exp. 2
Dak1		1.536664803	1.49864378
Pfrx		1.536287152	1.51676008
colt	Congested-like trachea protein	1.535579388	1.498284506
Cpr73D		1.532637489	1.44845664
CG6543		1.531768844	1.5814277
Adam	Eukaryotic translation initiation factor 3 subunit J	1.528841664	1.416290194
Stim	Stromal interaction molecule homolog	1.526205044	1.78176887
hoe1		1.526181771	1.79124813
CG4670		1.525273755	1.42572002
M(2)21AB; Sam-S	S-adenosylmethionine synthase	1.524181173	1.59729103
Nplp2	Neuropeptide-like 2	1.5240881	1.71218216
CG4646	UPF0587 protein CG4646	1.523530941	1.53071384
Fmrf	FMRFamide-related peptides; FMRFamide A; Corticotropin-releasing factor-like; AAMDRY-amide; DPKQDFMRF-amide; TPAEDFMRF-amide; SDNFMRF-amide; SPKQDFMRF-amide; PDNFMRF-amide; SAPQDFVRS-amide; MDSNFIRF-amide	1.521884634	1.40289847
Vha16-1	V-type proton ATPase 16 kDa proteolipid subunit	1.518210885	1.452011017
TH1	Negative elongation factor D	1.517980439	1.462458615
Blast: BcDNA.GH05536 (98.1)		1.514967873	1.63313302
CG10361		1.512378767	1.62765722
Dic1		1.512035697	1.50916066
cpx		1.512012954	1.71641415
CG9977	Adenosylhomocysteinase	1.511007792	1.62298133
Blast: CG11858 (98.4)		1.509160662	1.431208837
A0A034VU53		1.509115158	1.58995144
CG4019		1.50843204	1.8679717
Irp-1B		1.504913536	1.51611638
Nurf-38	Inorganic pyrophosphatase	1.504076034	1.470782892
PCB	Pyruvate carboxylase	1.50242638	1.54009634
CG2658		1.50024009	1.51708235

Table A16: List of upregulated proteins after FLAG-d4E-BP[TA] overexpression in _Drosophila_. FLAG-d4E-BP[TA] was overexpressed in flies raised on light food only. The inverted normalised ratio of proteins from flies raised on light and heavy food is indicated (H/L) for experiment 1 and 2. Major protein IDs, which could not be matched with _Drosophila melanogaster_ genes were analysed with BLAST and the result listed in the gene name column along with % sequence identity in brackets. If no result was detectable, the protein IDs were listed instead of a gene name.

Gene name/ Protein IDs	Protein name	H/L ratio WT Exp. 1	H/L ratio WT Exp. 2
Blast: AnxB9 (91.7)		18.83913735	21.19138536
Sgs3	Salivary glue protein Sgs-3	14.79486882	5.385028574
Cyp6a2	Cytochrome P450 6a2	11.23014772	8.888888313
_CG8768_		10.60164329	20.11424944
Cyp12d1-p; Cyp12d1-d	Probable cytochrome P450 12d1 proximal, mitochondrial; Probable cytochrome P450 12d1 distal, mitochondrial	9.232760095	5.576310904
Tep4; TepIV		7.536360617	8.528783631
Blast: cry (86.9)		7.418399691	6.975932111
cry	Cryptochrome-1	5.977287764	4.221547655
_CG3513_		5.858575829	6.012145815
Act79B	Actin, larval muscle	5.60380984	4.48913661
Blast: CG8757 (96.1)		4.60341657	5.335893974
_CG3702_		3.931434995	4.813245467
_CG5853_		3.900916182	5.844534002
A0A098AQR2		3.290124096	3.356154194
_CG13059_		3.258177045	4.218876921
Ugt86Dd		3.09770122	2.755656379
obst-B		2.976987162	2.275934439
_CG12119_		2.965951486	2.618417228
desat1		2.961822123	2.712084257
_CG11395_		2.836156219	3.675389123
slik		2.789555007	1.703896849
C0R325		2.730600015	2.660139677
msps		2.64151939	1.759417296
woc		2.573539632	2.214790133
Cyp12a5	Probable cytochrome P450 12a5, mitochondrial	2.541425606	1.906577664
_CG10517; CG33056_		2.524614307	2.562066638
_CG2950_		2.496069319	2.309681627
_CG8243_		2.444150292	3.050919258
_CG3680_		2.442717456	2.103358841
mop		2.392573094	1.706513822
_CG2509_		2.320724072	1.968193958
grass		2.30637963	1.850823472
asparagine-synthetase	Asparagine synthetase	2.287963441	2.323366902
Blast: Pax (89.1)		2.279878592	2.472127239

Appendix

Gene name/ Protein IDs	Protein name	H/L ratio WT Exp. 1	H/L ratio WT Exp. 2
CG8399	Putative ferric-chelate reductase 1 homolog	2.227519405	2.124855891
A0A098AS71; Q4EC26; C0R5R0		2.178934758	2.203662063
CG32549; CG6247		2.139404084	1.674368877
Cpr76Bd		2.133834078	2.395095198
Mo25	Protein Mo25	2.12815761	2.332742396
Crag		2.123277595	1.886507715
CG42353		2.100222243	1.839520304
CG12997; CG34327		2.083767044	2.440332955
Cpr49Ac		2.082899167	1.735086875
BG: DS00180.2		2.061557928	1.998281457
Nup214	Nuclear pore complex protein Nup214	1.988664631	2.777238353
CG8192		1.979609952	1.877899037
trpl	Transient-receptor-potential-like protein	1.96714854	1.626677325
Cpr30B		1.963170942	1.733582987
CG6564		1.943899186	1.897209109
bun	Protein bunched, class 2/F/G isoform; Protein bunched, class 1/class 3/D/E isoforms	1.931061217	1.887006117
EG: 125H10.1; CG3777		1.92737634	1.601101535
Blast: CG4612 (93.5)		1.924002002	1.810610342
Blast: CG30197 (98.9)		1.915819044	3.942596316
CG14184		1.910840288	2.585449275
CG5721	Armadillo repeat-containing protein 6 homolog	1.897677191	2.078569518
nocte		1.870697257	1.898686084
Cpr97Ea		1.860465064	2.104067517
CG3760	Protein CDV3 homolog	1.857596681	1.892935561
CG15100		1.844235765	1.807762435
CG15118		1.843284041	1.62237587
larp	La-related protein	1.842944212	1.771604786
M9WTB4; C0F9X1; A0A098ASQ2; Q4ED38; C0R4N4		1.823985423	1.694484453
CG6126		1.805249697	1.91259459
Cas	Exportin-2	1.788940867	1.720489396
Ndae1		1.784471426	1.715619002
ste24a		1.778979517	1.681972596
Blast: Mhc (93.8)		1.769660974	1.859980634
TpnC41C	Troponin C, isoform 1	1.765598978	1.871432742
Bx42	Puff-specific protein Bx42	1.758427191	1.790766829
Hsp22	Heat shock protein 22	1.740038346	1.812283679
Amun; CG2446		1.737076029	1.518095657

Appendix

Gene name/ Protein IDs	Protein name	H/L ratio WT Exp. 1	H/L ratio WT Exp. 2
VGlut		1.733462828	2.607425442
Srp68	Signal recognition particle subunit SRP68	1.732952126	1.667222323
CG5991		1.72494098	1.800082839
Blast: vlc (95.4)		1.722979456	1.645982161
Lmpt		1.718774168	1.946055425
Stam		1.713854815	1.658759928
lig	Protein lingerer	1.709840083	1.647907998
CG4045	tRNA (guanine-N(7)-)-methyl-transferase	1.702214564	1.835502272
anon-66Db		1.698081143	1.784280335
DnaJ-1	DnaJ protein homolog 1	1.684267279	1.732231682
mbt	Serine/threonine-protein kinase PAK mbt	1.670788015	1.609632009
Cka		1.663423017	1.764135163
Ccp84Ae		1.657577471	1.743466447
CG17078		1.656479214	1.801087785
CG9780		1.655930817	1.737287353
EG: 52C10.2; aft		1.65182769	1.619485779
l(2)tid	Protein tumorous imaginal discs, mitochondrial	1.645602967	1.651064178
Mlp84B	Muscle LIM protein Mlp84B	1.645277915	1.744104883
CG1910; anon1A3		1.642710555	1.757716258
CG34205		1.637760275	1.689788518
CG2199	Zinc finger protein CG2199	1.634841759	1.74456131
CG10289		1.629619897	2.42124824
CG31869		1.629088974	1.833213989
CG16721		1.626174977	1.586042796
CG9572		1.623376574	1.605858193
tn		1.621928475	1.69643917
Paf-AHalpha	Platelet-activating factor acetylhydrolase IB subunit beta homolog	1.615691661	1.664890737
clu	Protein clueless	1.615404429	1.521606907
CG1124		1.615091388	1.683246774
Aats-glupro	Bifunctional glutamate/proline–tRNA ligase; Glutamate–tRNA ligase; Proline–tRNA ligase	1.614179032	1.575969594
exba	Protein extra bases	1.613553709	1.521328914
Blast: CdsA (94.2)		1.612669049	1.727891705
elav	Protein elav	1.602666783	1.500285014
CG3860	Oxysterol-binding protein	1.60061474	1.667166739
RanBP3		1.594972666	1.607458621

Appendix

Gene name/ Protein IDs	Protein name	H/L ratio WT Exp. 1	H/L ratio WT Exp. 2
Aats-ala; AATS	Alanine–tRNA ligase, cytoplasmic	1.568135363	1.503420311
Cnot4		1.564945158	1.863134078
Dsp1	High mobility group protein DSP1	1.560646726	1.518049569
Dmn	Probable dynactin subunit 2	1.535532236	1.664114959
CG13023		1.529075348	1.740644036
ens		1.518625986	1.577859558
Cul-3; gft		1.514508946	1.617704163
unc-45		1.509775772	1.626915589
bsf		1.507954502	1.582128303
Obp99b	General odorant-binding protein 99b	1.50371421	1.799305551
Fs(2)Ket	Importin subunit beta	1.501095745	1.709606265
Cht5		1.490957258	1.513592138
l(3)neo43		1.488316853	1.776514421
Tap42		1.482447692	1.518141853
CG1598	ATPase ASNA1 homolog	1.48042869	1.546168766
CG4673	Nuclear protein localization protein 4 homolog	1.480341059	1.617939655
Synd		1.478655736	1.837559672
CG3493		1.477213958	1.641820379
deltaCOP		1.476363525	1.651173246
CG7945		1.474273918	1.61676254
vimar		1.471648675	1.672800154
CG8547		1.46970204	1.505593286
LqfR; lqfR		1.464471888	1.835199114
GluClalpha	Glutamate-gated chloride channel	1.462544174	1.623086738
CG12269		1.460962958	1.615013249
CG9281		1.460600268	1.705756838
Cpr30F		1.454714661	1.60169139
CycY		1.451863579	1.600768297
mRpL39	39S ribosomal protein L39, mitochondrial	1.447722808	2.092619484
Blast: ArgK (99.5)		1.44686388	1.631640814
l(2)k09913		1.445985214	1.500217629
path		1.44262667	2.997242887
CG8858	Proteasome-associated protein ECM29 homolog	1.439470277	1.777303669
Asator; CG11533		1.438538467	1.659750861
CG9186		1.438538467	1.593523947
by; tensin		1.438414331	1.604801545
CG6299		1.437938526	1.880582894
140up	RPII140-upstream gene protein	1.436368779	1.595201642
Marf	Transmembrane GTPase Marf	1.435440967	1.552048026

Gene name/ Protein IDs	Protein name	H/L ratio WT Exp. 1	H/L ratio WT Exp. 2
Blast: CG4250 (79.3)		1.435090779	1.732952126
c11.1		1.430901734	1.570154582
zormin; CG33484		1.423467249	1.544663943
vnc		1.42021249	1.547460624
p120ctn		1.41880203	1.631241405
CG14688		1.417092861	1.80622773
Fuca	Putative alpha-L-fucosidase	1.416571086	1.586747533
GckIII		1.414607191	1.584183438
Zpr1		1.414207093	1.527090539
Hrs	Hepatocyte growth factor-regulated tyrosine kinase substrate	1.408907113	1.669421204
CG1737		1.402937754	1.879911309

Table A17: List of commonly upregulated proteins after FLAG-d4E-BP[WT] or FLAG-d4E-BP[TA] overexpression in *Drosophila*. FLAG-d4E-BP[WT] was overexpressed in flies raised on light food only. The inverted normalised ratio of proteins from flies raised on light and heavy food is indicated (H/L) for experiment 1 and 2. Major protein IDs, which could not be matched with *Drosophila melanogaster* genes were analysed with BLAST and the result listed in the gene name column along with % sequence identity in brackets. If no result was detectable, the protein IDs were listed instead of a gene name.

Gene name/ Protein IDs	Protein name	H/L ratio WT Exp. 1	H/L ratio WT Exp. 2	H/L ratio TA Exp. 1	H/L ratio TA Exp. 2
GstE1		51.06210118	69.16105638	29.43773976	79.9424565
Blast: CG6910 (98.3)		13.04273932	14.60472208	3.766477732	2.862704982
Blast: Tudor-SN (90.4)		9.879472409	11.6495797	21.43989596	18.5078961
CG8665		6.639667517	6.865772244	2.368825621	2.48453351
ssp7		6.132711142	4.569549688	10.39673767	1.400776028
CG7787	Guanine nucleotide exchange factor MSS4 homolog	4.677488155	4.402957748	5.769010943	4.919323734
Blast: CG4686 (96.7)		4.664178493	5.045152925	2.54019808	2.347473709
C0FAB9; A0A098ASB8; Q4EB96; M9WRT3; C0R2L2		4.477880413	4.490748725	2.275106372	2.405755455
CG32523		3.873567822	3.315868974	1.466103749	2.304200087
A0A098AS94; C0R4H2; M9WPT5		3.593632798	3.440208489	2.062664242	1.881679866

Appendix

Gene name/ Protein IDs	Protein name	H/L ratio WT Exp. 1	H/L ratio WT Exp. 2	H/L ratio TA Exp. 1	H/L ratio TA Exp. 2
CG3800	CCHC-type zinc finger protein CG3800	3.556945822	3.163856135	3.926649973	3.750656133
Q4EC24; C0R3A2; A0A098ATU3; M9WW69		3.495158788	2.870016438	2.37428151	2.299220771
Q4EC22; M9WSG7; C0R3A4; C0F9U7; A0A098ARP1		3.457576088	3.147128312	2.039234943	2.087203112
A0A098ATY0; Q4ECV2; C0R4Y6		3.456021039	4.168750415	2.152064026	2.247090143
Q4EBJ5; M9WX60; C0R4R4; A0A098ATS1		3.393396474	3.399741371	2.01474744	2.188088362
A0A098ATG3; Q4EBH1; M9X042; C0R3W7; C0F9Q0		3.292505841	2.749972135	1.983103947	2.031075684
Q4E981; C0R550; A0A098AR50; M9WT71; C0F980		3.055206724	3.065133689	1.919569905	2.051870954
A0A098AT29		3.047666415	3.726755056	2.72866257	2.224396543
A0A098ASQ0; Q4ED86; M9WUP1; C0R577; C0FA23		2.974951193	3.467046053	2.081512179	2.102784492
Q4EBZ2; M9X0Q6; C0R4L4; A0A098ATM8; C0F9Y9; Q4E9I5		2.794389254	2.868369734	1.721318539	2.290111752
M9WUN3; C0R3I9; A0A098ARK9		2.788155452	2.630747892	1.746145284	1.856320863
Blast: CG4577 (96.4)		2.77600468	2.635531618	1.6536854	1.749107912
BEST: GH09393		2.691064556	2.805364049	1.589395539	1.719306075
CG32638		2.613354792	2.443672587	3.661797471	4.183049297

Gene name/ Protein IDs	Protein name	H/L ratio WT Exp. 1	H/L ratio WT Exp. 2	H/L ratio TA Exp. 1	H/L ratio TA Exp. 2
A0A098ASS6; M9WUM0; Q4E8N0; C0R3L0; C0F8Y9		2.457001945	2.420603865	1.665195656	1.678443647
Cyp12b2	Probable cytochrome P450 12b2, mitochon-drial	2.397219476	2.479728205	1.463314631	1.693709442
stnA	Protein stoned-A	2.275106372	1.878569251	1.926039913	1.831367595
lbm	Protein late bloomer	2.267727044	1.903275622	1.575200091	1.815936682
Blast: CG10924 (71.4)		2.256928947	2.377329704	2.671938867	2.463174778
CG5065	Puta-tive fatty acyl-CoA reductase CG5065	2.196016661	2.134197958	1.46374313	1.677796102
Past1		2.182167734	2.187227065	1.843453723	1.771196897
Caps	Calcium-dependent secretion activator	2.180645114	1.985939537	2.045031407	1.970715202
CG15562		2.144679399	2.72635608	2.364568604	1.698802339
GM130		2.136478798	2.283261342	1.931061217	2.203613185
CG5973		2.083159059	1.930800091	1.404553618	1.538603505
CG32544		2.083029109	2.275882381	2.210189392	2.028520665
Blast: CG15515 (96.7)		2.05706303	1.985426977	1.836749778	1.698917857
didum		2.049348015	2.224347205	1.766909319	1.619564359
CG34325		2.030663231	1.847848143	2.732614599	1.904290396
Yp2	Vitellogenin-2	1.992627308	1.844133885	1.53306036	1.662952776
btz		1.980550929	1.965408636	2.377329704	2.072066062
Capr; rngi	Caprin ho-molog	1.973126018	1.796590114	2.766634381	2.976102056
CG5945		1.945525244	2.025029605	1.452327381	1.507704398
wdp		1.937721589	2.208236972	1.805282356	1.51272202
PP2A-B		1.926485463	2.253724237	2.047292163	1.697418257
BcDNA.GH10229		1.922448432	1.639236712	1.859012409	1.828521259
CG1311	CTL-like protein 1	1.921007964	1.799888454	1.76109044	2.475798669
CSN4	COP9 sig-nalosome complex subunit 4	1.910037416	1.741401897	1.933749743	2.103624202

Appendix

Gene name/ Protein IDs	Protein name	H/L ratio WT Exp. 1	H/L ratio WT Exp. 2	H/L ratio TA Exp. 1	H/L ratio TA Exp. 2
Orct	Organic cation transporter protein	1.903311902	1.738979228	1.808874353	1.6536854
CG6180		1.896669491	1.760873414	1.542067696	1.495103438
Pp2B-14D	Serine/ threonine-protein phos-phatase 2B catalytic subunit 2	1.887219722	1.845529246	1.634921877	1.62432599
IscU		1.885511827	2.058502214	1.699726472	1.659613272
CG2604		1.873185272	1.964790922	1.531229469	1.482557644
Yp3	Vitellogenin-3	1.860984449	1.893473329	1.541710945	1.676530233
Cpr51A		1.860603441	1.841925998	2.498314324	2.669443474
Yp1	Vitellogenin-1	1.852709643	1.736261681	1.460429686	1.61365795
Sgs7	Salivary glue protein Sgs-7	1.851646117	2.022490604	8.64304097	6.61506806
eIF5	Eukaryotic translation initiation factor 5	1.842876382	1.704070945	1.987952933	1.903927839
exo70	Exocyst complex component 7	1.833684585	2.104155025	1.648097964	1.476189056
DENR		1.827018066	1.812152288	1.933076725	2.266237402
Vm34Ca	Vitelline membrane protein Vm34Ca	1.819505106	3.861750613	3.847485795	1.848258054
Mgstl		1.817917337	2.025685213	1.565018705	1.572104589
Cyp313a1	Probable cytochrome P450 313a1	1.817884323	1.822024679	1.637116625	1.507658834
Ote	Otefin	1.814915022	1.472840803	2.835430904	2.021795389
brm	ATP-dependent helicase brm	1.811594293	1.544186922	1.874379005	1.989653768
CG9689		1.804142382	1.660908964	1.812185197	1.97308704
Lsd-1	Lipid storage droplets surface-binding protein 1	1.797655785	1.702098703	2.476842274	2.293473122

Gene name/ Protein IDs	Protein name	H/L ratio WT Exp. 1	H/L ratio WT Exp. 2	H/L ratio TA Exp. 1	H/L ratio TA Exp. 2
UQCR-6.4		1.777809449	1.908069207	1.962631472	1.7988848
jeb		1.776451498	1.552048026	1.505615933	1.443064015
CG11134	Probable methylthio- ribulose- 1-phosphate dehydratase	1.769911471	1.9648296	1.735568732	1.749046809
Lsp2	Larval serum protein 2	1.757623665	1.863481375	2.744839895	2.910614959
ple	Tyrosine 3-mono- oxygenase	1.757623665	1.917214691	2.065945219	1.746450315
Lasp	LIM and SH3 domain protein Lasp	1.747884918	1.781070718	1.435956355	1.577834622
CG11857		1.739342082	2.348907661	2.86976977	2.631854987
PpD3		1.738646458	1.714295602	1.800601467	1.664087391
Sgt1; CG9617		1.723098172	1.626122	1.892792287	1.77345829
CanA-14F	Serine/ threonine- protein phos- phatase 2B catalytic subunit 3	1.716974008	1.893616655	1.652865234	1.41057649
CG3967	Alpha- tubulin N-acetyl- transferase 1	1.715030579	1.881538226	1.593473029	1.491557712
endoA	Endophilin- A	1.710805559	1.931023873	1.530713837	1.485464677
Pepck	Phospho- enolpyru- vate car- boxykinase [GTP]	1.706280814	1.81409172	1.798722961	1.739523778
dre4	FACT complex subunit spt16	1.688020003	1.419688385	2.128792009	2.303510222
NAT1; l(2)01424		1.667111271	2.065091921	2.30255561	1.732952126

Appendix

Gene name/ Protein IDs	Protein name	H/L ratio WT Exp. 1	H/L ratio WT Exp. 2	H/L ratio TA Exp. 1	H/L ratio TA Exp. 2
ninaA	Peptidyl-prolyl cis-trans isomerase; Peptidyl-prolyl cis-trans isomerase, rhodopsin-specific isozyme	1.657193079	1.5240881	1.836581095	1.632919647
VAChT	Vesicular acetyl-choline transporter	1.643682672	1.66430887	1.647989328	1.582078187
I-2		1.6252763	1.679486734	1.699610663	1.432069788
tral		1.617311754	2.18111978	1.996246945	1.979139768
CG43737		1.599385817	1.484582533	1.680757049	1.552891465
BcDNA:GH08902; CG32444	Aldose 1-epimerase	1.591520456	1.61859439	1.577983916	1.557559633
Rab10		1.582078187	1.817851184	1.422940562	1.688561704
Ncc69		1.573366095	2.070007507	1.871888107	1.948292247
sdt		1.568110907	1.519595137	1.504800361	1.533930587
Ranbp9		1.554653748	1.745840427	1.773332663	2.039151549
CG14715	Peptidyl-prolyl cis-trans isomerase	1.550868539	1.449926732	1.598593358	1.707387829
RanGap; Ran-GAP	Ran GTPase-activating protein	1.539290471	1.505593286	1.491001801	1.586697161
eIF4G		1.529192257	1.47288419	1.416390429	1.853396304
CG6523		1.523693473	1.41470731	1.484450308	1.526577677
CG8635	Zinc finger CCCH domain-containing protein 15 homolog	1.484516471	1.542424422	1.796557736	2.130969582
Blast: pasi2 (92.7)		1.471930241	1.510551216	2.769852208	2.409986392
Blast: Hsc70-5 (92.3)		1.466576676	1.595277938	1.648369872	1.56948909
unc-104	Kinesin-like protein unc-104	1.461603608	1.588158608	1.513889914	1.483217427
Rtnl1		1.450684107	1.517174365	1.868530224	1.982946701

Gene name/ Protein IDs	Protein name	H/L ratio WT Exp. 1	H/L ratio WT Exp. 2	H/L ratio TA Exp. 1	H/L ratio TA Exp. 2
CG4747	Putative oxidore-ductase GLYR1 homolog	1.446006162	1.537728175	1.517312554	1.47177874
CG4721; CG4721		1.402898467	1.663146205	1.407023866	1.521629899

Table A18: List of downregulated proteins after FLAG-d4E-BP[WT] overexpression in *Drosophila*. FLAG-d4E-BP[WT] was overexpressed in flies raised on light food only. The inverted normalised ratio of proteins from flies raised on light and heavy food is indicated (H/L) for experiment 1 and 2. Major protein IDs, which could not be matched with *Drosophila melanogaster* genes were analysed with BLAST and the result listed in the gene name column along with % sequence identity in brackets.

Gene name	Protein name	H/L ratio WT Exp. 1	H/L ratio WT Exp. 2
Cpr76Bd		0.498976923	0.404024028
Blast: Cpr64Ac (74.7)		0.496425799	0.567859175
SP1029		0.496154726	0.523916789
Rpi; CG30410		0.490027969	0.517625143
fon		0.484496114	0.388545646
l(2)34Fc	Defense protein l(2)34Fc	0.484097316	0.488543523
Ance	Angiotensin-converting enzyme	0.482462595	0.503043407
aay	Phosphoserine phosphatase	0.480284448	0.500926729
Mhc		0.479777365	0.461424976
CG8515; Cpr49Ah		0.47778319	0.448611653
Hn; Henna	Protein henna	0.476099824	0.472947516
Cht5		0.471053882	0.508388394
Cchl		0.466439865	0.526371251
mgl		0.46468404	0.401445209
Neb-cGP		0.462855894	0.400608795
CG7860	Probable isoaspartyl peptidase/L-asparaginase CG7860; Probable isoaspartyl peptidase/L-asparaginase CG7860 alpha chain; Probable isoaspartyl peptidase/L-asparaginase CG7860 beta chain	0.451916144	0.441053325
CG4098		0.451711954	0.543507821
Blast: CG14291 (97.5)		0.44696724	0.567988215
GstE11		0.443892119	0.574778738
CG34205		0.443360762	0.426712122
Blast: CG34424 (96.8)		0.443242769	0.514006675

Appendix

Gene name	Protein name	H/L ratio WT Exp. 1	H/L ratio WT Exp. 2
Cpr100A		0.430311112	0.442204006
Skeletor	Protein Skeletor, isoforms B/C; Protein Skeletor, isoforms D/E	0.423244727	0.333411091
CG12997; CG34327		0.419550971	0.486333879
Blast: Cpr76Bd (93.4)		0.418637658	0.510073976
CG13044		0.418287561	0.396636678
Ugt58Fa		0.413393898	0.471076086
Cpr30B		0.412575198	0.421034979
Ccp84Ab; Ccp84Aa		0.412541168	0.380589852
Blast: CalpA (88.3)		0.408680411	0.418427623
Blast: EG:BACR7A4.14 (90.2)		0.404907424	0.359376007
Plod; CG6199		0.403893547	0.356036733
Clect27		0.403095896	0.394617543
Blast: RpS6 (95.2)		0.401574064	0.429166092
CG30296		0.397582731	0.507202267
Hsp22	Heat shock protein 22	0.392942739	0.41628515
CG6762	Putative sulfiredoxin	0.383038948	0.391757554
Phk-3		0.364737136	0.316195557
CG8757		0.361480568	0.29814251
Cht2	Probable chitinase 2	0.359479399	0.302041774
Blast: Unc-89 (91.1)		0.34712592	0.37461615
Cyp6a23	Probable cytochrome P450 6a23	0.344530593	0.206543276
CG13043		0.341658518	0.373454917
CG11835		0.341099135	0.367012982
Cpr64Aa		0.339870253	0.335514262
Blast: Obp99b (73.7)		0.331477075	0.332236849
ras	Inosine-5-monophosphate dehydrogenase	0.33024005	0.320965469
Obp99b	General odorant-binding protein 99b	0.324390843	0.32427529
Tsp		0.32248702	0.458358077
Gasp		0.31614559	0.338398012
Hsp27	Heat shock protein 27	0.315826033	0.395194562
se		0.312890986	0.334314075
Blast: CG9782 (94.7)		0.308441972	0.127599891
Cyp4s3	Probable cytochrome P450 4s3	0.306626226	0.42702191
CG6891		0.29928461	0.137691748
CG5653		0.291655665	0.309061746
poe	Protein purity of essence	0.290040043	0.387011945
wupA		0.289796284	0.294932967
CG9427		0.27154722	0.301404529
CG13065		0.262123208	0.294247487
Blast: CG10417 (94.4)		0.219096448	0.048883012

Gene name	Protein name	H/L ratio WT Exp. 1	H/L ratio WT Exp. 2
EG:125H10.1; CG3777		0.204215036	0.230621992
l(2)NC136		0.201588605	0.236551957
Blast: CG40485 (92.3)		0.192559473	0.225830461
serp		0.189609348	0.16689481
Blast: TpnC47D (95.5)		0.18860097	0.193061313
TpnC73F	Troponin C, isoform 3	0.183833679	0.184382802
CG5172		0.178034162	0.14663191
CG4898		0.176003619	0.184246868
Blast: RpLP1 (96.4)		0.175706808	0.178794963
Blast: Cda5 (85.7)		0.170085375	0.414645115
Cpr49Af		0.167591165	0.514482675
Obp83g		0.15044833	0.171975029
CG7900		0.137686021	0.173121163
CG31606		0.129518582	0.197612759
Sclp		0.126583915	0.112794295
CG15369		0.102488433	0.106674629
Blast: verm (96.8)		0.099641324	0.197957139
Pu		0.086707704	0.054232858
Pbprp5	Pheromone-binding protein-related protein 5	0.070596526	0.078265646
Pebp1		0.060779179	0.068446283
Blast: Lsp1beta (84.4)		0.044806877	0.049433984
anon-3B1.2	Circadian clock-controlled protein	0.043963773	0.043417847
Mhc		0.03714848	0.057863684
Blast: Fbp1 (95.8)		0.032018444	0.016963821
Blast: PPO1 (94.5)		0.030726686	0.028439797
Blast: Mtpalpha (98)		0.02297741	0.145353025
Blast: Lsp1gamma (96.5)		0.022904788	0.047499166
CG14961		0.02230599	0.006888473
Lsp1gamma	Larval serum protein 1 gamma chain	0.018333487	0.019210448
Fbp2	Fat body protein 2	0.009225092	0.052996981

Table A19: List of downregulated proteins after FLAG-d4E-BP[TA] overexpression in *Drosophila*. FLAG-d4E-BP[TA] was overexpressed in flies raised on light food only. The inverted normalised ratio of proteins from flies raised on light and heavy food is indicated (H/L) for experiment 1 and 2. Major protein IDs, which could not be matched with *Drosophila melanogaster* genes were analysed with BLAST and the result listed in the gene name column along with % sequence identity in brackets.

Gene name	Majority protein IDs	H/L ratio TA Exp. 1	H/L ratio TA Exp. 2
CG9338		0.499226354	0.567859175
Blast: Cyt-b5-r (83.7)		0.492853576	0.497933505
Blast: MetRS (84.4)		0.492150341	0.398692397
CG6812-RA; CG6812		0.491545544	0.442967881
lva	Protein lava lamp	0.483676048	0.591086387

Appendix

Gene name	Majority protein IDs	H/L ratio TA Exp. 1	H/L ratio TA Exp. 2
Blast: dj-1beta (98.9)		0.481742129	0.46753005
Drs	Drosomycin	0.475669689	0.542240546
gag		0.475556282	0.551663257
CD98hc		0.472567396	0.548005281
Blast: CG6543 (97.6)		0.472188235	0.545167098
sesB	ADP,ATP carrier protein	0.471408932	0.463585388
Blast: Got2 (98.8)		0.469968836	0.300652321
Cyp6g1	Cytochrome P450 6g1	0.468450008	0.485036425
PGRP-SD	Peptidoglycan-recognition protein SD	0.463478076	0.449095135
TepII; Tep2		0.460978062	0.451671253
Vha16-1	V-type proton ATPase 16 kDa proteolipid subunit	0.451793682	0.464425148
Blast: Droj2 (92.1)		0.448792664	0.560506691
Blast: aralar1 (99.1)		0.444938857	0.420981576
trol		0.443301761	0.515277999
Pbprp2; Obp19d	Pheromone-binding protein-related protein 2	0.440664627	0.449458245
Blast: PPO1 (98.4)		0.440199069	0.588235272
CG18279; IM10	Immune-induced peptides; Immune-induced peptide 10; Immune-induced peptide 12; Immune-induced peptide 13; Immune-induced peptide 24	0.435483209	0.497586759
CG30491; CG30495		0.435179952	0.506893757
Blast: CG5787 (90.8)		0.422833035	0.422012021
Blast: Sod (93.5)		0.414095951	0.488495779
Mal-B2; CG14935		0.398390458	0.401977596
ade3		0.383847724	0.37560105
Cyp6d5	Probable cytochrome P450 6d5	0.382819175	0.375883372
CG11951		0.379449027	0.352447677
Blast: ade3 (80.8)		0.35161731	0.345077425
Blast: CG32700 (95.9)		0.349113246	0.296243622
Blast: wal (95.9)		0.337997622	0.339431885
l(3)03670		0.290368528	0.513452492
CG1161	Uncharacterized protein CG1161	0.272449925	0.362292539
Act88F	Actin, indirect flight muscle	0.214128094	0.221395684

Table A20: List of downregulated proteins after FLAG-d4E-BP[WT] or FLAG-d4E-BP[TA] overexpression in *Drosophila*. FLAG-d4E-BP[WT/TA] was overexpressed in flies raised on light food only. The inverted normalised ratio of proteins from flies raised on light and heavy food is indicated (H/L) for experiment 1 and 2. Major protein IDs, which could not be matched with *Drosophila melanogaster* genes were analysed with BLAST and the result listed in the gene name column along with % sequence identity in brackets. If no result was detectable, the protein IDs were listed instead of a gene name.

Gene name/ Protein IDs	Protein name	H/L ratio WT Exp. 1	H/L ratio WT Exp. 2	H/L ratio TA Exp. 1	H/L ratio TA Exp. 2
CG6726		0.491521354	0.492659233	0.37068612	0.567214965
Nep2		0.483161699	0.55769336	0.459115804	0.435198956
bt		0.482043751	0.433801817	0.461701716	0.496524221
Stalker; HDC10856		0.469947011	0.476621851	0.409282532	0.389787573
futsch	Microtubule-associated protein futsch; Futsch heavy chain; Futsch light chain LC(f)	0.468164679	0.475782792	0.433425818	0.331950263
uzip	Protein un-zipped	0.468011537	0.50599604	0.44194998	0.529997882
Rbcn-3A		0.457582252	0.569054762	0.433576058	0.309243248
Blast: Cyt-c-p (97.2)		0.448873241	0.50916498	0.294750466	0.300751951
Glycogenin		0.443655882	0.430644706	0.402835854	0.446050203
Dhc64C	Dynein heavy chain, cytoplasmic	0.435843772	0.391404704	0.458064289	0.51329432
GstO2		0.427697595	0.48311515	0.357232192	0.424124286
EG: BACR7A4.14; CG3699		0.42204771	0.446987379	0.183979127	0.170776693
Unc-89		0.413308517	0.400176124	0.420928471	0.41466236
GstS1	Glu-tathione S-transferase S1	0.408947628	0.427661132	0.446767764	0.417658586
Blast: Glycogenin (90.1)		0.405646515	0.282877434	0.448450607	0.405646515
kst		0.404056795	0.556049799	0.355252326	0.38807812
CG17525; GstE4		0.390899867	0.391926221	0.251104885	0.249097077
CG13022		0.380894405	0.381956434	0.469263124	0.502588338
Cyp6a20	Proba-ble cy-tochrome P450 6a20	0.373426962	0.385460518	0.425350779	0.434990561
CG34309		0.344982241	0.387326737	0.206748247	0.219630604

Appendix

Gene name/ Protein IDs	Protein name	H/L ratio WT Exp. 1	H/L ratio WT Exp. 2	H/L ratio TA Exp. 1	H/L ratio TA Exp. 2
Blast: CG10602 (98.7)		0.328623145	0.285983933	0.387131606	0.350508175
Blast: Unc-89 (88.6)		0.32557391	0.342278126	0.367728271	0.327804372
Hexo2	Beta-hexos-aminidase	0.318481395	0.323446723	0.271127621	0.558222662
Mlp60A	Muscle LIM protein 1	0.299016293	0.29724738	0.369795097	0.387717027
Vps13		0.295290122	0.459157813	0.345996896	0.327257237
CG9497		0.291689832	0.288650174	0.179739699	0.20297557
Tsp42Ed		0.288375599	0.269498286	0.249382822	0.232233982
CG17544	Acyl-coenzyme A oxidase	0.277816271	0.29232072	0.448792664	0.435767951
Pbprp1	Pheromone-binding protein-related protein 1	0.207395716	0.111450423	0.067796612	0.075809266
pr	6-pyruvoyl tetrahy-dro-biopterin synthase	0.204185879	0.211349411	0.296366647	0.392557257
antdh		0.197515257	0.202105992	0.080051264	0.07026417
CG5804		0.184815543	0.269324056	0.181277654	0.123811395
CG11391		0.179581545	0.096543705	0.093257463	0.053989849
Gp150		0.156494515	0.193787175	0.187059222	0.195476624
ORF1		0.132310091	0.131707189	0.163851184	0.163923659
Cyp4p1	Cy-tochrome P450 4p1	0.124685188	0.193978814	0.108140812	0.147344795
Prosalpha7	Protea-some sub-unit alpha type-3	0.112952257	0.172398963	0.04898599	0.111410723
Jhedup; CG8424		0.11055468	0.062007821	0.10775166	0.062668401
Cht6		0.1055665	0.116192592	0.134972837	0.205854515
Scp1		0.102824574	0.104348155	0.231048239	0.234142706
fln	Flightin	0.102244277	0.1958633	0.021782223	0.092284937
Pbprp3	Pheromone-binding protein-related protein 3	0.065389418	0.038140274	0.208428866	0.03444831

Appendix

Gene name/ Protein IDs	Protein name	H/L ratio WT Exp. 1	H/L ratio WT Exp. 2	H/L ratio TA Exp. 1	H/L ratio TA Exp. 2
Lsp1beta	Larval serum protein 1 beta chain	0.05552164	0.05744818	0.388878128	0.418637658
Blast: TppII (98.5)		0.051082962	0.088347003	0.04539471	0.266254903
Obp83b; Os-E	Pheromone-binding protein-related protein 6	0.045993921	0.042777085	0.027124531	0.027262808
a10	Putative odorant-binding protein A10	0.039837474	0.070716368	0.050563775	0.047328303
TpnC4		0.033215973	0.073174308	0.026213703	0.029042752
C6FGJ6; A0A0F7LVX2; A0A0F7LZN9; A0A0F7LZE6; A0A0F7LZ62; A0A0F7LXG1; A0A0F7LXF3; A0A0F7LZJ9; A0A0F7LZC0; A0A0F7LZ46; A0A0F7LXD4; A0A0F7LZN7; A0A0F7LZN1; A0A0F7LZA9; A0A0F7LXE5; A0A0F7LVW2; A0A0F7LVS2		0.01348381	0.013518079	0.010968043	0.010707556
Lsp1alpha	Larval serum protein 1 alpha chain	0.012755268	0.004687573	0.390838637	0.4544215
hts	Protein hu-li tai shao	0.012634076	0.169425508	0.057843594	0.026989817

Definitions of PANTHER database categories

Table A21: List of GO terms used by PANTHER to categorise proteins according to their molecular function.

GO term	Definition
antioxidant activity (GO:0016209)	Inhibition of the reactions brought about by dioxygen (O_2) or peroxides. Usually the antioxidant is effective because it can itself be more easily oxidized than the substance protected. The term is often applied to components that can trap free radicals, thereby breaking the chain reaction that normally leads to extensive biological damage.
binding (GO:0005488)	The selective, non-covalent, often stoichiometric, interaction of a molecule with one or more specific sites on another molecule.
catalytic activity (GO:0003824)	Catalysis of a biochemical reaction at physiological temperatures. In biologically catalyzed reactions, the reactants are known as substrates, and the catalysts are naturally occurring macromolecular substances known as enzymes. Enzymes possess specific binding sites for substrates, and are usually composed wholly or largely of protein, but RNA that has catalytic activity (ribozyme) is often also regarded as enzymatic.
enzyme regulator activity (GO:0030234)	Modulates the activity of an enzyme.
nucleic acid binding transcription factor activity (GO:0001071)	Interacting selectively and non-covalently with a DNA or RNA sequence in order to modulate transcription. The transcription factor may or may not also interact selectively with a protein or macromolecular complex.
protein binding transcription factor activity (GO:0000988)	Interacting selectively and non-covalently with any protein or protein complex (a complex of two or more proteins that may include other nonprotein molecules), in order to modulate transcription. A protein binding transcription factor may or may not also interact with the template nucleic acid (either DNA or RNA) as well.
receptor activity (GO:0004872)	Combining with an extracellular or intracellular messenger to initiate a change in cell activity.
structural molecule activity (GO:0005198)	The action of a molecule that contributes to the structural integrity of a complex or assembly within or outside a cell.
translation regulator activity (GO:0045182)	Any molecular function involved in the initiation, activation, perpetuation, repression or termination of polypeptide synthesis at the ribosome.
transporter activity (GO:0005215)	Enables the directed movement of substances (such as macromolecules, small molecules, ions) into, out of or within a cell, or between cells.

Table A22: List of GO terms used by PANTHER to categorise proteins according to their biological process.

GO term	Definition
apoptotic process (GO:0006915)	A programmed cell death process which begins when a cell receives an internal (e.g. DNA damage) or external signal (e.g. an extracellular death ligand), and proceeds through a series of biochemical events (signaling pathways) which typically lead to rounding-up of the cell, retraction of pseudopodes, reduction of cellular volume (pyknosis), chromatin condensation, nuclear fragmentation (karyorrhexis), plasma membrane blebbing and fragmentation of the cell into apoptotic bodies. The process ends when the cell has died. The process is divided into a signaling pathway phase, and an execution phase, which is triggered by the former.
biological adhesion (GO:0022610)	The attachment of a cell or organism to a substrate or other organism.
biological regulation (GO:0065007)	Any process that modulates a measurable attribute of any biological process, quality or function.
cellular component organization or biogenesis (GO:0071840)	A process that results in the biosynthesis of constituent macromolecules, assembly, arrangement of constituent parts, or disassembly of a cellular component.
cellular process (GO:0009987)	Any process that is carried out at the cellular level, but not necessarily restricted to a single cell. For example, cell communication occurs among more than one cell, but occurs at the cellular level.
developmental process (GO:0032502)	A biological process whose specific outcome is the progression of an integrated living unit: an anatomical structure (which may be a subcellular structure, cell, tissue, or organ), or organism over time from an initial condition to a later condition.
immune system process (GO:0002376)	Any process involved in the development or functioning of the immune system, an organismal system for calibrated responses to potential internal or invasive threats.
localization (GO:0051179)	Any process in which a cell, a substance, or a cellular entity, such as a protein complex or organelle, is transported to, and/or maintained in a specific location.
metabolic process (GO:0008152)	The chemical reactions and pathways, including anabolism and catabolism, by which living organisms transform chemical substances. Metabolic processes typically transform small molecules, but also include macromolecular processes such as DNA repair and replication, and protein synthesis and degradation.
multicellular organismal process (GO:0032501)	Any biological process, occurring at the level of a multicellular organism, pertinent to its function.
reproduction (GO:0000003)	The production by an organism of new individuals that contain some portion of their genetic material inherited from that organism.
response to stimulus (GO:0050896)	Any process that results in a change in state or activity of a cell or an organism (in terms of movement, secretion, enzyme production, gene expression, etc.) as a result of a stimulus. The process begins with detection of the stimulus and ends with a change in state or activity or the cell or organism.